THE ROTATION OF VENUS

PART I. ATMOSPHERIC TIDES

PART II. OBLIQUITY AND EVOLUTION

Thesis by

Anthony Robert Dobrovolskis

In Partial Fulfillment of the Requirements

for the Degree of

Doctor of Philosopy

California Institute of Technology

Pasadena, California

1979

(Submitted 25 August 1978)

ERRATA

p. 16, eq. (2:25): $\Gamma_+ = \Gamma + - \frac{1}{\Delta}$ (etc.) should be $\Gamma_+ = \Gamma - \frac{1}{\Delta}$ (etc.)

p. 18, eq. (2:33): a should be *a*

p. 22, eq. (2:38): add the term $- \frac{i\sigma}{g} \delta \Omega$ to the right-hand side

p. 133, eq. (3:10): $[- \frac{3}{32} (1 - \cos \beta)^4]$ should be $[\frac{3}{32} (1 - \cos \beta)^4]$

p. 133, eq. (3:10): the second $b(2\omega - 2n)$ should be $b(2\omega + 2n)$

p. 133, eq. (3:11): " " " " " "

p. 134, eq. (3:12): " " " " " "

p. 229, line 10: should read $\Theta_{\ell,s} (\theta) \propto P_{21} (\cos \theta) \propto \sin \theta \cos \theta$

p. 78, eq. (5:19): $Ae^{(\xi + i\lambda)x}$ should be $Ae^{(\xi + i\lambda_o)x}$

p. 78, eq. (5:20): both λ_o should be λ_∞

p. 79, line 18: furthur should be further

p. 81, eq. (5:25): $\Pi_{ns}\Lambda_4^{\ 1}$ should be $\Pi\Lambda_4$

To my parents

Francis M. Dobrovolskis

Helen R. Dobrovolskis

ACKNOWLEDGEMENTS

Much of the credit for this work is due to my research advisor, Prof. Andrew P. Ingersoll, who suggested the topic of this dissertation in the first place. His unflagging interest in the problem has not only helped to shape this product, but has also taught me much about the meaning of scientific research, for which I am grateful.

Thanks are also due to the members of my examining committee for reading this thesis and making helpful comments: Drs. Don Anderson, Andy Ingersoll, Peter Goldreich, Stan Peale, Jim Williams, Bill Ward, and Dick Zurek.

My student collegues have been a wellspring of encouragement and good fellowship for the last several years; while they are numerous (my good fortune), one and all are appreciated more than they know. In particular, though, among the faculty Prof. Dewey Muhleman has won lasting respect for his equanimity and true concern for the fledglings.

Certainly I am much indebted to (the long-suffering) Ms. Hallee Kelso for typing the manuscript and almost single-handedly seeing it through to its final form.

ABSTRACT

Earth-based radar observations reveal that the surface of Venus rotates very slowly in the retrograde sense. Tides raised by the sun in the body of Venus tend to slow its rotation further. The spin of Venus might be in a steady state if thermal tides in the atmosphere balance the tidal torque on the crust. Part I of this dissertation presents a quantitative theory of atmospheric tides applicable to Venus. It is found that the thermal tide is capable of maintaining the rotation of Venus in its current state indefinitely.

Part II examines the effects of obliquity, the frequency-dependence of the tides, core-mantle coupling, possible resonances, and other phenomena. It appears most likely that Venus originated with an obliquity greater than 90°.

CONTENTS

CONTENTS (continued)

FIGURES

ix

FIGURES (continued)

FIGURES (continued)

FIGURES (continued)

TABLES

Page

THE ROTATION OF VENUS

PART I. ATMOSPHERIC TIDES

1. The Rotation of Venus

Earth-based radar observations reveal that the surface of Venus rotates with a very long sidereal period of 243 days, and in the retrograde sense; its orbital and spin angular momenta form an angle (the obliquity) within a few degrees of 180° (Shapiro et al., 1978). Such a slow rotation is unlikely to be primordial, but there are several influences that may affect the rotation.

The gravitational field of the Sun raises tides in the body of Venus, on which it exerts a retarding torque. In the absence of other effects, within about 10^8 years this torque should be capable of slowing Venus down from the present rate to the synchronous state, with one hemisphere always facing the Sun. Furthermore, Goldreich and Peale (1970) found that a retrograde obliquity is unstable on the same time scale as the despinning. So either we happen to be observing the final stages of Venus' tidal evolution, an unlikely circumstance, or else Venus has already reached a stable equilibrium in which other influences balance the solar body tide.

There is the additional complication that the spin of Venus appears to be affected by the orbit of the Earth, so that Venus presents nearly the same hemisphere to the Earth at each close approach. This is hard to account for, since the Earth's influence ought to be much weaker than the solar torque on the body tides, and in any case cannot by itself stabilize the obliquity (Goldreich and Peale, 1970). It appears that a third influence at least is needed to account for the present rotation state.

Thermal tides in the atmosphere of Venus may provide the necessary balance of torques. This state of affairs is depicted in Fig. 1, after Hinch (1970). Since only the semidiurnal components of the tides contribute to the torques, it is convenient to picture the effects produced both by the real sun and by an identical image sun on the opposite side of the planet. The suns are held stationary in the figure, so that Venus is rotating clockwise as seen from north of its orbit plane.

The suns' gravitational influence elongates the solid body of Venus, represented by the inner oval in the diagram. Internal dissipation produces a lag angle between the subsolar points and the positions of high tide. The planet's rotation pulls the tidal bulges forward into the afternoon sector, but they remain fixed relative to the suns. The daily cycle of heating and cooling also redistributes the mass of the atmosphere. The outer oval represents a surface of constant pressure; it may also be regarded as the surface of an ocean with equivalent mass. Solar radiation raises the air temperature highest in the afternoon, causing mass to flow to the colder morning region.

The gravitational attraction of the suns, represented by arrows in the figure, thus exerts contrary torques on the atmosphere

Figure 1

Balance of Torques on Venus

Since only the semidiurnal components of the tides produce
a torque, an "image sun" is shown diametrically opposite the true
sun, in order to make the picture symmetrical and to aid in visuali-
zation. The sun is held fixed in this sketch so that Venus is
rotating clockwise as seen from north of its orbit plane. The inner
oval represents the tidally distorted figure of Venus, while the outer
oval represents a surface of constant atmospheric pressure; the outer
oval may also be regarded as the surface of an ocean of equivalent mass.
Solar radiation raises the air temperature in the afternoon and causes
mass to flow to the colder morning region. The high-pressure areas
as well as the tidal bulges in the body of Venus are fixed with
respect to the sun (but not with respect to the surface). The
gravitational attraction of the sun, represented by arrows in the
diagram, thus exerts contrary torques on the atmosphere and body of
Venus.

HIGH P

LOW P

HOT

COLD

5
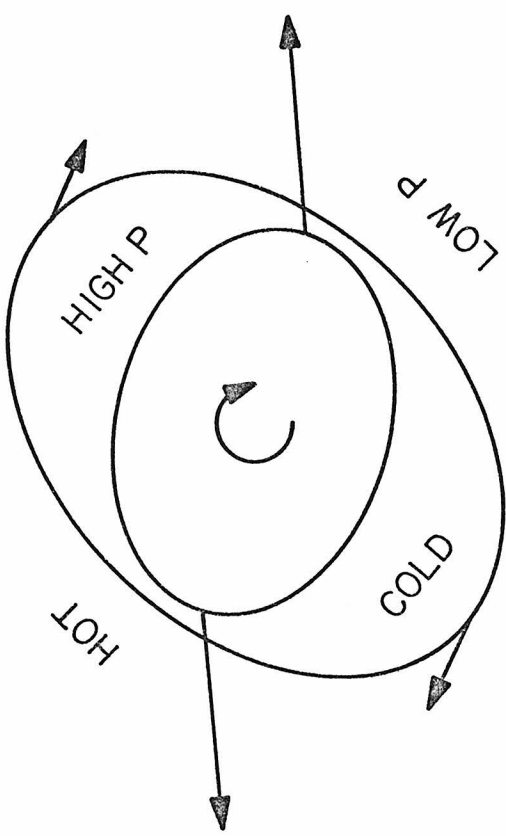
and body of Venus. It will be shown in chapter 7 that the net torque on the atmosphere depends only on the semidiurnal component of the surface pressure variation. If this amounts to only as much as a few millibars, the atmospheric torque could cancel the decelerating tidal torque on the crust. In that case, the spin has no tendency either to slow down or to speed up, and the current rotation of Venus may be in a steady state.

Various authors (MacDonald, 1964; Gold and Soter, 1969, 1971; Hinch, 1970; Kundt, 1977; Cazenave and Fouchard, 1977; see also Holmberg, 1952) have considered the effects of atmospheric tides on the rotation of Venus. However, realistic calculations have not been possible before, for lack of adequate data and of a theory of atmospheric tides applicable to Venus. Part I of this work develops an approximate theory of atmospheric tides suitable for Venus, and applies it to recent data, mostly returned by the Soviet Venera spacecraft. From this we predict the periodic variations in wind, temperature, and pressure at the surface. The resulting torque on the atmosphere does cancel the torque due to tides in the body of Venus, for reasonable values of the dissipation. The observed rotation of Venus can then be understood as an equilibrium between atmospheric and body tides, and possibly also the influence of the Earth.

2. Tidal Theory Including Mean Zonal Winds

Classical theory treats tides as the response of a linear oscillator to a periodic thermal or gravitational forcing. The traditional approach treats an atmosphere in uniform rotation; no mean winds or horizontal temperature gradients are considered. As a result, the horizontal and vertical structures of the oscillations are separable. For Venus, these assumptions are not justified (Lindzen, 1970b), primarily because of the substantial difference in rotation rate between the upper and lower atmospheres. In the following chapter, we develop a generalized linear theory of atmospheric tides that can be applied in the presence of a large shear in the mean zonal wind. The derivations closely follow the work of Chapman and Lindzen (1970) and of Lindzen and Hong (1974).

A. Primitive Equations.

To a sufficiently high accuracy, it is valid to treat atmospheric tides on Venus as hydrostatic. In terms of the conventional variables, the hydrostatic law is

$$\frac{\partial p}{\partial z} = - g\rho. \tag{2:1}$$

As long as the oscillations are hydrostatic, it is simpler to develop the governing equations in isobaric coordinates, where altitude z is considered a function of pressure p instead of _vice versa_. Define the new "height" coordinate $x = -\ln\left(p/p_o\right)$ where the constant p_o is

the mean surface pressure at the equator, and let its corresponding

speed be $\eta = \dfrac{dx}{dt} = -\dfrac{1}{p}\dfrac{dp}{dt}$. Define also the geopotential $\Phi = \displaystyle\int_0^z gdz$,

the tidal potential Ω, and the total geopotential $\psi = \Phi + \Omega$.

Since the acceleration of gravity g is nearly constant, the hydro-

static law (2:1) becomes

$$\frac{\partial\psi}{\partial x} \approx \frac{\partial\Phi}{\partial x} \approx g\frac{\partial z}{\partial x} = p/\rho = RT, \qquad (2:2)$$

where we have combined it with the equation of state for an ideal

gas.

Now let a be the radius of Venus, and ω_{φ} its sideral rate of

rotation at the surface, considered positive. Also let θ be the

colatitude, measured from the right-hand rotation pole, let φ be

the longitude relative to the surface in the direction of rotation,

and let the corresponding velocities relative to the ground be

$u = a\left(\dfrac{d\theta}{dt}\right)_p$ and $v = a\,\sin\theta\left(\dfrac{d\varphi}{dt}\right)_p$. This coordinate system is described

by Figure 2, after Lindzen (1970b).

The inviscid equations of horizontal momentum then take the follow-

ing form:

$$\frac{du}{dt} - \left(\frac{v}{a\,\sin\theta} + 2\omega_{\varphi}\right)v\cos\theta = -\frac{1}{a}\left(g\frac{\partial z}{\partial\theta} + \frac{\partial\Omega}{\partial\theta}\right) = -\frac{1}{a}\frac{\partial\psi}{\partial\theta} \qquad (2:3)$$

$$\frac{dv}{dt} + \left(\frac{v}{a\,\sin\theta} + 2\omega_{\varphi}\right)u\cos\theta = -\frac{1}{a\,\sin\theta}\left(g\frac{\partial z}{\partial\varphi} + \frac{\partial\Omega}{\partial\varphi}\right) = -\frac{1}{a\,\sin\theta}\frac{\partial\psi}{\partial\varphi} \qquad (2:4)$$

where we may write the $\dfrac{d}{dt}$ operator as

$$\frac{d}{dt} = \frac{\partial}{\partial t} + \frac{u}{a}\frac{\partial}{\partial\theta} + \frac{v}{a\,\sin\theta}\frac{\partial}{\partial\varphi} + \eta\frac{\partial}{\partial x}. \qquad (2:5)$$

Figure 2

Coordinate system for tidal theory
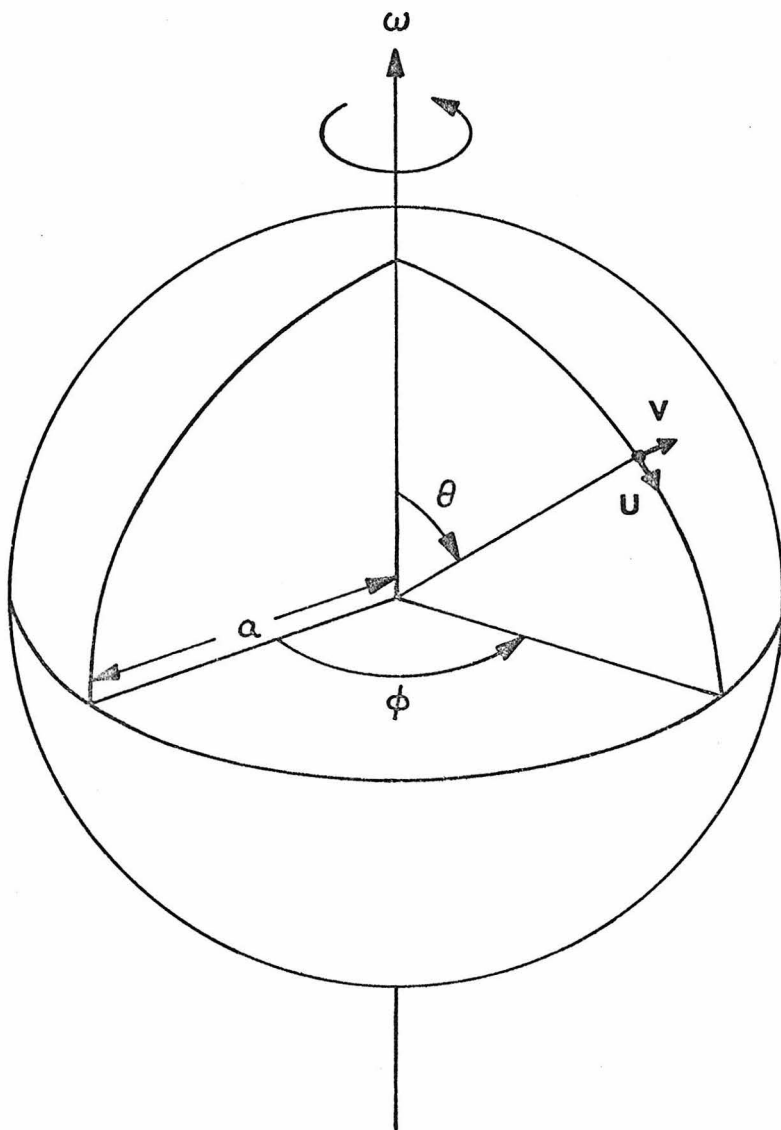
We also introduce the equation of continuity in isobaric coordinates:

$$0 = \frac{1}{a\sin\theta}\ \frac{\partial}{\partial\theta}\left(u\ \sin\theta\right) + \frac{1}{a\sin\theta}\ \frac{\partial v}{\partial\varphi} + \frac{\partial\eta}{\partial x} - \eta. \qquad (2:6)$$

B. Linearization

In order to linearize the basic equations about a reference state, we split all dependent variables into a mean part and a variation. The mean part, designated by an overbar, is zonally and temporally averaged, so that it depends only on θ and x, while the variation depends also on φ and t. Furthermore we shall represent all variation quantities as complex Fourier series in φ and t in order to eliminate their dependence on longitude and time. For example, the total geopotential would then be written

$$\psi\ (\theta,x,\varphi,t) = \overline{\psi}(\theta,x) + \text{Real}\sum_{\sigma,s} \delta\psi^{\sigma,s}(\theta,x)\ e^{i(\sigma_\varphi t + s\varphi)}, \qquad (2:7)$$

where s is the zonal wavenumber and σ_φ is the angular time frequency of the oscillation at a point fixed on the surface. Note that s must be an integer for continuity, and that the symbol δ will signify a complex variation quantity depending on σ and s.

For convenience, we also define ω, the (position-dependent) mean rotation rate of the atmosphere relative to inertial space, and its corresponding Doppler-shifted tidal frequency σ:

$$\omega(\theta,x) = \omega_\varphi + \overline{\frac{d\varphi}{dt}} = \omega_\varphi + \frac{\overline{v}}{a\sin\theta} \qquad ,$$

$$\sigma(\theta,x) = \sigma_\varphi + \frac{s\overline{v}}{a\sin\theta} \qquad . \qquad (2:8)$$

The mean meridional and vertical velocities $\bar{u}$ and $\bar{\eta}$ are small

on Venus, and so are the nonlinear correlation terms such as $\overline{uv} - \bar{u}\,\bar{v}$

(Suomi, 1974). Scaling the equations of motion shows that those

terms can be neglected in the following treatment.

Then the equations of the basic state reduce to

$$\frac{\partial}{\partial x}\,\bar{\psi} \approx g\,\frac{\partial}{\partial x}\,\bar{z} = R\bar{T}\,, \tag{2:9}$$

$$\frac{\partial}{\partial \theta}\,\bar{\psi} = a^2\,\sin\theta\,\cos\theta\,(\omega^2 - \omega_o^2)\,, \tag{2:10}$$

where ω_o is the rotation rate of the atmosphere at the ground, not

necessarily equal to ω_o. The above may be combined to give the

cyclostrophic balance condition for Venus (the "thermal wind";

Leovy, 1973):

$$\frac{\partial}{\partial \theta}\,R\bar{T} = a^2\,\sin\theta\,\cos\theta\,\frac{\partial}{\partial x}\,\omega^2 = 2a\omega\,\cos\theta\,\frac{\partial}{\partial x}\,\bar{v}\,. \tag{2:11}$$

For reasonable choices of $\omega(\theta, x)$, the mean equations show that

the average surface pressure and temperature change by about one

part in 10^4 between the equator and the poles. It is possible,

however, that the mean state represented by the averaged equations

(2:9) and (2:11) would be baroclinically (or otherwise) unstable;

the actual mean balance might be maintained by some more complicated

mechanisms. Even so, this would affect the linearization about

the mean only slightly, and we shall see that the results are not

sensitive to the exact choice of the mean state.

In order to obtain a linearized system, we may now expand the
primitive equations (2:2) – (2:6) to first order in variation
quantities. Subtracting the equations (2:9) and (2:10) of the basic
state then removes the zeroth-order terms, which balance in the mean.
Finally, applying the Fourier decomposition (2:7) to the linearized
equations gives for each individual component

$$\frac{\partial}{\partial x} \delta\psi = R \, \delta T \tag{2:12}$$

$$i\sigma \, \delta u - 2\omega \, \cos\theta \, \delta y = -\frac{1}{a} \frac{\partial}{\partial\theta} \delta\psi \tag{2:13}$$

$$i\sigma \, \delta v + 2\omega \, \delta u \cos\theta + \delta u \sin\theta \, \frac{\partial}{\partial\theta} \omega$$
$$+ \delta\eta \, a\sin\theta \, \frac{\partial}{\partial x} \omega = -\frac{is}{a \sin\theta} \, \delta\psi \tag{2:14}$$

$$0 = \frac{1}{a \sin\theta} \frac{\partial}{\partial\theta} (\delta u \sin\theta) + \frac{is}{a \sin\theta} \delta v$$
$$+ \frac{\partial}{\partial x} \delta\eta - \delta\eta \tag{2:15}$$

where we have omitted the superscript σ,s for the sake of clarity.

C. Thermodynamic Relations

Now for each σ,x component equations (2:12)-(2:15) represent
four equations in five unknowns: δu, δv, $\delta\eta$, $\delta\psi$ and δT. We proceed
to eliminate δT in terms of the other variables and a known forcing.

To first order in δ-quantities, applying the $\frac{d}{dt}$ operator (2:5) to
the temperature T gives

$$\delta\left(\frac{dT}{dt}\right) = i\sigma \, \delta T + \delta u \, \frac{1}{a} \frac{\partial}{\partial\theta} \bar{T} + \delta\eta \, \frac{\partial}{\partial x} \bar{T} \tag{2:16}$$

What is $\left(\frac{dT}{dt}\right)$? Ignoring other effects, define the solar heating
$J = T \frac{dS}{dt}$ where S is the entropy per unit mass. By making use of
the thermodynamic relation

$$dS = c_p \frac{dT}{T} - R \frac{dp}{p} = c_p \frac{dT}{T} + Rdx \qquad (2:17)$$

and by regarding T as a function of S and p only, we find

$$\frac{dT}{dt} = \left(\frac{\partial T}{\partial p}\right)_S \frac{dp}{dt} + \left(\frac{\partial T}{\partial S}\right)_p \frac{dS}{dt} = -\left(\frac{RT}{pc_p}\right) p\eta + \left(\frac{T}{c_p}\right) \frac{J}{T} \qquad (2:18)$$

$$= \eta \left(\frac{RT}{c_p}\right) + \frac{J}{c_p} \qquad .$$

Since the atmospheric heat balance is steady in the long term, averaging eq. (2:18) above must give $\bar{J} = 0$. Furthermore, to simulate the damping of the temperature variations, we introduce a Newtonian cooling term $\frac{dT}{dt} = (\bar{T}-T)/\tau$ in addition to the above, where $1/\tau$ is the Newtonian cooling coefficient, and τ is the time constant of the damping. We choose to simulate the effects of dissipation this way, not only because it is a natural model for radiative damping, but also because it is the simplest; i.e., it is the only way known to parameterize the damping which preserves the separability of the classical tidal equations without raising their order (Lindzen and McKenzie, 1967; Dickinson and Geller, 1968).

Now combining equation (2:18) with (2:16) and including Newtonian cooling allows us to rewrite the hydrostatic law (2:13) as

$$(i\sigma + 1/\tau) \frac{\partial}{\partial x} \delta\psi = (i\sigma + 1/\tau) R\delta T \qquad (2:19)$$

$$= \varkappa \delta J - \Gamma \delta \eta - \delta u \frac{1}{a} \frac{\partial}{\partial \theta} R\bar{T} \quad ,$$

where we have put $\varkappa = \frac{R}{c_p} \approx .20$ and written δJ by analogy with $\delta\psi$. We have also defined Γ, the stratification or static stability, as

$$\Gamma = \frac{\partial}{\partial x} R\bar{T} + \varkappa R\bar{T} = \varkappa \bar{T} \frac{\partial}{\partial x} \bar{S} \ . \qquad (2{:}20)$$

Note that Γ may not be negative in a stably stratified atmosphere. According to the cyclostrophic relation (2:10), Γ increases toward the equator on Venus for any realistic choice of $\omega(\theta, x)$.

D. Elimination of Variables

Now equations (2:13), (2:14), (2:15), and (2:19) constitute four coupled equations in four unknowns. Since we eliminated the φ and t dependences, we can solve (2:13) and (2:14) algebraically for δu and δv in terms of $\delta\eta$ and $\delta\psi$:

$$\delta u = -\frac{1}{\Delta} \left[i\sigma \frac{1}{a} \frac{\partial}{\partial\theta} \delta\psi + i \frac{2s\omega}{a} \frac{\cos\theta}{\sin\theta} \delta\psi + \delta\eta \, a \, \sin\theta \, \cos\theta \, \frac{\partial}{\partial x} \omega^2 \right] \qquad (2{:}21)$$

$$\delta v = \frac{1}{\Delta} \left[+ (\sin\theta \, \frac{\partial}{\partial\theta} \omega + 2\omega \cos\theta) \frac{1}{a} \frac{\partial}{\partial\theta} \delta\psi + \frac{\sigma s}{a \sin\theta} \delta\psi \right.$$
$$\left. - i\sigma \, \delta\eta \, a \, \sin\theta \, \frac{\partial}{\partial x} \omega \right] \qquad . \qquad (2{:}22)$$

Substituting (2:21) and (2:22) into (2:15) and (2:19) to eliminate δu and δv gives

$$0 = i\Lambda_1 \frac{\partial^2}{\partial\theta^2} \delta\psi + i\Lambda_2 \frac{\partial}{\partial\theta} \delta\psi + i\Lambda_3 \delta\psi + \Lambda_4 \frac{\partial}{\partial\theta} \delta\eta$$

$$\qquad (2{:}23)$$

$$- \frac{\partial}{\partial x} \delta\eta + \Lambda_5 \delta\eta$$

$$0 = (i\sigma + 1/\tau) \frac{\partial}{\partial x} \delta\psi + i\Lambda_6 \frac{\partial}{\partial\theta} \delta\psi + i\Lambda_7 \delta\psi + \Gamma_+ \delta\eta - \varkappa \delta J \qquad (2:24)$$

where we have defined the following real coefficients:

$$\Delta = -\sigma^2 + \sin\theta \cos\theta \frac{\partial}{\partial\theta} \omega^2 + 4\omega^2 \cos^2\theta$$

$$\Lambda_1 = \frac{\sigma}{a^2 \Delta}$$

$$\Lambda_2 = \frac{\sigma}{a^2} \frac{1}{\sin\theta} \frac{\partial}{\partial\theta} \left(\frac{\sin\theta}{\Delta} \right)$$

$$\Lambda_3 = \frac{2s}{a^2} \frac{1}{\sin\theta} \frac{\partial}{\partial\theta} \left(\frac{\omega \cos\theta}{\Delta} \right) - \frac{\sigma s^2}{a^2 \Delta \sin^2\theta}$$

$$\Lambda_4 = \frac{1}{\Delta} \sin\theta \cos\theta \frac{\partial}{\partial x} \omega^2 = \frac{2\omega}{a\Delta} \cos\theta \frac{\partial}{\partial x} \bar{v} \qquad (2:25)$$

$$\Lambda_5 = 1 - \frac{\sigma s}{\Delta} \frac{\partial}{\partial x} \omega + \frac{1}{\sin\theta} \frac{\partial}{\partial\theta} \left(\frac{\sin^2\theta \cos\theta}{\Delta} \frac{\partial}{\partial x} \omega^2 \right)$$

$$= 1 - \frac{\sigma s}{\Delta} \frac{\partial}{\partial x} \omega + \frac{\partial}{\partial\theta} \Lambda_4 + \frac{\cos\theta}{\sin\theta} \Lambda_4$$

$$\Lambda_6 = -\frac{\sigma}{\Delta} \sin\theta \cos\theta \frac{\partial}{\partial x} \omega^2 = -\sigma\Lambda_4$$

$$\Lambda_7 = -\frac{2s\omega}{\Delta} \cos^2\theta \frac{\partial}{\partial x} \omega^2 = -2s\omega \frac{\cos\theta}{\sin\theta} \Lambda_4$$

$$\Gamma_+ = \Gamma + -\frac{1}{\Delta} \left(a \sin\theta \cos\theta \frac{\partial}{\partial x} \omega^2 \right)^2 = \Gamma - a^2 \Delta \Lambda_4^2$$

It is interesting to examine the significance of the term $\Gamma_+ - \Gamma = -a^2 \Delta \Lambda_4^2$. This quantity, which is positive near the equator, seems to represent an added contribution to the static stability from the shear. In fact, the presence of an outward gradient of

angular momentum in a rotating fluid does help to stabilize it against convection. Yet that cannot be the significance of this term, since it vanishes at the equator while the momentum gradient does not. Rather it represents the horizontal advection of heat which is coupled to vertical motions.

Next we would like to reduce (2:23) and (2:24) to a single equation in one unknown. If $\frac{\partial}{\partial x} \omega \ll \omega$, as it is on Earth, we could separate variables in a manner parallel to the traditional theory. For example, suppose that the frequency σ (as well as ω and $\bar{v}$) depends only on colatitude θ, but that $\sigma\tau$ depends only on height x. Then Γ_+ becomes $\Gamma(x)$, Λ_5 becomes 1, and $\Lambda_4 = \Lambda_6 = \Lambda_7 = 0$, while equations (2:23) and (2:24) become

$$0 = i\Lambda_1 \frac{\partial^2}{\partial \theta^2} \delta\psi + i\Lambda_2 \frac{\partial}{\partial \theta} \delta\psi + i\Lambda_3 \delta\psi - \frac{\partial}{\partial x} \delta\eta + \delta\eta \qquad (2:26)$$

$$0 = (i\sigma + 1/\tau) \frac{\partial}{\partial x} \delta\psi + \Gamma\delta\eta - \varkappa\delta J. \qquad (2:27)$$

Differentiating (2:26) with respect to x and using (2:27) to eliminate $\delta\psi$ then yields

$$0 = \left[\Lambda_1 \frac{\partial^2}{\partial \theta^2} + \Lambda_2 \frac{\partial}{\partial \theta} + \Lambda_3 \right] \left(\frac{\Gamma\delta\eta - \varkappa\delta J}{\sigma - i/\tau} \right) + \frac{\partial^2}{\partial x^2} \delta\eta$$

$$- \frac{\partial}{\partial x} \delta\eta \qquad . \qquad (2:28)$$

Now we put

$$\delta\eta = \sum_{\ell} \delta\eta_{\ell}(x)\,\Theta_{\ell}(\theta) \qquad \text{and}$$

$$\qquad\qquad\qquad\qquad\qquad\qquad\qquad (2:29)$$

$$\delta J = \sum_{\ell} \delta J_{\ell}(x)\,\Theta_{\ell}(\theta) \qquad .$$

Then separating variables in eq. (2:28) gives for each component

$$\frac{\varkappa\delta J_{\ell}}{gh_{\ell}(1 - \frac{i}{\sigma\tau})} = \frac{d^2}{dx^2}\,\delta\eta_{\ell} - \frac{d}{dx}\,\delta\eta_{\ell} + \frac{\Gamma\delta\eta_{\ell}}{gh_{\ell}(1 - \frac{i}{\sigma\tau})} \qquad (2:30)$$

$$\frac{1}{gh_{\ell}}\,\Theta_{\ell} = \left[\Lambda_1\,\frac{d^2}{d\theta^2} + \Lambda_2\,\frac{d}{d\theta} + \Lambda_3\right]\left(\frac{\Theta_{\ell}}{\sigma}\right) \qquad , \qquad (2:31)$$

where h_{ℓ} is a constant of separation conventionally called the equivalent depth. In the traditional case, where ω and σ are constant, we may write (2:30) and (2:31) above in their more familiar forms:

$$\frac{d^2}{dx^2}\,y_{\ell} + y_{\ell}\left[\frac{\Gamma}{gh_{\ell}(1 - \frac{i}{\sigma\tau})} - \frac{1}{4}\right] = e^{-x/2}\,\frac{\varkappa\delta J_{\ell}}{gh_{\ell}(1 - \frac{i}{\sigma\tau})} \qquad (2:32)$$

$$\frac{d}{d\mu}\left[\left(\frac{1-\mu^2}{f^2-\mu^2}\right)\frac{d}{d\mu}\,\Theta_{\ell}\right] - \left(\frac{1}{f^2-\mu^2}\right)\left[\left(\frac{s^2}{1-\mu^2}\right) + \frac{s}{f}\left(\frac{f^2+\mu^2}{f^2-\mu^2}\right)\right]\Theta_{\ell}$$

$$= -\frac{4a^2\omega^2}{gh_{\ell}}\,\Theta_{\ell} \qquad\qquad (2:33)$$

where we define $y_{\ell} = e^{-x/2}\delta\eta_{\ell}$, $\mu = \cos\theta$, and $f = \frac{\sigma}{2\omega}$.

Thus we see that latitudinal gradients of the mean zonal wind do not in themselves alter the separability of the tidal theory (provided also that the lower boundary is taken at $x = 0$ instead of a sphere); this appears to be a new result. Unfortunately,

the presence of a vertical shear as on Venus prevents the separation
of the latitude and height dependences.

It is instructive to consider σ as a slowly varying function of
x; then the vertical and horizontal structure equations (2:30) and
(2:31) remain nearly valid. However, the separation "constant h_n now
varies with height roughly as $\sigma^2(x)$, according to eq. (2:31). Since
the rotation rate of the Venusian upper atmosphere is nearly 30 times
faster than the motion of the surface relative to the subsolar point, the
equivalent depth is nearly three orders of ten greater high in the
atmosphere than close to the ground. The effects of the stratification
and heating which appear in eq. (2:32) will thus be correspondingly
reduced, compared to an atmosphere rotating uniformly with height.
This interpretation is borne out by both our more rigorous
analytical and numerical solutions of the tidal equations.

In the realistic case of Venus, $\frac{1}{\omega} \frac{\partial}{\partial x} \omega$ is of order unity, so
that the "slowly varying" approximation cannot strictly be made.
Although we cannot then obtain eq. (2:28), eqs. (2:23) and (2:24)
can still be combined to yield a single exact relation in $\delta\psi$. As
long as $\Gamma_+ \neq 0$, we can invert (2:24) for $\delta\eta$:

$$\delta\eta = \frac{-1}{\Gamma_+} \left[(i\sigma + 1/\tau) \frac{\partial}{\partial x} \delta\psi + i\Lambda_6 \frac{\partial}{\partial\theta} \delta\psi + i\Lambda_7 \delta\psi - \kappa\delta J \right] \quad (2:34)$$

Substituting (2:34) into (2:23) to eliminate $\delta\eta$, multiplying by Γ_+,

and rearranging gives

$$i\Xi = \Lambda_{\theta\theta} \frac{\partial^2}{\partial\theta^2} \delta\psi + \Lambda_{xx} \frac{\partial^2}{\partial x^2} \delta\psi + \Lambda_{\theta x} \frac{\partial^2}{\partial\theta\partial x} \delta\psi$$

$$+ \Lambda_\theta \frac{\partial}{\partial\theta} \delta\psi + \Lambda_x \frac{\partial}{\partial x} \delta\psi + \Lambda_o \delta\psi \quad , \tag{2:35}$$

where we define the coefficients

$$\Xi - \Lambda_4 \frac{\partial}{\partial\theta} (\varkappa\delta J) - \Lambda_4 \left(\frac{1}{\Gamma_+} \frac{\partial}{\partial\theta} \Gamma_+\right) \varkappa\delta J + \Lambda_5 \varkappa\delta J - \frac{\partial}{\partial x} (\varkappa\delta J)$$

$$+ \left(\frac{1}{\Gamma_+} \frac{\partial}{\partial x} \Gamma_+\right) \varkappa\delta J$$

$$\Lambda_{\theta\theta} = \Gamma_+ \Lambda_1 - \Lambda_4 \Lambda_6 = \Gamma\Lambda_1$$

$$\Lambda_{xx} = \sigma - i/\tau$$

$$\Lambda_{\theta x} = \Lambda_6 - \Lambda_4 (\sigma - i/\tau) = (-2\sigma + i/\tau) \Lambda_4 \tag{2:36}$$

$$\Lambda_\theta = \Gamma_+ \Lambda_2 - \Lambda_4 \frac{\partial}{\partial\theta}\Lambda_6 + \left(\frac{1}{\Gamma_+} \frac{\partial}{\partial\theta} \Gamma_+\right) \Lambda_4 \Lambda_6 + \frac{\partial}{\partial x} \Lambda_6 - \left(\frac{1}{\Gamma_+} \frac{\partial}{\partial x} \Gamma_+\right)\Lambda_6$$

$$- \Lambda_4 \Lambda_7 - \Lambda_5 \Lambda_6$$

$$\Lambda_x = - \Lambda_4 \frac{\partial}{\partial\theta} (\sigma - i/\tau) + \Lambda_4 \left(\frac{1}{\Gamma_+} \frac{\partial}{\partial\theta} \Gamma+\right) (\sigma - i/\tau) + \frac{\partial}{\partial x} (\sigma - i/\tau)$$

$$- \left(\frac{1}{\Gamma_+} \frac{\partial}{\partial x} \Gamma_+\right)(\sigma - i/\tau) - \Lambda_5 (\sigma - i/\tau) + \Lambda_7$$

$$\Lambda_o = \Gamma_+ \Lambda_3 - \Lambda_4 \frac{\partial}{\partial\theta} \Lambda_7 + \Lambda_4 \left(\frac{1}{\Gamma_+} \frac{\partial}{\partial\theta} \Gamma_+\right) \Lambda_7 + \frac{\partial}{\partial x} \Lambda_7 - \left(\frac{1}{\Gamma_+} \frac{\partial}{\partial x} \Gamma_+\right) \Lambda_7$$

$$- \Lambda_5 \Lambda_7 \quad .$$

Now (2:35) above is the required equation in one unknown, but it is generally not separable unless $\frac{\partial}{\partial x} \bar{v} = 0$. Lindzen and Hong (1974) have developed similar equations in altitude coordinates, including mean zonal winds and latitudinal temperature gradients, and used a finite-difference scheme to calculate tides

in the Earth's atmosphere. It is doubtful

whether such an approach could be applied directly to Venus,

with its regions of small or vanishing stratification where eq. (2:34)

does not apply. This difficulty might possibly be overcome by

integrating the finite-difference forms of (2:23) and (2:24)

simultaneously. In chapter 5 and 6 we shall describe two simpler

methods of predicting the general features of atmospheric tides on Venus.

E. Boundary conditions.

If $s \neq 0$, the solutions for $\delta\psi$ and $\delta\eta$ must vanish at the

poles, so that the tidal fields are continuous there (but not

necessarily differentiable). When $s = 0$, continuity is assured

so we may impose a condition of zero gradient at the poles. In

the separable case these conditions combined with the

horizontal structure equation (2:31) or (2:33) form a

Sturm-Liouville type problem. Its solution set consists

of the eigenfunctions $\theta_{\ell}^{\sigma,s}$ (called Hough modes when σ is

constant), with their associated eigenvalues $h_{\ell}^{\sigma,s}$.

Any function of colatitude can be represented in terms

of the complete set of Hough modes; thus both the forcing

and the tidal fields may be represented as eigenfunction

expansions in colatitude when separation of variables is

employed.

We must also impose boundary conditions on the vertical

structure of the tidal fields. In our coordinate system, the

vertical velocity w may be written

$$\delta w = \delta \left(\frac{dz}{dt} \right) = \frac{\partial}{\partial t} \, \delta z + \frac{\delta u}{a} \, \frac{\partial}{\partial \theta} \, \bar{z} + \delta \eta \, \frac{\partial}{\partial x} \, \bar{z} \tag{2:37}$$

$$= i\sigma \, (\delta \psi - \delta \Omega)/g + \delta u \, \frac{a}{g} \, \sin\theta \, \cos\theta \left(\omega^2 - \omega_o^2 \right) + H \, \delta\eta,$$

where $H = R\bar{T}/g = \frac{\partial}{\partial x} \, \bar{z}$ is defined as the scale height.

In the classical case, when $h_\ell \neq \infty$, this becomes

$$\delta w = H\delta\eta + h_\ell \left[\frac{d}{dx} \, \delta\eta - \delta\eta \right]. \tag{2:38}$$

Since the air must not flow through the planet's surface,
we shall require

$$w = \frac{dZ}{dt} \tag{2:39}$$

at the ground,   where Z is the height of the gravitational
tide raised in the crust. To first order, condition (2:39)
can be applied at z = 0, or at $\bar{z}$ = 0, instead of at z = Z;
since eq. (2:9) shows that $\bar{z}$ (θ, x = 0) is on the order of a
meter for Venus, condition (2:39) can even be applied at
x = 0 with comparable accuracy.

The upper boundary condition is much more subtle. Since
the tidal equation (2:36) is of complex or position-dependent type,
the familiar variety of conditions do not apply. First of
all, we demand that the energy density in the tidal fields
remains bounded as height increases indefinitely. (Siebert
(1961) further requires the total kinetic energy to be bounded,
but for practical purposes these are the same.) When this is not
sufficient, we shall apply the radiation condition, also
called the outgoing wave condition: at great heights the tidal

waves must carry a non-negative upward flux of energy, or in other words, their group velocities must have a non-negative upward component. This simulates the effects of dissipative processes which become important at very high altitudes, such as viscosity, thermal conductivity, radiation, and nonlinear effects. For a uniformly rotating atmosphere with constant stratification and negligible forcing above some level, the radiation condition is equivalent to requiring the tidal fields to vary as $e^{(1/2 + i\lambda)x}$, where λ is a positive constant (Wilkes, 1949). In comparison, the boundedness condition demands that $e^{-x/2} \delta\eta \to 0$ as $x \to \infty$. The former may be obtained from the latter by retaining the damping $1/\tau$ in the solution, applying the condition of boundedness, and finally neglecting the damping. Instead of the usual "rigid" lower boundary condition, it might be appropriate to apply an analogous "ingoing" wave or boundedness condition in the event that there is no solid surface, or if the lower boundary is very remote from the region of forcing, as is the case for thermal tides in the Jovian planets.

Finally, the boundedness condition sometimes permits the existence of nonzero solutions, or free oscillations, even when the forcing terms δJ and $\delta\Omega$ vanish. While such phenonmena, possibly including baroclinic instability or the like, may play some role in maintaining the basic state of the Venus

atmosphere, we shall assume that all free solutions either are damped out or else do not interact with the tidal fields.

3. Model Atmospheres

In this chapter we shall develop simple analytic models for the basic state of the Venus atmosphere, which are needed for the numerical and analytical exploration of the tides.

On the basis of stratification, the atmosphere is divided into a troposphere and a stratosphere. These two regions are separated by the tropopause, which generally slopes with latitude in the presence of a vertical shear. Numerical calculations for the Earth's atmosphere suggest that such sloping interfaces reduce interference effects among the tidal waves, and eliminate the sensitivity of the surface pressure variation to details of the basic state (Lindzen and Hong, 1974). Furthermore, since we intend to study tides mainly near Venus' equator, where the slope vanishes, for our purposes we may take the tropopause at a constant pressure level $p = p_t \approx 600$ mb, or $x = x_t \approx 5.0$, corresponding roughly to the bottom of the cloud deck at an altitude of $z = z_t \approx 50$km.

The Venera 8, 9, and 10 data on zonal wind speed versus altitude are presented in Fig. 3 (Keldysh, 1977). The Venera 9 and 10 speeds level off at about 60 m/s, while the Venera 8 velocities exceed 100 m/s at the top; the difference may reflect temporal variations. In our models we shall adopt an intermediate value of 90 m/s in the stratosphere, corresponding to the ultraviolet cloud motions observed by Mariner 10 (Suomi, 1974).

Figure 3

Zonal wind speed as a function of altitude

Figure 4

Top: Entropy versus pressure

Bottom: Stratification versus pressure

Figure 5

Temperature versus altitude

Figure 6

Pressure p or height x as a function of altitude z
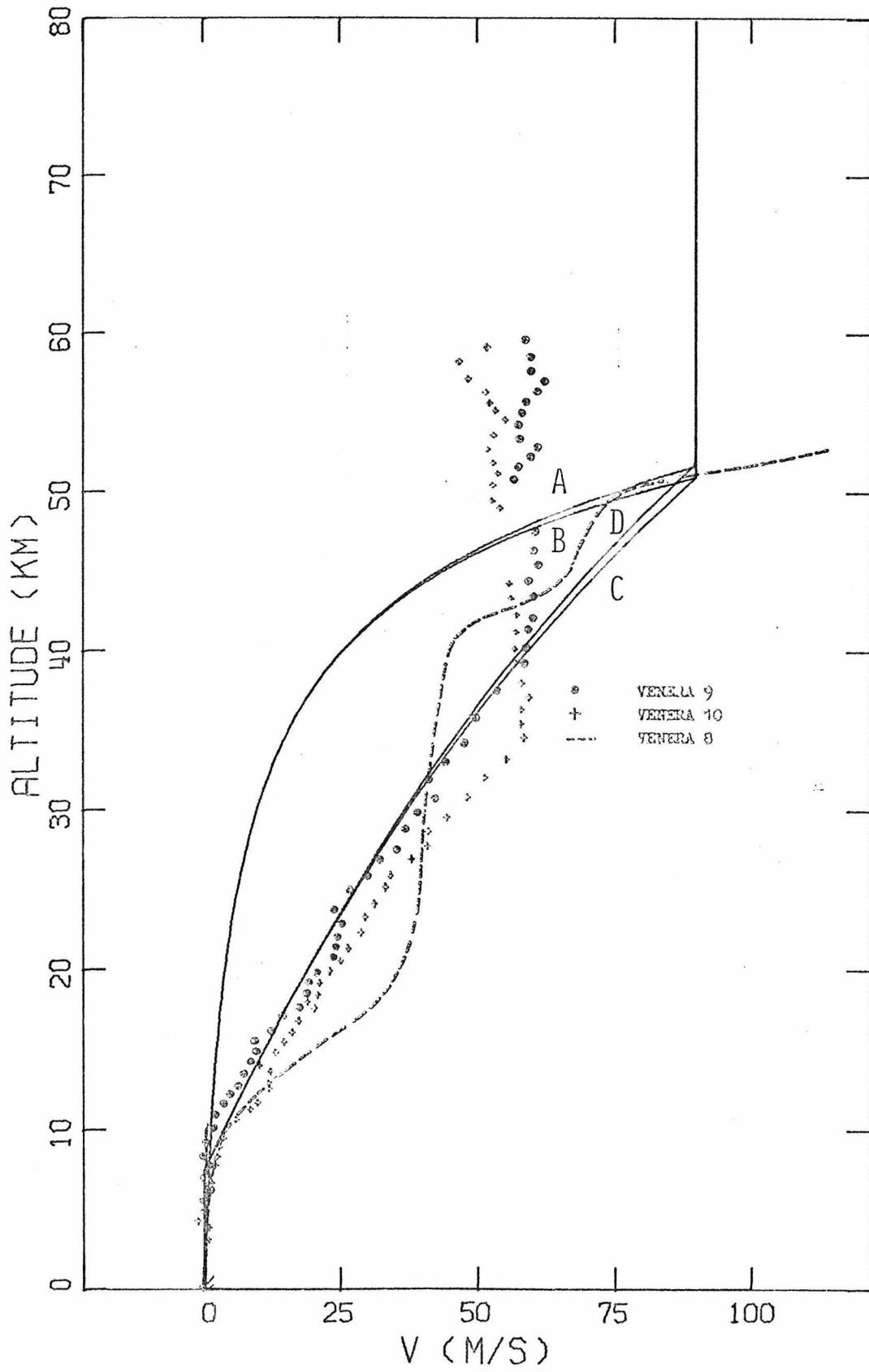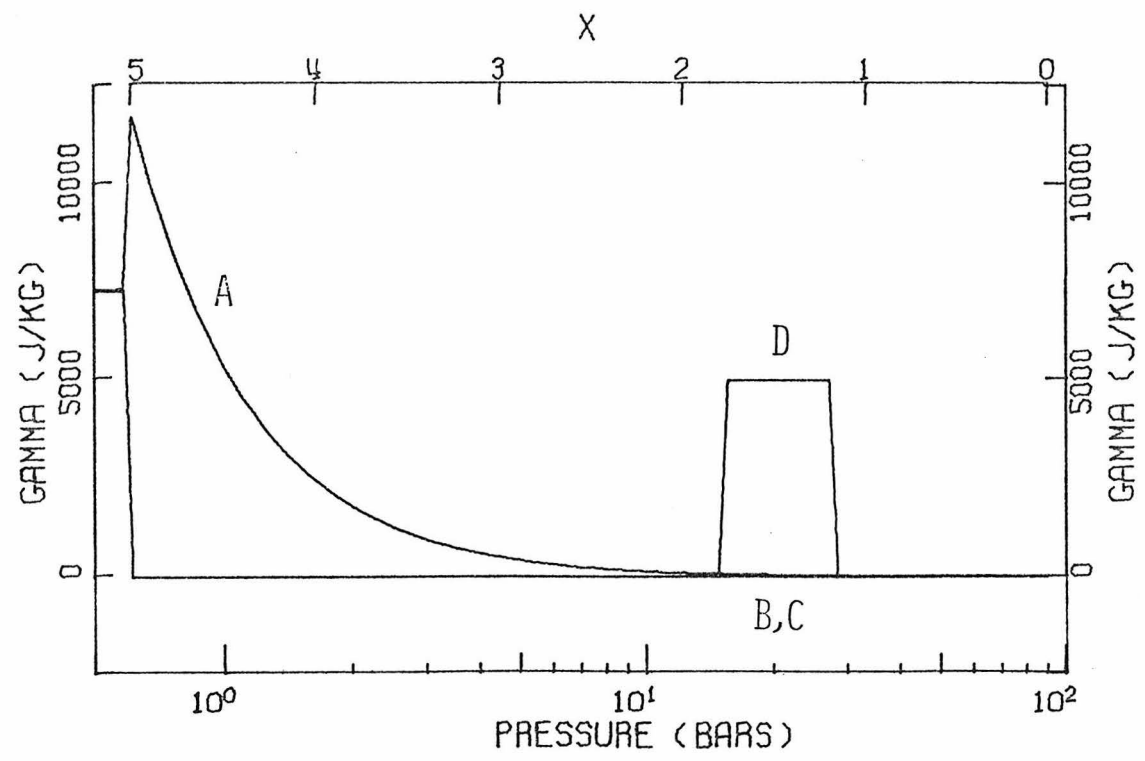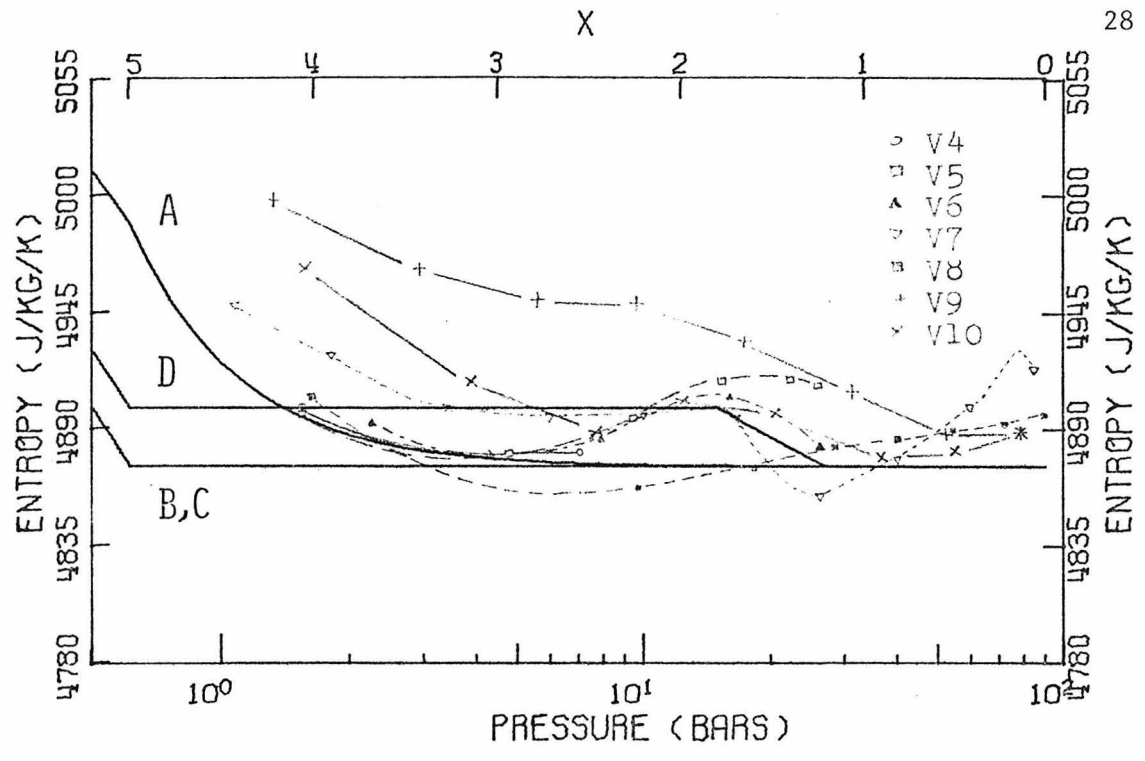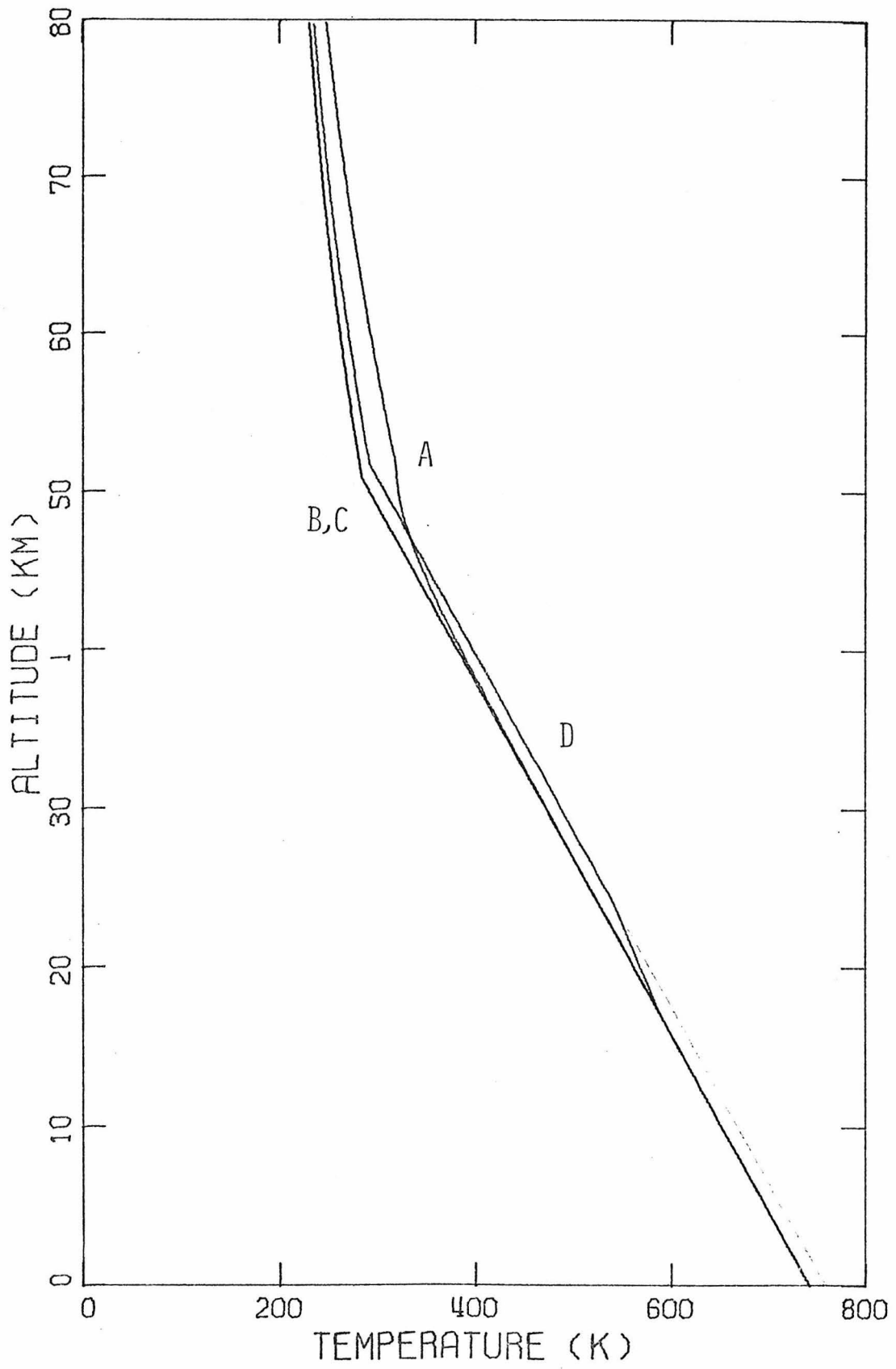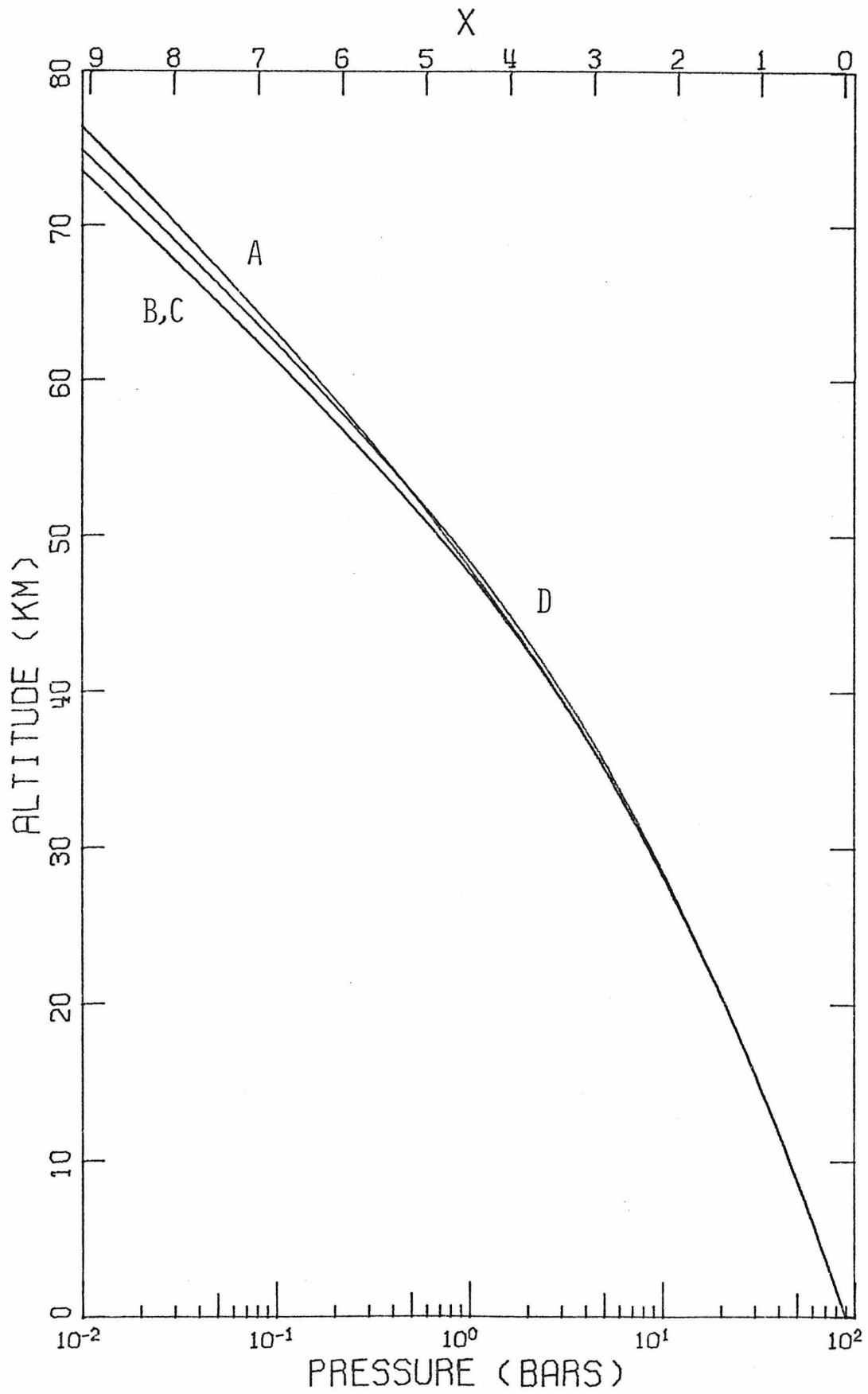
With this alteration, the Venera probe data are fitted
fairly well by a mean wind profile which vanishes in the bottom half
scale height, is constant in the stratosphere, and linear
in x in between. Stated analytically, this model becomes

$$\bar{v} = 0, \qquad x \leq .5$$

$$\bar{v} = \left(\frac{x - .5}{x_t - .5}\right) \cdot 90 \text{ m/s} \qquad , \qquad .5 < x < x_t \qquad (3:1)$$

$$\bar{v} = 90 \text{ m/s} \qquad , \qquad x \geq x_t \quad .$$

This model is graphed in Fig. 3 as the curves labeled C and D;
the slight difference is due to a minor change in the scale of
altitude versus pressure.

The linear dependence of $\bar{v}$ on x adopted above is fairly
realistic for use in the numerical computations, but it is not
convenient for studying the tides analytically. We shall be
able to simplify the mathematical analysis considerably by
use of an "exponential wind" model:

$$\omega = \omega_o \, e^{fx} \quad \rightleftarrows \quad \bar{v} = a \, \omega_o \, (e^{fx} - 1) \quad , \qquad x < x_t \; ;$$

$$\omega = \omega_o \, e^{fx_t} = \omega_\infty \quad \rightleftarrows \quad \bar{v} = a \, \omega_o \, (e^{fx_t} - 1) = 90 \text{ m/s} \, , \qquad (3:2)$$

$$x \geq x_t; \; f \approx .785$$

This alternative wind profile is depicted in Fig. 3 by the
curves labeled A and B.

We also require models of the static stability profile
$\Gamma(x)$. In order to simplify the upper boundary condition,
it suffices to take $\Gamma(x) = \Gamma_\infty = \text{constant} \approx 7560$ J/kg in

the stratosphere, corresponding to an asymptotic temperature

$$T_\infty = \frac{\Gamma_\infty}{\mu R} \approx 200K.$$

If the troposphere were strictly adiabatic, as in a vigorously convecting atmosphere, we should put $\Gamma = 0$, as represented by the horizontal line labeled B,C in Fig. 4 (bottom). However, the Russian entropy measurements (Marov et al., 1973; Keldysh, 1977) presented in Fig. 4 (top) suggest the presence of a stably stratified layer near the twenty-bar level; accordingly we define the following alternative model for the static stability in the atmosphere of Venus:

$$
\begin{aligned}
\Gamma &= 0 \ , & x &< 1.2 \\
\Gamma &= 5000 \ J/kg \ , & 1.2 &< x < 1.8 \\
\Gamma &= 0 \ , & 1.8 &< x < x_t \\
\Gamma &= \Gamma_\infty \ , & x &> x_t
\end{aligned}
\qquad (3:3)
$$

The stratified layer is labeled D in Fig. 4.

Again, the above profile is not convenient for solving the tidal equations analytically. Along with the exponential wind, eq. (3:2), it is convenient to adopt an exponential stratification

$$
\begin{aligned}
\Gamma &= \Gamma_0 \ e^{2fx} \ , & x &< x_t \\
\Gamma &= \Gamma_\infty \ , & x &> x_t
\end{aligned}
\qquad (3:4)
$$

where Γ_0 may have any value greater than or equal to zero. Yet if the cyclostrophic relation (2:10) applies, the minimum stratification must occur at the poles. Assuming that the

troposphere is strictly adiabatic at the poles (and that the circulation period is not strongly dependent on latitude) then gives a lower limit on Γ_o at the equator:

$$\Gamma_o \approx (2f^2 + \varkappa f) \; \alpha^2 \; \omega_o^2 \approx 4.5 \; \text{J/kg} \qquad . \qquad (3:5)$$

The corresponding profile is plotted as curve A in Fig. 4 (bottom).

For the numerical calculations, we shall use four different models for the mean state of the Venus atmosphere;

model A, defined by eqs. (3:2) and (3:4);

model B, described by eq. (3:2) with $\Gamma = 0$

in the troposphere;

model C, described by eq. (3:1) with $\Gamma = 0$

in the troposhere; and

model D, defined by eqs. (3:1) and (3:3)   .

Only models A and B, based on the exponential wind profile, will be used to study the tides analytically.

Of course, each model of the stratification corresponds to a certain distribution of temperature, pressure, and entropy, which may be found by integrating eq. (2:2). We have chosen $\bar{T}_o = 750$ K at the ground. Average temperature is shown as a function of altitude by the solid lines in Fig. 5, while Fig. 6 may be regarded as giving the conversion between altitude z and pressure p, or the height coordinate x. The entropy profile corresponding to each model

is plotted in Fig. 4 (top) for ease of comparison with the
Venera data. The data do not enable us to chose among these
several models at present, although the upcoming Pioneer and
Venera spacecraft missions should help further to constrain
the picture of the Venus atmosphere.

4. The Distribution of Heating

Once the basic state of the atmosphere has been defined,
we need to specify the forcing function. Atmospheric tides
driven by the gravitational influence of the sun are treated
in a later chapter, and have little effect on the net torque.
In this chapter we are concerned with the thermal forcing of
atmospheric tides.

A. Absorption of sunlight in the atmosphere

At the subsolar point, Venus receives a solar flux of about
2600 W/m^2, but it only absorbs 600 ± 180 W/m^2 (Irvine, 1968).
Of this, about 100 W/m^2 is absorbed by the ground
(Avduevskii et al., 1976a),so that about 500 W/m^2 must be absorbed
directly in the atmosphere and cloud layers.

The total flux absorbe F is related to the solar heating
rate per unit mass J through

$$F = \int_o^\infty J\frac{}{\rho}\ dx = \int_0^{Po} J\ \frac{dp}{g} = \int_0^\infty J\ \frac{p}{g}\ dx = \frac{Po}{g}\ \int_0^\infty J\ e^{-x}\ dx. \quad (4:1)$$

Lacis (1975) has modeled heating rates in the atmosphere of
Venus, using both ground-based observations and Venera 8
entry probe measurements. Concerning the day side, he
concludes (Lacis, 1975): "Above $\sim$ 20 mb ($x \approx 8.4$), the
heating rates are nearly the same over the whole sunlit
hemisphere... In the deep atmosphere the ratio of heating
rates remains constant and is roughly proportional to the cosine
of solar zenith angle." Naturally, the insolation vanishes

on the night side of the planet. Combined, these statements can
be expressed as follows:

$$J = J_\odot (x) \cos \zeta \quad \text{if } \cos \zeta > 0 \qquad ,$$

$$J = 0 \qquad \text{if } \cos \zeta \leq 0 \qquad ,$$

(4:2)

where ζ is the solar zenith angle and $J_\odot (x)$ is the vertical
profile of the heating rate at the subsolar point. On the
other hand, comparison of the Venera 8, 9, and 10 measurements
(Avduevskii et al.,1973; Avduevskii et al., 1976a) suggests that
the illumination varies roughly as $(\cos \zeta)^{1.5 \sim 2}$ below the
cloud deck. For simplicity's sake we shall assume that the
heating has the horizontal structure described by (4:2) above.
While more elaborate models are possible, the results would
be affected only slightly, as discussed in chapter 4 of Part II.

Now we need to express the forcing (4:2) in terms
periodic in longitude and time. Suppose that the obliquity
of Venus is $180° - \beta'$, where β' is a small angle between the
equator and orbit planes (two or three degrees, according
to the radar studies of Shapiro et al., 1978).To first order
in β' (and neglecting the small eccentricity of Venus' orbit),
the longitude $\varphi_\odot$ of the subsolar point decreases uniformly
with time, while its latitude $\frac{\pi}{2} - \theta_\odot$ varies sinusoidally over
an orbit:

$$\varphi_\odot = \omega_o t - nt \quad , \quad \theta_\odot = \frac{\pi}{2} + \beta' \sin nt \quad , \qquad (4:3)$$

where both time and longitude are measured from the northern
vernal equinox. This small-obliquity approximation will be

made exact in Part II. Then we find for the cosine of the solar zenith angle

$$\cos \zeta = \sin \theta \cos (\varphi - \varphi_\odot) - \beta' \cos \theta \sin nt \quad . \qquad (4:4)$$

However, when it is half-rectified as (4:2) requires, we find to first order in β'.

$$\left\{ \begin{array}{c} \cos \zeta \text{ if } \cos \zeta > 0 \\ 0 \text{ otherwise} \end{array} \right\} = \sin \theta \cdot \left\{ \begin{array}{c} \cos (\varphi - \varphi_\odot) \text{ if } \cos (\varphi - \varphi_\odot) > 0 \\ 0 \text{ otherwise} \end{array} \right\}$$

$$- \beta' \cos \theta \sin nt \cdot \left\{ \begin{array}{c} 1 \text{ if } \cos (\varphi - \varphi_\odot) > 0 \\ 0 \text{ otherwise} \end{array} \right\}$$

$$= \sin \theta \left[\frac{1}{\pi} + \frac{1}{2} \cos (\varphi - \varphi_\odot) + \frac{2}{3\pi} \cos (2\varphi - 2\varphi_\odot) - \frac{2}{\pi} \sum_{\substack{s = 4, \\ \text{even}}}^{\infty} \right.$$

$$\left. \frac{(-1)^{s/2}}{s^2 - 1} \cos (s\varphi - s\varphi_\odot) \right] \qquad (4:5)$$

$$- \beta' \cos \theta \left\{ \sin nt + \frac{1}{\pi} \sin (\varphi - \omega_\odot t - 2nt) + \frac{1}{\pi} \sin (\varphi - \omega_\female t) \right.$$

$$+ \frac{1}{\pi} \sum_{\substack{s = 3, \\ \text{odd}}}^{\infty} \frac{(-1)^{\frac{s-1}{2}}}{s} \left[\sin (s\varphi - s\omega_\female t - (s + 1) nt) \right.$$

$$\left. \left. + \sin (s\varphi - s\omega_\female t - (s - 1) nt) \right] \right\} \quad .$$

Note that when $\beta' = 0$ in (4:4), the heating rates are symmetrical with respect to the equator, while the presence of β' introduces an antisymmetrical part. Except for the diurnal ($s = 1$) terms we also note that all the even values of s arise from the symmetrical part, while all the odd wavenumbers arise from the antisymmetrical forcing; however, this is an artifact of the simple horizontal structure (4:2) assumed.

The first term of the expansion (4:5) does not vary with time. Since the insolation cannot of course be negative, $\frac{1}{\pi} \sin \theta$ is simply the average of the heating, relative to the subsolar value. This steady energy input must be carried away by internal processes (such as the Newtonian cooling term $1/\tau$) and ultimately reradiated to space; thus in setting $\bar{J} = 0$ we may remove the first term from (4:5).

The equivalent gravity mode approach applied in a later chapter also requires us to express both the forcing and response in terms of spherical surface harmonics. The terms $\sin \theta \cdot 1/2 \cos (\varphi - \varphi_\odot) - \beta' \cos \theta \sin nt$ in (4:5) are already in the proper form, since $\sin \theta = P_{1,1} (\cos \theta)$ and $\cos \theta = P_{1,0} (\cos \theta)$ are suitable Legendre functions. In all other cases, the latitude distributions $\sin \theta$ and $\cos \theta$ must be decomposed into Legendre functions of different order s. For the semidiurnal component, the leading term is

$$\frac{15}{64} \sin^2 \theta \cos (2\varphi - 2\varphi_\odot) \qquad , \qquad (4:6)$$

while the leading term of the antisymmetric diurnal component is

$$- \beta' \frac{15}{32} \sin \theta \cos \theta \left\{ \sin (\varphi - \omega_{\venus} t - 2nt) + \sin (\varphi - \omega_{\venus} t) \right\} . \quad (4:7)$$

Both expressions (4:6) and (4:7) above represent spherical harmonics of the second degree ($\ell = 2$). None of the other components contribute second degree terms (because $1 \geq s$), and since only second degree harmonics are capable of producing a substantial torque, we need not consider any higher order terms.

The distribution of heating with height is not well
known, so we shall use a combination of the simple models
depicted in Fig. 7. Here the horizontal scale is logarithmic
in $J_\odot$ (x), the heating rate per unit mass at the subsolar
point. The vertical scale is linear in x, or logarithmic in
pressure p, in order to avoid complications due to slight
differences in the relation between pressure and attitude z.
Each of the profiles in this figure is normalized using eq.
(4:27) so that the total insolation F absorbed at the subsolar
point is 500 W/m^2 for models I, II, and III, but is 100 W/m^2
for the rest.

The profile labeled I in the figure represents a uniform
heating per unit mass above the nominal level of the cloud tops,
$x = x_a \approx 7.5$ or $p \approx 50$ mb. When normalized using (4:1), this
model becomes

$$\delta J = \delta F \; \frac{g}{P_o} e^{x_a} \quad , \qquad x > x_a \qquad\qquad (4:8)$$

$$\delta J = 0 \qquad\qquad , \qquad x \leq x_a$$

where δJ denotes a complex Fourier component of the total flux

absorbed in this manner. This profile corresponds to the
absorption of sunlight in an optically thin atmosphere above
a reflecting layer: if the clouds are not perfectly reflecting,
this model can be linearly combined with one or more of the others.

Model II is a delta function representing the absorption
of energy within the cloud layer itself, presumed to be

Figure 7

Heating rate J as a function of height x or pressure p at the subsolar point for several models of the thermal forcing in the Venus atmosphere. The upper scale gives $J/c_p \approx J/(945\ J/kg/K)$ in degrees Kelvin per day (86400 seconds). The upper profiles I, II, and III are each normalized to a total absorption of 500 W/m^2, while the lower profiles IV, V, and VIII are each normalized to 100 W/m^2. The twinning of profiles IV and V is related to differences in the mean zonal wind models and is explained in the text.
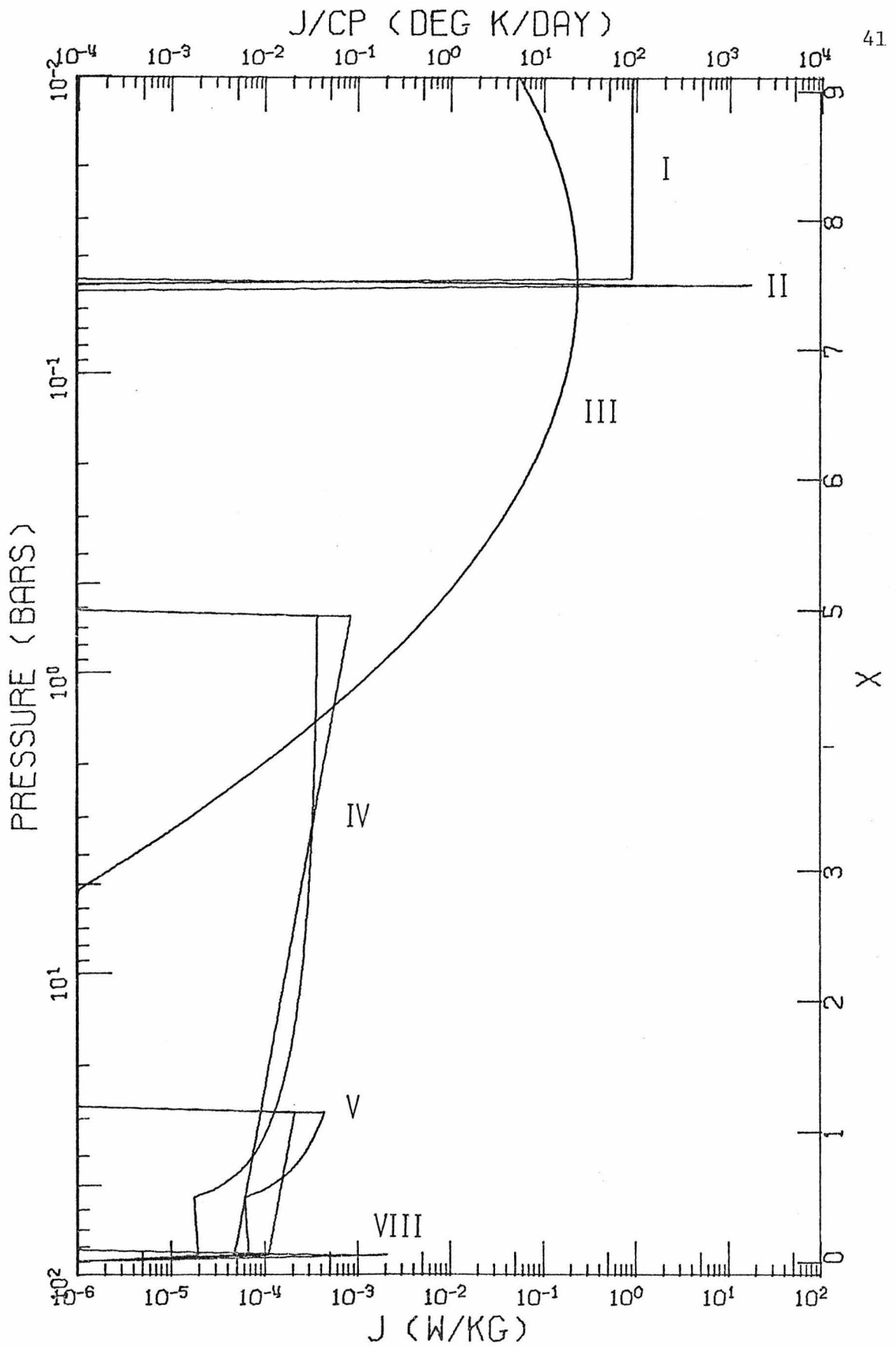
optically dense. Normalized, this may be written

$$\delta J = \delta F \ \frac{g}{P_o} \ e^{x_a} \ \delta \ (x - x_a) \ , \qquad (4:9)$$

where the latter δ- symbol must not be confused with a complex

variation quantity.

The curve labeled III in the figure represents a broader, more

realistic distribution of absorption in the clouds. We have

approximated the (inhomogeneous cloud) model calculations of

Lacis (1975) by a Gaussian heating profile. The distribution

peaks at the nominal level of cloud type ($x = x_a$) and has a

full width at half-maximum of $\sim$ 2.2 scale heights ($\sim$12 km);

when normalized, this can be written

$$\delta J(x) = \delta J(x_a) e^{- \frac{(x-x_a)^2}{1.75}} \ ;$$

$$\qquad (4:10)$$

$$\delta J(x_a) \approx 500 \ \frac{g}{P_o} \ \delta F \ \text{if} \ x_a \approx 7.5 \ .$$

Note that a Gaussian distribution appears as a parabola,

since Fig. 7 is a semi-logarithmic plot.

The remaining heating profile represents the redistribution

of heat absorbed by the ground, and will be described in

the remainder of this chapter.

B. A diffusive thermal boundary layer

The insolation absorbed by the ground also drives atmospheric tides, by means of heat exchange between the surface and the atmosphere. This is of course a subject of tremendous complexity, but we begin by analogy with the thermal boundary layer on Earth. In the following, we treat heat transport in the lower atmosphere of Venus as a process of diffusion.

After Chapman and Lindzen (1970), we set $\Gamma = 0$ and $\frac{\partial}{\partial \theta} R\bar{T} = 0$ in the heat equation (2:20), so that advection of heat is neglected. We then replace the source term $\varkappa\delta J$ by the vertical gradient of the diffusive heat flux, so that analogous heat diffusion equations apply in the atmosphere and in the soil:

$$i\sigma\,\delta T = \frac{1}{\bar{\rho}c_p}\frac{\partial}{\partial z}\left(K_a\frac{\partial}{\partial z}\delta T\right) = \frac{1}{\bar{\rho}c_p H}\frac{\partial}{\partial x}\left(\frac{K_a}{H}\frac{\partial}{\partial x}\delta T\right)\ ,\ z > 0;$$

$$i\sigma_{\rho}\,\delta T = \frac{1}{\rho_b c_b}\frac{\partial}{\partial z}\left(K_b\frac{\partial}{\partial z}\delta T\right)\qquad,\qquad z < 0\ .\qquad (4:11)$$

Here K_a and K_b are respectively the thermal conductivities of the lower atmosphere and of the ground, ρ_b is the density of the soil, and c_b is its specific heat capacity. In general, all of the parameters in eq. (4:11) above may vary with height, but for the sake of simplicity, we shall treat as constant the quantities K_a/H, $\sigma\bar{\rho}c_p H$, K_b, and $\sigma_{\rho}\rho_b c_b$; this is

tantamount to taking $K_a \propto 1/T \propto e^{\mu x}$ while $\sigma \propto 1/p \propto e^x$.

When we add the boundary condition that δT must be continuous at the surface $z = 0$, and must vanish at $z = \pm\infty$, the solution to (4:11) becomes a complex exponential function of height:

$$\delta T = \delta T_o \; e \; -(1 + i) \left(\frac{H_a}{D_a}\right) x \qquad , \qquad z > 0 \qquad ;$$

$$\delta T = \delta T_o \; e \; (1 + i) \; z/D_b \qquad , \qquad z < 0 \qquad , \tag{4:12}$$

where we have defined the constants

$$D_a = \sqrt{\frac{2K_a}{\sigma_o \bar{\rho}_o c_p}} \qquad \text{and} \qquad D_b = \sqrt{\frac{2K_b}{\sigma_\varphi \rho_b c_b}} \tag{4:13}$$

as the thermal skin depths in the atmosphere and soil, respectively. The atmospheric temperature variation from (4:12) above is graphed in Fig. 8, where the solid curve represents the real part and the dashed curve shows the imaginary part.

Figure 8

Temperature variation versus height

for a diffusive thermal boundary layer
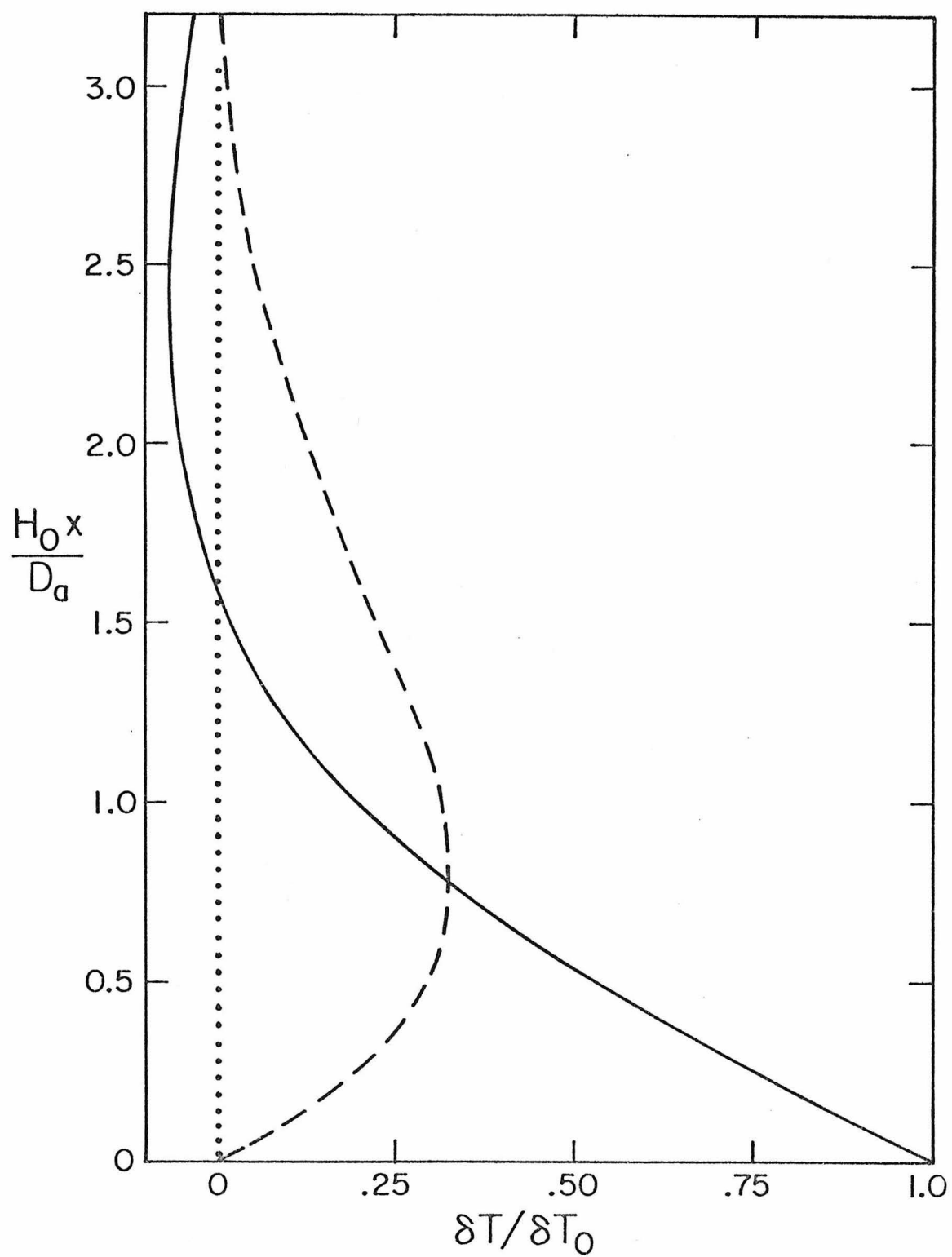
We also impose the condition that there is no net flux into the interface $z = 0$. This completes the solution by relating the surface temperature δT_o to the insolation δF absorbed by the ground:

$$\delta F = K_b \left[\frac{\partial}{\partial z} \delta T \right]_{0^-} - K_a \left[\frac{\partial}{\partial z} \delta T \right]_{0^+} \tag{4:14}$$

$$\rightarrow \delta T_o = \delta F \left(\frac{1 - i}{2} \right) \left(\frac{K_a}{D_a} + \frac{K_b}{D_b} \right)^{-1} \quad .$$

Note that both terms δT_o in (4:14) above have the same phase, so that the transfer of heat from the ground to the atmosphere is effectively instantaneous.

We proceed to estimate the values of these parameters appropriate to the lower atmosphere of Venus. The thermal conductivity due strictly to molecular diffusion would be on the order of 10^{-6} W/m/K vastly less efficient than other atmospheric processes. It may be that the dominant heat transfer mechanism in the thermal boundary layer is radiative; in an optically dense medium, radiative transfer reduces to a process of diffusion, with an effective thermal conductivity of

$$K_a \approx \frac{4}{3} (4 \sigma_{SB} \bar{T}_o^3) \bar{\ell} \approx 124 \text{ W/m}^2/K \cdot \bar{\ell}$$

(Goody, 1964), where σ_{SB} is the Stefan-Bolzmann constant, and $\bar{\ell}$ is the photon mean free path (the mean inverse of the absorption coefficient). The lower atmosphere of Venus contains about 0.1% water vapor (Moroz et al., 1977), so that $\bar{\ell}$ is probably on the order of 100 meters (Avduevsky et al.,

1970: Kuzmin and Marov, 1975). This leads to a thermal conductivity on the order of 10^4 W/m/K, corresponding to a skin depth of roughly 800 m.

This estimate of the conductivity is really a lower limit, since turbulent mixing may be the dominant heat transport process in the lower atmosphere of Venus. The thermal conductivity due to eddy diffusion is on the order of 10^4 W/m/K on Earth (Kuo, 1968), but eddy transport may be vastly more efficient on Venus, where the troposphere is about 50 times denser and nearly adiabatic. The competition between turbulence and radiative transfer fortunately does not complicate the problem; if eddy diffusion contributes a thermal conductivity K_E greater than the effective radiative conductivity K_R, Goody (1960) has shown that to lowest order in K_R/K_E, the results are just the same as if only the eddy contribution were present.

For typical surface materials, we estimate $K_b \approx 10$ W/m/K and $\rho_b c_b \approx 3 \times 10^6$ J/m^3/K, so that the thermal skin depth in the ground is about 3.3 m for the diurnal wave. We then find $\frac{K_b}{D_a} \approx 3$ W/m^2/K, while $\frac{K_a}{D_a} \gtrsim 15$ W/m^2/K. These remain in the same ratio for all frequencies, so that we are justified in neglecting the heat capacity of the soil relative to the atmosphere in eq. (4:14). This proves that effectively all of the heat

absorbed by the ground is immediately deposited at the bottom of the atmosphere. We can also estimate that daily temperature variations at the surface of Venus should not exceed a few degrees:

$$\delta T \approx \delta F \; (\frac{1 - i}{2}) \; (D_a/K_a) \leqslant (1 - i) \times 1.7 \; K \qquad (4:16)$$

for the diurnal component.

Following Chapman and Lindzen (1970), we regard the heating function J as derivable from the temperature field (4:12) by means of the heat equation (2:20), even when advection is not neglected:

$$\delta J = c_p i \sigma \delta T = \delta J_o \; (\frac{\sigma}{\sigma_o}) e^{-(1 + i)} \; (\frac{H_o}{D_a}) \; x \qquad (4:17)$$

While Chapman and Lindzen (1970) made the above substitution in altitude coordinates, it is more valid when expressed in isobaric coordinates like ours. However, substituting δT_o from (4:14) directly into (4:17) above is inexact because the solution was obtained effectively by assuming $\sigma = \sigma_o e^{x}$. Since the vertical form of δJ depends on the frequency as a function of height, δJ_o in (4:17) must be renormalized using eq. (4:1) for each model of the mean zonal winds.

We shall use the heating distribution (4:17) above to represent the effects or thermal diffusion in our numerical and analytical calculations despite the restriction mentioned above.

We define heating models VI and

VII with thermal conductivities K_a of 10^8 and 10^7 W/m/K

respectively, corresponding to thermal skin depths of roughly

4.4 and 1.4 scale heights for the diurnal wave according to

eq. (4:13). These are not shown in Fig. 7 for the sake of clarity.

Conductivities on the order of 10^6 W/m/K or less correspond

to shallow skin depths. Since the surface pressure cannot

respond to the fine structure of the forcing, a small conductivity

can be represented by a delta-function heating introduced just

above the ground. The "heating at the ground model" is written

$$\delta J = \delta F \frac{g}{p_o} \delta (x - 0^+) \qquad (4:18)$$

and is labeled profile VIII in Fig. 7.

On the other hand, the temperature gradient at the ground

is

$$\frac{\partial}{\partial z} \delta T_o = - \delta F/K_a \qquad . \qquad (4:19)$$

A thermal conductivity K_a less than about 10^5 W/m/K is thus

liable to drive the lapse rate unstable with respect to

convection. This possibility is discussed more fully in the

next section.

51

C. A simple approach to convection

Consider an atmosphere which is strictly isentropic up to some level $x = x_c$, and stably stratified above. Adding heat in a thin layer at the bottom would produce an unstable, superadiabatic temperature gradient. Buoyancy-driven convection would set in, and heat would rapidly be transported upwards, until an adiabatic lapse rate were re-established up to roughly the original height x_c. The stably stratified layer above the convective region would act as a lid to any further heat transport. If heat were then removed from the top of the convective zone, the entire process of readjustment would be reversed. This visualization suggests that the major effects of convection can be modeled simply by shifting an adiabat up and down on a plot of T (z), as the dashed line in Fig. 5 demonstrates. That sketch is exaggerated, though, since the total insulation absorbed by the ground over a Venus day would be able to raise the temperature of the bulk of the atmosphere by only about a tenth of a degree. This approach resembles Gierasch and Goody's (1968) treatment of the Martian thermal boundary layer, which was adapted by Zurek (1975) to study atmospheric tides on Mars.

In our isobaric coordinate system, the shifting adiabats described above are defined by

$$\bar{T} = \bar{T}_0 \, e^{-\varkappa x}, \quad \delta T = \delta T_0 \, e^{-\varkappa x}, \quad x \lesssim x_c. \tag{4:20}$$

As in the previous section, the heat equation (2:20)
allows us to represent convection approximately by a special
heating distribution;

$$\delta J = (i\sigma + i/\tau)\ c_p\ \delta T = (i\sigma + 1/\tau)\ c_p\ \delta T_o e^{-\varkappa x}. \qquad (4:21)$$

This type of forcing is illustrated in Fig. 7 by the profiles
labeled IV and V; the tops of the convective layers are chosen
so as to coincide with the levels of stable stratification of
$x_c = 5.0$ and $x_c = 1.2$ respectively, as suggested by the static
stability profile shown in Fig. 4 (bottom). Since the
convective heating rate (4:21) depends on the forcing frequency,
two curves are shown in Fig. 7 for each convective model;
the straight profiles correspond to the "exponential wind"
model (3:2) of the basic state, while the curves with kinks
at $x = 0.5$ are related to model (3:1) of the mean wind.
For the purpose of presentation, these curves are drawn for
$1/\tau = 0$ and an obliquity of exactly 180° ($\beta' = 0$), so that
all of the component frequences are multiples of $(\omega + n)$
and these have the same dependence on height. This restriction
does not apply to the numerical calculations. Finally each of
the profiles IV through VIII shown in Fig. 7 is normalized by
numerical integration of (4:1) to comprise 100 w/m^2, the total
insolation absorbed by the ground at the subsolar point.

It is worth remembering that the technique developed above
is a linear means of dealing with a fundamentally nonlinear

process. Convective instability may also be tied to other types of instabilities and to nonlinear phenomena beyond the scope of the tidal theory. Naive though this approach may be, it is adequate to its purpose: to show the principal effects of distributing the heat absorbed at the ground throughout the lower atmosphere.

5. The Equivalent Gravity Mode Approach

Three major difficulties arise in calculating tidal effects
in the atmosphere of Venus: uncertainties in the basic state,
ignorance of the heating distribution, and the nonseparability
of the tidal equations in latitude and height which arises
from the large vertical shear in the mean zonal wind. Ultimately
we shall show that these problems have little impact on the
conclusions regarding the net atmospheric tidal torque on Venus.

A. Theoretical basis

Nonseparability is not a fundamental obstacle, since the
nonseparable tidal equations could be solved by a two-dimensional
finite-difference scheme, as Lindzen and Hong (1974) did for
the Earth. Such an attack is prone to numerical pitfalls;
furthermore, present knowledge of the basic state and heating
profile does not warrant such rigor. Accordingly we shall not
seek global solutions, but instead assume a latitudinal structure
as if the solutions were separable, in order to solve for the
vertical structure at the equator. This approximate
approach indicates that the surface pressure variations are
mainly forced by heating near the ground, for which the question
of separability is not as important.

The appellation "equivalent gravity mode" was coined by
Lindzen (1970a) in a study of gravity waves on a nonrotating
plane, which have a sinusoidal structure in both horizontal

directions. A concise description is found in the sequel
(Lindzen and Blake, 1971): "In Part I (Lindzen 1970a) we
defined 'equivalent' gravity modes as internal gravity waves
on a non-rotating plane whose frequencies are equal to tidal
frequencies, whose east-west wavenumbers are equal to those
of the tidal modes at the equator, and whose meridional
wavenumbers are *chosen* so that the vertical structures of the
'equivalent' gravity modes are identical... with the vertical
structures of tidal modes appropriate to a rotating sphere.
In addition, the horizontal structure of the 'equivalent'
gravity modes (E. G. M.'s) approximates that of tidal modes in
the neighborhood of the equator."

The technique was further developed in Lindzen (1971)
and in Lindzen and Hong (1973). By using properties of the
horizontal structure found from the separable case, one can
more readily study the effects on the vertical structure of
a variety of phenomena, such as viscosity and thermal conductivity,
which lead to nonseparability of the tidal equations on a
rotating sphere. We shall use an approach slightly modified
from the one described above to study atmospheric tides on
Venus.

The spin and orbital periods of Venus are comparable,
so no distinction is made between seasonal and diurnal timescales.

Accordingly the basic state is assumed symmetrical about the equator. Then the coefficients of eqs. (2:23) and (2:24) given in (2:25) naturally divide into a symmetric set (Δ, Λ_1, Λ_3, Λ_5, Λ_7, Γ_+) and an antisymmetric set (Λ_2, Λ_4, Λ_6).

These coefficients, as well as the dependent variables $\delta\eta$ and $\delta\psi$ in (2:23) and (2:24), may now be replaced by their Taylor series expansions about the equator. Since the tropical region is the most important for calculating the tidal torques, we retain only the first two terms of the resulting expansions. For forcings symmetrical with respect to the equator, all of the coefficients then take their values at the equator, so that the antisymmetric coefficients vanish. For antisymmetrial forcings, however, the symmetrical coefficients are again set to their values at the equator, while the antisymmetrical ones are replaced by their first derivatives with respect to θ, evaluated at the equator.

We can further simplify the resulting tidal equations by defining a new, height-dependent "equivalent depth" $h(x)$ by analogy with eq. (2:31). For symmetrical modes, let

$$\frac{1}{gh} = \frac{1}{\sigma}\left[\Lambda_1 \frac{1}{\delta\psi}\frac{\partial^2}{\partial\theta^2}\delta\psi + \Lambda_3\right] \qquad , \qquad (5:1)$$

while for antisymmetrical modes, we put

$$\frac{1}{gh} = \frac{1}{\sigma}\left[\Lambda_1\left(\frac{\partial}{\partial\theta}\delta\psi\right)^{-1}\frac{\partial^3}{\partial\theta^3}\delta\psi + \Lambda_2 + \Lambda_3\right] \qquad , \qquad (5:2)$$

where all derivatives are evaluated at the equator. Choosing
a value for h is thus tantamount to assuming the ratio of $\delta\psi$
to its second derivative (or of its first derivative to its third)
without solving for the horizontal structure of the tidal mode.
While this is somewhat arbitrary, ultimately we shall show that
the results are insensitive to the horizontal structure.

It is also convenient to introduce the notation

$\Pi = 0$ for symmetrical modes.

$\Pi = 1$ for antisymmetrical modes. $\qquad\qquad$ (5:3)

and $\chi = \dfrac{1}{\sigma^2}\dfrac{d}{dx}\omega^2 = \dfrac{\partial}{\partial\theta}\Lambda_4$ evaluated at the equator $\qquad$.

Then equations (2:23) and (2:24) can be written

$$\frac{i\sigma}{gh}\,\delta\psi = \frac{d}{dx}\,\delta\eta - (\Pi\chi + \Lambda_5)\,\delta\eta \qquad , \qquad (5:4)$$

$$\varkappa\delta J = (i\sigma + i/\tau)\frac{\partial}{\partial x}\,\delta\psi + i\Pi\chi\,\delta\psi + \Gamma\delta\eta \qquad . \qquad (5:5)$$

Now $\delta\eta$ may be eliminated between (5:4) and (5:5) above, to
give a single ordinary differential equation in the potential
$\delta\psi$ for each σ,s mode:

$$\begin{aligned}
i\varkappa\delta J\left(\Lambda_5 + \Pi\chi + \frac{1}{\Gamma}\frac{d}{dx}\Gamma\right) &- i\frac{d}{dx}\varkappa\delta J = (\sigma - i/\tau)\frac{d^2}{dx^2}\delta\psi \\
&+ \frac{d}{dx}\delta\psi\left[-(\sigma - i/\tau)\left(\Lambda_5 + \Pi\chi + \frac{1}{\Gamma}\frac{d}{dx}\Gamma\right)\right. \\
&\left.+ \frac{d}{dx}(\sigma - i/\tau) - \Pi\sigma\chi\right] + \delta\psi\left[\frac{\sigma\Gamma}{gh} + \Pi\sigma\chi\left(\Lambda_5 + \chi + \frac{1}{\Gamma}\frac{d}{dx}\Gamma\right)\right. \\
&\left.- \Pi\frac{d}{dx}(\sigma\chi)\right] \qquad .
\end{aligned} \qquad (5:6)$$

Equation (5:6) above could have been obtained directly by
expanding eq. (2:35) about the equator. However, it is more

convenient to eliminate $\delta\psi$ between (5:4) and (5:5) in order to obtain a single equation in the vertical velocity $\delta\eta$, as in the classical approach.

If h is finite, subsituting $\delta\psi$ from (5:4) and (5:5) and rearranging gives

$$
\frac{\varkappa\delta J}{(1 - \frac{i}{\sigma\tau})gh} = \frac{d^2}{dx^2}\delta\eta - \frac{d}{dx}\delta\eta\left[\Lambda_5 + \Pi\chi + \frac{\Pi\chi}{(1 - \frac{i}{\sigma\tau})} - \frac{\sigma}{gh}\frac{d}{dx}(\frac{gh}{\sigma})\right]
$$
$$
+ \delta\eta\left[\frac{\Gamma}{(1 - \frac{i}{\sigma\tau})gh} - \frac{d}{dx}(\Lambda_5 + \Pi\chi) + (\Lambda_5 + \Pi\chi)\frac{\Pi\chi}{(1 - \frac{i}{\sigma\tau})}\right. \tag{5:7}
$$
$$
\left. - (\Lambda_5 + \Pi\chi)\frac{\sigma}{gh}\frac{d}{dx}(\frac{gh}{\sigma})\right] \quad .
$$

Now eq. (5:7) (or else (5:6)) can be solved either analytically or by the simple numerical method described by Chapman and Lindzen (1970). Once $\delta\eta$ (x) is known $\delta\psi$ can easily be found through eq. (5:4). Then (2:19) and (2:22) give expressions for the temperature variation:

$$
\delta T = \frac{1}{R}\frac{\partial}{\partial x}\delta\psi = \frac{1}{R}(i\sigma + 1/\tau)^{-1}\left[i\sigma\,\Pi\chi\,\delta\psi - \Gamma\delta\eta + \varkappa\delta J\right]. \tag{5:8}
$$

Equations (2:21) and (2:22) can also be expanded so as to give the horizontal wind speeds δu and δv and their colatitudinal derivatives at the equator for each mode. If $\delta\psi$ and $\delta\eta$ are symmetric, we find at the equator

$$
\delta u = 0 \quad , \quad \frac{\partial}{\partial\theta}\delta u = \frac{-i}{a\sigma}[\ell(\ell + 1) - s^2 + 2s\,\omega/\sigma]\delta\psi
$$
$$
- \frac{2a\omega}{\sigma^2}\left(\frac{\partial\omega}{\partial x}\right)\delta\eta; \tag{5:9}
$$
$$
\delta v = \frac{-s}{a\sigma}\delta\psi + i\frac{a}{\sigma}\left(\frac{\partial\omega}{\partial x}\right)\delta\eta \quad , \quad \frac{\partial}{\partial\theta}\delta v = 0 \quad .
$$

Similarly, if $\delta\psi$ and $\delta\eta$ are antisymmetric we find

$$\delta u = \frac{i}{a_\sigma}\frac{\partial}{\partial\theta}\,\delta\psi \quad , \quad \frac{\partial}{\partial\theta}\,\delta u = 0 \quad ;$$

$$\delta v = 0 \quad , \quad \frac{\partial}{\partial\theta}\,\delta v = \frac{1}{\sigma^2}\,(s\sigma - 2\omega + \frac{\partial^2}{\partial\theta^2}\,\omega)\,\frac{\partial}{\partial\theta}\,\delta\psi + \tag{5:10}$$

$$i\,\frac{a}{\sigma}\left(\frac{\partial\omega}{\partial x}\right)\frac{\partial}{\partial\theta}\,\delta\eta \quad .$$

We can also substitute the above results into eq. (2:37) to find the dimensionalized vertical velocity:

$$\delta w = \frac{i\sigma}{g}\,(\delta\psi - \delta\Omega) - \Pi\,i\,\delta\psi\left(\frac{\omega^2 - \omega_o^2}{g\sigma}\right) + H\,\delta\eta$$

$$= h\left[1 - \Pi\left(\frac{\omega^2 - \omega_o^2}{\sigma^2}\right)\right]\left[\frac{d}{dx}\,\delta\eta - (\Lambda_4 + \Lambda_5)\,\delta\eta\right] \tag{5:11}$$

$$+ H\,\delta\eta - \frac{i\sigma}{g}\,\delta\Omega \quad .$$

Eq. (5:11) combined with (2:39) then constitutes the lower boundary condition for eq. (5:7). Since the equivalent depth is typically four orders of ten less than the scale height at the ground, for Venus the lower boundary condition is almost identical to requiring $\delta\eta = 0$ at $x = 0$.

C. Equivalent depths

The equivalent gravity mode approach of the preceding
section has now reduced the tidal problem to one dimension,
where it is more easily dealt with. For the purposes of the
numerical calculations, we still need to evaluate the
equivalent depths.

Suppose that the tidal problem were separable in the upper
atmosphere of Venus. The equivalent depths could then be
obtained by dividing the known values for the Earth by 23.1, the
ratio of the quantity $\dfrac{a^2 \omega^2}{g}$ between the two planets
(assuming mean zonal winds of 90 m/s at the equator in the
stratosphere of Venus). The resulting approximate values of
h are listed in Table 1 under the heading "classical", for
the four modes of lowest order at each of the important
forcing frequencies. The terrestrial values for the inertial
diurnal modes ($\sigma = \omega$) were taken from Lindzen (1967), while
all of the others were taken from the corresponding synodic
modes ($\sigma = s\omega + sn$) tabulated by Flattery (1967).

The least arbitrary technique of extending these equivalent
depths throughout the atmosphere would be to scale the tabulated
stratospheric values to the height-dependent frequency at each level.
Since the equations are not separable in the first place,
such a refinement would be an unnecessary complication. By
comparing several approaches we shall show that it is adequate

to assume a plausible distribution over colatitude, independent
of height, which gives simple formulae for the equivalent
depth as a function of frequency.

The simplest way (method 0) of approximating the
equivalent depth is to neglect $\frac{\partial^2}{\partial\theta^2}\delta\psi$ and $\frac{\partial^3}{\partial\theta^3}\delta\psi$ altogether in
eqs. (5:1) and (5:2). Then $\delta\psi$ and $\delta\eta$ will have the same
distribution over colatitude as the forcing, while (5:1) and (5:2)
become,

$$\frac{1}{gh} = \frac{1}{\sigma}[\Pi\,\Lambda_2 + \Lambda_3] = \Pi\,\frac{1}{a^2\sigma^4}[\sigma^2 - 8\omega^2 + (2s\sigma - 4\omega)$$
$$\frac{\partial^2}{\partial\theta}\,\omega] + \frac{2s\omega}{a^2\sigma^3} + \frac{s^2}{a^2\sigma^2} \qquad . \tag{5:12}$$

Table 1 shows that the equivalent depths obtained this way
do not agree well with the "classical" values, so that the
traditional case cannot be recovered.

It is more satisfactory to scale the equivalent depths of
the separable problem approximately to each level of the Venus
atmosphere. No explicit formula is known for the equivalent
depths in the classical case. Based on an equational beta-plane
approximation, Lindzen (1967) gives a formula which predicts
some of the eigenvalues quite well, but only for the diurnal
modes. Green (1965) replaces the Coriolis parameter $2\omega\cos\theta$
in the classical primitive equations by a constant value $s_o^2\,\omega^2$
for midlatitudes. The eigenfunctions of the resulting separable
problem are Legendre functions $P_{\ell s}(\cos\theta)$ of degree ℓ and
order s, with corresponding equivalent depths given by

$$h_\ell = \frac{a^2}{g} \cdot \frac{\sigma^2 - s_o^2 \omega^2}{\ell (\ell + 1)} \tag{5:13}$$

The resulting values are listed under method 1 in Table 1, where following Green (1965) we use $s_o^2 = 0.95$ for diurnal tides, and $s_o^2 = 2.0$ otherwise. Note that (5:13) above is an exact solution to the Hough equation (2:33) for a nonrotating planet ($\omega = 0$).

The comparison between the equivalent depths obtained by means of method 1 and the classical values is much more satisfactory. The Legendre functions are very convenient for representing the forcing and response for several reasons: (1) they resemble the known Hough functions for low degree and order, (2) they are simple and well known, (3) they automatically fit the polar boundary condition, and (4) they are natural for treating the resulting gravitational torques. Therefore we shall adopt formula (5:13) as the principal method for estimating equivalent depths in the numerical computations.

However, it might be more consistent with our original approach to obtain the equivalent depths from eqs. (5:1) and (5:2) applied to Legendre functions, than from eq. (5:13). Then it is easy to find the quotients

$$\frac{1}{\delta\psi} \frac{\partial^2}{\partial\theta^2} \delta\psi = \lim_{\theta \to \pi/2} \frac{1}{P_{\ell s}(\cos\theta)} \frac{\partial^2}{\partial\theta^2} P_{\ell s}(\cos\theta) =$$

$$-\ell(\ell + 1) + s^2, \tag{5:14}$$

$$\left(\frac{\partial}{\partial\theta} \delta\psi^{-1}\right) \frac{\partial^3}{\partial\theta^3} \delta\psi = \lim_{\theta \to \pi/2} \left[\left(\frac{\partial}{\partial\theta} P_{\ell s}(\cos\theta)^{-1}\right) \frac{\partial^3}{\partial\theta^3} P_{\ell s}(\cos\theta)\right]$$

σ	s	ℓ	Π	classical	method 0	method 1	method 2
				Table 1	Equivalent depths h_ℓ high in the atmosphere (m)		
ω + n	1	1	0	29.9	336.	44.3	251.
		2	1	3.48×10^4	−268.	14.8	3.44×10^3
		3	0	5.21	336.	7.39	71.2
		4	1	10.3	−268.	4.43	69.5
ω	1	1	0	30.2	317.	23.8	238.
		2	1	∞	−238.	7.94	∞
		3	0	5.24	317.	3.97	68.0
		4	1	10.4	−238.	2.38	68.0
ω + 2n	1	1	0		355.	65.3	264.
		2	1		−301.	21.8	1.85×10^3
		3	0		355.	10.9	74.4
		4	1		−301.	6.53	71.1
ω − 2n	1	1	0		283.	−15.9	213.
		2	1		−188.	−5.32	-1.36×10^3
		3	0		283.	−2.66	62.0
		4	1		−188.	−1.59	65.3
2ω + 2n	2	2	0	340.	667.	345.	499.
		3	1	158.	788.	172.	330.
		4	0	91.3	667.	103.	181.
		5	1	59.2	788.	69.0	132.
2ω	2	2	0		635.	317.	476.
		3	1		762.	159.	317.
		4	0		635.	95.2	173.
		5	1		762.	63.5	127.
2ω − 2n	2	2	0		604.	291.	454.
		3	1		736.	145.	305.
		4	0		604.	87.2	166.
		5	1		736.	58.1	122.
−2n	0	0	0		∞	∞	∞
		1	1		-3.94×10^{-4}	−952.	-3.94×10^{-4}
		2	0		∞	−317.	0.289
		3	1		-3.94×10^{-4}	−159.	-3.94×10^{-4}
3ω + 3n	3	3	0	558.	816.	586.	641.
		4	1	332.	805.	352.	424.
		5	0	220.	816.	235.	280.
		6	1	157.	805.	168.	207.
4ω + 4n	4	4	0	665.	885.	700.	724.
		5	1	443.	860.	466.	505.
		6	0	316.	885.	333.	362.
		7	1	237.	860.	250.	277.

$$= -\ell(\ell+1) + s^2 + 1 \qquad .$$

Substituting (5:14) above into (5:1) and (5:2) then yields

$$\frac{1}{gh} = \frac{1}{a^2\sigma^4}\left[\sigma^2\,\ell(\ell+1) + 2s\,\omega\sigma - 8\,\omega^2\,\Pi + \Pi\,(2s\sigma + 4\omega)\right.$$
$$\left. \frac{\partial^2}{\partial\theta^2}\,\omega\right] \qquad . \tag{5:15}$$

The results of formula (5:15) above are also listed in Table 1 under method 2, but do not appear to reproduce the separable results as well as those from method 1. Formula (5:15) will therefore be used as an alternative for comparison with (5:13) in the numerical computations.

It is worth noting that the first antisymmetric mode of the inertial diurnal frequency $\sigma = \omega$ has a formally infinite equivalent depth in the classical case, which only method 2 of the approximate formulae has reproduced. This is significant because an infinite equivalent depth may lead to vanishing surface pressure variations; the behavior of tidal modes with infinite equivalent depths is treated more fully in Appendix I. However, Table 1 was made by setting $\frac{\partial^2}{\partial\theta^2}\,\omega = 0$ in eqs. (5:12) and (5:15), and so represents an ideal case. In reality, the substantial horizontal wind shear observed on Venus (Suomi, 1974) keeps the equivalent depth small so that this particular tidal mode probably behaves qualitatively the same as the others. Several of the tabulated equivalent depths are infinite for the $\sigma = -2n$ semiannual tides as well; this also is an artifact of the formulae used and does not occur either in the exact

solutions of the Hough equation or in reality. These questions could probably be resolved by two-dimensional finite-difference computations, like those of Lindzen and Hong (1974), but as we have already mentioned, these are subject to limitations of their own.

Meanwhile the equivalent depth scales roughly as $\sigma^2(x)$, the square of the frequency at each height, according to all of the approximate formulae (5:12), (5:13), and (5:15). As a result, the equivalent depths decrease by roughly three orders of magnitude from the upper atmosphere down to the surface of Venus. The equivalent depths of the surface are listed in Table 2, which has the same format as Table 1, except that the "exact" values of the equivalent depths are less meaningful and are therefore omitted.

Table 2				Equivalent depths h_ℓ at the surface (meters)		
σ	s	ℓ	Π	method 0	method 1	method 2
$\omega + n$	1	1	0	0.818	0.626	0.542
		2	1	1.44	0.209	0.314
		3	0	0.818	0.104	0.124
		4	1	1.44	0.0626	0.0839
ω	1	1	0	0.123	9.25×10^{-3}	0.0925
		2	1	-0.0925	3.08×10^{-3}	∞
		3	0	0.123	1.54×10^{-3}	0.0264
		4	1	-0.0925	9.25×10^{-4}	0.0264
$\omega + 2n$	1	1	0	2.27	1.68	1.41
		2	1	2.02	0.559	0.635
		3	0	2.27	0.279	0.293
		4	1	2.02	0.168	0.187
$\omega - 2n$	1	1	0	-0.699	0.0750	1.78
		2	1	-0.0893	0.0250	-0.310
		3	0	-0.699	0.0125	0.0488
		4	1	-0.0893	7.50×10^{-3}	0.0405
$2\omega + 2n$	2	2	0	1.29	0.946	0.922
		3	1	1.17	0.473	0.513
		4	0	1.29	0.284	0.306
		5	1	1.17	0.189	0.210
2ω	2	2	0	0.247	0.123	0.185
		3	1	0.296	0.0617	0.123
		4	0	0.247	0.0370	0.0673
		5	1	0.296	0.0247	0.493
$2\omega - 2n$	2	2	0	-4.91×10^{-4}	-0.122	-5.45×10^{-4}
		3	1	-3.17×10^{-5}	-0.0608	-3.24×10^{-5}
		4	0	-4.91×10^{-4}	-0.0365	-2.30×10^{-3}
		5	1	-3.17×10^{-5}	-0.0243	-3.44×10^{-5}
$-2n$	0	0	0	∞	∞	∞
		1	1	-2.45	0.496	5,93
		2	0	∞	0.165	0.289
		3	1	-2.45	0.0827	0.168
$3\omega + 3n$	3	3	0	1.45	1.14	1.11
		4	1	1.34	0.685	0.695
		5	0	1.45	0.456	0.466
		6	1	1.34	0.326	0.338
$4\omega + 4n$	4	4	0	1.51	1.25	1.22
		5	1	1.44	0.831	0.832
		6	0	1.51	0.593	0.597
		7	1	1.44	0.445	0.451

C. Numerical calculations

The tidal equations were solved numerically in one dimension according to the equivalent gravity mode formulation, using both methods 1 and 2 described in the preceding section. The finite-difference scheme employed is standard in tidal problems and is given in Chapman and Lindzen (1970); see also Lindzen and Kuo (1969). We used a fully complex double precision program with a vertical step size x ≤ .05 for accuracy.

Table 3 displays the tidal variations in surface pressure δp_o resulting from each of the heating distributions I – VIII, for models A – D of the basic state. For the main synodic diurnal mode ($\sigma = \omega + n$), heating profiles I, II, and III are normalized to a total absorbed insolation of $1/2 \times 500$ W/m^2, while distributions IV through VIII are normalized to $1/2 \times 100$ W/m^2. This tidal mode has a large amplitude, but does not affect the torque on the planet. It will be shown in chapter 7 that the net accelerating torque on the atmosphere is proportional to the imaginary part of the semidiurnal component ($\sigma = 2\omega + 2n$) of the surface pressure variation. In order for this mode to be consistent with eq. (4:6), heating models I – III must be normalized to a total flux of $\frac{15}{64} \times 500$ W/m^2, and profiles IV – VIII to $\frac{15}{64} \times 100$ W/m^2. All of the other modes tabulated appear only when the obliquity is not exactly 180°. They influence the behavior of Venus' obliquity, and will be discussed further in Part II of this work. Here they have been normalized

SIGMA = 1*OMEGA + 1*N   S = 1   DEGREE = 1   PARITY = 0

| J | MODEL | DELTA P (MILLIBARS) | |
		METHOD 1	METHOD 2
I	A	0.0 +I* 0.0	0.159 +I* 0.528E-01
	B	-0.756E-03+I* 0.280E-03	-0.202E-03+I* 0.173E-03
	C	-0.402E-03+I* 0.171E-03	-0.260E-03+I* 0.223E-03
	D	-0.368E-03+I* 0.157E-03	0.175E-02+I*-0.149E-02
II	A	1.48 +I*-0.134	0.164 +I*-0.259
	B	0.117E-02+I* 0.329E-02	0.218E-03+I* 0.435E-03
	C	0.718E-03+I* 0.175E-02	0.281E-03+I* 0.560E-03
	D	0.660E-03+I* 0.160E-02	-0.186E-02+I*-0.375E-02
III	A	0.628E-03+I*-0.740E-02	-0.103E-01+I*-0.638E-01
	B	-0.256E-04+I* 0.227E-03	0.863E-04+I* 0.614E-04
	C	-0.113E-04+I* 0.262E-04	0.112E-03+I* 0.430E-04
	D	-0.103E-04+I* 0.240E-04	-0.747E-03+I*-0.290E-03
IV	A	-2.32 +I* 5.30	-0.887 +I* 3.60
	B	-0.482E-04+I* 3.43	-0.710E-05+I* 2.92
	C	-0.151E-04+I* 0.879	-0.498E-05+I* 0.835
	D	-0.105E-04+I* 0.869	-0.248E-04+I* 0.838
V	A	-3.02 +I* 9.42	-0.965 +I* 6.74
	B	-0.189E-04+I* 6.08	-0.277E-05+I* 5.24
	C	-0.101E-04+I* 2.45	-0.301E-05+I* 2.33
	D	-0.844E-05+I* 2.43	-0.134E-03+I* 2.35
VI	A	-1.95 +I* 8.04	-0.504 +I* 5.62
	B	0.433 +I* 5.02	0.344 +I* 4.36
	C	0.139 +I* 2.99	0.128 +I* 2.88
	D	0.137 +I* 2.98	0.129 +I* 2.89
VII	A	0.109 +I* 10.5	0.838 +I* 7.39
	B	1.55 +I* 6.32	1.26 +I* 5.61
	C	0.590 +I* 4.20	0.549 +I* 4.06
	D	0.583 +I* 4.18	0.553 +I* 4.08
VIII	A	-0.335 +I* 10.0	-0.111 +I* 9.66
	B	-0.185E-05+I* 9.49	-0.279E-06+I* 9.35
	C	-0.140E-05+I* 9.35	-0.414E-06+I* 9.32
	D	-0.118E-05+I* 9.35	-0.185E-04+I* 9.32

SIGMA = 2*OMEGA + 2*N		S = 2	DEGREE = 2	PARITY = 0

J	MODEL	DELTA P (MILLIBARS)	
		METHOD 1	METHOD 2
I	A	0.0 +I* 0.0	-0.198 +I* 0.186
	B	-0.167E-03+I* 0.357E-02	0.193E-02+I* 0.195E-02
	C	0.172E-03+I* 0.310E-02	0.226E-02+I* 0.169E-02
	D	-0.237E-03+I*-0.414E-02	-0.257E-02+I*-0.191E-02
II	A	-0.124 +I*-0.401	0.121 +I* 0.314
	B	0.514E-02+I* 0.171E-02	0.315E-02+I*-0.130E-02
	C	0.459E-02+I* 0.993E-03	0.300E-02+I*-0.181E-02
	D	-0.615E-02+I*-0.132E-02	-0.340E-02+I* 0.206E-02
III	A	-0.955E-01+I*-0.734E-01	0.997E-01+I* 0.851E-01
	B	0.144E-02+I*-0.393E-03	0.814E-03+I*-0.101E-02
	C	0.120E-02+I*-0.534E-03	0.665E-03+I*-0.119E-02
	D	-0.161E-02+I* 0.718E-03	-0.750E-03+I* 0.135E-02
IV	A	-0.160 +I* 0.863	-0.181 +I* 1.22
	B	-0.733E-04+I* 0.752	-0.448E-04+I* 0.704
	C	-0.429E-04+I* 0.224	-0.312E-04+I* 0.217
	D	0.137E-04+I* 0.216	0.801E-05+I* 0.210
V	A	-0.143 +I* 1.57	-0.150 +I* 1.81
	B	-0.257E-04+I* 1.32	-0.166E-04+I* 1.25
	C	-0.271E-04+I* 0.617	-0.201E-04+I* 0.599
	D	-0.486E-04+I* 0.609	-0.259E-04+I* 0.590
VI	A	0.114E-01+I* 1.39	0.985E-01+I* 1.69
	B	0.135 +I* 1.16	0.123 +I* 1.10
	C	0.550E-01+I* 0.794	0.525E-01+I* 0.777
	D	0.531E-01+I* 0.787	0.506E-01+I* 0.769
VII	A	0.502 +I* 1.88	0.690 +I* 2.06
	B	0.494 +I* 1.56	0.458 +I* 1.50
	C	0.250 +I* 1.22	0.240 +I* 1.20
	D	0.245 *I* 1.21	0.235 +I* 1.19
VIII	A	-0.160E-01+I* 2.26	-0.175E-01+I* 2.28
	B	-0.267E-05+I* 2.21	-0.180E-05+I* 2.20
	C	-0.361E-05+I* 2.20	-0.265E-05+I* 2.20
	D	-0.647E-05+I* 2.20	-0.341E-05+I* 2.20

SIGMA = 1*OMEGA + 0*N   S = 1   DEGREE = 2   PARITY = 1

J	MODEL	DELTA P (MILLIBARS)		
		METHOD 1		METHOD 2
I	A	0.0	+I* 0.0	0.0	+I* 0.0
	B	0.489E-09	+I*-0.832E-09	0.0	+I* 0.0
	C	-0.929E-12	+I* 0.167E-11	0.0	+I* 0.0
	D	-0.380E-13	+I* 0.686E-13	0.0	+I* 0.0
II	A	0.113E-04	+I*-0.710E-04	0.0	+I* 0.0
	B	-0.953E-08	+I*-0.301E-08	0.0	+I* 0.0
	C	0.190E-10	+I* 0.550E-11	0.0	+I* 0.0
	D	0.780E-12	+I* 0.224E-12	0.0	+I* 0.0
III	A	0.913E-07	+I* 0.656E-07	0.0	+I*-0.601E-09
	B	-0.248E-09	+I* 0.585E-07	0.0	+I*-0.601E-09
	C	0.218E-12	+I* 0.866E-09	0.0	+I*-0.586E-10
	D	0.885E-14	+I* 0.867E-09	0.0	+I*-0.586E-10
IV	A	-0.507	+I*-0.896E-01	0.0	+I*-0.155
	B	-0.177E-06	+I* 1.79	0.0	+I*-0.155
	C	0.889E-10	+I* 0.795	0.0	+I*-0.552E-01
	D	0.157E-12	+I* 0.795	0.0	+I*-0.552E-01
V	A	-1.19	+I*-0.192	0.0	+I*-0.360
	B	-0.343E-06	+I* 4.15	0.0	+I*-0.360
	C	0.303E-09	+I* 2.75	0.0	+I*-0.191
	D	0.508E-12	+I* 2.75	0.0	+I*-0.191
VI	A	-1.24	+I*-0.121	-0.930E-02	+I*-0.334
	B	0.113	+I* 3.81	-0.930E-02	+I*-0.334
	C	0.127	+I* 4.68	-0.848E-02	+I*-0.325
	D	0.127	+I* 4.69	-0.849E-02	+I*-0.326
VII	A	-1.72	+I*-0.827E-01	-0.365E-01	+I*-0.430
	B	0.439	+I* 4.88	-0.365E-01	+I*-0.430
	C	0.507	+I* 6.04	-0.339E-01	+I*-0.421
	D	0.508	+I* 6.05	-0.340E-01	+I*-0.421
VIII	A	-8.12	+I* 14.2	0.0	+I* -2.12
	B	-0.157E-06	+I* 17.2	0.0	+I* -2.12
	C	0.178E-09	+I* 18.0	0.0	+I* -1.55
	D	0.299E-12	+I* 18.0	0.0	+I* -1.55

SIGMA = 1*OMEGA + 2*N   S = 1   DEGREE = 2   PARITY = 1

J	MODEL	DELTA P (MILLIBARS)	
		METHOD 1	METHOD 2
I	A	0.240E-02+I*-0.327E-02	0.352E-03+I*-0.322E-03
	B	0.819E-05+I* 0.206E-04	0.859E-05+I*-0.197E-04
	C	0.968E-05+I* 0.218E-04	-0.538E-05+I*-0.153E-04
	D	-0.331E-05+I*-0.734E-05	0.127E-04+I* 0.358E-04
II	A	-0.207E-01+I*-0.138E-01	0.289E-04+I*-0.305E-03
	B	0.124E-03+I*-0.562E-04	-0.438E-05+I*-0.131E-04
	C	0.131E-03+I*-0.657E-04	-0.914E-05+I*-0.496E-05
	D	-0.441E-04+I* 0.224E-04	0.214E-04+I* 0.116E-04
III	A	-0.766E-04+I*-0.583E-04	-0.228E-04+I*-0.143E-03
	B	-0.275E-05+I* 0.677E-04	-0.461E-05+I*-0.381E-05
	C	-0.150E-05+I* 0.468E-05	-0.658E-05+I*-0.202E-05
	D	0.496E-06+I*-0.158E-05	0.154E-04+I* 0.470E-05
IV	A	-1.58 +I* 1.85	-0.159E-02+I* 3.46
	B	-0.943E-04+I* 2.73	-0.514E-05+I* 2.05
	C	-0.395E-04+I* 0.782	-0.132E-05+I* 0.696
	D	-0.300E-05+I* 0.758	-0.569E-05+I* 0.693
V	A	-2.20 +I* 3.75	-0.181E-02+I* 5.33
	B	-0.760E-04+I* 4.37	-0.408E-05+I* 3.42
	C	-0.769E-04+I* 1.91	-0.248E-05+I* 1.70
	D	-0.877E-05+I* 1.85	-0.136E-04+I* 1.70
VI	A	-1.71 +I* 3.20	0.582 +I* 4.49
	B	0.414 +I* 3.67	0.275 +I* 2.85
	C	0.128 +I* 2.10	0.105 +I* 1.90
	D	0.122 +I* 2.05	0.105 +I* 1.90
VII	A	-0.976 +I* 5.29	1.97 +I* 5.45
	B	1.47 +I* 4.68	1.03 +I* 3.82
	C	0.565 +I* 3.09	0.478 +I* 2.84
	D	0.544 +I* 3.04	0.475 +I* 2.84
VIII	A	-0.263 +I* 6.01	-0.213E-03+I* 6.10
	B	-0.786E-05+I* 5.98	-0.430E-06+I* 5.80
	C	-0.147E-04+I* 5.82	-0.466E-06+I* 5.77
	D	-0.167E-05+I* 5.81	-0.256E-05+I* 5.77

SIGMA = 2*OMEGA + 0*N   S = 2   DEGREE = 2   PARITY = 0

| J | MODEL | DELTA P (MILLIBARS) | |
		METHOD 1	METHOD 2
I	A	-0.346 +I* 0.381	0.743E-01+I*-0.369
	B	-0.191E-03+I* 0.801E-03	0.808E-03+I* 0.102E-02
	C	-0.625E-04+I* 0.453E-03	0.522E-03+I* 0.487E-03
	D	0.563E-03+I*-0.368E-02	-0.717E-03+I*-0.666E-03
II	A	0.451 +I* 0.689	-0.402 +I*-0.257
	B	0.116E-02+I* 0.617E-03	0.158E-02+I*-0.485E-03
	C	0.677E-03+I* 0.279E-03	0.815E-03+I*-0.393E-03
	D	-0.547E-02+I*-0.235E-02	-0.112E-02+I* 0.541E-03
III	A	0.204 +I* 0.742E-01	-0.179 +I*-0.109E-01
	B	0.331E-03+I*-0.346E-04	0.419E-03+I*-0.434E-03
	C	0.181E-03+I*-0.491E-04	0.189E-03+I*-0.281E-03
	D	-0.147E-02+I* 0.378E-03	-0.258E-03+I* 0.386E-03
IV	A	-1.69 +I* 0.160	-0.629 +I* 1.36
	B	-0.256E-04+I* 1.49	-0.305E-04+I* 1.49
	C	-0.768E-05+I* 0.432	-0.933E-05+I* 0.432
	D	-0.567E-04+I* 0.434	0.262E-05+I* 0.430
V	A	-3.36 +I* 1.53	-0.963 +I* 3.83
	B	-0.123E-04+I* 3.33	-0.147E-04+I* 3.33
	C	-0.619E-05+I* 1.49	-0.752E-05+I* 1.49
	D	-0.410E-03+I* 1.51	-0.141E-04+I* 1.49
VI	A	-2.73 +I* 1.79	-0.673 +I* 3.39
	B	0.186 +I* 3.01	0.186 +I* 3.01
	C	0.108 +I* 2.63	0.108 +I* 2.63
	D	0.109 +I* 2.65	0.107 +I* 2.63
VII	A	-3.03 +I* 3.74	-0.132 +I* 4.91
	B	0.717 +I* 4.02	0.717 +I* 4.02
	C	0.465 +I* 3.71	0.465 +I* 3.71
	D	0.470 +I* 3.73	0.464 +I* 3.71
VIII	A	-0.739 +I* 8.64	-0.188 +I* 8.98
	B	-0.189E-05+I* 8.61	-0.226E-05+I* 8.61
	C	-0.121E-05+I* 9.05	-0.147E-05+I* 9.05
	D	-0.803E-04+I* 9.05	-0.277E-05+I* 9.04

SIGMA = 0*OMEGA +-2*N   S = 0   DEGREE = 2   PARITY = 0

J	MODEL	DELTA P (MILLIBARS)			
		METHOD 1		METHOD 2	
I	A	0.0	+I*-0.189E-32	0.0	+I*-0.228E-51
	B	0.0	+I*-0.855E-32	0.0	+I* 0.209E-60
	C	0.0	+I* 0.732E-40	0.0	+I* 0.0
	D	0.0	+I* 0.496E-40	0.0	+I* 0.0
II	A	0.0	+I*-0.425E-32	0.0	+I* 0.268E-49
	B	0.0	+I*-0.192E-31	0.0	+I*-0.246E-58
	C	0.0	+I* 0.165E-39	0.0	+I* 0.0
	D	0.0	+I* 0.112E-39	0.0	+I* 0.0
III	A	0.0	+I* 0.126E-07	0.0	+I*-0.105E-04
	B	0.0	+I* 0.298E-07	0.0	+I*-0.430E-06
	C	0.0	+I* 0.462E-09	0.0	+I*-0.887E-09
	D	0.0	+I* 0.462E-09	0.0	+I*-0.887E-09
IV	A	0.0	+I* -3.63	0.0	+I* -3.30
	B	0.0	+I* -2.57	0.0	+I* -4.90
	C	0.0	+I* -1.72	0.0	+I* -2.66
	D	0.0	+I* -1.72	0.0	+I* -2.66
V	A	0.0	+I* -4.86	0.0	+I* -5.29
	B	0.0	+I* -3.45	0.0	+I* -6.38
	C	0.0	+I* -2.30	0.0	+I* -3.56
	D	0.0	+I* -2.30	0.0	+I* -3.56
VI	A	0.111	+I* -3.70	0.289E-01	+I* -3.38
	B	0.419E-01	+I* -2.63	0.428	+I* -4.95
	C	0.378E-01	+I* -1.76	0.126	+I* -2.71
	D	0.378E-01	+I* -1.76	0.126	+I* -2.71
VII	A	0.560	+I* -5.46	0.484	+I* -5.22
	B	0.280	+I* -4.01	1.57	+I* -6.27
	C	0.195	+I* -2.64	0.541	+I* -3.82
	D	0.195	+I* -2.64	0.542	+I* -3.83
VIII	A	0.0	+I* -10.0	0.0	+I* -8.94
	B	0.0	+I* -9.28	0.0	+I* -8.73
	C	0.0	+I* -8.22	0.0	+I* -8.44
	D	0.0	+I* -8.22	0.0	+I* -8.44

to twice the total absorption as the main semidiurnal mode.

Inspection of the semidiurnal results shows that absorption in the upper atmosphere (profiles I-III) produces only a small torque, likely to have either sign. In constrast, heating in the lower atmosphere (models IV-VIII) seems always to generate a net accelerating torque on the planet. Heating deeper in the atmosphere generally has the greatest effect at the ground. This was anticipated by scaling the equivalent depth, and will be elucidated more fully in the following sections. The different basic state models A-D and EGM methods 1 and 2 do not seem to have as much effect as the choice of heating distribution; mostly they appear to alter the coupling between the upper and lower atmospheres. There is one exception; for the antisymmetric inertial diurnal mode ($\sigma = \omega$, $s = 1$) the surface pressure variations obtained through method 2 are about an order of magnitude less than those from method 1, or vanish altogether, as expected; this provides a nice check on the consistency of the calculations.

Along with the torques and pressure variations, the numerical program also calculated temperature and wind fields. In addition it generated the correlation terms such as $\overline{pw}$ and $\overline{vw}$, which are related to energy and momentum transport (Reynolds stresses), respectively. Those correlations which ought to vanish according to symmetry or to the lower boundary condition did so, while the upward energy flux was always positive or negligible, consistent with the upper boundary condition. However, the

correlations were quite sensitive both to the heating distribution and to the basic state model, while the EGM method used did not matter as much.

The numerical program also solves for the height at which the exponentially growing tides become nonlinear, and at which they presumably dump a large part of the outgoing energy flux. This is taken as the level where $\delta T/\overline{T} = - \delta\rho/\overline{\rho}$ first exceeds unity in magnitude. While this height was variable, it was always above the cloud tops for the properly normalized solar input.

The Newtonian cooling term $1/\tau$ was also retained explicitly in the numerical program. At first we used the thermal time constant as a function of height obtained by Pollack and Young (1975), which becomes comparable with the rotation period above $x \approx 8$ or $z \approx 70$ km, along with the appropiate upper boundary condition at the top ($\Delta \delta\eta / \Delta x = 0$ at $x = 15$; see Lindzen and Hong (1974) for a discussion). Subsequently we found that the inclusion of this damping only affected the amplitudes and phases of the tidal fields by 10% or less at the surface. Interestingly, dissipation growing with height tended to increase the amplitudes at the ground; this is interpreted as due to enhanced reflection or "trapping" of gravity waves in the troposphere. For the sake of definiteness, all of the values presented in Table 3 were obtained by neglecting damping (setting $1/\tau = 0$)

and imposing either the boundedness or outgoing wave condition at
the top, as appropriate. In order to obtain more definitive
results, it is necessary to gather better data on the heating
distribution and on the basic state.

D. Free modes and gravitational forcing

In the following two sections, we shall use the equivalent gravity mode approach to explore the atmospheric tides analytically. This will also be of value in interpreting the numerical results.

In order to render the problem analytically tractable, we shall neglect the difference between σ and $s\omega$. This is a good approximation high in the atmosphere where $\omega >> n$, and is often done in the terrestrial theory. Close to the ground it is off by about a factor of two (for the principal semidiurnal mode), while the frequency σ retains more significance than $s\omega$.

Under the above approximation, equations (5:1) and (5:2) for the equivalent depth can be related

$$h_\ell^{\sigma,s}(x) = h_\ell^{\sigma,s}(0) \left[\frac{\sigma(x)}{\sigma(0)}\right]^2 \qquad . \qquad (5:16)$$

We also employ the "exponential wind" model (3:2) for the variation of frequency with height:

$$\sigma(x) = \sigma_o\, e^{fx} \quad , \quad x < x_t;$$

$$\qquad\qquad\qquad\qquad (5:17)$$

$$\sigma(x) = \sigma_o\, e^{fx_t} \quad , \quad x \geq x_t \qquad . $$

When the damping $1/\tau$ is neglected for simplicity, the tidal equation (5:7) has constant coefficients in the troposphere:

$$\frac{\varkappa \delta J}{gh_o} = \frac{d^2}{dx^2}\,\delta\eta - \frac{d}{dx}\,\delta\eta\left[1 + (2 + 4\,\Pi)\,\frac{f}{s^2}\right]$$

$$+ \delta\eta\left[\frac{\Gamma_o}{gh_o} - f\left(1 + f + \frac{2f}{s^2}\right) + \Pi\left(\frac{2f}{s^2} + \frac{8f^2}{s^4}\right)\right]\quad, \tag{5:18}$$

where we have written h_o for $h\ell\,(0)$ and h_∞ for $h\ell\,(\infty)$:

It is easily verified that the general solution to eq. (5:18) above is

$$\delta\eta\,(x) = A\,e^{(\xi + i\lambda)\,x} + B\,e^{(\xi - i\lambda_o)\,x}$$

$$+ \frac{\varkappa}{gh_o}\,\frac{1}{2i\,\lambda_o}\,e^{(\xi + i\lambda_o)x}\int_0^x e^{-(\xi + i\lambda_o)x'}\,e^{-2fx'}$$

$$\cdot\,\delta J\,(x')\,dx' \tag{5:19}$$

$$- \frac{\varkappa}{gh_o}\,\frac{1}{2i\lambda}\,e^{(\xi + i\lambda_o)x}\int_0^x e^{-(\xi - i\lambda_o)x'}\,e^{-2fx'}$$

$$\cdot\,\delta J\,(x')\,dx'\quad .$$

In the stratosphere, $f = 0$ and we recover the "classical" vertical structure equation (2:30), whose solution is similarly

$$\delta\eta\,(x) = C\,e^{(1/2 + i\lambda_o)\,(x - x_c)} + D\,e^{(1/2 - i\lambda_o)\,(x - x_c)}$$

$$+ \frac{\varkappa}{gh_\infty\left(1 - \frac{i}{\sigma\tau}\right)}\,\frac{1}{2i\lambda_\infty}\,e^{(1/2 + i\lambda_\infty)x}\int_\infty^x e^{-(1/2 + i\lambda_\infty)x'}$$

$$\cdot \delta J\ (x') \ dx'$$

$$-\ \frac{\varkappa}{gh_\infty\ (1 - \frac{i}{\sigma\tau})}\ \frac{1}{2i\lambda_o}\ e^{(1/2 - i\lambda_\infty)x}\ \int_\infty^x e^{-(1/2 - i\lambda_\infty)x'} \qquad (5{:}20)$$

$$\cdot \delta J\ (x') \ dx' \qquad .$$

In the above expressions, A, B, C, and D are constants of

integration, and we have defined

$$\xi\ =\ 1/2 + \frac{f}{s^2} + \Pi\ (\frac{2f}{s^2})$$

$$\lambda_o{}^2\ =\ \frac{\Gamma_o}{gh_o} - f\ (1 + f + \frac{2f}{s^2}) + \Pi\ (\frac{2f}{s^2} + \frac{8f^2}{s^4}) - \xi^2$$

$$\qquad (5{:}21)$$

$$=\ \frac{\Gamma_o}{gh_o} - \frac{1}{4} - f\ (1 + f + \frac{2f}{s^2} + \frac{1}{s^2} + \frac{f}{s^4})\ \neq 0$$

$$\lambda_\infty{}^2\ =\ \frac{\Gamma_o}{gh_\infty}\ (1 - \frac{i}{\sigma\tau})^{-1} - \frac{1}{4} \neq 0 \qquad .$$

If the expression for λ^2 or $\lambda_\infty{}^2$ above should be positive,

we take the (real) positive root; if the expression

is negative (or complex due to damping), we take the root

lying in the first quadrant of the complex plane. We must

treat separately the possibility that $\lambda_o = 0$ or $\lambda_\infty = 0$.

Note that the presence of shear represented by $f > 0$

in (5:21) above always reduces the value of $\lambda_o{}^2$, making the

tidal modes more likely to be evanescent, or "trapped". Thus

vertical shear furthur decouples the upper and lower atmospheres,

in addition to the effective increase of equivalent depth with

height discussed previously.

Given the choice of square roots above, the upper boundary condition requires us to set D = 0 in (5:20). The lower boundary condition also provides a relation among the remaining constants of integration. Combining eq. (5:19) with (5:11) and (2:39) at x = 0 gives

$$i\sigma_o \; \delta Z + i\sigma_o \; \delta\Omega/g = AH_+ + BH_- \qquad , \qquad (5:22)$$

where we have defined H_+ and H_- by

$$H_{\pm} = H_o + h_o \; (\xi \pm i\lambda_o - \Pi \chi - \Lambda_5) \left[1 - \Pi \left(\frac{\omega_o^2 - \omega_\varphi^2}{\sigma_o^2} \right) \right] (5:23)$$

In order to complete the solution, we also need two matching conditions at the interface x = x_o, to relate the solutions for the two regions. Since the oscillations are hydrostatic, the pressure p decreases continuously with altitude z, according to equation (2:1). Conversely z must be a continuous function of p, so that by eq. (2:2), $\delta\psi$ (x) must be continuous across the tropopause. Conservation of mass further requires that the velocity normal to the interface be continuous; at the equator, this is equivalent to continuity of $\delta\eta$ (x). Therefore we shall adopt continuity of $\delta\eta$ and $\delta\psi$ as our matching conditions at x = x_o.

For the time being, let us leave out the thermal forcing. Then the requirement of continuity of $\delta\eta$ at x = x_o gives

$$C = A e^{(\xi + i\lambda_o)x_t} + B e^{(\xi - i\lambda_o)x_t} \qquad . \qquad (5:24)$$

$\delta\psi$ (x) can be found from (5:19) and (5:20) by use of (5:4);
continuity at $x = x_t$ then requires

$$\left(\frac{h_\infty}{h_o \, e^{2f \, x_t}}\right) (-1/2 + i \, \lambda_\infty) \, C = A \, (\xi + i \, \lambda_o - \Lambda_5 - \Pi \quad \Lambda_4)$$

$$\cdot \, e^{(\xi + i \, \lambda_o)x_t}$$

$$+ \, B \, (\xi - i \, \lambda_o - \Lambda_5 - \Pi_{ns} \, \Lambda_4^1) \, e^{(\xi - i \, \lambda_o)x_t} \, . \qquad (5:25)$$

Solving (5:24) and (5:25) simultaneously with (5:23) then gives

$$A = i c_o \, (\delta Z + \delta\Omega/g) \, \xi_- \quad (\xi_+ + H_- - \xi_- \, H_+)^{-1}$$

$$B = i c_o \, (\delta Z + \delta\Omega/g) \, \xi_+ \quad (\xi_+ + H_- - \xi_- \, H_+)^{-1}$$

$$C = i c_o \, (\delta Z + \delta\Omega/g) \left[\xi_+ \, e^{(\xi - i \, \lambda_o)x_t} - \xi_- \, e^{(\xi + i \, \lambda_o)x_t} \right]$$

$$\cdot \, (\xi_+ \, H_- - \xi_- \, H_+)^{-1}$$

(5:26)

where we have defined ξ_+ and ξ_- by

$$\xi_\pm = \left[\xi \pm i \, \lambda_o - \Lambda_5 - \Pi \quad \Lambda_4 + (1/2 - i \, \lambda_\infty) \left(\frac{h_\infty}{h_o \, e^{2fx_t}}\right) \right]$$

$$\cdot \, e^{(\xi \pm i \, \lambda_o)x_t}$$

(5:27)

For the time being, we presume that the quantity $\left(\xi_+ \, H_- - \xi_- \, H_+\right)$

cannot vanish, and is of order $\xi_\pm \, H_o$.

At a level of constant pressure p, or of constant x, the altitude z varies by an amount

$$\delta z = \delta \phi / g = (\delta \psi - \delta \Omega)/g \qquad . \qquad (5{:}28)$$

Relative to a fixed altitude z, the pressure p varies by an amount

$$\delta p_z = - \delta z \left(\frac{\partial}{\partial z} \bar{p}\right) = g\bar{\rho} \, \delta z = \bar{\rho} \, \delta \psi - \bar{\rho} \, \delta \Omega \qquad . \qquad (5{:}29)$$

The surface of the planet also experiences a pressure variation by virtue of the tidal motion of the ground up and down relative to the mean pressure gradient. Combining this effect with the above gives for the total pressure variation at the ground

$$\delta p_Z = \bar{\rho}_o \, \delta \psi_o - \bar{\rho}_o \, \delta \Omega - \bar{\rho}_o \, g \, \delta Z \qquad , \qquad (5{:}30)$$

where the subscript noughts signify a quantity evaluated at x = 0.

By virtue of eq. (5:4), we find

$$\delta \psi_o = \frac{g h_o}{i \sigma_o} \left[A (\xi + i \lambda_o) + B (\xi - i \lambda_o) - (A + B) \right. $$
$$\left. \cdot (\Lambda_5 + \Pi \, \Lambda_4) \right] \qquad . \qquad (5{:}31)$$

Substituting A and B from (4:17) into the above then gives

$$\delta \psi_o = (\delta \Omega + g \, \delta Z) \left[\xi_+ (\xi - i \lambda_o - \Lambda_5 - \Pi \, \Lambda_4) \right.$$
$$\left. - \xi_- (\xi + i \lambda_o - \Lambda_5 - \Pi \, \Lambda_4) \right] h_o (\xi_+ H_- - \xi_- H_+)^{-1} \qquad (5{:}32)$$

Since h_o is on the order of a meter for Venus, the dynamic response of the atmosphere to the gravitational forcing is negligible. The resulting surface pressure variation $\overline{\rho}_o \delta\psi_o$ is on the order of $\overline{\rho}_o \delta\Omega \, h_o \approx 10^{-4}$ mb from eq. (5:32) above, while the accompanying wind and temperature variations are correspondingly small.

When the small dynamic term $\overline{\rho}_o \, \delta\psi_o$ is neglected in eq. (5:30), the result becomes independent of the EGM approach. The surface pressure variation for <u>all</u> latitudes is then given by

$$\delta p_Z \approx -\overline{\rho}_o(\delta\Omega + g \, \delta Z) \approx -\overline{\rho}_o \, \delta\Omega_\odot \, (1 + k - ik/Q - j + ij/Q)$$

$$\approx 1.8 \text{ mb sin } \theta \quad . \tag{5:33}$$

In formula (5:33) above, j and k are respectively the height and potential Love numbers while Q is the "quality factor" for body tides; these quantities are described more fully in chapter 7. Note that the gravitationally induced pressure variation is mostly due to the equipotential surfaces' moving up and down farther than the ground; if Venus were a perfectly fluid body (j = 1 +k) with no dissipation (1/Q = 0), the forcing term ($\delta\Omega + g \, \delta Z$) would vanish entirely.

The gravitationally induced surface pressure variation (5:33) has a substantial amplitude but the phase lead is much too small to produce a significant torque. This is because

the imaginary part of the surface pressure variation is produced merely by the tidal bulge in the crust displacing the air, while the density of the soil is about fifty times greater than that of the air. Thus only the thermal forcing can produce a substantial torque on the atmosphere of Venus.

There is one exception to the treatment above. When both the thermal and gravitational forcings vanish, the response of the atmosphere remains indeterminate provided that the quantity $(\xi_+ H_- - \xi_- H_+)$ vanishes also. This circumstance defines the free modes of the atmosphere, as discussed previously. In general, the response of a free mode to either type of forcing is formally unbounded, or resonant.

As long as the oscillations do not interact with the basic state, physical intuition dictates that there can be no free modes in the presence of damping (complex $\lambda_o{}^2$ or $\lambda_\infty{}^2$), or if the outgoing wave condition is applied (λ_∞ positive). In pursuing free oscillations, we may then restrict our attention to evanescent modes (λ_∞ imaginary), although for Venus most tidal modes are in fact propagating (λ_∞ positive).

Note that $\xi_+ H_- - \xi_- H_+$ always vanishes as λ_o tends to zero. However, all of the tidal fields generally remain finite in this limit, as the explicit solution for $\lambda_o = 0$ confirms.

In the classical case ($f = 0$), if the atmosphere is adiabatic everywhere, we find

$$\lambda_o = \lambda_\infty = i/2, \quad \xi_+ = 0 \quad , \quad \xi_- = e^{x_t} \quad ,$$

$$H_+ = H_o - h_\ell^{\sigma,s} \quad , \quad H_- = H_o \qquad \qquad . \tag{5:34}$$

Thus we recover the usual result that free modes in a strictly adiabatic atmosphere only occur when $h_\ell^{\sigma,s} = H_o$.

For Venus, the low frequencies of the tides allow us to neglect h_o/H_o. If we regard both λ_o and λ_∞ as imaginary, we always find $\xi_+ < \xi_-$, so that free modes of short period cannot exist. If we suppose that λ_o is positive, we get a purely imaginary expression:

$$\xi_+ H_- - \xi_- H_+ \approx H_o \, (\xi_+ - \xi_-) = H_o \, 2ie^{\xi x_t} \left\{ \lambda_o \, \cos, (\lambda_o x_t) \right.$$

$$+ \left[\xi - \Lambda_5 - \Pi \quad \Lambda_4 + (1/2 - i \lambda_\infty) \left(\frac{h_\infty}{h_o \, e^{2fx_t}} \right) \right] \tag{5:35}$$

$$\left. \sin \, (\lambda_o x_t) \right\} \qquad \qquad .$$

Therefore free modes of short period can only exist if the Venus atmosphere fulfills the special condition (5:35) above. Since this would be a rather fortuitous circumstance, henceforth we shall exclude the possibility of resonant atmospheric tides.

E. The Green's function

Since our system of equations is linear, we can treat the thermal and gravitational forcings separately, and add the solutions together at the end to obtain the combined effects. The gravitational forcing was treated in the preceding section: if now we leave it out, the lower boundary condition becomes homogenous. Then it becomes convenient for analytical purposes to formulate the response of the atmosphere to a thermal forcing in terms of Green's functions.

For our purposes the Green's function is merely the response produced by a forcing in a thin layer. Consider the heating as a Dirac delta-function at the level $x = x_J$:

$$\delta J\ (x) = \delta J_J\ \delta\ (x - x_J) \qquad , \qquad (5:36)$$

where the latter δ symbol denotes the Dirac function and not a complex variation quantity, while the multiplier δJ_J furnishes the proper dimensions of power per unit mass.

If $x_J < x_t$ so that the heating is in the troposphere, subsituting the above forcing (5:36) into the formula (5:19) and applying the upper boundary condition gives the solution

$$\delta \eta = A\ e^{(\xi + i\,\lambda_o)\ x} + B\ e^{(\xi - i\,\lambda_o)x} \quad , \quad x < x_J$$

$$\delta \eta = A\ e^{(\xi + i\,\lambda_o)\ x} + B\ e^{(\xi - i\,\lambda_o)x}$$

$$+ \frac{\varkappa \delta J_J}{gh_o} \frac{1}{2i\lambda_o} e^{(\xi + i \lambda_o)(x - x_J)} e^{-2fx_J} \qquad (5:37)$$

$$- \frac{\varkappa \delta J_J}{gh_o} \frac{1}{2i\lambda_o} e^{(\xi - i \lambda_o)(x - x_J)} e^{-2fx_J} \quad , \quad x_J < x < x_t$$

$$\delta\eta = C e^{(1/2 + i \lambda_\infty)(x - x_t)} \quad , \quad x > x_t \quad .$$

Note that according to (5:37) above, $\delta\eta$ and $\delta\psi$ suffer an abrupt change in amplitude and phase at the heating level $x = x_J$. Still, we require $\delta\eta$ and $\delta\psi$ to be continuous at the interface $x = x_t$. This matching condition, along with the homogeneous form of the lower boundary condition (5:22), gives for the constants of integration

$$A = - \frac{\varkappa \delta J_J}{gh_o} \frac{1}{2i\lambda_o} e^{-2fx_J} H_- \left[\xi_+ e^{-(\xi + i \lambda_o)x_J} - \xi_- e^{-(\xi - i \lambda_o)x_J} \right]$$

$$\cdot (\xi_+ H_- - \xi_- H_+)^{-1}$$

$$B = \frac{\varkappa \delta J_J}{gh_o} \frac{1}{2i\lambda_o} e^{-2fx_J} H_+ \left[\xi_+ e^{-(\xi + i \lambda_o)x_J} - \xi_- e^{-(\xi - i \lambda_o)x_J} \right]$$

$$\cdot (\xi_+ H_- - \xi_- H_+)^{-1} \qquad (5:38)$$

$$C = \frac{\varkappa \delta J_J}{gh_o} e^{-2fx_J} e^{2\xi x_t} \left[H_+ e^{-(\xi + i \lambda_o)x_J} - H_- e^{-(\xi - i \lambda_o)x_J} \right]$$

$$\cdot (\xi_+ H_- - \xi_- H_+)^{-1} \qquad ,$$

which leads to a surface pressure variation

$$\delta p_o = \bar{\rho}_o \; \delta\psi_o = - \bar{\rho}_o \; \frac{\varkappa\delta J_J}{i\sigma_o} \; e^{-2fx_J} \; H_o \left[\xi_+ \; e^{-(\xi + i \lambda_o)x_J} \right.$$

$$\left. - \; \xi_- \; e^{-(\xi - i \lambda_o)x_J} \right] \; (\xi_+ \; H_- - \xi_- \; H_+)^{-1} \; . \tag{5:39}$$

The response of the atmosphere to a heating at the ground (model VIII) can now be obtained directly by subsituting eq. (4:18) for (5:36) in the results above. Then δJ_J is replaced by $\delta F \frac{g}{po}$, $x_J = 0$, and the surface pressure variation becomes simply

$$\delta p_o = \bar{\rho}_o \; \delta\psi_o = - \bar{\rho}_o \; \frac{\varkappa\delta F}{i\sigma_o} \; \frac{gH_o}{p_o} \; (\xi_+ - \xi_-) \; (\xi_+ \; H_- - \xi_- \; H_+)^{-1}$$

$$= i \; \frac{\varkappa\delta F}{\sigma_o} \; \left(\frac{\xi_+ - \xi_-}{\xi_+ \; H_- - \xi_- \; H_+} \right) \approx i \; \frac{\varkappa\delta F}{\sigma_o H_o} \; . \tag{5:40}$$

For the main semidiurnal mode, eq. (5:40) gives $\delta p_o \approx i \times 2.3$ mb, which corresponds to a substantial torque. Note that the solution (5:40) above is virtually independent of the basic state of the atmosphere; actually this result is still more general, and we shall return to it shortly.

On the other hand if $x_J > x_t$ so that the heating is in the stratosphere, substituting eq. (5:36) into (5:20) yields

$$\delta\eta = A \; e^{(\xi + i \lambda_o)x} + B \; e^{(\xi - i \lambda_o)x} \; , \quad x < x_t$$

$$\delta\eta = C\, e^{(1/2 + i\,\lambda_o)\,(x - x_t)} - \frac{\varkappa\delta J_J}{gh_\infty\,(1 - \frac{i}{\sigma_\infty T})}\,\frac{1}{2i\lambda_\infty}$$

$$\left[e^{(1/2 + i\,\lambda_\infty)\,(x - x_J)} - e^{(1/2 - i\,\lambda_\infty)\,(x - x_J)} \right],\ x_t < x < x_J$$

$$\tag{5:41}$$

$$\delta\eta = C\, e^{(1/2 + i\,\lambda_\infty)\,(x - x_t)}\ ,\quad x > x_J\quad .$$

Applying the boundary and matching conditions again gives

$$A = \frac{\varkappa\delta J_J}{gh_o\,(1 - \frac{i}{\sigma_\infty t})}\ e^{-2fx_t}\ e^{(1/2 - i\,\lambda_\infty)\,(x_t - x_J)}\left(\frac{H_-}{\xi_+\,H_- - \xi_-\,H_+} \right)$$

$$B = \frac{-\varkappa\delta J_J}{gh_o\,(1 - \frac{i}{\sigma_\infty T})}\ e^{-2fx_t}\ e^{(1/2 - i\,\lambda_\infty)\,(x_t - x_J)}\left(\frac{H_+}{\xi_+\,H_- - \xi_-\,H_+} \right)$$

$$\tag{5:42}$$

$$C = A\, e^{(\xi + i\,\lambda_o)x_t} + B\, e^{(\xi - i\,\lambda_o)x_t} + \frac{\varkappa\delta J_J}{gh_\infty\,(1 - \frac{i}{\sigma_\infty T})}\,\frac{1}{2i\lambda_\infty}$$

$$\cdot\left[e^{(1/2 + i\,\lambda_\infty)\,(x_t - x_J)} - e^{(1/2 - i\,\lambda_\infty)\,(x_t - x_J)} \right]\quad .$$

Similarly we find for the surface pressure variation

$$\delta p_o = -\,\bar{\rho}_o\,\frac{\varkappa\delta J_J}{\sigma_o\,(1 - \frac{i}{\sigma_\infty T})}\ e^{-2fx_t}\ e^{(1/2 - i\,\lambda_\infty)\,(x_t - x_J)}$$

$$\tag{5:43}$$

$$\left(\frac{2\,\lambda_o\,H_o}{\xi_+\,H_- - \xi_-\,H_+} \right)\qquad\qquad .$$

We note that eqs. (5:42) and (5:43) above match (5:38)

and (5:39) when the heating is at the tropopause and the

stratospheric damping is neglected ($x_J = x_t$, $1/\tau = 0$).

The effects of heating distribution II can now be found

directly by replacing eq. (5:36) with (4:9), so that δJ_J

becomes $\delta F \dfrac{g}{p_o} e^{x_a}$ and x_J becomes x_a.

A distributed heating $\delta J(x)$ can always be represented

as a generalized linear combination of delta functions:

$$\delta J(x) = \int_0^\infty \delta J(x_J)\, \delta(x - x_J)\, dx_J \qquad (5:49)$$

If the problem is linear with homogenous boundary condition,

the solution is then just the heating distribution convolved with

the response to the delta-function forcing. In particular,

combining the surface pressure variation (5:43) arising from

a delta-function forcing with eq. (4:8) for model I of the heating

yields

$$\delta p_o = -\bar{\rho}_o \int_{x_a}^\infty \frac{\varkappa \delta F_I}{(\sigma_\infty - i/\tau)} \frac{g}{p_o} e^{x_a} e^{(1/2 - i\lambda_\infty)(x_t - x_J)}$$

$$\cdot 2\lambda_o H_o (\xi_+ H_- - \xi_- H_+)\, dx_J \qquad (5:45)$$

$$= -\frac{\bar{\rho}_o}{(1/2 - i\lambda_\infty)} \frac{\varkappa \delta F}{\sigma_o (1 - i/\sigma_\infty \tau)} \frac{g}{p_o} e^{x_a} e^{-2fx_t}$$

$$\cdot e^{(1/2 - i\lambda_\infty)(x_t - x_a)} 2\lambda_o H_o (\xi_+ H_- - \xi_- H_+) \,.$$

Note that the result (5:45) above is the same as for model II of the heating, except δF is replaced by δF $(1/2 - i\lambda_\infty)^{-1}$. This ratio agrees with the numerical calculations, which also show that the Gaussian heating distribution (4:10) of model III has a comparable effect at the ground. This demonstrates that the breadth of the absorption profile in the upper atmosphere generally does not affect the order of magnitude of the resulting surface pressure variations.

We are able to estimate this effect for the main semidiurnal tide by inserting $\delta F \approx \frac{15}{64} \times 500$ W/m^2 into formula (5:45):

$$\left| \delta P_o \right| \approx \frac{15}{64} \times 500 \, \frac{W}{m^2} \, \bar{\rho}_o \, \frac{\varkappa g}{\sigma_o P_o} \, e^{x_a/2} \, e^{-(2f + f/S^2)x_t}$$

$$\approx 10^{-1} \text{ mb} \quad , \tag{5:46}$$

which agrees well with the numerical calculations. The drop in density with height tends to increase the effect of heating high in the atmosphere through the factor $e^{x_a/2}$, but is overcome by the "impedance mismatch" between the stratosphere and the ground represented by the factor $e^{-(2f + \frac{f}{S^2}) x_t}$. Thus the surface pressure variation driven by the direct absorption of sunlight high in the atmosphere is about an order of magnitude too weak to counteract to despinning torque due to body tides.

Heating in the troposphere ought to produce a greater torque because of the slower rotation of the lower atmosphere. The exponential dependence of frequency upon height makes it easy to normalize the diffussive heating profile (4:17):

$$\delta J\,(x) = \delta J_o\; e^{fx}\; e^{-(1+i)\left(\frac{H_o}{D_a}\right)x} \rightarrow \delta J_o = \frac{g}{p_o}\,\delta F$$
$$\cdot\left[1 - f + (1+i)\left(\frac{H_o}{D_a}\right)\right] \quad . \tag{5:47}$$

Convolving (5:47) above with the Green's function (5:39) for the troposphere then gives

$$\delta p_o = -\,\bar{\rho}_o\;\frac{\varkappa\,\delta J_o}{i\sigma_o}\;\left(\frac{H_o}{\xi_+\,H_- - \xi_-\,H_+}\right)\left\{\xi_+\left[2f + \xi + i\,\lambda_o\right]\right.$$
$$\left. + (1+i)\left(\frac{H_o}{D_a}\right)\right]^{-1} - \xi_-\left[2f + \xi - i\lambda_o + (1+i)\left(\frac{H_o}{D_a}\right)\right]^{-1}\right\}, \tag{5:48}$$

where we have neglected the changes at the tropopause. The convective forcing function (4:21) is treated similarly:

$$\delta J\,(x) = \delta J_o\; e^{fx}\; e^{-\varkappa x}\;,\; x < x_c \rightarrow \delta J_o = \frac{g}{p_o}\,\delta F\left[\frac{1 + \varkappa - f}{1 - e^{-(1 + \varkappa - f)x_c}}\right];$$

$$\delta p_o = -\,\bar{\rho}_o\;\frac{\varkappa\delta J_o}{i\sigma_o}\left(\frac{H_o}{\xi_+\,H_- - \xi_-\,H_+}\right)\left\{\xi_+\left[\frac{1 - e^{-(\xi + i\lambda_o + f + \varkappa)x_c}}{\xi + i\lambda_o + f + \varkappa}\right]\right.$$
$$\left. - \xi_-\left[\frac{1 - e^{-(\xi - i\lambda_o + f + \varkappa)x_c}}{\xi - i\lambda_o + f + \varkappa}\right]\right\} \quad . \tag{5:49}$$

It is gratifying to note that numerical evaluations of the above formulae agree very closely with the finite-difference calculations for the same cases.

In the limit where the convective and diffusive layers are much thinner than a scale height ($x_c << 1$ and $D_a << H_o$), the results above reduce to the solution (5:40) for heating at the ground, as expected. As the net heating moves farther from the surface, it ought to become less effective at driving surface pressure variations. However, estimating δp_o from the above formulae gives roughly the same result for thick heated layers ($x_c > 1$ and $D_a > H_o$) as for heating at the ground; the numerical calculations confirm that they are of the same order of magnitude. The single most important parameter controlling the atmospheric tidal torque on Venus is therefore the amount of sunlight absorbed by the ground. In the next chapter, we shall be able to account for this result more simply.

6. Heating at the Ground

In this chapter we derive the tidal effects at the surface independently of the equivalent gravity mode approximation. In this context it is noteworthy that Hinch (1970) obtained essentially the same surface pressure variation as (5:40), by applying a much simpler approach to a strictly isentropic atmosphere corotating with the ground on a cylindrical planet. However, his model was heated radiatively at the top. We can understand why he arrived at the same result as ours for heating at the ground by considering the Green's function for a stationary, adiabatic atmosphere. Using the parameters from (5:34) in eq. (5:43) then gives

$$\delta p_0 = i\bar{\rho}_0 \; \frac{\varkappa}{\sigma - i/\tau} \; \frac{H_0}{H_0 - h_\ell^{\sigma,s}} \int_0^\infty \delta J(x_J) \, e^{-x_J} \, dx_J$$

$$= \frac{\varkappa \delta F}{(\sigma - i/\tau)\left(H_0 - h_\ell^{\sigma,s}\right)}$$

(6:1)

When $1/\tau$ and h/H_0 are neglected, the result (6:1) above is the same as (5:40). Therefore to the extent that the troposphere of Venus can be considered isentropic and stationary, the details of the heating distribution in the lower atmosphere are irrelevant for our purposes, because the same surface pressure variation is obtained no matter how the net absorbed insolation is distributed in such an atmosphere.

Since the result for heating at the ground is so
prominent, we present another derivation which shows how
little formula (6:1) depends on any specific assumptions. We
begin by supposing only that all of the energy absorbed by
the ground is immediately redeposited in a thin layer of air
at the surface. Then the heating distribution becomes the
same as for model VIII:

$$J(x) = \frac{g}{P_o} F \delta (x - 0^+) \quad . \qquad (6:2)$$

We can then substitute the above forcing into the form
(2:24) of the heat equation. Since all tidal fields
(except δJ) must remain finite, integrating (2:24) across
the heated layer gives

$$0 = (i\sigma_o + i/\tau) [\delta\psi (0^+) - \delta\psi (0^-)] - \frac{g}{P_o} \varkappa\delta F \quad . \qquad (6:3)$$

Because h_o/H_o is negligible on Venus (with the possible
exception of the antisymmetric $\sigma = \omega$ mode), the lower
boundary condition reduces to $\delta\eta = 0$ at $x = 0$. Now eq.
(2:23) shows that $\frac{\partial}{\partial x} \delta\eta$ is also finite, so that $\delta\eta$ itself
must furthermore be continous. Therefore $\delta\eta$ vanishes
immediately above the heated layer as well. As long as no
other forcings or free modes are present, $\delta\eta$ vanishes
everywhere. Then by eq. (2:23), $\delta\psi$ must also vanish
everywhere above the boundary layer. (The upper boundary
condition does not enter, because we have dealt with a

system of only first order in height x.) Thus (with the

single possible exception mentioned above) eq. (6:3) gives for

the pressure variation at the ground

$$\delta p_o = \bar{\rho}_o \ \delta\psi \ (0^-) = - \bar{\rho}_o \ \frac{g}{p_o} \ \varkappa\delta F = i \ \frac{\varkappa\delta F}{(\sigma_o - i/\tau)} \ H_o \quad . \qquad (6:4)$$

Formula (6:4) above is essentially the same eq. (5:40)

for heating model VIII, eq. (6:1) for heating anywhere in a

stationary isentropic atmosphere, and the result obtained

by Hinch (1970). Although eq. (6:4) was obtained by

assuming a very shallow heated layer, it is independent of

the assumptions involved in the equivalent gravity mode

approach and of the model atmosphere chosen. Since a surface

pressure variation with the magnitude and phase of (6:4)

above is capable of exerting the dominant torque on the

atmosphere of Venus, we shall adopt this simple formula for a

semiquantitative study of the surface wind field and for

a discussion of the evolution of Venus' rotation.

It is useful to notice that formula (6:4) is equivalent

to the solution of the differential equation

$$\frac{d}{dt} \ P_o + (P_o - \bar{P}_o) \ /\tau_o = - \varkappa \ F/H_o \quad \rightarrow$$

$$P_o \ (t) = P_o \ (0) - \frac{\varkappa}{H_o} \ e^{-t/\tau_o} \int_0^t e^{t'/\tau_o} \ F \ (t') \ dt' \quad . \qquad (6;5)$$

Formula (6:5) above permits us to find the total surface

pressure variation $P_o - \bar{P}_o$, including all Fourier components

δp_o at once, given the time dependence of the insolation

absorbed by the ground. As an example, using the half-
rectified sine wave given by eq. (4:5), with F = 100 W/m^2
at the subsolar point, and neglecting β' and $1/\tau_o$ then yields

$$p_o - \overline{P}_o \approx 19.7 \text{ mb} \cdot \sin \theta \; (\frac{\varphi_\odot}{\pi} - \sin \varphi_\odot), \; -\frac{\pi}{2} < \varphi_\odot < \frac{\pi}{2}$$

$$p_o - \overline{P}_o \approx 19.7 \text{ mb} \cdot \sin \theta \; (\frac{\varphi_\odot}{\pi} - 1), \; \frac{\pi}{2} < \varphi_\odot < \frac{3\pi}{2} \quad . \quad (6:6)$$

This variation in surface pressure in depicted in Figure 9
as a set of isobars on a grid of latitude and longitude
relative to the subsolar point. The solid curves denote
a pressure greater than or equal to the mean, while the
dashed lines represent negative values of the pressure
variation; the contour interval is one millibar. This pattern
migrates eastward (right) with the sun so that the solid
surface is moving toward the west (left) relative to this
map. Note that the pressure is high on the morning side
and low in the afternoon, so that the sun does indeed exert an
accelerating torque on the atmosphere.

Given formula (6:4) for the surface pressure variations,
it is simple to use eqs. (2:21) and (2:22) in order to find
the tidal wind field at the surface. For example, supposing
that $\omega_o = \omega_\varphi$ so that on the average the lowest layers of the
atmosphere are corotating with the ground, the surface winds
for the same case as (6:6) then become

$$\delta u_o = i \; \frac{\delta P_o}{a \; \overline{\rho}_o} \; \left[\frac{\sigma \cos \theta + 2 \, s\omega \; \cos \theta}{(\sigma^2 - 4\omega^2 \cos^2 \theta)\sin \theta} \right]$$

$$(6:7)$$

$$\delta v_o = - \; \frac{\delta P_o}{a \; \overline{\rho}_o} \; \left[\frac{\sigma \, s + 2\omega \cos^2 \theta}{(\sigma^2 - 4\omega^2 \cos^2 \theta)\sin \theta} \right]$$

Figure 9

Surface pressure and temperature variations, no damping ($1/\tau = 0$)

Figure 10

Surface wind field, no damping ($1/\tau = 0$)
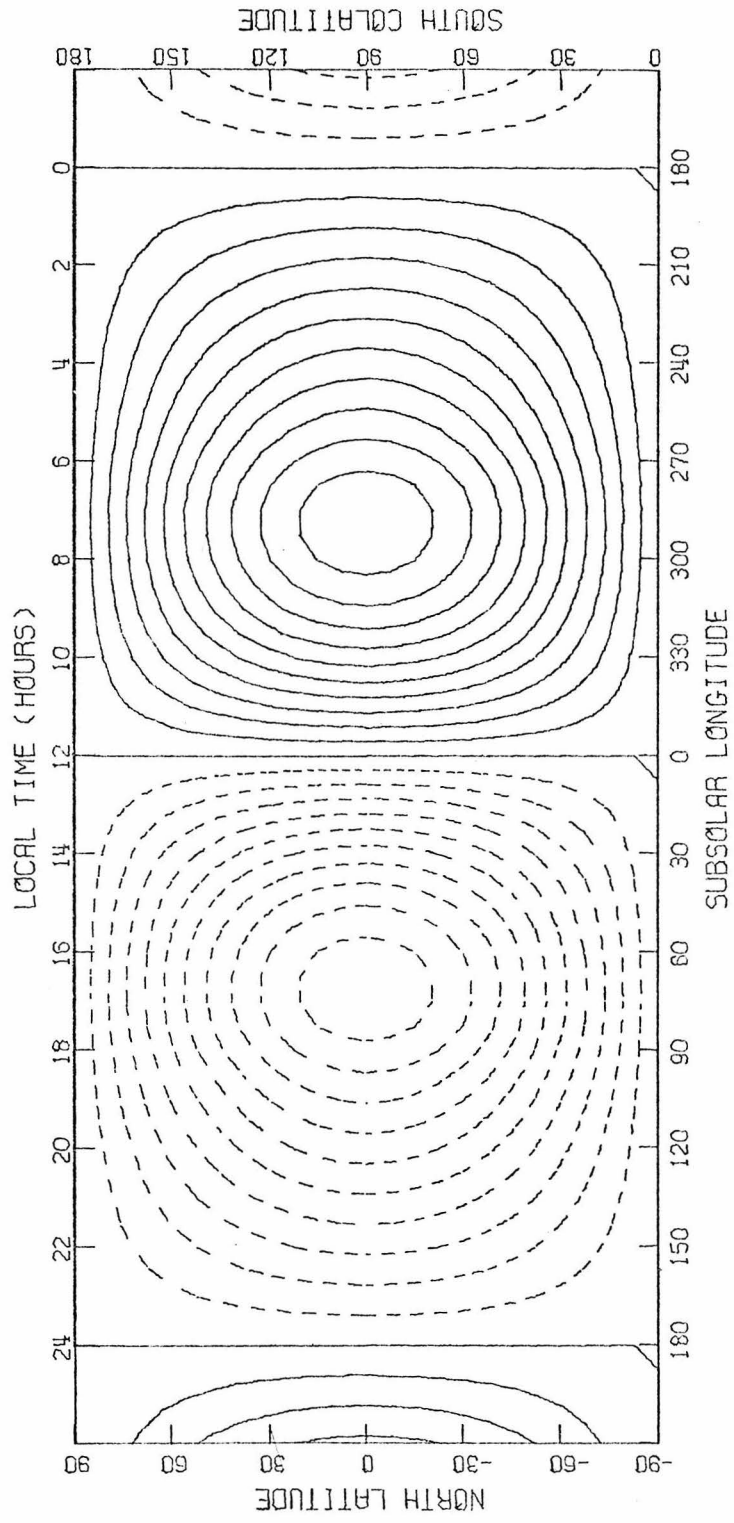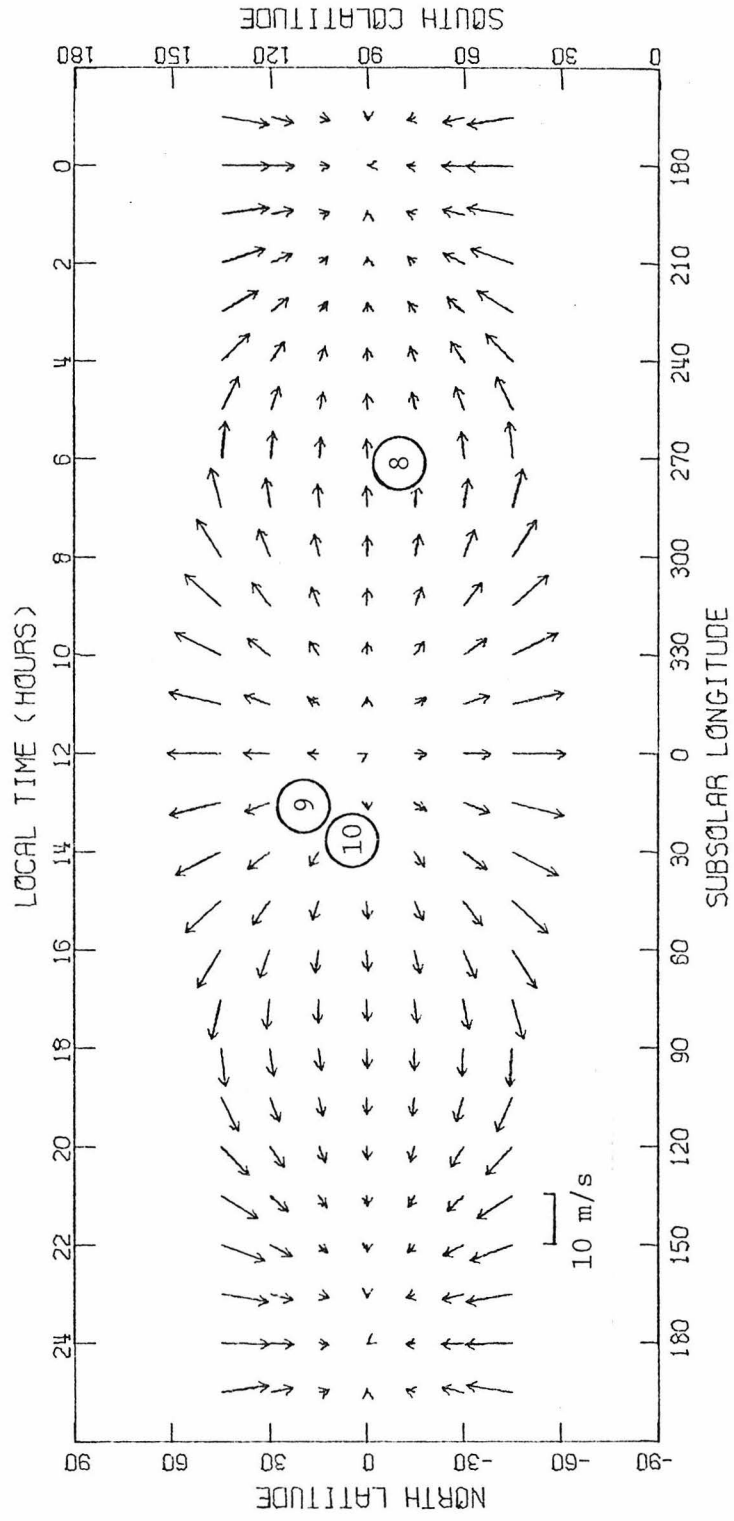
This wind field is mapped in Figure 10, corresponding with Figure 9 for the undamped surface pressure field. The lengths of the arrows are proportional to the wind speeds (the scale is given at the lower left of the figure). Their orientations give the correct direction relative to the local meridian, but it is interesting to note that these arrows do not represent displacements accurately; the zonal wind components are de-emphasized at high latitudes in this projection. The winds are only plotted up to a latitude of $\pm\ 45°$, because the speed and direction of the wind are finite but undefined at the poles; however, this is only an artifact of the simple heating distribution which does not take the "airmass effect" into account. It is evident from the figure that near the ground the subsolar point is a region of divergence, while the antisolar point is an area of convergence.

The landing sites of the Venera 8, 9, and 10 probes relative to the subsolar coordinates are indicated in Fig. 10 by small circles. Surface wind speeds measured by the Venera 9 and 10 anemometers averaged $\sim$ 0.5 m/s and 1.0 m/s, respectively (Avduevskii et al., 1976b), while radar tracking of Venera 8 gives an upper limit of $\sim$2 m/s near the ground (Marov et al. 1973). Inspection of the figure suggests that the observed winds are several times slower than eq. (6:7) predicts. However the anemometers on the Venera 9 and 10 landers were mounted only

about one meter off the ground, undoubtedly well within the frictional boundary layer, so that such measurements are not conclusive.

The expressions (6:7) for the surface winds are not easy to integrate analytically for all components at once, except at the equator where the zonal component is proportional to the pressure variation:

$$v_o = -\frac{(P_o - \overline{P_o})}{\overline{\rho}_o \, v_\odot} \qquad (6:8)$$

Here $v_\odot = a(\omega_{\venus} + n) \approx 3.76$ m/s is the speed at which the subsolar point travels eastward over the surface of Venus. However, when $1/\tau_o$ and β' are neglected so that eq. (6:6) applies, the peak surface wind speed given by (6:8) above is 4.50 m/s occurring at about 71° away from the subsolar point. Since this exceeds $v_\odot$, the relative motion of the sun, a critical region might develop on the morning side where the frequency of the forcing felt by the gas locally vanishes. Strictly speaking, this is inconsistent with the original linearization fundamental to all tidal theories, and suggests that either nonlinear effects or substantial damping may occur.

In addition to the critical phenomena suggested above, friction with the ground must tend to reduce the surface winds. Our formulae really apply only above the frictional

boundary layer, provided that it is thinner than the heated

layer. Other effects which might conspire to reduce the

amplitude and phase of the surface pressure variation

include turbulent viscosity and the development of baroclinic

or other instabilities in the tidal fields. For the sake of

simplicity, we choose to parameterize all of these unmodeled

effects by means of a Newtonian cooling. A thermal time constant

τ comparable to the forcing period has a substantial impact

on the tidal fields, as Figures 11 and 12 illustrate.

These are the same as Figures 9 and 10, except that now we

have included a Newtonian cooling with $\tau \approx 10$ days. It is

evident that a substantial damping both

reduces the amplitude of the tidal variations, and alters

their phases so that the dynamic response of the atmosphere

comes to resemble a static situation. This ought to remain

qualitatively true for any dissipative mechanism. Damping

of the atmospheric tides can also have important effects

on the rotation of Venus, as shown in the remainder of

this work.

Figure 11

Surface pressure and temperature variations,

damping included (τ = 10 days)

Figure 12

Surface wind field, damping included (τ = 10 days)
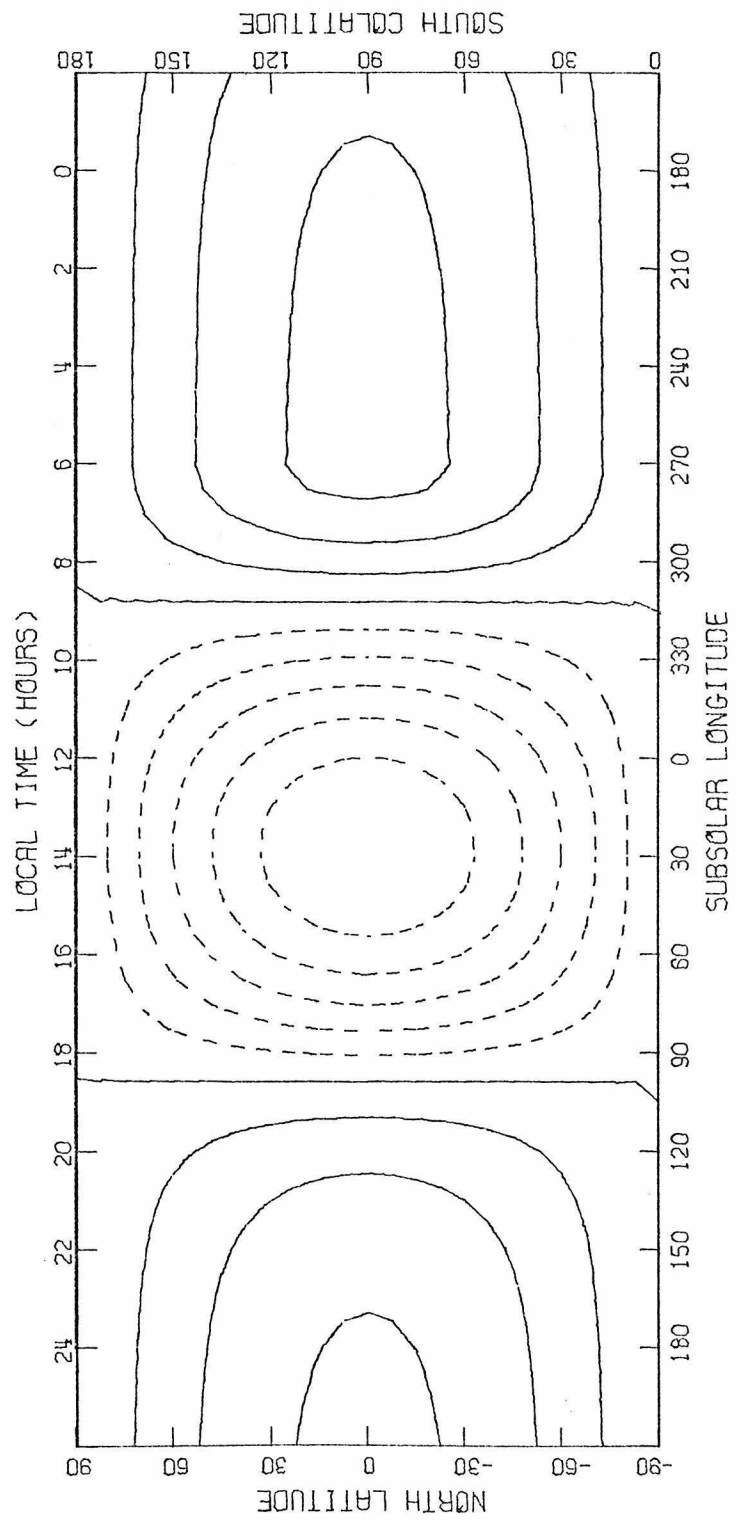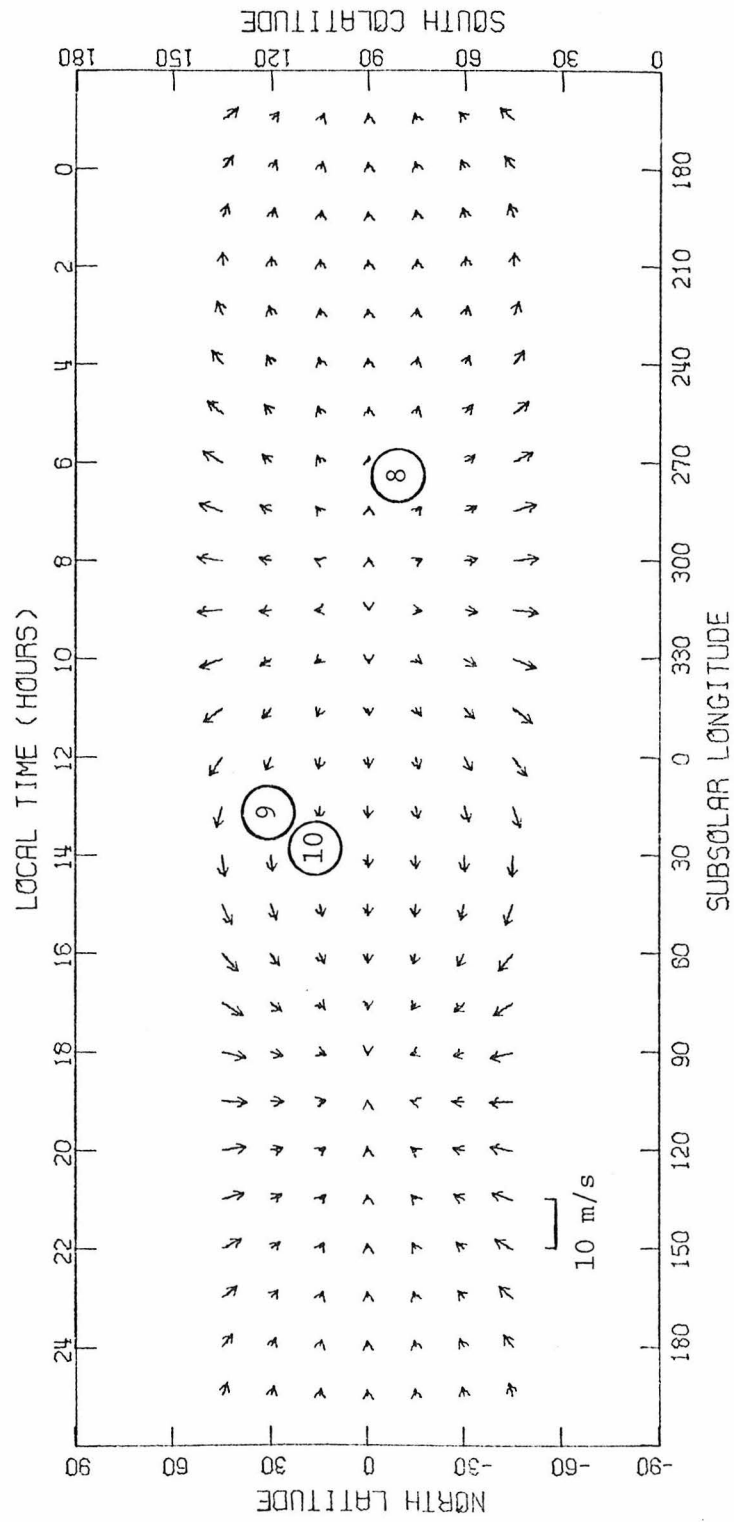
7. Tidal Torques and Conclusions

The sun's gravitational influence exerts torques on both the body and atmosphere of Venus, which are evaluated in this chapter. At the surface of Venus, the solar tidal potential may be written

$$\Omega_\odot = - \frac{3}{2} GM_\odot \frac{a^2}{r^3} (\cos^2 \zeta - \frac{1}{3}) \approx - 5.75 \frac{J}{kg} (\cos^2 \zeta - \frac{1}{3}) \quad . \quad (7:1)$$

Here G is the universal constant of gravitation, $M_\odot$ is the mass of the sun, a is the radius of Venus, r is the distance between Venus and the sun, and ζ is the local zenith angle of the sun.

For simplicity, we neglect the orbital eccentricity so that r is taken as constant. Furthermore we assume an obliquity of exactly 180° ($\beta' = 0$). These restriction will be relaxed somewhat in Part II of this work. Meanwhile, eq. (7;1) above may be simplified by substitution from eq. (4:4):

$$\Omega_\odot = - \frac{3}{2} GM_\odot \frac{a^2}{r^3} (1/2 \sin^2 \theta \cos 2\varphi_\odot + 1/2 \sin^2 \theta - 1/3). \quad (7:2)$$

The colatitude θ is still measured northward from the pole, while the new longitude $\varphi_\odot$ is measured westward from the subsolar point.

The solar tidal potential $\Omega_\odot$ raises a bulge in the surface of Venus whose height Z is given by

$$Z(\theta, \varphi_\odot) = -\frac{j}{g} \Omega_\odot (\theta, \varphi_\odot - \frac{\epsilon}{2}) \qquad . \qquad (7:3)$$

The phase lag ϵ arises because internal dissipation retards the time of high tide. This tidal bulge generates its own gravitational potential

$$\Omega_o (\theta, \varphi_\odot) = k (\frac{a}{d})^3 \Omega_\odot (\theta, \varphi_\odot - \frac{\epsilon}{2}) \qquad , \qquad (7:4)$$

falling off as the inverse cube of the distance d from the center of Venus. Self-gravitation is negligible in the atmosphere, so that the total tidal potential is just $\Omega = \Omega_\odot + \Omega_o$. The induced potential interacts in turn with the mass of the sun. By reaction, the sun exerts a torque on the tidal bulge, given by

$$(\text{body torque}) = M_\odot (\frac{a}{r})^3 \frac{\partial}{\partial \varphi_\odot} \Omega_o (\frac{\pi}{2}, 0)$$

$$= -\frac{3}{2} k \, GM_\odot^2 \frac{a^5}{r^6} \sin \epsilon \approx -2.0 \times 10^{18} \, J \times \frac{k}{Q} \qquad . \qquad (7:5)$$

The negative sign appearing above means that the body torque tends to reduce the rotation rate.

The constants j and k in the above formulae are called the Love numbers for height and potential, respectively, while $Q = \cot \epsilon$ is known as the tidal "quality factor". Presuming that Venus has the same internal distribution of density and rigidity as the Earth, the terrestrial values of the Love numbers (Munk and MacDonald, 1975) may be rescaled

to j ≈ .51 and k ≈ .25 for Venus. If Venus has zero rigidity, we may use the Love numbers j ≈ 1.96, k ≈ .96 for a fluid Earth (Munk and MacDonald, 1975). Scaling Q is more dubious, but values comparable with the other terrestrial planets may be expected: Q ≈ 80 for Mars, (Smith and Born, 1976), derived from the secular acceleration of Phobos; Q ≈ 10 for the Moon (Yoder et al., 1978), from an offset in the Cassini state (see chapter 7 of Part II); and 30 ≤ Q ≤ 100 for the solid Earth (Munk and MacDonald, 1975), from damping of the Chandler wobble. However, the lunar and terrestrial values quoted above may include nontidal effects due to core—mantle friction or to other sources of dissipation which tend to reduce the apparent Q, as discussed in chapter 7 of Part II.

wobble. However, the latter two values may be too low, because of   core—mantle friction (also discussed in chapter 7 of Part II), or other effects.

The sun exerts a net torque on the atmosphere as well, given by the volume integral of $-\rho \frac{\partial}{\partial \varphi_\odot} \Omega_\odot$. By virtue of the hydrostatic law (2:1), the integral over altitude z may be converted to one over pressure p. Since $\Omega_\odot$ does not change sensibly through the depth of the atmosphere (H ≪ a), the integral can then be evaluated in terms of the pressure p_Z at the ground z = Z:

$$(\text{atmospheric torque}) = - \int_0^{\pi} \int_0^{2\pi} \int_Z^{\infty} \left(\frac{\partial}{\partial\varphi_\odot} \Omega_\odot\right) \rho dz \, a \, d\varphi_\odot \, a \sin\theta d\theta$$

$$(7:6)$$

$$= - \int_0^{\pi} \int_0^{2\pi} \int_{pZ}^{0} \left(\frac{\partial}{\partial\varphi_\odot} \Omega_\odot\right) \rho \left(-\frac{dp}{g\rho}\right) a \, d\varphi_\odot \, a \sin\theta d\theta$$

$$= - \int_0^{\pi} \int_0^{2\pi} \left(\frac{\partial}{\partial\varphi_\odot} \Omega_\odot\right) \left[\frac{p_Z}{g}\right] a \, d\varphi_\odot \, a \sin\theta d\theta \quad .$$

When $\left(\frac{\partial}{\partial\varphi_\odot} \Omega_\odot\right)$ is written out in full, and the Fourier decomposition (2:7) is applied to the surface pressue p_Z, it is apparent that only the imaginary part of the semidiurnal pressure variation contributes to the net torque:

$$(\text{atmospheric torque}) = - \int_0^{\pi} \int_0^{2\pi} \frac{3}{2} \frac{GM_\odot}{g} \frac{a^4}{r^3} \sin^2\theta \sin 2\varphi_\odot$$

$$\left\{\overline{p}_o + \sum_{\sigma,s} \left[\text{Real} (\delta p_Z^{\sigma,s}) \cos (s\varphi_\odot) - \text{Im} (\delta p_Z^{\sigma,s}) \sin (s\varphi_\odot)\right]\right\}$$

$$d\varphi_\odot \sin\theta d\theta \qquad (7:7)$$

$$= \frac{3}{2} \frac{M_\odot}{M_o} \frac{a^6}{r^3} \int_0^{\pi} \int_0^{2\pi} \text{Im} (\delta p_Z^{\sigma,s}) \sin^2(2\varphi_\odot) \, d\varphi_\odot \sin^3\theta d\theta$$

$$= \pi \frac{3}{2} \frac{M_\odot}{M_o} \frac{a^6}{r^3} \int_0^{\pi} \text{Im} (\delta p_Z^{\sigma,2}) \sin^3\theta d\theta \quad .$$

The pressure variation appearing in eq. (7:7) above is

still a function of the colatitude θ. By analogy with the Earth, Gold and Soter (1969) estimated $\delta p_Z^{\sigma,2}(\theta) = \delta p_Z^{\sigma,2}(\frac{\pi}{2}) \sin^3\theta$; the resulting integral of $\sin^6\theta \, d\theta$ in eq (7:7) yields a factor of $\frac{5}{16}\pi$. On the other hand, the equivalent gravity mode approach defined in chapter 5 assumes $\delta p_Z^{\sigma,2}(\theta) = \delta p_Z^{\sigma,2}(\frac{\pi}{2}) \sin^2\theta$, so that the net torque on the atmosphere becomes simply

$$\text{(atmospheric torque)} = \pi \frac{3}{2} \frac{M_\odot}{M_o} \frac{6}{r^3} \, \text{Im}\left(\delta p_Z^{\sigma,s}(\frac{\pi}{2})\right) \int^\pi \sin^5\theta \, d\theta \tag{7:8}$$

$$= \pi \frac{3}{2} \frac{M_\odot}{M_o} \frac{6}{r^3} \, \text{Im}\left(\delta p_Z^{\sigma,s}(\frac{\pi}{2})\right) \cdot \frac{16}{15} \approx 7.95 \times 10^{13} \, m^3 \, \text{Im}\left(\delta p_Z^{\sigma,s}(\frac{\pi}{2})\right).$$

This approach was used for numerical calculations of the surface pressure variations, as described in chapter 5; the resulting values for $\delta p_Z^{\sigma,2}(\frac{\pi}{2})$ are listed in Table 3 under the synodic semidiurnal mode ($\sigma = 2\omega + 2n$).

According to formula (6:4), the surface pressure variation $\delta p_Z^{\sigma,s}$ has the same latitudinal structure as the insolation $\delta F^{\sigma,s}$ when the heating at the ground model applies. If δF is distributed as $\cos\theta$ on the sunlit side, substituting the expansion (4:5) into eq. (7:7) then yields

$$\text{(atmospheric torque)} = \pi \frac{3}{2} \frac{M_\odot}{M_o} \frac{a^6}{r^3} \, \text{Im}\left(\delta p_Z^{\sigma,s}(\frac{\pi}{2})\right) \int_0^\pi \sin\theta \, d\theta$$

$$= \pi \frac{3}{2} \frac{M_\odot}{M_o} \frac{a^6}{r^3} \, \text{Im}\left(\delta p_Z^{\sigma,s}(\frac{\pi}{2})\right) \cdot \frac{3}{8}\pi \tag{7:9}$$

$$= \pi \frac{3}{2} \frac{M_\odot}{M_o} \frac{a^6}{r^3} \frac{2}{3\pi} \frac{\varkappa F_\odot}{\sigma_o H_o} \left(\frac{1}{1 + \sigma_o^{-2} \tau_o^{-2}}\right) \frac{3}{8}\pi$$

$$\approx \frac{1.8 \times 10^{16} \, J}{1 + (2\omega+2n)^{-2} \tau_o^{-2}} \quad .$$

The net solar torque on the atmosphere is transmitted to the body of Venus in two ways. Following an idea by G. Colombo (private communication, 1978), when the body phase lag is neglected, it is easy to show that the atmospheric pressure distribution exerts an accelerating torque on the tidal bulge in the surface of Venus, which is just the height Love number j times the net solar torque on the atmosphere from eq. (7:6). However, in order for the atmospheric circulation to be steady (over a time scale of $\sim 10^3$ years), the remainder of the net torque on the atmosphere must be transmitted to the crust. Reynolds stresses vanish at the lower boundary, but sufficient frictional coupling would be produced by mean zonal wind speeds on the order of 1 cm/s at the ground (Hinch, 1970).

If the rotation of the crust is also steady over geologic time, the atmospheric and body tidal torques must balance (or nearly so if the rotation of Venus is resonant with the orbit of the Earth). Comparison of eqs. (7:5) and (7:9) shows that the atmospheric and body tides balance if

$$Q \approx \frac{2.0 \times 10^{18} \text{ J}}{1.8 \times 10^{16} \text{ J}} \cdot k \left[1 + (2\omega_o \tau_o + 2n \tau_o)^{-2} \right] \approx 28 \quad , \quad (7:10)$$

where we have set k = .25 and neglected $1/\tau_o$.

Figure 13, after Gold and Soter (1969), shows the various torques on Venus as functions of the diurnal frequency $\frac{2\pi}{\omega + n}$

Figure 13

Torques on Venus versus rotation rate. Horizontal
line: body tidal torque for Q = 30 = constant. Vertical
spikes: Earth resonances. Curve: atmospheric
tidal torque.
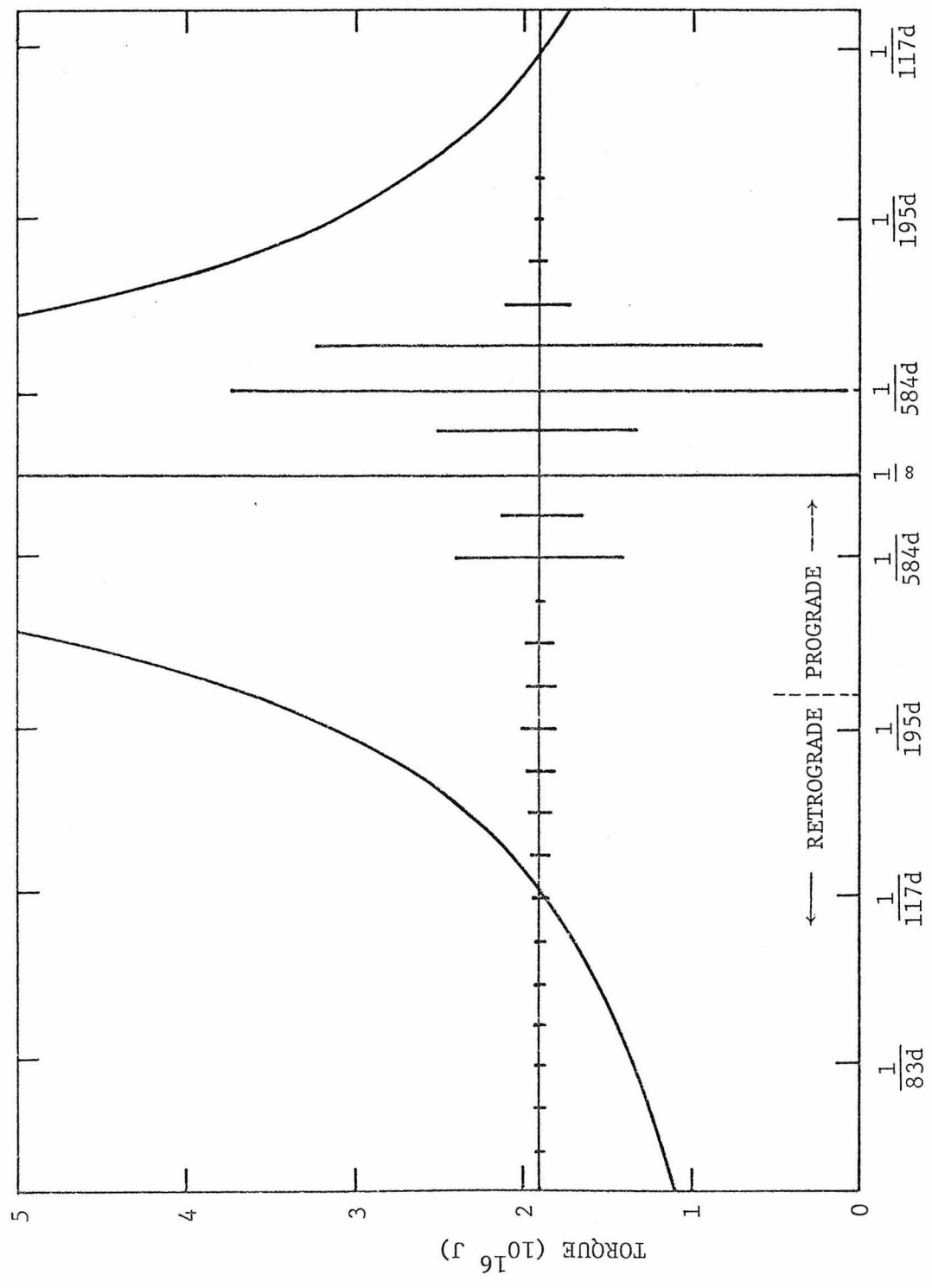
(the inverse of the solar day). The curve shows the torque due
to atmospheric tides, using eq. (7:9) for heating at the ground
with $1/\tau_0 = 0$, so that damping and nonlinearities are neglected.
Then the atmospheric torque varies as the inverse of the frequency
The horizontal line represents the magnitude of the body tidal
torque, assuming Q = constant $\approx$ 30. The vertical spikes on this
line give the strengths of the spin resonances with the Earth,
using the terrestrial value of 2.2 x 10^{-5} ($= \frac{B-A}{C}$, where A $\leq$ B $\leq$ C
are the principal moments of inertia) for the permanent gravita-
tional quadrupole moment of Venus.

The body tides tend to despin the planet towards synchronous
rotation, while the atmospheric tides tend to drive it away.
Where the two curves cross in the figure, the net torque on
the planet vanishes. This is a position of stable equilibrium
with respect to changes in period, since the frequency dependence
of the torque tends to return any changed value of the rotation
rate back to the equilibrium state. Thus Venus could have
begun with a rapid retrograde rotation and been gradually
despun by body tides, evolving to the right in the figure, until
the increasing influence of atmospheric tides overcame the
body tidal torque, and Venus remained with a slow retrograde
rotation as in the present day.

In despinning from a rapid retrograde rotation, Venus would have to pass through a number of special rotation rates corresponding to resonances between the spin of Venus and the orbit of the Earth. Currently the rotation period of Venus is very close, but apparently not equal, to one of these resonant values (Shapiro et al., 1978). If Venus does in fact occupy this resonance, its special rotation rate can only be maintained if the interaction between the Earth and the permanent quadrupole moment of Venus is stronger than the sum of the other torques on the planet. For the value of $\frac{B-A}{C}$ used to draw Fig. 13, the Earth's influence is about an order of magnitude too weak to overcome the net tidal torque, unless the atmospheric and body tides cancel near the resonant frequency. In that case, the present rotation rate of Venus may be explained as a balance among all three influences.

However, none of the above effects can provide Venus with a sufficient mechanism for capture into a resonance of this kind. According to Goldreich and Peale (1967, 1970), viscous coupling between the hypothetical core and mantle of Venus may supply the required dissipation. It is interesting to speculate that once Venus had evolved to a balance between the atmospheric and body tides, small variations in its orbital eccentricity or changes in its climate might have driven the

equilibrium across the resonant period many times, until capture finally occurred.

Finally, note that there are actually two equilibrium states shown in Fig. 13, corresponding to prograde and retrograde spins with the same diurnal period. Why should Venus occupy the retrograde state and not the prograde one? This problem really has a third dimension, the obliquity; when this is taken into account many equilibria can occur at all possible obliquities. Part II of this work will address these questions, along with several other problems concerning the rotation of Venus.

THE ROTATION OF VENUS

PART II. OBLIQUITY AND EVOLUTION

1. The Obliquity of Venus

The theory developed in Part I provides a means of
calculating the net tidal torque on the atmosphere of Venus.
The conclusions show that the planet's observed rotation
period may represent a balance between the torques due to
atmospheric and body tides, as well as possibly a spin
resonance with the orbit of the Earth. Actually, the problem
involves a third dimension, the obliquity, not adequately
dealt with in Part I. When another degree of freedom is
included, the current spin state may become unstable, while
other stable and unstable equilibria can appear at all
obliquities. Part II considers not only these aspects of the
present spin, but also the whole history of the rotation
of Venus.

Chapter 2 following describes the basic technique for
treating arbitrary obliquities, while chapter 3 develops the
theory of linear body tides. In chapter 4 the results of Part I
are used to generalize the theory of atmospheric tides to
obliquities other than 180°. The possibility of spin resonances
with either the Earth or the sun is studied in chapter 5,
while chapter 6 explores the effects of precession, nutation,
core-mantle friction, and other phenomena. Finally chapter
7 arrives at the conclusions that Venus has probably always
spun retrograde, and that core-mantle friction may play an
important role in maintaining its current obliquity.

2. Coordinates and Equations of Motion

Goldreich and Peale (1970) have developed an elegant formalism for investigating the rotation of Venus. We shall follow their method closely and obtain results which can be compared directly with theirs.

Define two right-handed Cartesian coordinate systems: a set of inertial axes $(\hat{I}, \hat{J}, \hat{K})$, where $\hat{K}$ lies in the direction of the orbital angular momentum of Venus, and a set of axes $(\hat{i}, \hat{j}, \hat{k})$ fixed to the body of Venus along the directions of the principal moments of inertia (A, B, C). We further define the (northern vernal for Venus) equinox $e = \dfrac{\hat{K} \times \hat{k}}{|\hat{K} \times \hat{k}|}$ as the "ascending mode" of the $(\hat{i}, \hat{j})$ plane on the $(\hat{I}, \hat{J})$ plane, and the usual Euler angles α, β, γ, where $\cos \alpha = \hat{I} \cdot \hat{e}$, $\cos \beta = \hat{K} \cdot \hat{k}$, and $\cos \gamma = \hat{e} \cdot \hat{i}$ (see Fig. 1). The Euler angles can be used to transform between inertial and body coordinates as follows:

$$\hat{i} = \hat{I} \, [\cos \alpha \cos \gamma - \sin \alpha \cos \beta \sin \gamma]$$
$$+ \hat{J} \, [\sin \alpha \cos \gamma + \cos \alpha \cos \beta \sin \gamma]$$
$$+ \hat{K} \, \sin \beta \sin \gamma$$

$$\hat{j} = \hat{I} \, [- \cos \alpha \sin \gamma - \sin \alpha \cos \beta \cos \gamma]$$
$$+ \hat{J} \, [- \sin \alpha \sin \gamma + \cos \alpha \cos \beta \cos \gamma]$$
$$+ \hat{K} \, \sin \beta \cos \gamma$$

(2:1)

Figure 1

Coordinates and Euler angles
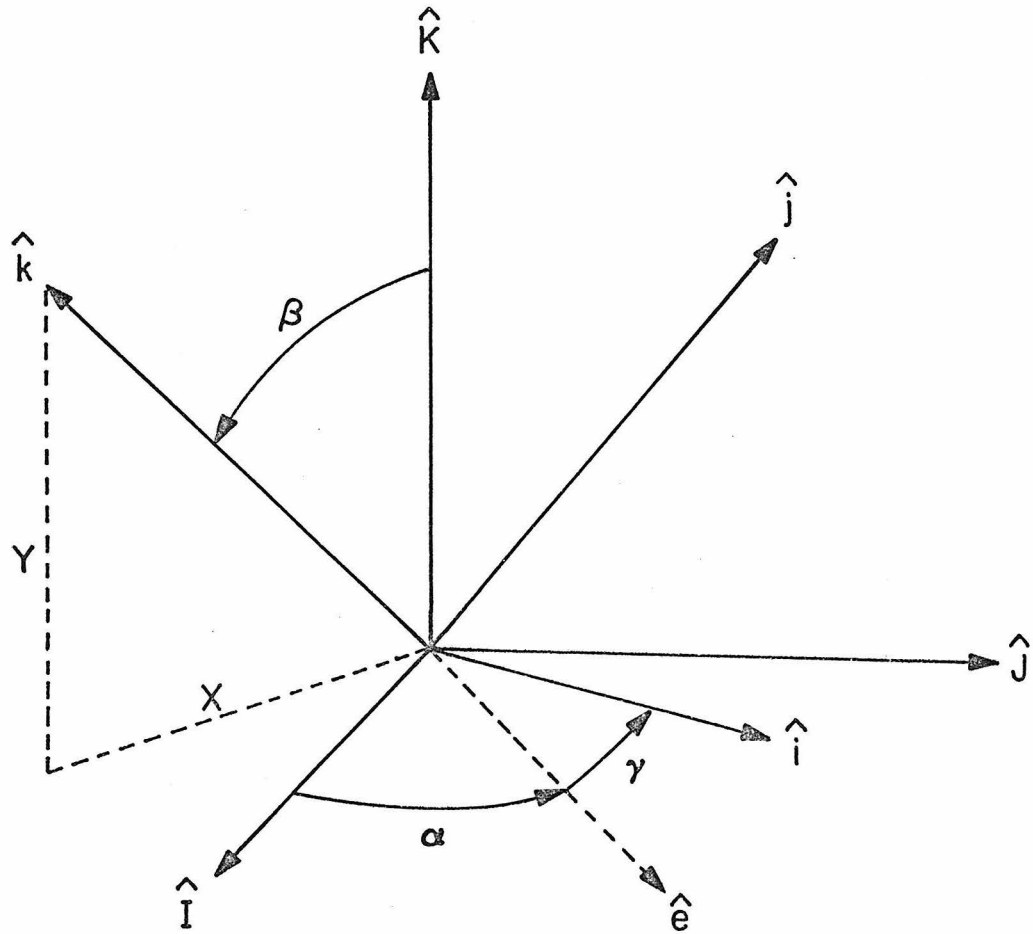
$$\hat{k} = \hat{i} \; \sin \alpha \; \sin \beta - \hat{j} \cos \alpha \; \sin \beta \div \hat{K} \cos \beta \qquad .$$

The planetocentric colatitude θ and longitude φ are measured from the $\hat{k}$ and $\hat{i}$ axes, respectively, as shown in Fig. 2 of Part I. Then a point $\vec{a} = a \; \hat{a}$ on the surface of Venus may be located by

$$\hat{a} = \hat{i} \; \sin \theta \; \cos \varphi + \hat{j} \; \sin \theta \; \sin \varphi + \hat{k} \; \cos \theta \qquad . \qquad (2:2)$$

Now let $\vec{r} = r \; \hat{r}$ be the position of the sun relative to Venus in the orbit plane. When the small orbital eccentricity is neglected, both the distance r and the orbital angular velocity n are constant. If the origin of time t is then chosen so that $\hat{r} = \hat{I}$ at $t = 0$, we may write simply

$$\hat{r} = \hat{i} \; \cos \; nt + \hat{j} \; \sin \; nt \qquad . \qquad (2:3)$$

The problem is simplified considerably by assuming that Venus always rotates about $\hat{k}$, its axis of greatest moment of inertia, C; this will be justified a posteriori in chapter 6. Then β becomes the obliquity, currently near 180°; recall that $0 \le \beta \le 180°$. Let the inertial rate of rotation be ω, counterclockwise about $\hat{k}$, so that the spin angular momentum of Venus is $\omega \; C \; \hat{k}$.

By applying the Hamilton-Jacobi technique of analytical dynamics under the above assumptions, Goldreich and Peale (1970) obtained the equations of motion governing the system:

$$\frac{d}{dt} (\omega C) = -\frac{\partial H}{\partial \gamma} \tag{2:4}$$

$$\frac{d\beta}{dt} = \frac{1}{\omega C} \frac{1}{\sin\beta} \frac{\partial H}{\partial \alpha} - \frac{1}{\omega C} \frac{\cos\beta}{\sin\beta} \frac{\partial H}{\partial \gamma} \tag{2:5}$$

$$\frac{d\alpha}{dt} = -\frac{1}{\omega C} \frac{1}{\sin\beta} \frac{\partial H}{\partial \beta} \tag{2:6}$$

$$\frac{d\gamma}{dt} = \frac{\partial H}{\partial (\omega C)} - \frac{1}{\omega C} \frac{\cos\beta}{\sin\beta} \frac{\partial H}{\partial \beta} \tag{2:7}$$

(Goldreich and Peale's (1970) eq. (5) contains a sign error, in (2:4) above, while their eq. (6) contains an extra term dropped from (2:7).)

The Hamiltonian for the rotation of Venus may be written

$$H (\omega C, \alpha, \beta, \gamma) = 1/2 \; \omega^2 C + 1/2 \; \omega^2 \Delta C + U + V + W \quad . \tag{2:8}$$

The first term in (2:8) above describes unperturbed steady rotation; when $H = 1/2 \; \omega^2 C$, the equations of motion become simply

$$\frac{d\omega}{dt} = \frac{d\beta}{dt} = \frac{d\alpha}{dt} = 0 \quad , \quad \frac{d\gamma}{dt} = \omega \quad . \tag{2:9}$$

Variations in γ itself are not of much interest, so eq. (2:7) will not be considered further. Meanwhile $\frac{d\alpha}{dt}$ represents axial precession, so discussion of eq. (2:6) will be postponed until chapter 6. It remains to examine the effects on ω and β of the other terms in the Hamiltonian.

The second term in (2:8) represents the contribution to the kinetic energy of rotation, due to changes in the moment of inertia induced by the tides. When the orbital eccentricity is neglected (and the missing exponent 5 is supplied on the planet's radius), equation (12) of Goldreich and Peale (1970) becomes, in our notation,

$$1/2 \; \omega^2 \Delta C = k_o \; \frac{\omega^2}{3} \; \frac{M_\odot \; a^5}{r^3} \; (3/4 \sin^2 \beta - 1/2) \quad . \qquad (2{:}10)$$

Here k_o is the secular (zero frequency) Love number for a second-degree potential. Note that expression (2:10) above contains neither α nor γ, so that according to (2:4) and (2:5) it cannot affect ω or β. Additional contributions to the Hamiltonian can arise from changes in the mean moments of inertia caused either by tectonic processes or by tidal despinning, but these are negligible, since much greater changes in the angular velocity occur over the same timescale (Goldreich and Peale, 1970; Goldreich and Toomre, 1969). Henceforth C will be considered constant.

The term U appearing in (2:8) represents the gravitational potential energy associated with tides in the body of Venus, while V is the interaction between external potentials and its permanent gravitational quadupole moment. We have also added the term W to take atmospheric tides into account. The next three chapters will examine the effects of these terms on the obliquity and rotation rate of Venus.

3. Body Tides

A. The component tides

The gravitational influence of the sun creates a tidal potential $\Omega_\odot$ at the surface of Venus, given to lowest order in $(\frac{a}{r})$ by eq. (7:1) of Part I:

$$\Omega_\odot = - GM_\odot \frac{a^2}{r^3} \frac{3}{2} (\cos^2 \zeta - \frac{1}{3}) \tag{3:1}$$

The tidal potential may be expanded as a multiply periodic function of time; this approach is traditionally associated with Sir George Darwin. Since the orbital eccentricity has been neglected, the solar zenith angle ζ can be found by using the coordinate transformation (2:1) to form the scalar product of eqs. (2:2) and (2:3):

$$\cos \zeta = \hat{a} \cdot \hat{r} = 1/2 (1 + \cos\beta) \sin \theta \cos (\varphi + \gamma + \alpha - nt)$$
$$+ 1/2 (1 - \cos \beta) \sin \theta \cos (\varphi + \gamma - \alpha + nt) + \sin \beta \tag{3:2}$$
$$\cos \theta \sin (\alpha - nt) .$$

To first order in $\beta' = 180° - \beta$, (3:2) above is equivalent to eq. (4:4) of Part I. Squaring (3:2) and collecting terms ultimately yields

$$\cos^2 \zeta = [\frac{1}{3} - \frac{1}{3} (\frac{3}{2} \cos^2 \beta - \frac{1}{2}) (\frac{3}{2} \cos^2 \theta - \frac{1}{2})]$$
$$+ [- \frac{1}{2} \sin^2 \beta (\frac{3}{2} \cos^2 \theta - \frac{1}{2})] \cos (2\alpha - 2nt)$$
$$+ [- \sin \beta \cos \beta \sin \theta \cos \theta] \sin (\varphi + \gamma) \tag{3:3}$$
$$+ [\frac{1}{2} \cos \beta (1 + \cos \beta) \sin \theta \cos \theta] \sin (\varphi + \gamma + 2\alpha - 2nt)$$
$$+ [- \frac{1}{2} \sin \beta (1 - \cos \beta) \sin \theta \cos \theta] \sin (\varphi + \gamma - 2\alpha + 2nt)$$

$$+ [\frac{1}{4} \sin^2 \beta \sin^2 \theta] \cos (2\varphi + 2\gamma) \tag{3:3}$$

$$+ [\frac{1}{8} (1 + \cos \beta)^2 \sin^2 \theta] \cos (2\varphi + 2\gamma + 2\alpha - 2nt)$$

$$+ [\frac{1}{8} (1 - \cos \beta)^2 \sin^2 \theta] \cos (2\varphi + 2\gamma - 2\alpha + 2nt) \quad .$$

Equation (3:3) above shows that the tidal potential $\Omega_{\odot}$ consists of only eight components, as long as the orbital eccentricity is neglected. Since $\frac{d\gamma}{dt} \approx \omega$ to a very close approximation, these correspond to frequencies of 0, −2n, ω, ω − 2n, ω + 2n, 2ω, 2ω − 2n, 2ω + 2n. In standard tidal theory, the respective components are labeled secular, semiannual, sidereal diurnal, slow diurnal, fast diurnal, sidereal semidiurnal, slow semidiurnal, and fast semidiurnal. This nomenclature seems hardly appropriate to Venus, since its orbital angular velocity n $\approx \frac{2\pi}{225d}$ is somewhat greater than its present rotation rate $\omega \approx \frac{2\pi}{243d}$; thus for example, not only is the slow semidiurnal frequency 2ω − 2n less than the sidereal diurnal frequency ω, but it is formally negative! We shall see that this need not complicate the analysis unduly.

We can gain insight into the roles of the various components by considering their dependences upon the obliquity β. When β = 0, all the terms of (3:3) vanish, except for the secular and slow semidiurnal components. Similarly all but the secular and fast semidiurnal terms vanish for β = 180°. Clearly, the slow semidiurnal frequency 2ω − 2n is associated with "progradeness" while the fast semidiurnal frequency 2ω + 2n

is associated with "retrogradeness". The other nonsecular
components represent seasonal effects occurring at intermediate
obliquities.

Now the solar potential $\Omega_\odot$ raises a bulge in the surface
of Venus, which has its own gravitational potential $\Omega_\venus$.
Because the strains involved are so small (from Part I, about
$\frac{0.3 \text{ m}}{6 \times 10^6 \text{m}} = 5 \times 10^{-8}$), we suppose that the material composing
the body responds linearly to the stresses. Then each component
$(\Omega_\odot)_\sigma$ of the forcing, corresponding to a particular frequency σ,
gives rise to a distinct component $(\Omega_\venus)_\sigma$ of the induced potential
with the same frequency. The ratio of the amplitude of $(\Omega_\venus)_\sigma$
to $(\Omega_\odot)_\sigma$ is known as the potential Love number k_σ.

Dissipation of tidal energy in the body of Venus also
introduces phase lags ϵ_σ between the maxima of $(\Omega_\odot)_\sigma$ and
$(\Omega_\venus)_\sigma$. The tidal "quality factor" Q is a dimensionless
measure of damping, defined as the inverse of the "specific"
dissipation, and related to the phase lag by

$$\tan \epsilon_\sigma = \frac{1}{Q} = \frac{\Delta E}{2\pi E} \quad . \tag{3:4}$$

where E is the peak mechanical energy stored in the body
tides and ΔE is the energy dissipated per cycle. In general,
both k_σ and Q depend upon the frequency σ; geophysical studies
indicate $30 \leqslant Q \leqslant 100$ for both solid Earth tides and the
Chandler wobble, while seismic waves and free body oscillations
have Q's of several hundred (Munk and MacDonald, 1975).

Since Q and k_σ are always positive, we must add to (3:4) above the physically reasonable codicil that ϵ_σ must have the same sign as σ. The secular terms can have no phase lag, so we must put $\epsilon_\sigma = 0$ if $\sigma = 0$.

We are now able to write the form of the induced potential:

$$
\Omega_{\substack{\varphi}} = - GM_\odot \frac{a^2}{r^3} \left(\frac{a}{d}\right)^3 \cdot \frac{3}{2} \left\{ \left[-\frac{1}{3} \left(\frac{3}{2} \cos^2 \beta^* - \frac{1}{2}\right) \left(\frac{3}{2} \cos^2 \theta - \frac{1}{2}\right) \right] k_o \right.
$$

$$
+ \left[-\frac{1}{2} \sin^2 \beta^* \left(\frac{3}{2} \cos \theta^2 - \frac{1}{2}\right) \right] k_{-2n} \cos (2\alpha^* - 2nt - \epsilon_{-2n})
$$

$$
+ \left[-\sin \beta^* \cos \beta^* \sin \theta \cos \theta \right] k_\omega \sin (\varphi + \gamma^* - \epsilon_\omega)
$$

$$
+ \left[\frac{1}{2} \sin \beta^* (1 + \cos \beta^*) \sin \theta \cos \theta \right] k_{\omega - 2n}
$$

$$
\cdot \sin (\varphi + \gamma^* + 2\alpha^* - 2nt - \epsilon_{\omega - 2n})
$$

$$
+ \left[-\frac{1}{2} \sin \beta^* (1 - \cos \beta^*) \sin \theta \cos \theta \right] k_{\omega + 2n}
$$

$$
\cdot \sin (\varphi + \gamma^* - 2\alpha^* + 2nt - \epsilon_{\omega + 2n}) \tag{3:5}
$$

$$
+ \left[\frac{1}{4} \sin^2 \beta^* \sin^2 \theta \right] k_{2\omega} \cos (2\varphi + 2\gamma^* - \epsilon_{2\omega})
$$

$$
+ \left[\frac{1}{8} (1 + \cos \beta^*)^2 \sin^2 \theta \right] k_{2\omega - 2n} \cos (2\varphi + 2\gamma^* + 2\alpha^*
$$

$$
- 2nt - \epsilon_{2\omega - 2n})
$$

$$
+ \left[\frac{1}{8} (1 - \cos \beta^*)^2 \sin^2 \theta \right] k_{2\omega + 2n} \cos (2\varphi + 2\gamma^* - 2\alpha^*
$$

$$
\left. + 2nt - \epsilon_{2\omega + 2n}) \right\} .
$$

After Goldreich and Peale (1970), we have put asterisks on
the Euler angles (α^*, β^*, γ^*) in (3:5) above in order
mathematically to distinguish   . the body raising the tides
from the body interacting with the tides, although here they are
physically the same. The factor $(\frac{a}{d})^3$ is included in (3:5)
in order to show that the induced potential falls off as the
inverse cube of the distance d from the center of Venus.

This induced potential $\Omega_\venus$ attracts the Sun in turn.
The reaction produces a tidal torque on Venus, by virtue of
the phase lags between the subsolar point and the position
of "high tide". For our purposes it is more convenient
to regard the tidal bulge as a distribution of mass over the
surface of Venus, equivalent to a density per unit area of

$$m_b = -\frac{5\Omega_\venus}{4\pi G a} \tag{3:6}$$

(Kaula, 1968, p. 67). Then the contribution U to the
Hamiltonian due to body tides is just the potential energy
of the mass distribution (3:6) in the gravitational field of the Sun:

$$U = \int_0^{2\pi} \int_0^\pi m_b \, \Omega_\odot \, a^2 \, d\varphi \, \sin\theta \, d\theta \tag{3:7}$$

$$= \int_0^{2\pi} \int_0^\pi \frac{5\Omega_\venus \, \Omega_\odot}{4\pi G a} a^2 \, d\varphi \, \sin\theta \, d\theta \quad .$$

When the trigonometric series (3:3) and (3:5) are multiplied together in the integrand of (3:7) above, only products of terms with the same zonal wavenumber s contribute to the integral over longitude φ. Performing the integration over colatitude θ as well then leaves

$$
\begin{aligned}
U = - \frac{GM_{\bigcirc}^2 a^5}{r^6} \Bigg\{ & k_o \left[(\tfrac{3}{4} \sin^2 \beta^* - \tfrac{1}{2}) (\tfrac{3}{4} \sin^2 \beta - \tfrac{1}{2}) \right] \\
& + k_{-2n} \left[\tfrac{9}{32} \sin^2 \beta^* \sin^2 \beta \right] \cos (2\alpha^* - 2\alpha - 4nt - \epsilon_{-2n}) \\
& + k_{-2n} \left[\tfrac{9}{32} \sin^2 \beta^* \sin^2 \beta \right] \cos (2\alpha^* - 2\alpha - \epsilon_{-2n}) \\
& + \left[\tfrac{3}{4} \sin \beta^* \cos \beta^* \sin \beta \cos \beta \right] k_\omega \cos (\gamma^* - \gamma - \epsilon_\omega) \\
& + \left[\tfrac{3}{16} \sin \beta^* (1 + \cos \beta^*) \sin \beta (1 + \cos \beta) \right] k_{\omega - 2n} \\
& \qquad \cdot \cos (\gamma^* - \gamma + 2\alpha^* - 2\alpha - \epsilon_{\omega - 2n}) \\
& + \left[\tfrac{3}{16} \sin \beta^* (1 - \cos \beta^*) \sin \beta (1 - \cos \beta) \right] k_{\omega + 2n} \\
& \qquad \cdot \cos (\gamma^* - \gamma - 2\alpha^* + 2\alpha - \epsilon_{\omega + 2n}) \\
& + \left[\tfrac{3}{16} \sin^2 \beta^* \sin^2 \beta \right] k_{2\omega} \cos (2\gamma^* - 2\gamma - \epsilon_{2\omega}) \\
& + \left[\tfrac{3}{64} (1 + \cos \beta^*)^2 (1 + \cos \beta)^2 \right] k_{2\omega - 2n} \\
& \qquad \cdot \cos (2\gamma^* - 2\gamma + 2\alpha^* - 2\alpha - \epsilon_{2\omega - 2n})
\end{aligned}
$$

(3:8)

$$+ [\frac{3}{64} (1 - \cos \beta^*)^2 (1 - \cos \beta)^2] k_{2\omega+2n}$$

$$\cdot \cos (2\gamma^* - 2\gamma - 2\alpha^* + 2\alpha - \epsilon_{2\omega+2n}) \Bigg\} \cdot \qquad (3:8)$$

Note that the second term in (3:8) varies with a short
(semiannual) period, although we are primarily interested in
secular changes. Such seasonal effects can formally be
eliminated simply by averaging U over an orbital period.
If the Love number k_σ is taken as constant, (3:8) above is
then identical with eq. (10) of Goldreich and Peale (1970),
when expanded to zeroth   order in the orbital eccentricity
(and when an omitted square is supplied on $M_\odot$).

At this point it is convenient to introduce the notation

$$b (\sigma) = k_\sigma \sin \epsilon_\sigma = \frac{\pm k_\sigma}{\sqrt{Q_\sigma^2+1}} \approx \frac{\pm k_\sigma}{Q_\sigma} \quad , \quad U_o = \frac{GM_\odot^2 a^5}{r^6}$$

$$\approx 1.332 \times 10^{18} \text{ J} \qquad . \qquad (3:9)$$

Now according to eq. (2:4) we can find $\frac{d\omega}{dt}$ by differentiating
U with respect to γ (unstarred); dropping the asterisks
subsequently gives

$$\frac{d\omega}{dt} = - \frac{1}{C} \frac{\partial U}{\partial \gamma} = - \frac{U_o}{C} \Bigg\{ b (\omega) [\frac{3}{4} \sin^2\beta \cos^2\beta]$$

$$+ b (\omega - 2n) [\frac{3}{16} \sin^2\beta (1 + \cos \beta)^2] + b (\omega + 2n)$$

$$\cdot [\frac{3}{16} \sin^2\beta (1 - \cos \beta)^2]$$

$$+ b (2\omega) [\frac{3}{8} \sin^4\beta] \qquad (3:10)$$

$$+ b (2\omega - 2n) [\tfrac{3}{32} (1 + \cos \beta)^4] + b (2\omega - 2n)$$

$$\cdot [- \tfrac{3}{32} (1 - \cos \beta)^4] \Bigg\} \quad . \tag{3:10}$$

It is easy to see from (3:10) above that $\frac{d\omega}{dt} < 0$ whenever

$\omega \geq 2n$; thus body tides always tend to despin a rapidly

rotating planet. Similarly, differentiating U with respect

to α yields

$$\frac{\partial U}{\partial \alpha} = U_o \Bigg\{ b (-2n) [\tfrac{9}{16} \sin^4 \beta]$$

$$+ b (\omega - 2n) [\tfrac{3}{8} \sin^2 \beta (1 + \cos \beta)^2] + b (\omega + 2n)$$

$$\cdot [- \tfrac{3}{8} \sin^2 \beta (1 - \cos \beta)^2]$$

$$\tag{3:11}$$

$$+ b (2\omega - 2n) [\tfrac{3}{32} (1 + \cos \beta)^4] + b (2\omega - 2n)$$

$$\cdot [- \tfrac{3}{32} (1 - \cos \beta)^4] \Bigg\} \quad ;$$

combining (3:10) and (3:11) above with eq. (2:5) then gives

$$\frac{d\beta}{dt} = \frac{1}{\omega C} \frac{1}{\sin \beta} \frac{\partial U}{\partial \alpha} - \frac{1}{\omega C} \frac{\cos \beta}{\sin \beta} \frac{\partial U}{\partial \gamma}$$

$$= \frac{U_o}{\omega C} \Bigg\{ - b (2n) [\tfrac{9}{16} \sin^3 \beta] + b (\omega) [\tfrac{3}{4} \sin \beta \cos^3 \beta]$$

$$\tag{3:12}$$

$$+ b (\omega - 2n) [\tfrac{3}{16} \sin \beta (1 + \cos \beta)^2 (2 - \cos \beta)$$

$$\cdot + b (\omega+2n) [- \tfrac{3}{16} \sin \beta (1-\cos \beta)^2 (2+\cos \beta)]$$

$$+ b\ (2\omega)\ [\ -\frac{3}{8}\ \sin\ ^3\beta\ \cos\ \beta\ ] + b\ (2\omega - 2n)$$

$$\cdot\ [\frac{3}{32}\ \sin\ \beta\ (1+\cos\ \beta)^3] + b\ (2\omega-2n) \qquad (3{:}12)$$

$$\cdot\ [\ -\frac{3}{32}\ \sin\ \beta\ (1-\cos\ \beta)^3]\Big\} \qquad .$$

When the obliquity is very small, to first order in β

eqs. (3:10) and (3:12) reduce to

$$\frac{d\omega}{dt} = -\frac{U_o}{C}\ \frac{3}{2}\ b\ (2\omega - 2n) = -\frac{U_o}{C}\ \frac{3}{2}\ k_{2\omega-2n}\ \sin\ \epsilon_{2\omega-2n} \qquad (3{:}13)$$

$$\frac{1}{\beta}\ \frac{d\beta}{dt} = \frac{U_o}{\omega C}\ \frac{3}{4}\ [\ b\ (2\omega - 2n) + b\ (\omega - 2n) - b\ (\omega)\ ] \qquad (3{:}14)$$

For retrograde rotations, we define $\beta' = 180° - \beta$ as the

supplement of the obliquity. Then to first order in β'

$$\frac{d\omega}{dt} = -\frac{U_o}{C}\ \frac{3}{2}\ b\ (2\omega + 2n) = -\frac{U_o}{C}\ \frac{3}{2}\ k_{2\omega+2n}\ \sin\ \epsilon_{2\omega+2n} \qquad (3{:}15)$$

$$\frac{1}{\beta'}\ \frac{d\beta'}{dt} = \frac{U_o}{\omega C}\ \frac{3}{4}\ [b\ (2\omega + 2n) + b\ (\omega + 2n) - b\ (\omega)\ ] \quad . \quad (3{:}16)$$

Equation (3:15) above is really the same as eq. (7:5) of Part I.

In the strictly planar problem where the obliquity is

either 0 or 180°, expressions (3:13) and (3:15) show that the

spin period always tends to evolve towards synchronism

(ω = n), while (3:14) and (3:16) give $\frac{d\beta}{dt} = 0$ (as we might

expect from symmetry considerations). However, the stability

of an exactly prograde or retrograde obliquity depends on the

tendency for an infinitesimal β or β' to grow or decay with time.

For a rapid rotation ($\omega > >n$), normally $b (\omega - 2n)$ $\approx b (\omega) \approx b (\omega + 2n)$, so that an obliquity of either 0 or 180° would be unstable. For $\omega \leq n$, as for Venus, eq. (3:14) shows that a zero obliquity would be stable under the influence of body tides alone. According to eq. (3:16), though, the stability of the observed retrograde rotation of Venus is contingent upon the frequency dependence of the dissipation. Accordingly the remainder of this chapter will examine three different models of body tides, while atmospheric tides will be included in the next chapter.

B.   The viscous model

Analytically the simplest way to model tidal friction is to treat the Love number k_σ as constant, and to assume that the response has the same form as the equilibrium tidal bulge in the absence of dissipation, but with the position of "high tide" shifted from the subsolar point to wherever the subsolar point had been at a time Δt before. The resulting picture of tidal evolution is very valuable for its clarity.

MacDonald   (1964) developed the above approach in order to simplify the Darwinian tidal theory; it is generally known as the "weak friction" approximation, but as Gerstenkorn (1967) has pointed out, that is truly a misnomer. Many authors have used models for the time lag Δt as a function of the tidal amplitude or of the speed of the subsolar point which are inconsistent with the assumption of linearity, no matter how weak or strong the tidal forces may be. If a nonzero obliquity or inclination is involved, the peak displacement generally does not coincide with the position of the subsolar point at any time past; in general, the net distortion does not even have the same shape as an equilibrium tidal bulge!

The "weak friction" model can still be made linear, provided that the time lag is the same for all of the component tides. Since a time lag Δt corresponds to a phase lag

$\epsilon_\sigma = \sigma \Delta t$, then to first order the dissipation must be

proportional to the frequency:

$$b\ (\sigma) = k_\sigma \sin \epsilon_\sigma \approx k\ \epsilon_\sigma = k\sigma \Delta t \approx \frac{k}{Q_n}\ \frac{\sigma}{n} \qquad , \qquad (3:17)$$

where Q_n is the value of the quality factor Q at the annual

frequency $\sigma \approx n$. (Note, however, that the strict proportionality

cannot persist for arbitrarily high frequencies, since $\sin \epsilon_\sigma$

cannot exceed 1.) Relation (3:17) above is graphed in Fig. 2

as the straight line labeled "viscous", because this type of

physical behavior is related to the effects of viscosity,

which will be discussed more fully in the final section of

this chapter.

The simple analytic form of the dissipation in

this model permits us to obtain compact expressions for the

tidal evolution at arbitrary obliquities. Substituting

(3:17) into (3:9) and (3:11) gives, after considerable

simplification,

$$\frac{d\omega}{dt} = -\frac{3}{2}\ \frac{U_o}{C}\ \frac{k}{nQ_n}\ [\omega\ (1 + \cos^2 \beta) - 2n \cos \beta] \quad , \qquad (3:18)$$

$$\frac{d\beta}{dt} = \frac{3}{2}\ \frac{U_o}{\omega C}\ \frac{k}{nQ_n}\ [(\omega \cos \beta - 2n) \sin \beta] \quad . \qquad (3:19)$$

Eq. (3:19) above is equivalent to equation (19) of Goldreich

and Peale (1970), found by consideration of the vector torque

acting on the displaced tidal bulge; it shows that the obliquity

β tends to increase as long as $\omega \cos \beta > 2n$, but decreases

Figure 2

Models for frequency dependence of tidal torque.
Abcissa: forcing frequency σ. Ordinate: $b(\sigma) =$
$k_{\sigma} \sin \epsilon_{\sigma} \propto$ energy dissipation. τ_b is the
constant of an elasticoviscous body.
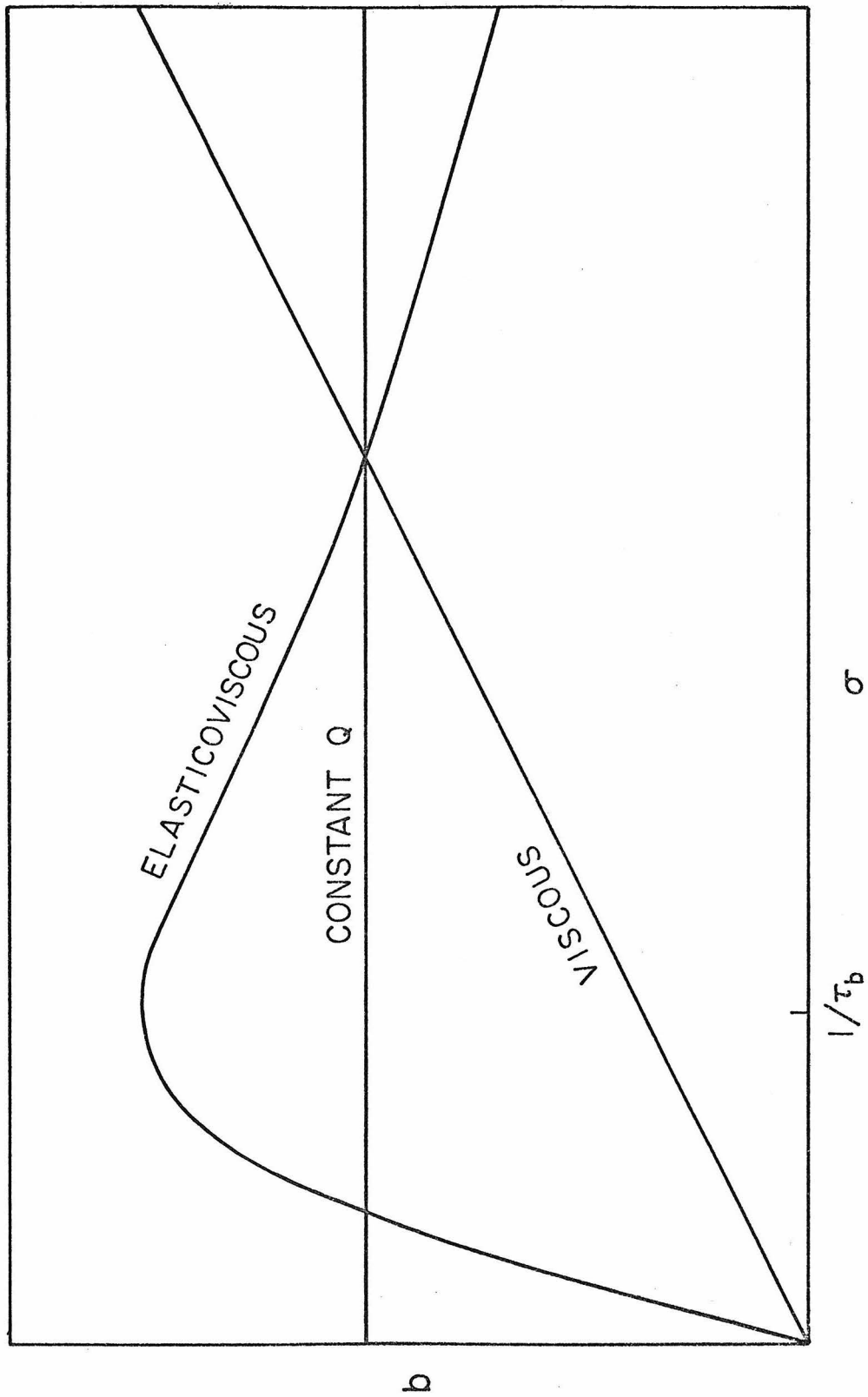
if $\omega \cos \beta < 2n$. Thus a prograde obliquity of 0 would be stable for a slowly rotating planet like Venus, while a strictly retrograde obliquity of 180° is unstable at any rotation rate.

The behavior is easier to visualize in a type of rectangular coordinates. Let $X = \omega \cos \beta$ be the component of the spin angular velocity ω parallel to the orbit normal $\hat{K}$, and let $Y = \omega \sin \beta$ be the component of ω lying in the plane of the orbit, perpendicular to $\hat{K}$. In these coordinates, (3:18) and (3:19) may be restated as follows:

$$\frac{dX}{dt} = \frac{d\omega}{dt} \cos \beta - \omega \sin \beta \frac{d\beta}{dt} = -\frac{1}{C} \frac{\partial H}{\partial \alpha}$$
(3:20)
$$= -\frac{3}{2} \frac{U_o}{C} \frac{k}{nQ_n} (2\omega \cos \beta - 2n) = -\frac{3}{2} \frac{U_o}{C} \frac{k}{Q_n n} (2X - 2n)$$

$$\frac{dY}{dt} = \frac{d\omega}{dt} \sin \beta + \omega \cos \beta \frac{d\beta}{dt}$$
(3:21)
$$= -\frac{3}{2} \frac{U_o}{C} \frac{k}{Q_n n} \omega \sin \beta = -\frac{3}{2} \frac{U_o}{C} \frac{k}{Q_n n} Y \qquad .$$

This model of tidal evolution is pictured graphically in Fig. 3, where expressions (3:20) and (3:21) above are plotted as vectors showing the rate and direction of evolution on a rectangular grid of X and Y. The lengths of the arrows are normalized to show the change in rotation over 3.0×10^7 years for $k = .25$ and $Q_{2\omega_o + 2n} \approx 35$, but the pattern does not

Figure 3

Spin evolution for the viscous model of
body tides; time interval = $3.0 \times 10^7 y$
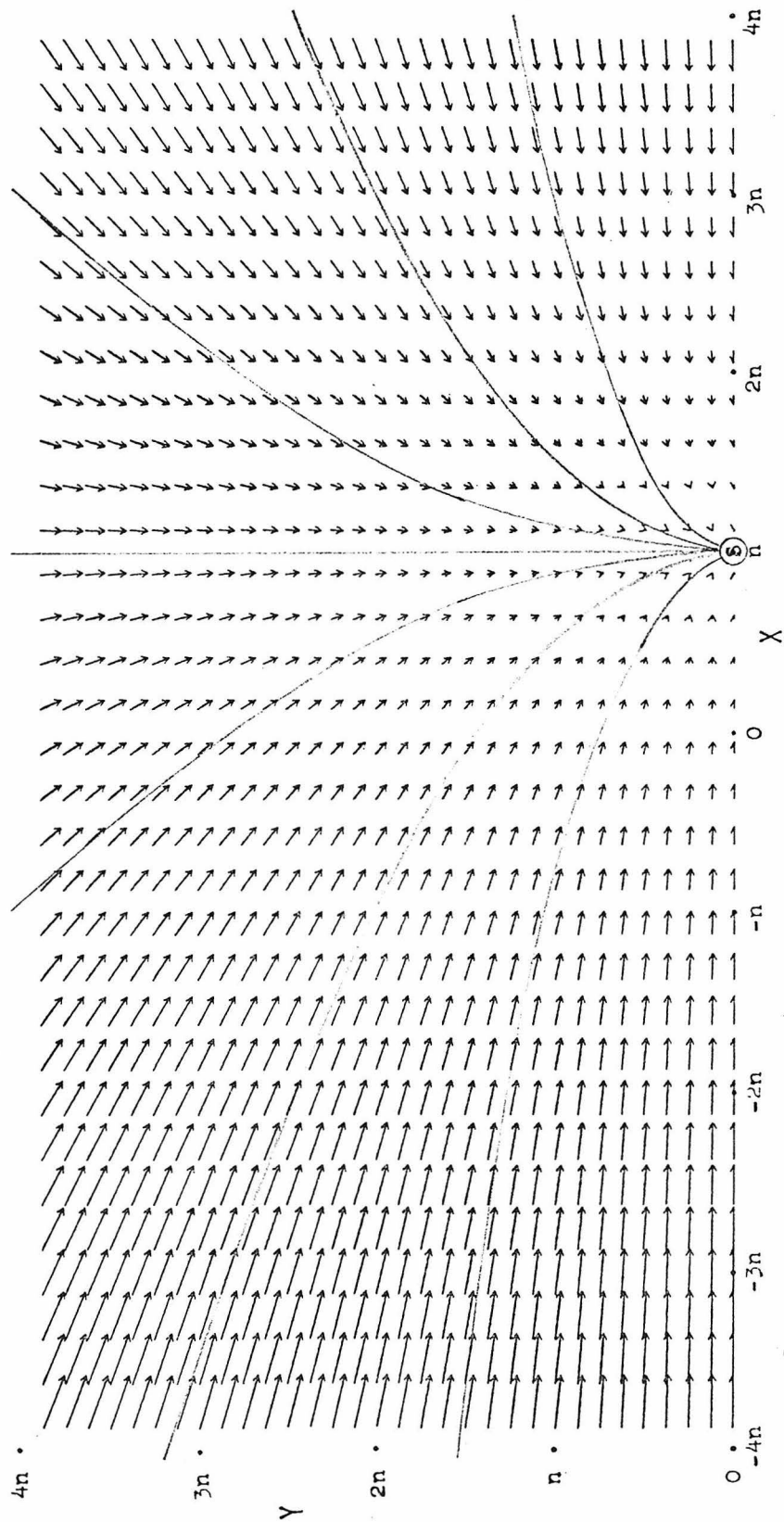
depend on the choice of parameters. It does not appear that
such a diagram has ever been presented for planetary rotations,
although it is not limited in application to Venus alone.
Greenberg (1974) has given similar graphs for the tidal
evolution of satellite orbits. (Although he used MacDonald's
approach with constant Q, has arrows should have the same direction
as if he used the more consistent relation (3:17).)

For this particularly simple model of tidal dissipation,
it is easy to integrate (3:20) and (3:21):

$$X(t) = X(0) e^{-2t/T} + n; \quad Y(t) = Y(0) e^{-t/T} ;$$

$$T = \frac{2}{3} \frac{C}{U_o} \frac{Q_n n}{k} \quad . \tag{3:22}$$

It is clear that the trajectory, or path of evolution of a
planet in the X, Y plane, must be a vertical or horizontal
straight line ending at the synchronous state, or else a
parabola with a horizontal axis and vertex at $X = n$, $Y = 0$.
Several representative trajectories have been plotted in
Fig. 3 as an aid to visualization.

The expression above has a very natural interpretation,
given by Goldreich and Peale (1970). The tidal torque can be
regarded as operating separately on the components of the spin
angular velocity $\bar{\omega}$ perpendicular and parallel to the orbital

plane. The torque perpendiular to the orbit acts continually, and the corresponding component X of the spin decays exponentially toward the synchronous value. The torque on the oblique component Y of the spin varies seasonally; it peaks at the equinoxes, and vanishes at the solstices. Thus the Y component of ω decays exponentially to zero, but with a time constant T twice as long as for the X component of the spin. When the viscous type of tidal dissipation is the only influence acting on the rotation, an initially prograde planet always remains prograde, while any retrograde rotation must eventually turn prograde.

C.   Constant Q

Since Q for the Earth changes by less than an order of magnitude between the Chandler wobble period of ~ 440 days and seismic periods of a few seconds, it is common to treat the specific dissipation as well as the Love numbers as independent of frequency. In order to satisfy our physical restriction on sign, we then adopt for the constant Q model

$$
\begin{aligned}
b &= k_\sigma \sin \, \epsilon_\sigma \approx k/Q && \text{if } \sigma > 0 \\
b &= 0 && \text{if } \sigma = 0 \\
b &= - k_\sigma \sin \, \epsilon_\sigma \approx - k/Q && \text{if } \sigma < 0 \quad .
\end{aligned}
\tag{3:23}
$$

This behavior is represented by the horizontal line in Fig. 2. Substituting (3:25) above into (3:14) gives, to first order in the obliquity β,

$$
\frac{d\beta}{dt} = \frac{U_o}{\omega C} \; \frac{3}{4} \; \beta \; x \; \frac{k}{Q} \; x
\begin{cases}
1 & \text{if } \omega > 2n \\
0 & \text{if } \omega = 2n \\
-1 & \text{if } n < \omega < 2n \\
-2 & \text{if } \omega = n \\
-3 & \text{if } \omega < n
\end{cases}
\tag{3:24}
$$

Eq. (3:24) above shows that a zero obliquity would be stable for Venus with its present rotation rate $\omega < n$. Meanwhile to first order in $\beta' = 180° - \beta$, (3:16) gives simply

$$
\frac{d\beta'}{dt} = \frac{U_o}{\omega C} \; \frac{3}{4} \; \beta' \; \frac{k}{Q}
\tag{3:25}
$$

Again for the constant Q tidal model, an obliquity
of 180° is unstable at any rotation rate.

Substituting (3:23) into (3:9) and (3:11) gives rise to
somewhat more complicated expressions for $\frac{d\omega}{dt}$ and $\frac{d\beta}{dt}$ at
arbitrary obliquities. The results are presented graphically
in Fig. 4; the format is the same as in Fig. 3, except that
now Q = 35 independent of frequency, and the time interval is
5.0×10^7 years. Discontinuous breaks in the pattern occur
where the frequencies $(\omega - n)$ and $(\omega - 2n)$ change sign , but
$\frac{d\omega}{dt}$ and $\omega \frac{d\beta}{dt}$ depend only on β in each of the three regions
separated by the semicircles $\omega = n$ and $\omega = 2n$. The obliquity
increases $(\frac{d\beta}{dt} > 0)$ only as long as $\omega > 2n$ and $0 < \beta \leqslant 67°$;
otherwise $\frac{d\beta}{dt} \leq 0$. Again we find that for this model of body
tides acting alone, all prograde planets remain prograde, while
retrograde planets eventually become prograde.

Figure 4

Spin evolution for the constant Q model

of body tides: time interval = 5.0 x 10^{7}y
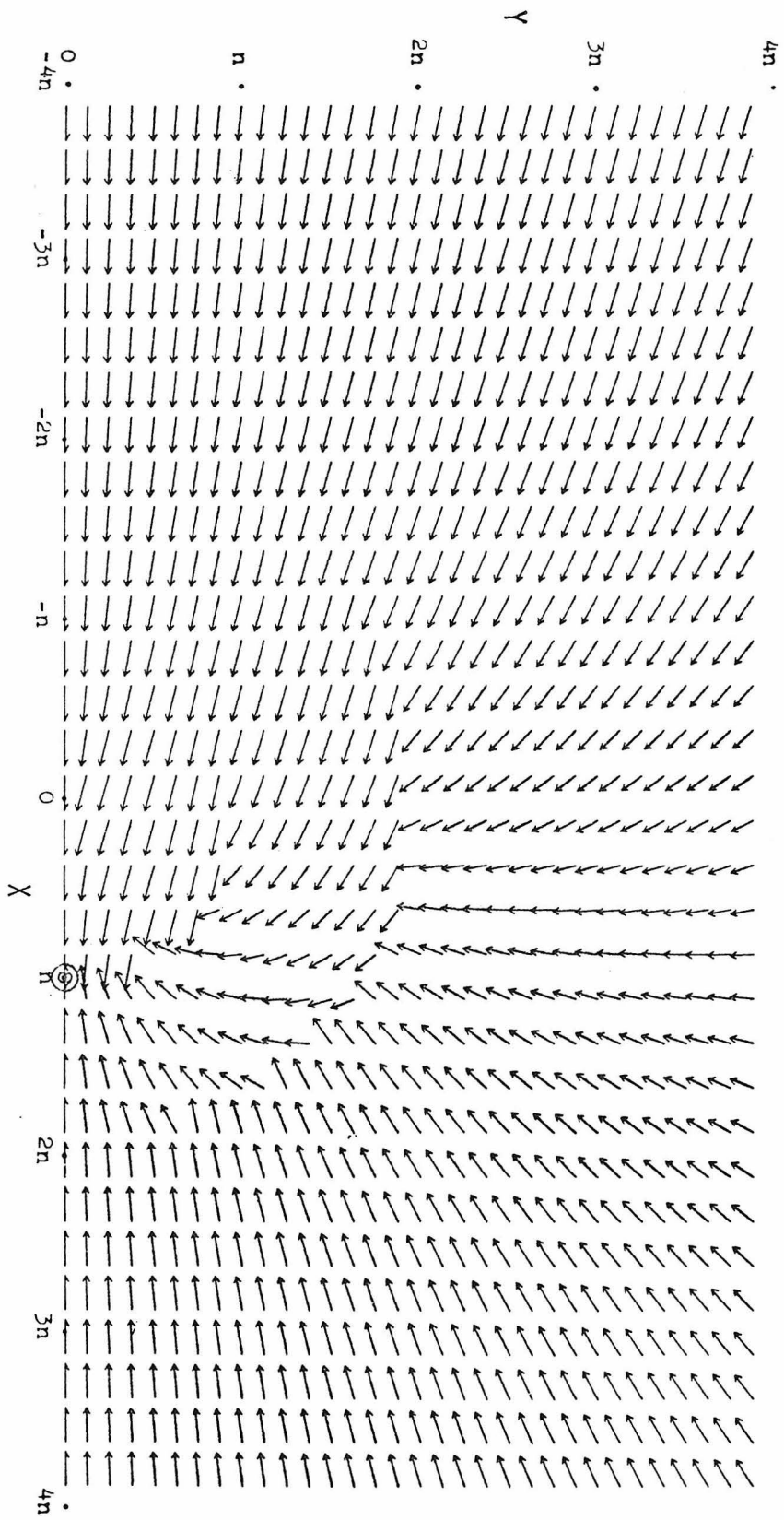
D. Elasticoviscosity

While an obliquity of exactly 180° is unstable for both of the tidal models considered so far, comparison of eq. (3:25) with (3:19) shows that the degree of instability indicated by $\frac{1}{\beta'}\frac{d\beta'}{dt}$ is several times less in the constant Q case than for the viscous model, where Q is inversely proportional to the tidal frequency. This suggests that a retrograde obliquity may actually be stable if Q increases with frequency. Although this possibility was not considered by Goldreich and Peale (1970), it is implicit in simple physical models of the dissipation mechanism.

Consider a mechanical oscillator composed of a massless spring and dashpot connected in series. Inertia can be neglected since tidal periods are much longer than free oscillation periods (about an hour or less); this system is therefore like a damped single harmonic oscillator driven always much more slowly than its resonant frequency. If this oscillator is driven at a very low frequency, it responds like the dashpot alone, dissipating energy in its internal viscosity. The specific dissipation 1/Q is then roughly proportional to the frequency σ, but only up to a point; above some characteristic forcing frequency the dissipation decreases again, and the system behaves more and more like the spring alone.

A material that responds to stresses in a manner analogous to the oscillator decribed above (except in shear instead of in compression) is called a Maxwell solid; this behavior is also known as elasticoviscosity. A Maxwell solid is presumed incompressible, and is characterized by a rigidity (or shear modulus) μ, as well as a viscosity ν, such that the shear stress and strain are related by the constitutive equation

$$\frac{1}{\mu} \frac{\partial}{\partial t} (\text{stress}) + \frac{1}{\nu} (\text{stress}) = \frac{\partial}{\partial t} (\text{strain}) \quad . \tag{3:26}$$

Such a law is found to describe empirically a great many substances. When the viscosity ν is formally infinite, (3:26) becomes the law of perfect elasticity; conversely when the rigidity μ is infinite (3:26) is the law of viscous flow. Thus a Maxwell body behaves like an elastic solid over short time scales, but flows like a Newtonian liquid over long periods of time.

Sir George Darwin (1908) performed elaborate calculations of tides in an elasticoviscous planet. Although he supposed the body to have a constant density ρ, we shall interpret ρ as the mean density of Venus. Darwin (1908) then gives

$$k_\sigma = k_f [1 + \sigma^2 \nu^2/\mu^2]^{1/2} [1 + \frac{\sigma^2 \nu^2}{\mu^2} (1 + \frac{19\mu}{2g\,\rho a})^2]^{-1/2} \tag{3:27}$$

$$\sin (\epsilon_\sigma) = \frac{19\,\nu\sigma}{2g\,\rho a} [1 + \sigma^2 \nu^2/\mu^2]^{-1/2} [1 + \frac{\sigma^2 \nu^2}{\mu^2} (1 + \frac{19\mu}{2g\,\rho a})^2]^{-1/2}$$

$$b(\sigma) = k_\sigma \sin(\epsilon_\sigma) = k_f \frac{19 \; \nu\sigma}{2g \; \rho a} \left[1 + \frac{\sigma^2 \; \nu^2}{\mu^2} \left(1 + \frac{19\mu}{2g \; \rho a} \right)^2 \right]^{-1}, \quad (3:27)$$

when k_f is the Love number pertaining to a perfectly fluid body with the same mass distribution as the actual planet. The quantity $\frac{19}{2g\rho a}$ appearing above may be regarded in effect as an added rigidity due to the planet's self-gravity.

The curve labled elasticoviscous in Fig. 2 depicts the frequency-dependence of this model for the dissipation. For low frequencies, eq. (3:27) above reduces to the viscous model, where the dissipation $b(\sigma) = k_\sigma \sin(\epsilon_\sigma)$ is proportional to the frequency:

$$k_\sigma \approx k_f \approx .96 \; ; \; \sin(\epsilon_\sigma) \approx \frac{19 \; \sigma\nu}{2g \; \rho a} \approx \frac{\sigma}{nQ_n} \approx \epsilon_\sigma \approx \sigma\Delta t \quad (3:28)$$

However, $b(\sigma)$ reaches a maximum at the frequency $\sigma = 1/\tau_b$, where τ_b is the time constant for damping of the body tides, given by

$$\tau_b = \frac{\nu}{\mu} \left(1 + \frac{19\mu}{2g \; \rho a} \right) \quad (3:29)$$

Above this frequency, b decreases again, falling off roughly as $1/\sigma$ for $\sigma >> \tau_b$.

Studies of the Chandler wobble yield the following values of the mean elasticoviscous parameters for the Earth:

$$\mu = (8.35 \pm 0.36) \times 10^{11} \text{ dy} \cdot \text{cm}^{-2} \; ; \; \nu \approx 10^{20} \text{ poise}; \; k_f \approx 0.96$$
(3:30)

(Munk and MacDonald, 1975). Presuming these values apply to Venus as well, inserting (3:30) into eq (3:29) gives

$$\tau_b = 10^{20} \times (\frac{10^{-11}}{8.35} + 3.367 \times 10^{-12}) \text{ s} \approx 4.564 \times 10^8 \text{ s} \approx 14.5 \text{ years}$$
(3:31)

for Venus, as compared with about $\tau_b \approx 13$ years for the Earth. For our purposes, $\sigma\tau_b$ is always much greater than unity, and the elasticoviscous model (3:27) gives

$$k_\sigma \approx k_f (1 + \frac{19\mu}{2g\rho a})^{-1} \approx 0.96 (1 + 2.81)^{-1} \approx .252$$

$$\sin \epsilon_\sigma \approx \frac{19\mu}{2g\rho a} \frac{1}{\sigma\tau_b} \approx \frac{2.81}{\sigma\tau_b} \approx \frac{6.16 \times 10^{-9} \text{ s}^{-1}}{\sigma} \approx \frac{1}{Q}$$
(3:32)

$$b(\sigma) = k_\sigma \sin \epsilon_\sigma \approx \frac{19\nu}{2g\rho a} \frac{1}{\sigma\tau_b^2} \approx \frac{.712}{\sigma\tau_b} \approx \frac{1.56 \times 10^{-9} \text{ s}^{-1}}{\sigma} \; .$$

At the current semidiurnal frequency ($\sigma = \frac{4\pi}{116.8d} \approx 1.245 \times 10^{-6} \text{ s}^{-1}$), eq. (3:42) above leads to a value of $Q \approx 200$ for Venus. Yet even presuming that the elasticoviscous model is appropriate, Q may actually be much lower if the high temperatures in the crust of Venus reduce its effective viscosity ν.

From eqs. (3:16) and (3:27) we find that the present obliquity of Venus would be stable if $\tau_b \geqslant 3.5 \times 10^6 \text{s} \approx 40$ days. Thus a tidal model where Q increases with frequency exhibits qualitatively different behavior in this respect

from the models usually considered. This also raises the
question whether past studies on the remote history of the
Earth-moon system are sufficiently general.

The expressions (3:9) and (3:11) for $\frac{d\omega}{dt}$ and $\frac{d\beta}{dt}$ at
arbitrary obliquities do not admit of much simplification in
the elasticoviscous case. The tidal evolution in the (ω, β)
plane is plotted in Fig. 5, where we have taken $\nu \approx 1.73 \times 10^{19}$
poise so that $\tau_b \approx 7.90 \times 10^7$ s ≈ 914 d ≈ 2.50y and $Q \approx 35$.
In order to improve legibility, only the direction of evolution
is shown, using arrows of arbitrary lengh. For this choice of
parameters, the current obliquity of Venus would be steady
although the rotation rate would still be decreasing. In the
absence of other influences, synchronous rotation is again
the only possible final state.

For the elasticoviscous model of solid body tides, like the other
cases treated above, it can be shown analytically that any
rapid rotation evolves toward an intermediate, but prograde
obliquity. Even if Venus had originated with a short rotation
period and an obliquity very close to 180°, it could hardly
have despun to its present slow spin rate under the influence
of body tides alone without turning prograde. One means of
avoiding this difficulty is described in the following chapter.

Figure 5

Spin evolution for the elasticoviscous model of
body tides; arrows show direction only

X

Y
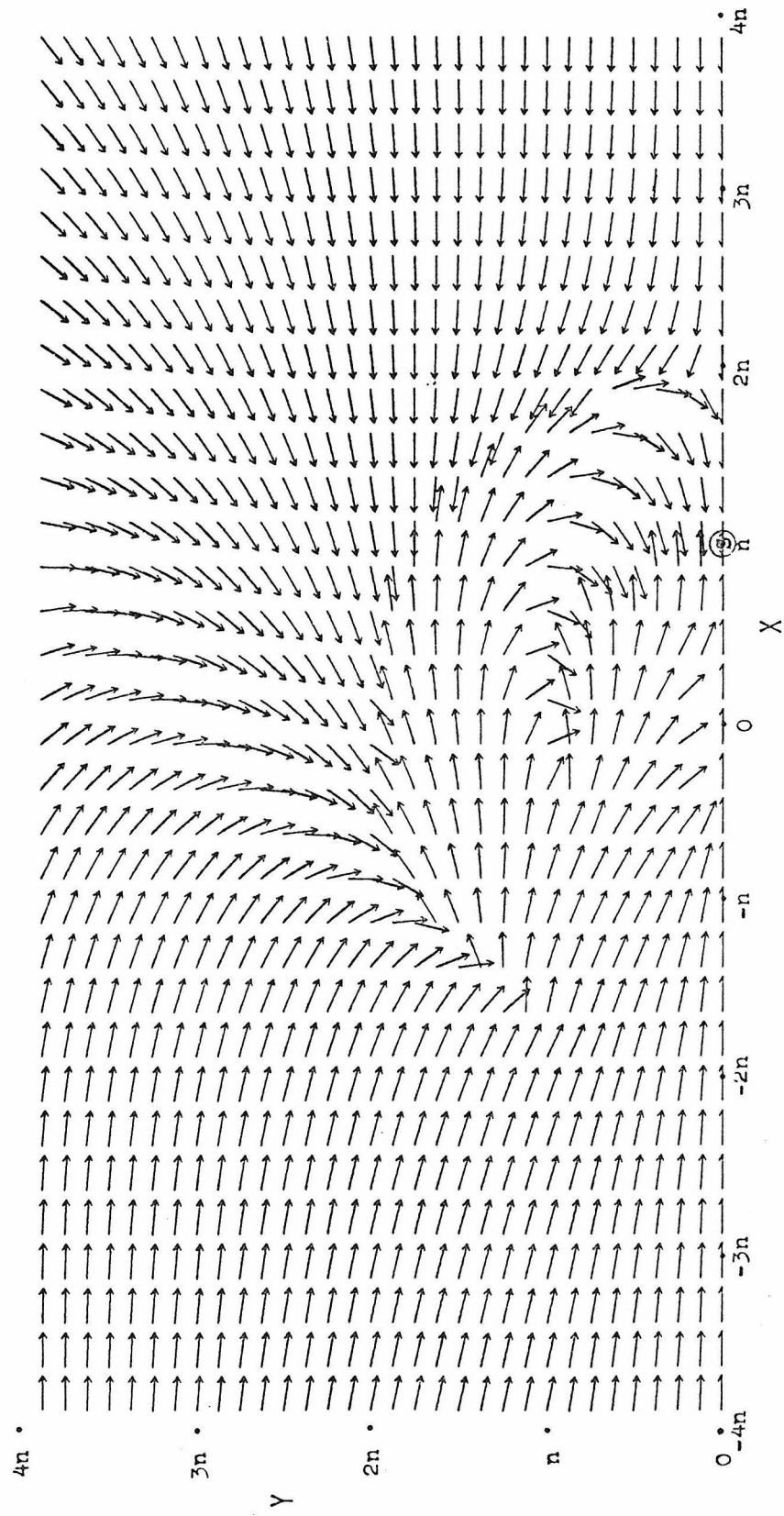
4. Atmospheric Tides

Tides in the atmosphere also affect the rotation of Venus, as demonstrated in Part I. In this chapter we shall apply the Hamiltonian formalism to our earlier results. The numerical calculations tabulated in chapter 5 of Part I permit us to examine the effect of atmospheric tides on the current rotation of Venus, while the heating at the ground model developed in chapter 6 of Part I is extended to cover all possible obliquities and a wide range of rotation rates.

A. Contribution to the Hamiltonian

The distribution of mass in the atmosphere also contributes to the gravitational field of Venus, as shown in chapter 7 of Part I. By virtue of the hydrostatic law (eq. (2:1) of Part I), the atmosphere is equivalent to a mass density m_a per unit area, which depends only on the pressure p_Z at the ground:

$$m_a = \int_Z^\infty \rho \, dz = \frac{p_Z}{g} = p_Z \frac{a^2}{GM_\varphi} \qquad . \qquad (4:1)$$

When the gravitational potential of Venus is analyzed in terms of spherical harmonics, to lowest order only terms of the second degree are capable of exerting a torque on the sun. Therefore only the second degree part of the surface pressure variation enters the total Hamiltonian for the rotation of Venus.

The theory of atmospheric tides as developed in chapter 2
of Part I is separable in longitude and time. Thus each Fourier
component of the forcing gives rise to tides with the same
frequency and zonal wavenumber. In the classical problem,
the tides are further separable into functions of height x and
Hough modes depending on colatitude θ. This is not strictly
true on Venus, because of the large vertical wind shear.
The equivalent gravity mode formalism developed in chapter 5
of Part I nevertheless assumes that the latitudinal structure
of the tides is nearly separable in terms of Legendre functions
$P_{\ell,s}$ (cos θ), which resemble Hough modes for low orders.
As a result, each spherical harmonic component of the forcing
gives rise only to the corresponding component of the surface
pressure variation. The same is naturally true for the heating
at the ground model defined in chapter 6 of Part I, which
does not involve separation of colatitude and height.

The following analysis is simplified considerably by
expanding the second-degree part of the surface pressure or
mass distribution in a manner parallel to expression (3:5)
for the induced potential of the body tides. This step will
be justified in the next section. In the complex δ-notation
of Part I, the atmospheric analogues of the Love numbers
k_σ may be written as $\delta p_Z^{\sigma,s}$, which have the dimensions of

pressure. The secular Love number k_o has no counterpart, though, because the mean pressure distribution properly belongs to the atmosphere's basic state. Then the second-degree part of the surface pressure, designated below by angle brackets, may be expressed in terms of the following components:

$$
\begin{aligned}
\langle gm_a \rangle = \langle p_z \rangle = & \left| \delta p_Z^{-2n,0} \right| \left[-\frac{1}{2} \sin^2 \beta* \left(\frac{3}{2} \cos^2 \theta - \frac{1}{2} \right) \right] \\
& \cdot \cos (2\alpha* - 2nt - \epsilon_{-2n}) \\
& + \left| \delta p_Z^{\omega,1} \right| \left[-\sin \beta* \cos \beta* \sin \theta \cos \theta \right] \\
& \cdot \sin (\varphi + \gamma* - \epsilon_\omega) \\
& + \left| \delta p_Z^{\omega-2n,1} \right| \left[\frac{1}{2} \sin \beta* (1 + \cos \beta*) \sin \theta \cos \theta \right] \\
& \cdot \sin (\varphi + \gamma* + 2\alpha* - 2nt - \epsilon_{\omega-2n}) \\
& + \left| \delta p_Z^{\omega+2n,1} \right| \left[-\frac{1}{2} \sin \beta* (1 - \cos \beta*) \sin \theta \cos \theta \right] \\
& \cdot \sin (\varphi + \gamma* - 2\alpha* + 2nt - \epsilon_{\omega+2n}) \qquad (4:2) \\
& + \left| \delta p_Z^{2\omega,2} \right| \left[\frac{1}{4} \sin^{-2} \beta* \sin^2 \theta \right] \cos (2\varphi + 2\gamma* - \epsilon_{2\omega}) \\
& + \left| \delta p_Z^{2\omega-2n,2} \right| \left[\frac{1}{8} (1 + \cos \beta*)^2 \sin^2 \theta \right] \\
& \cdot \cos (2\varphi + 2\gamma* + 2\alpha* - 2nt - \epsilon_{2\omega-2n}) \\
& + \left| \delta p_Z^{2\omega+2n,2} \right| \left[\frac{1}{8} (1 - \cos \beta*)^2 \sin^2 \theta \right] \\
& \cdot \cos (2\varphi + 2\gamma* - 2\alpha* + 2nt - \epsilon_{2\omega+2n}) \qquad .
\end{aligned}
$$

The phase lags ϵ_σ in (4:2) above now refer to the atmospheric tides, and are defined by

$$\epsilon_\sigma = -\text{Arcsin}\left[\frac{\text{Im}\,(\delta p_Z^{\sigma,s})}{\left|\delta p_Z^{\sigma,s}\right|}\right] = -\text{Arcos}\left[\frac{\text{Real}\,(\delta p_Z^{\sigma,s})}{\left|\delta p_Z^{\sigma,s}\right|}\right]. \qquad (4:3)$$

The atmospheric contribution W to the Hamiltonian may also be developed similarly to the body tides. Substituting m_a from eq. (4:3) for m_b in eq. (3:7), and averaging over an orbital period, then gives the atmospheric analogue to expression (3:8) for U:

$$W = \int_0^{2\pi}\int_0^{\pi} m_a\,\Omega_\odot\,a^2\,\sin\theta\,d\theta\,d\varphi = \frac{a^4}{GM_\varphi}\int_0^{2\pi}\int_0^{\pi} p_Z$$

$$\cdot\,\Omega_\odot\,\sin\theta\,d\theta\,d\varphi$$

$$= -\frac{8\pi}{15}\frac{M_\odot}{M_\varphi}\frac{a^6}{r^3}\left\{\left|\delta p_Z^{-2n,0}\right|\,[\frac{9}{32}\sin^2\beta^*\,\sin^2\beta]\right.$$

$$\cdot\,\cos\,(2\alpha^* - 2\alpha - \epsilon_{-2n})$$

$$+\left|\delta p_Z^{\omega,1}\right|\,[\frac{3}{4}\sin\beta^*\,\cos\beta^*\,\sin\beta\,\cos\beta]\,\cos\,(\gamma^* - \gamma - \epsilon_\omega)$$

$$+\left|\delta p_Z^{\omega-2n,1}\right|\,[\frac{3}{16}\sin\beta^*\,(1+\cos\beta^*)\,\sin\beta\,(1+\cos\beta)]$$

$$\cdot\,\cos\,(\gamma^* + 2\alpha^* - \gamma - 2\alpha - \epsilon_{\omega-2n})$$

$$+\left|\delta p_Z^{\omega+2n,1}\right|\,[\frac{3}{16}\sin\beta^*\,(1-\cos\beta^*)\,\sin\beta\,(1-\cos\beta)]$$

$$\cdot\,\cos\,(\gamma^* - 2\alpha^* - \gamma + 2\alpha - \epsilon_{\omega+2n}) \qquad (4:4)$$

$$+\left|\delta p_Z^{2\omega,2}\right|\,[\frac{3}{16}\sin^2\beta^*\,\sin^2\beta]\,\cos\,(2\gamma^* - 2\gamma - \epsilon_{2\omega})$$

$$+ \left| \delta p_Z^{2\omega-2n,2} \right| \left[\frac{3}{64} (1 + \cos \beta*)^2 (1 + \cos \beta)^2 \right]$$

$$\cdot \cos (2\gamma* - 2\gamma + 2\alpha* - 2\alpha - \epsilon_{2\omega-2n})$$

$$+ \left| \delta p_Z^{2\omega+2n,2} \right| \left[\frac{3}{64} (1 - \cos \beta*)^2 (1 - \cos \beta)^2 \right]$$

$$\cdot \cos (2\gamma* - 2\gamma - 2\alpha* + 2\alpha - \epsilon_{2\omega+2n}) \Bigg\} \qquad .$$

Inserting W from (4:4) above into the equations of motion (2:4) and (2:5) then gives $\frac{d\omega}{dt}$ and $\frac{d\beta}{dt}$; the resulting expressions can also be found by replacing U_o and b (σ) in eqs. (3:10) and (3:12) by W_o and $- a\ (\sigma)$, where we define

$$a\ (\sigma) = - \left| \delta p_Z^{\sigma,s} \right| \sin \epsilon_\sigma = Im\ (\delta p_Z^{\sigma,s}), \quad W_o = \frac{8\pi}{15} \frac{M_\odot}{M_\varphi} \frac{a^6}{r^3}$$

$$\approx 2.65 \times 10^{13}\ m^3 \qquad . \qquad (4:5)$$

Under these substitutions, eqs. (3:13) and (3:19) for small obliquities become

$$\frac{d\omega}{dt} = \frac{W_o}{C} \frac{3}{2} a\ (2\omega - 2n) = \frac{4\pi}{5C} \frac{M_\odot}{M_\varphi} \frac{a^6}{r^3} Im\ (\delta p_Z^{2\omega+2n,2}) \qquad (4:6)$$

$$\frac{1}{\beta} \frac{d\beta}{dt} = - \frac{W_o}{\omega C} \frac{3}{4} [a\ (2\omega - 2n) + a\ (\omega - 2n) - a\ (\omega)] \quad , \qquad (4:7)$$

while the analogues of eqs. (3:15) and (3:16) for retrograde rotations are

$$\frac{d\omega}{dt} = \frac{W_o}{C} \frac{3}{2} a\ (2\omega + 2n) = \frac{4\pi}{5C} \frac{M_\odot}{M_\varphi} \frac{a^6}{r^3} Im\ (\delta p_Z^{2\omega+2n,2}) \qquad (4:8)$$

$$\frac{1}{\beta'} \frac{d\beta'}{dt} = - \frac{W_o}{\omega C} \frac{3}{4} [a\ (2\omega + 2n) + a\ (\omega + 2n) - a\ (\omega)] \quad . \qquad (4:9)$$

When the change of normalization (explained in the next section)is taken into account, eq. (4:8) above is just the same as eq. (7:7) of Part I. Thus as shown in that chapter, the net torque on the atmosphere of Venus currently depends only on the semidiurnal variation of the surface pressure. Meanwhile eq. (4:9) for the stability of a retrograde obliquity also involves the $\sigma = \omega + 2n$ and $\sigma = \omega$ frequency components. The following section applies the above formulation to the numerical results for these tidal modes obtained in Part I.

B. Stability of the present state

For the current spin of Venus, atmospheric tides can be studied by means of the equivalent gravity mode approach developed in chapter 5 of Part I. As shown therein, gravitationally induced tides are negligible in the Venus atmosphere, so only thermally driven tides are considered in the following.

By equation (4:2) of Part I, the direct absorption of sunlight in the atmosphere of Venus was assumed separable into the form $J_{\odot}(x) \cos \zeta$ on the day side, where $J_{\odot}(x)$ is the vertical profile of absorption at the subsolar point and ζ is the local zenith angle of the sun. Then the second degree components of the thermal forcing can be written in a form analogous to eq. (3:1) for the tidal potential $\Omega_{\odot}$:

$$\langle\!\langle J(\zeta, x)\rangle\!\rangle = \frac{15}{32} J_{\odot}(x) (\cos^2 \zeta - \frac{1}{3}) \qquad (4:10)$$

Consequently all of the tidal coefficients $\delta p_z^{\sigma,s}$ appearing in expression (4:3) correspond to a heating profile $\frac{15}{32} J_{\odot}(x)$. Actually this separation only applies to the stratospheric heating distributions I, II, and III. In the troposphere, models IV and V for convection, and VI and VII for thermal diffusion, cannot be expressed by eq. (4:10) above. Since eqs. (4:17) and (4:21) of Part I define these models in terms of $\frac{\sigma(x)}{\sigma_o}$, each frequency component of the spherical harmonic expansion of J has a slightly

different height dependence. This complication is really only
conceptual; in practice each component of the tropospheric
heating is normalized to a total absorbed flux of $\frac{15}{32}$ x 100 W/m^2,
where 100 W/m^2 is absorbed by the ground at the subsolar point.
Then each component of the surface pressure in eq.(4:2) still
corresponds to a similar component of the forcing. Finally,
the heating at the ground model, defined by eq. (4:18) of
Part I and further developed in chapter 6 of that Part, is trivially
separable because it does not involve height.

Although scattering and absorption may modify the
horizontal dependence of the heating from the cos ζ distribution
of the incident solar flux, the amplitudes of the low degree
harmonics will be nearly unaffected. For example, if the
heating actually varied as $\cos^2\zeta$ on the day side, the
normalization factor discussed above would become 1/2 instead
of $\frac{15}{32}$. Since such adjustments are easily made, we shall continue
to normalize the component tides by $\frac{15}{32}$ of the total flux
$F_\odot$ absorbed at the subsolar point.

The atmospheric contribution W to the Hamiltonian can then
be found by calculating the surface pressure variation
corresponding to each component of the forcing, as normalized
above. As described in chapter 5 of Part I, such calculations
were performed numerically, using two somewhat different

equivalent gravity mode (EGM) techniques. The resulting

variations in surface pressure are listed in Table 3 of Part I

for the most important tidal modes. The principal diurnal

pressure variation ($\sigma = \omega + n$), normalized by $1/2$ $F_\odot$, does

not appear in W because it represents a first degree spherical

harmonic. The tabulated results for the main semidiurnal

tide ($\sigma = 2\omega + 2n$) were normalized by $\frac{15}{64}$ in order to give the

surface pressure variation at the equator; those values must

be doubled to be consistent with the normalization

above. The modes with $\sigma = \omega - 2n$ and $\sigma = 2\omega - 2n$ were not

calculated, since these frequencies vanish somewhere between

the stratosphere and the surface of Venus; in the absence

of damping, the tidal theory becomes singular at such critical

levels. This omission is not important, though, because

inspection of eq. (4:4) shows that these components do not

contribute to W for obliquities near 180°. All of the other

second-degree modes listed in Table 3 of Part I were calculated

according to the normalization described above.

To first order in $\beta' = 180° - \beta$, eq. (4:8) for $\frac{d\omega}{dt}$

and eq. (4:9) for $\frac{d\beta'}{dt}$ involve only the tides of frequency

$2\omega + 2n$, $\omega + 2n$, and ω. The imaginary parts of the surface

pressure variations listed under these modes in Table 3 of

Part I may then be substituted directly into (4:8) and (4:9),

recalling that the semidiurnal values must be doubled. The

resulting contributions to $\frac{1}{\beta'} \frac{d\beta'}{dt}$ are listed under the

heading "atmosphere" in Table 1 following, versus EGM methods

1 and 2, basic state models A, B, C, and D, and heating

distributions I – VIII, all described in Part I.

As the tabulated results show, heating in the stratosphere

(profiles I, II, and III) has a comparatively small effect

on $\frac{1}{\beta'} \frac{d\beta'}{dt}$, distributed almost evenly between positive

(destabilizing) and negative (stabilizing) values. On the

other hand, the tropospheric forcing (distributions IV – VIII)

has a large influence on the obliquity. These conclusions

are similar to those for the net torque obtained in Part I.

While rather variable in strength, the results in Table 1

for EGM method 1 are all positive for heating at the ground

(model VIII) and tend to become negative for thicker heated

layers. In contrast, the values of $\frac{1}{\beta'} \frac{d\beta'}{dt}$ are nearly all

negative for EGM method 2. The primary reason for this

difference is that the equivalent depth of the $\sigma = \omega$ mode

becomes infinite according to EGM method 2, unlike EGM

method 1, as long as $\frac{\partial^2}{\partial\theta^2} \omega = 0$ at the equator. This leads to the

near-vanishing of the corresponding surface pressure variation,

as shown in Appendix I, but the special atmospheric conditions

leading to such an ideal situation are not likely to occur on

Venus.

Table 1		$\dfrac{1}{\beta'}\ \dfrac{d\beta'}{dt}$ for various cases (10^{-9} yr^{-1})							
J	MODEL	atmosphere		+ constant Q		+ viscous		+ elasticovisc.	
		EGM 1	EGM 2	EGM 1	EGM 2	EGM 1	EGM 2	EGM 1	EGM 2
I	A	.012	−1.32	.012	.001	.012	.689	.012	−3.75
	B	−.026	−.014	−7E−5	7E−5	.013	.007	−.072	0.404
	C	−.022	−.012	−8E−5	5E−5	.011	.006	−.063	−.034
	D	.030	.014	2E−5	−1E−4	−.015	−.007	.084	.039
II	A	2.91	−2.24	.049	.001	−1.44	1.17	8.17	−6.36
	B	−.012	.009	2E−4	5E−5	.007	−.005	−.034	.027
	C	−.007	.013	.002	2E−5	.006	−.007	−.018	.037
	D	−.009	−.015	−8E−5	−4E−5	−.006	.008	.027	−.042
III	A	.524	−.606	2E−4	5E−4	−.272	.316	1.49	−1.72
	B	.003	.007	−2E−4	1E−5	−.002	−.004	.008	.020
	C	.004	.008	−2E−5	7E−6	−.002	−.004	.011	.024
	D	−.005	−.010	6E−6	−2E−5	.003	.005	−.015	−.027
IV	A	−13.1	−21.6	−6.92	−12.9	−3.71	−8.39	−24.5	−37.5
	B	−8.70	−12.9	−3.35	−7.86	−.569	−5.25	−18.5	−22.1
	C	−.155	−4.23	.0464	−2.68	.877	−1.88	−4.49	−7.08
	D	−1.41	−4.16	.132	−2.67	.935	−1.89	−4.25	−6.92
V	A	−25.3	−33.2	−14.1	−20.3	−8.28	−13.6	−45.9	−57.0
	B	−10.2	−22.4	−.785	013.5	4.11	−8.86	−27.5	−38.8
	C	−.139	−13.5	3.00	−6.74	5.28	−4.51	−9.46	−18.9
	D	−1.14	−11.0	3.21	−6.74	5.47	−4.55	−9.15	−18.7
VI	A	−21.8	−29.2	−11.8	−17.2	−6.63	−11.0	−40.1	−51.3
	B	−7.74	−19.2	.499	−11.4	4.78	−7.32	−22.9	−33.7
	C	3.53	−13.5	9.20	−7.93	12.1	−5.06	−6.91	−23.6
	D	3.82	−13.4	9.41	−7.94	12.3	−5.08	−6.50	−23.5
VII	A	−32.5	−35.7	−19.2	−21.0	−12.2	−13.3	−57.2	−62.8
	B	−1.04	−25.9	.713	−15.1	6.48	−9.54	−30.8	−45.5
	C	1.82	−20.2	10.5	−11.6	15.0	−7.15	−14.2	−35.9
	D	2.07	−20.1	10.7	−11.6	15.2	−7.19	−13.9	−35.7
VIII	A	13.1	−45.6	29.2	−2.93	37.6	−20.8	−16.5	−75.5
	B	24.2	−43.9	40.0	−28.2	48.2	−20.1	−4.79	−72.7
	C	27.7	−41.8	43.4	−26.1	51.6	−18.0	−1.19	−70.7
	D	27.8	−4.18	43.5	−26.1	51.7	−18.0	−1.09	−70.6

Of course, the rotation of Venus is affected by tides in the body of the planet as well as those in the atmosphere. Combined body and atmospheric tides may be studied simply by adding the terms U and W of the Hamiltonian. For small obliquities, adding eq. (3:13) to (4:6) and eq. (3:14) to (4:7) yields

$$\frac{d\omega}{dt} = \frac{1}{C}\ \frac{3}{2}\ [U_o\ b\ (2\omega - 2n) - W_o\ a\ (2\omega - 2n)]$$

(4:11)

$$\frac{1}{\beta}\ \frac{d\beta}{dt} = \frac{1}{\omega C}\ \frac{3}{4}\ [U_o\ b\ (2\omega - 2n) - W_o\ a\ (2\omega - 2n)]$$

$$+ U_o\ b\ (\omega - 2n) - W_o\ a\ (\omega - 2n) - U_o\ b\ (\omega) + W_o\ a\ (\omega)]\ .$$

(4:12)

To first order in $\beta' = 180° - \beta$, combining eq. (3:15) and (4:8) and (3:16) with (4:9) similarly gives

$$\frac{d\omega}{dt} = -\frac{1}{C}\ \frac{3}{2}\ [U_o\ b\ (2\omega + 2n) - W_o\ a\ (2\omega + 2n)]$$

(4:13)

$$\frac{1}{\beta'}\ \frac{d\beta'}{dt} = \frac{1}{\omega C}\ \frac{3}{4}\ [U_o\ b\ (2\omega + 2n) - W_o\ a\ (2\omega + 2n)$$

$$+ U_o\ b\ (\omega + 2n) - W_o\ a\ (\omega + 2n) - U_o\ b\ (\omega) + W_o\ a\ (\omega)]\ .$$

(4:14)

The above equations (4:13) and (4:14) can be used to tell whether the retrograde spin of Venus is presently in a steady state. If the net tidal torques cancel so that the rotation rate in neither despinning nor accelerating, eq. (4:13) yields

$$\frac{d\omega}{dt} = 0\ \rightarrow\ U_o\ b\ (2\omega + 2n) = W_o\ a\ (2\omega + 2n)\ .$$

(4:15)

In order for the equilibrium also to be stable with respect to obliquity perturbations, $\frac{d\beta'}{dt}$ must be negative. Combined with (4:15) above, eq. (4:14) becomes

$$\frac{1}{\beta'} \frac{d\beta'}{dt} = \frac{1}{\omega C} \frac{3}{4} [U_o\, b\, (\omega + 2n) - W_o\, a\, (\omega + 2n) - U_o\, b\, (\omega) + W_o\, a\, (\omega)] \quad . \qquad (4:16)$$

Pursuing this line of reasoning any farther requires specific knowledge or assumptions regarding the frequency dependence of the dissipation in the body of Venus .

Suppose that the constant Q model applies, so the b (σ) as given by eq. (3:25) is essentially independent of frequency. Then the remaining terms due to body tides in eq. (4:16) above cancel, leaving

$$\frac{1}{\beta'} \frac{d\beta'}{dt} = \frac{W_o}{\omega C} \frac{3}{4} [- \quad a\, (\omega + 2n) + a\, (\omega)] \quad . \qquad (4:17)$$

As for the case of the atmosphere acting alone, the numerical values for the surface pressure variations from Table 3 of Part I were substituted into eq. (4:17); the results are listed in Table 1 under the heading "+ constant Q". The contributions of the various heating models to $\frac{1}{\beta'} \frac{d\beta'}{dt}$ again combine linearly in the same proportions as in the total surface pressure variation. As expected, the addition of constant Q body tides tends to destabilize a retrograde

obliquity. For equivalent gravity mode method 1, $\dfrac{1}{\beta'}\dfrac{d\beta'}{dt}$ generally becomes positive, while for EGM method 2 the values in the troposphere become smaller but remain negative.

As an alternative, consider the viscous model of body tides (3:17), where $b\,(\sigma)$ is proportional to the frequency. Combining this with eqs, (4:15) and (4:16) yields

$$
\begin{aligned}
\frac{1}{\beta'}\frac{d\beta'}{dt} &= \frac{1}{\omega C}\,\frac{3}{4}\,\left[U_o\,\left(\frac{\omega+2n}{2\omega+2n}\right)\,b\,(2\omega+2n) - W_o\,a\,(\omega+2n)\right.\\
&\qquad\left. - U_o\,\left(\frac{\omega}{2\omega+2n}\right)\,b\,(\omega) + W_o\,a\,(\omega)\right] \\
&= \frac{W_o}{\omega C}\,\frac{3}{4}\left[\left(\frac{2n}{2\omega+2n}\right)\,a\,(2\omega+2n) - a\,(\omega+2n) + a\,(\omega)\right].
\end{aligned}
\tag{4:18}
$$

The numerical values obtained from (4:18) above are also listed in Table 1, under the heading "+ viscous". The results are quite similar to those for the constant Q model, except that the negative values are smaller and the positive values are larger in general, so that an obliquity of 180° is stable for a still smaller range of parameters.

In the elasticoviscous model (3:43) for body tides, $b\,(\sigma)$ is almost inversely proportional to the frequency. In that case eq. (4:16) becomes

$$
\begin{aligned}
\frac{1}{\beta'}\frac{d\beta'}{dt} &= \frac{1}{\omega C}\,\frac{3}{4}\,\left[U_o\,\left(\frac{2\omega+2n}{\omega+2n}\right)\,b\,(2\omega+2n) - W_o\,a\,(\omega+2n)\right.\\
&\qquad\left. - U_o\,\left(\frac{2\omega+2n}{\omega}\right)\,b\,(\omega) + W_o\,a\,(\omega)\right]
\end{aligned}
\tag{4:19}
$$

$$= \frac{W_o}{\omega C} \frac{3}{4} \left[- (\frac{2n}{\omega}) \left(\frac{2\omega + 2n}{\omega + 2n} \right) a\ (2\omega + 2n) - a\ (\omega + 2n) \right.$$

$$\left. + a\ (\omega) \right] \qquad . \qquad (4:19)$$

The values obtained from (4:19), tabulated under "+ elasticovisc .",
are almost all negative, and especially large for EGM method
2. This is consistent with the result of chapter 3, that
elasticoviscous body tides can stabilize the obliquity of a
slow retrograde planet.

One more criterion must be met in order for the present
rotation of Venus to be in a steady state. For the spin
period to be stable with respect to small changes in the
rotation rate, we require

$$\frac{\partial}{\partial \omega} \left(\frac{d\omega}{dt} \right) < 0 \rightarrow U_o \frac{\partial}{\partial \omega} b\ (2\omega + 2n) > W_o \frac{\partial}{\partial \omega} a\ (2\omega + 2n) \ . \qquad (4:20)$$

Unfortunately, neither the full three-dimensional tidal theory
nor the equivalent gravity mode approximation can be used to
evaluate eq. (4:20) above, since it is not possible to say
for certain how the basic state of the atmosphere would
change if the solid planet were rotating with a different
period than observed. This limitation will be relaxed in the
following section, along with the restriction to an obliquity
near 180°.

C. Generalization to arbitrary obliquities

The complete theory of atmospheric tides cannot be applied to obliquities and rotation rates besides the current spin of Venus, because the results depend on the basic state, as explained above. Yet the essential features of the tides may be represented by the heating at the ground model, described in chapter 6 of Part I; then the surface pressure variations do not depend on the details of the basic state, as long as the atmosphere near the surface is corotating with the crust.

In the notation of this chapter, the result (6:4) of Part I may be written

$$\delta p_Z^{\sigma,s} = \frac{15}{32} \frac{\varkappa F_\odot}{(i\sigma + 1/\tau_a) H_o} \rightarrow \left| \delta p_Z^{\sigma,s} \right| = \frac{15}{32} \frac{\varkappa F_\odot}{\sigma H_o}$$

$$\cdot \sqrt{\frac{1}{1 + \sigma^{-2} \tau_a^{-2}}} \;,\; \epsilon_\sigma = \frac{15}{32} \frac{\varkappa F_\odot}{\sigma H_o} \left(\frac{1}{1 + \sigma^{-2} \tau_a^{-2}} \right) \quad (4:21)$$

$$\rightarrow a(\sigma) = \mathrm{Im}\left(\delta p_Z^{\sigma,s} \right) = - \left| \delta p_Z^{\sigma,s} \right| \sin \epsilon_\sigma = \frac{15}{32} \frac{\varkappa F_\odot}{\sigma H_o} \left(\frac{1}{1 + \sigma^{-2} \tau_a^{-2}} \right)$$

The Newtonian cooling coefficient $1/\tau_a$ is included in eq. (4:21) above in order to parameterize nonlinearities and damping in the thermal boundary layer. If $1/\tau_a$ is neglected, ϵ_σ becomes $-90°$ (always representing a phase lead) while $a(\sigma)$ is inversely proportional to the frequency. The magnitude of the atmospheric time constant τ_a is not known, and may depend on frequency, but we shall use a constant value for τ_a in order to gain qualitative insights into the heating at the ground model.

According to eq. (4:21) above, the atmospheric torque then has the same functional form as (3:27), the elasticoviscous model of body tides. The stability criterion (4:20) cannot then be met for an elasticoviscous planet, unless its time constant τ_a is shorter than the atmosphere's. If τ_a is so small, the body tides may just as well be represented by the viscous model (3:17), which always satisfies condition (4:20). If on the other hand the constant Q model (3:23) applies, eq. (4:20) is satisfied as long as $\tau_a > 1/(2\omega + 2n) \approx 9.29$ days.

One difficulty remains before the heating at the ground model can be applied to the question of obliquity. The simple formula (4:21) was derived under the assumption that the equivalent depth of the Venus atmosphere is negligible compared to the scale height near the ground. This approximation is excellent in most cases. However, for the particular mode with $\sigma = \omega$, $s = 1$, the principal equivalent depth may be very large or formally infinite, as described in Chapter 5 of Part I. In that case, the surface pressure variation $\delta p_z^{\omega,1}$ vanishes, as shown in Appendix I. This does not seem likely to occur on Venus, where the tidal modes are essentially nonseparable, but we shall examine both possibilities. Tides involving a (ω) obtained from eq. (4:21) will be referred to as type 1 atmospheric tides. Type 2 tides are obtained by setting a (ω) = 0 in eq. (4:2) et seq.

These two models are related to EGM methods 1 and 2, respectively and can now be compared with the detailed numerical calculations. The stability parameter $\frac{1}{\beta'} \frac{d\beta'}{dt}$ from eq. (4:9) is graphed in Figure 6, for various combinations of body tides and the heating at the ground model for atmospheric tides. The scale along the bottom shows the time constant τ_a of the atmosphere, while the upper scale gives the corresponding values of $b(2\omega + 2n) \approx k/Q$, the dissipation in the body of Venus required to balance the atmospheric torque at the current rotation rate. The curves labeled A, Q, and V respectively refer to atmospheric tides acting alone, added to body tides of the constant Q type, and combined with the viscous model of body tides. Comparing Fig. 6 with Table 1 shows that the effects of the heating at the ground on the stability of the retrograde obliquity broadly resemble the EGM calculations, but each basic state model and heating distribution does not correspond to a unique value of τ_a.

Because of the equivalence between heating at the ground and the elasticoviscous model, type 1 atmospheric tides can only help to stabilize the obliquity if $\tau_a \leqslant 40$ days. The elasticoviscous model is not included separately in Fig. 6, since for practical purposes it reduces to the viscous model whenever the rotation rate is stable, as explained above. Tides of type V_1 can stabilize the obliquity if $\tau_a < 1/\sqrt{5\omega^2 + 10n\,\omega + 4n^2} \approx 8.55$ days, but

Figure 6

Effects of τ_a on the stability of a

180° obliquity, for several tidal models
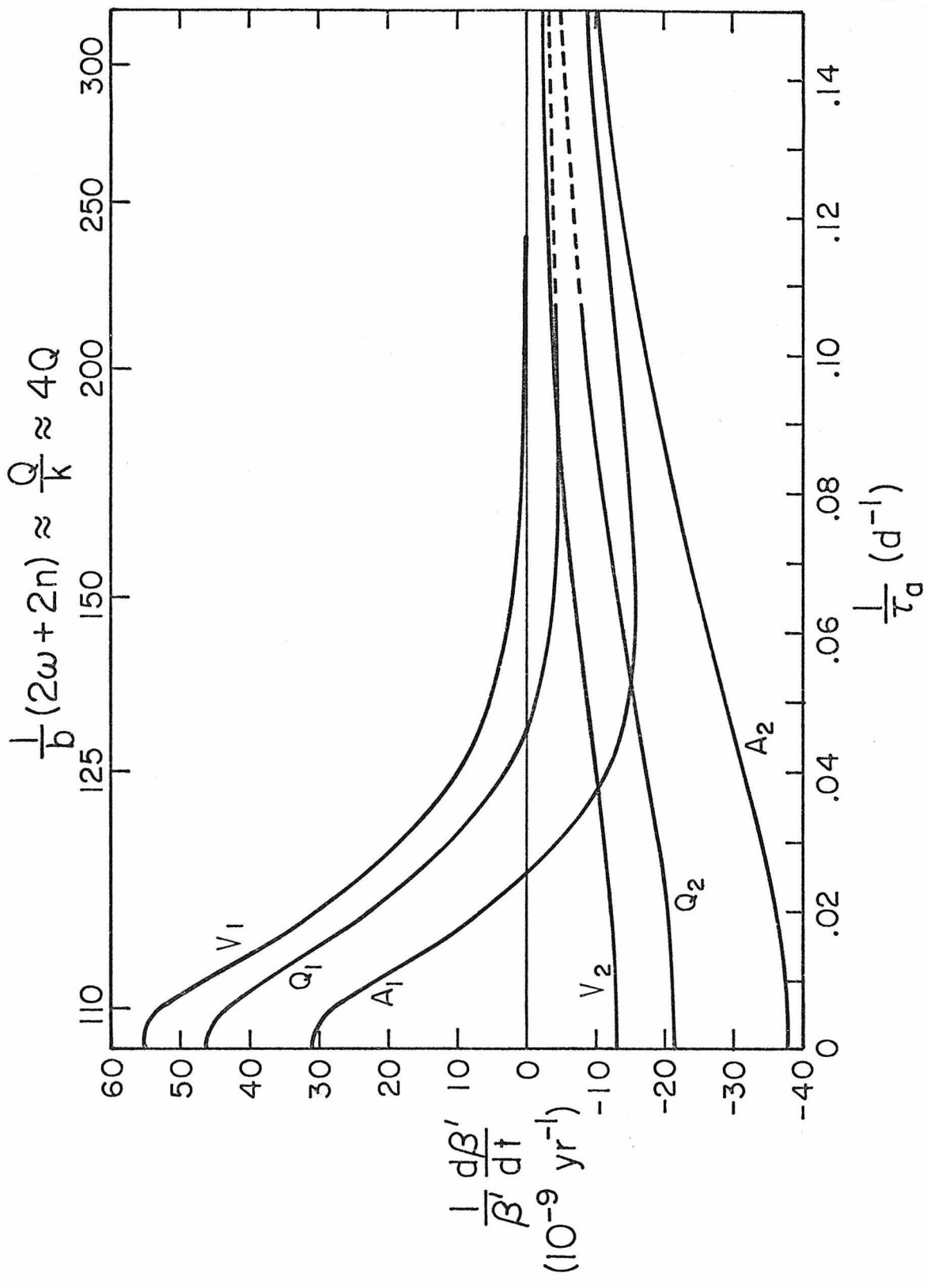
the negative branch of this curve is not shown in Fig. 6, since it is about three orders of magnitude weaker than the positive peak. For the Q_1 model, an obliquity near 180° is only stable when $\tau_a < 1/\sqrt{\omega\,(\omega + 2n)} \approx 21.8$ days; however, eq. (4:20) shows that the rotation rate is unstable for both Q_1 and Q_2 tides whenever $\tau_a \leqslant 9.29$ days, as indicated by the dashed portions of the corresponding curves. Finally, it is easy to show that a retrograde obliquity is always stable for each of these models combined with type 2 atmospheric tides.

Like all the models of body tides, the heating at the ground approach for atmospheric tides depends only on the frequency of each component. Consider the X-axis of the (ω, β) - plane, where $\beta = 0$ or $\beta = 180°$. The various torques on Venus are then symmetrical with respect to the prograde synchronous state $(\omega = n, \beta = 0)$, as shown in Fig. 13 of Part I. If the atmospheric and body tides cancel at $\beta = 180°$ and a rotation rate ω, another equilibrium must occur at $\beta = 0$ and rotation rate $w = \omega + 2n$, corresponding to the same semidiurnal freqency.

It is easy to see from eq. (4:20) that both equilibria must be equally stable or unstable with respect to perturbations in the rotation rate. Stability with respect to obliquity changes can be tested by comparing eq. (4:11) for the prograde state to eq. (4:13) for the retrograde state; for tides of type 1, this gives

$$\frac{1}{\beta} \frac{d\beta}{dt} = \frac{1}{\omega C} \frac{3}{4} [U_o \ b \ (w - 2n) - W_o \ a \ (w - 2n) - U_o \ b \ (w) + W_o \ a \ (w)]$$

$$= \frac{1}{\omega C} \frac{3}{4} [U_o \ b \ (\omega) - W_o \ a \ (\omega) - U_o \ b \ (\omega + 2n) + W_o \ a \ (\omega + 2n)]$$

$$= - \frac{\omega}{w} \frac{1}{\beta'} \frac{d\beta'}{dt} \quad . \tag{4:22}$$

Thus one of the equilibria is stable, and the other unstable, in this regard. Type 2 tides do not exhibit a comparable symmetry, but a prograde obliquity turns out to be stable for each of the models A_2, Q_2, and V_2. (In case an equilibrium occurs between $X = 0$ and $X = n$, it and its mirror configuration are both stable or both unstable for tides of type 1; the situation for type 2 tides is more complicated.)

In general, stable and unstable equilibria can also occur at intermediate obliquities. Figures 7 through 10 following display the configurations in the (ω, β) plane for the models V_1, V_2, Q_1, and Q_2. On the basis of Fig. 6, we have chosen τ_a = 17 days, k = .25, and $Q_{2\omega + 2n} \approx 35$, so that the torques balance at the present rotation rate, and a 180° obliquity is stable in all but the V_1 case. Atmospheric tides acting alone have not been plotted, since for this value of the time constant τ_a, the two types A_1 and A_2 appear quite alike and rather featureless.

In Fig. 7 for V_1-type tides, an unstable equilibrium (labeled U)appears for $\beta \approx 78°$, while a stable state (labeled S)

Figure 7

Spin evolution for type 1 atmospheric tides
plus viscous body tides;
time interval = 3.0×10^7 y

Figure 8

Spin evolution for type 2 atmospheric tides
plus viscous body tides;
time interval = 3.0×10^7 y

Figure 9

Spin evolution for type 1 atmospheric tides
plus constant Q body tides; time interval =
1.5×10^8 y

Figure 10
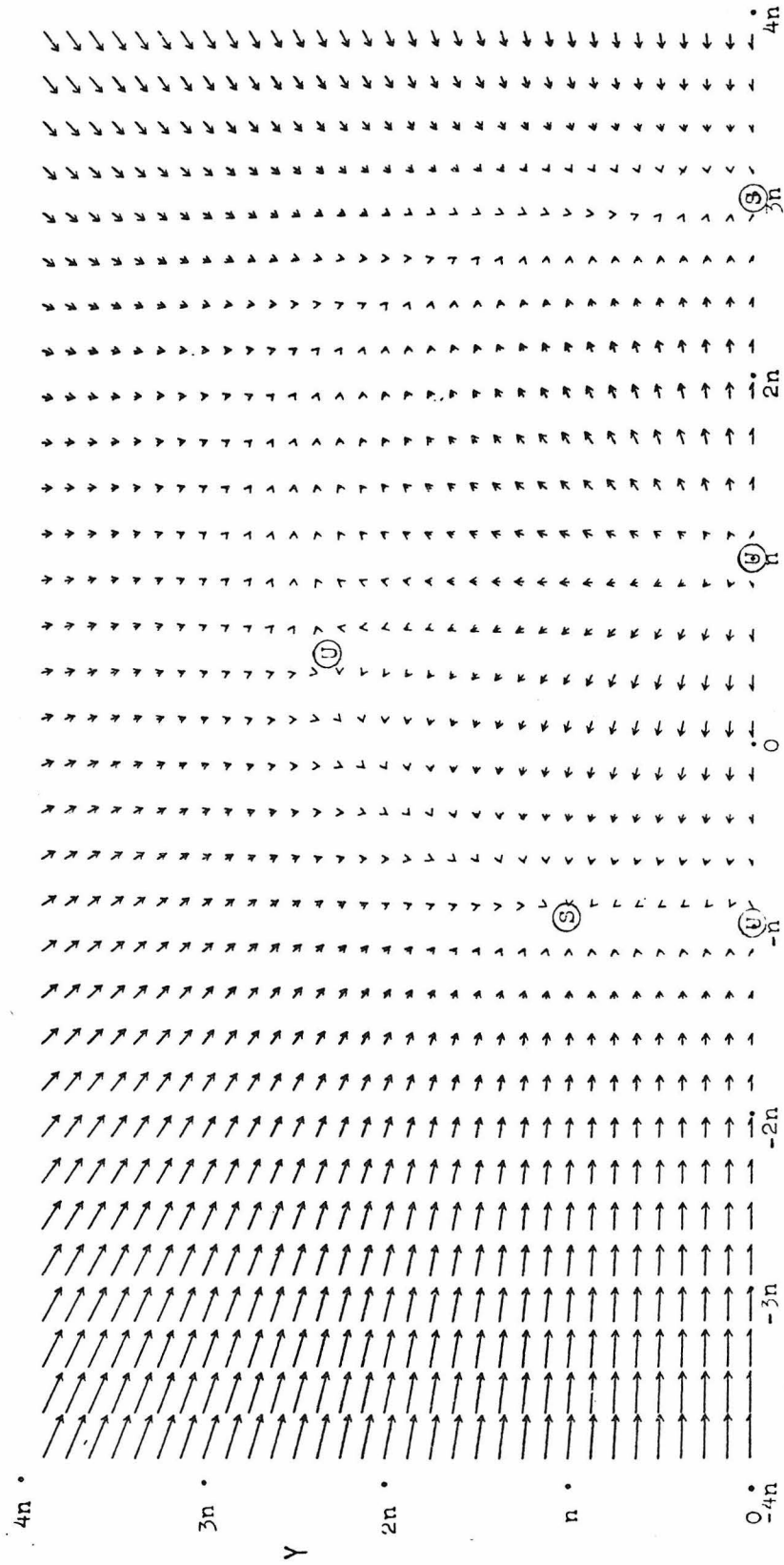
Spin evolution for type 2 atmospheric tides
plus constant Q body tides; time interval =
1.5×10^8 y
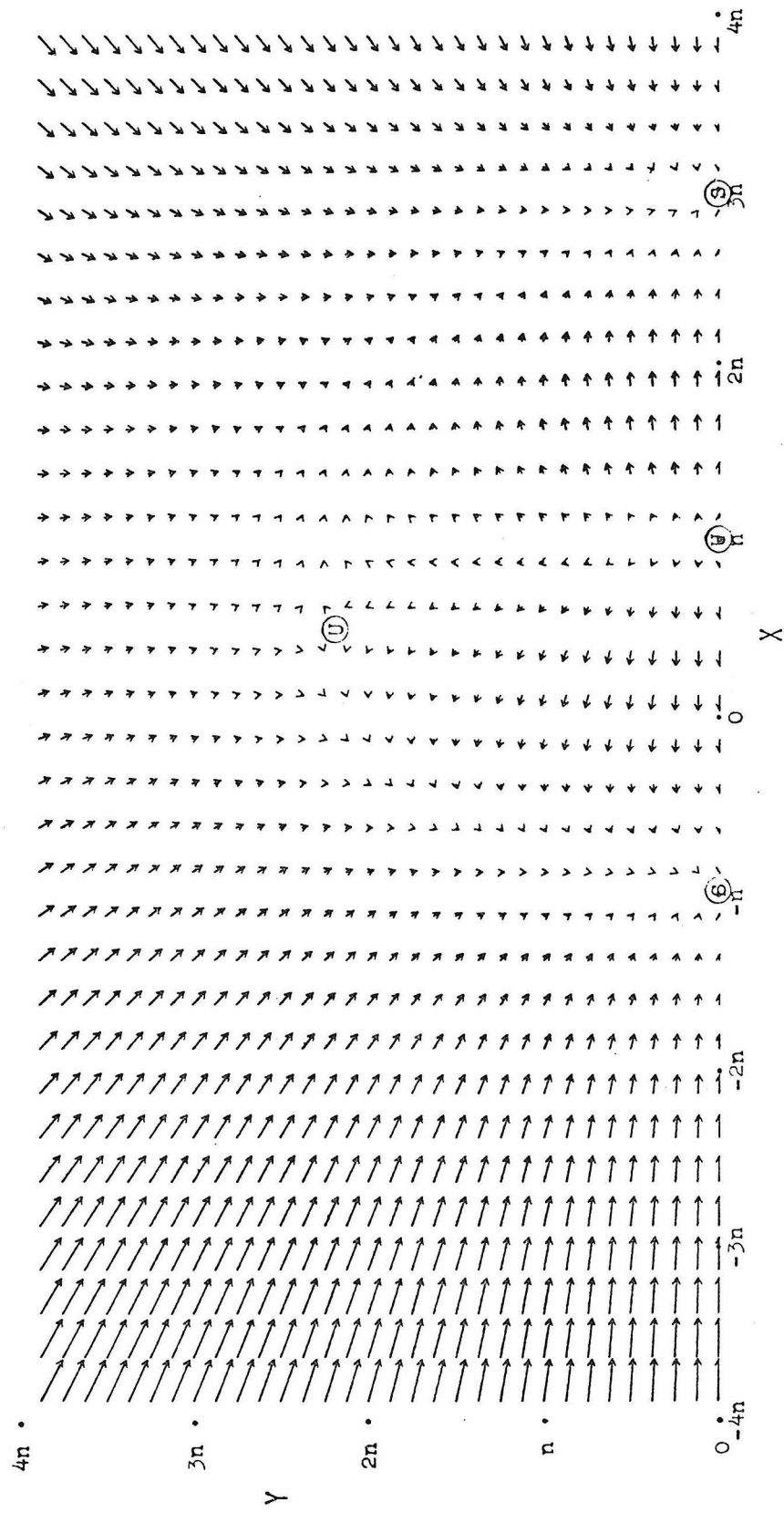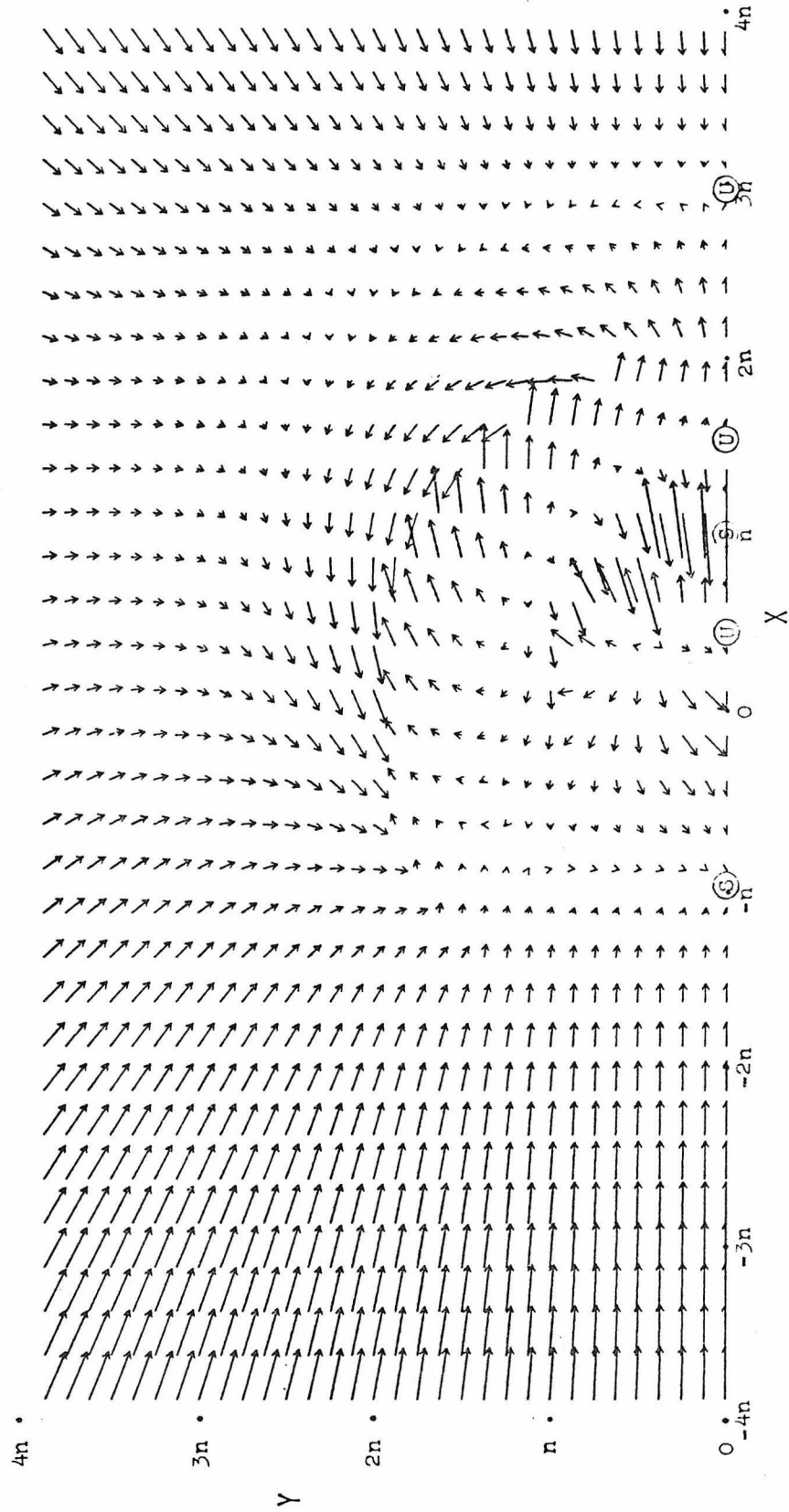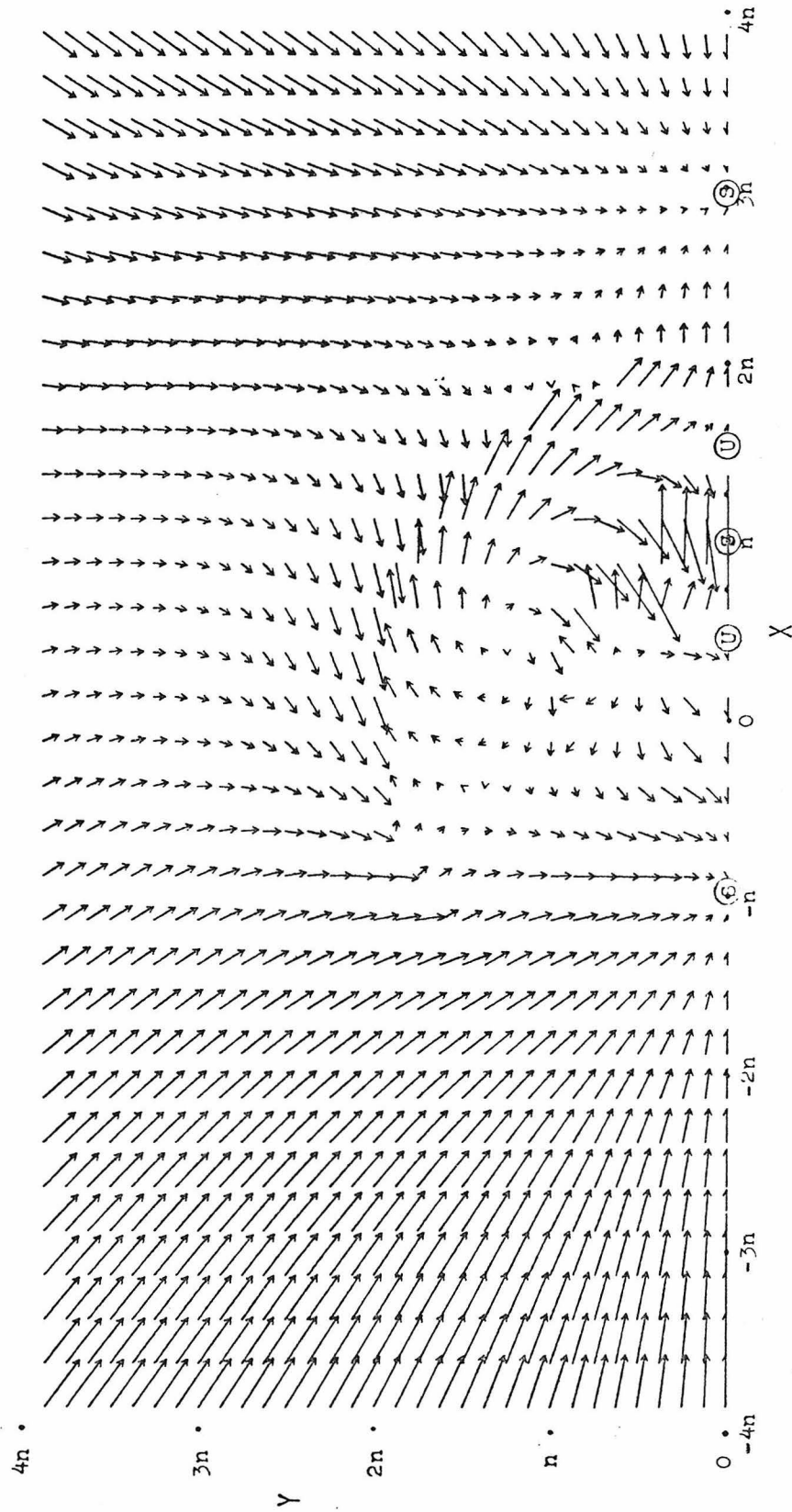
occurs at $\beta \approx 133°$. Since an obliquity of 180° is unstable,

the equilibrium at $\beta = 0$ must be stable. Thus the unstable

equilibrium at an intermediate obliquity is a branch point;

the planet may not cross the trajectory leading into that state,

and must wind up either with $\beta = 133°$ or $\beta = 0$, depending on

initial conditions.

Although we have not the space to show it, this picture

changes smoothly when the parameters vary. As the time constant

τ_a is shortened, and Q is correspondingly increased so as to

maintain the current rotation rate as an equilibrium, the

stable retrograde equilibrium migrates toward $\beta = 180°$, and

merges with the present state when $\tau_a \approx 8.55$ days. Simultaneously

the stable equilibrium at zero obliquity splits into an

unstable equilibrium at $\beta = 0$ and a stable state at a small

prograde obliquity. The picture is simpler for V_2-type tides;

as Fig. 8 shows, both stable equilibria occur on the horizontal

axis.

The situation is more complicated for body tides with

constant Q, shown combined with type 1 atmospheric tides in

Fig. 9. Several poorly-defined equilibria which we have not

bothered to label are visible at intermediate obliquities,

while only one state is stable out of four occurring on the X-axis.

Fig. 10 for the case Q_2 shows that deleting the $\sigma = \omega$ component
of the atmospheric tide affects this picture only slightly,
stabilizing the more rapid prograde equilibrium.

From these plots it appears that only a fraction of the
possible initial conditions lead ultimately to the present
rotation of Venus. Specifically, it appears unlikely that an
originally prograde planet could ever "roll over" and become
retrograde. It must be borne in mind, though, that the heating
at the ground model for atmospheric tides neglects the absorption
in the upper atmosphere of Venus. This forcing produces a
torque which varies in magnitude roughly as $\left(\dfrac{\text{period at the clouds}}{\text{period at the ground}}\right)^2$.

$\left(\dfrac{\text{density at the clouds}}{\text{density at the ground}}\right)^{-1/2}$. For the current basic state this torque
is about an order of magnitude less than that driven by the heating at
the ground, as described in chapter 5 of Part I. If the surface
of Venus were ever rotating several times faster than presently, all
other things being equal, the stratospheric torque might have been
dominant. Thus the simple model of atmospheric tides used above does
not apply much beyond the limits of these plots, and does not allow
firm conclusions regarding the spin history of Venus. In addition,
we much next examine several other influences besides the tides which
may also affect the rotation of Venus.

5. Resonances

The rotation of Venus may also involve the phenomenon of spin-orbit resonance. The present rotation rate may be stabilized by the weak torque exerted by the Earth on the permanent quadrupole moment of Venus, discussed in chapter 7 of Part I. This resonance would also have an effect on the obliquity comparable to the influence of the atmospheric and body tides. In the past, other resonances may have affected the history of Venus' spin.

First consider the gravitational interaction of the sun with the permanent quadrupole moment of Venus. Its contribution to the Hamiltonian is given by equation (11) of Goldreich and Peale (1970); in our notation, this may be written

$$
\begin{aligned}
V_\odot = \frac{GM_\odot}{2\bar{r}^3} \sum_{q=-\infty}^{\infty} \Bigg\{ & (2C-A-B)\ (\tfrac{3}{4}\sin^2\beta - \tfrac{1}{2})\ G_{21q}\ (e)\ \cos[qnt] \\
& - (2C-A-B)\sin^2\beta\ G_{20q}\ (e)\ \cos[2\tilde{\omega} - 2\alpha + (2+q)\ nt] \\
& - \tfrac{3}{4}\ (B-A)\sin^2\beta\ G_{21q}\ (e)\ \cos[qnt - 2\gamma] \\
& - \tfrac{3}{8}\ (B-A)\ (1+\cos\beta)^2\ G_{20q}\ (e)\ \cos[2\tilde{\omega} - 2\alpha + (2+q)nt - 2\gamma] \\
& - \tfrac{3}{8}\ (B-A)\ (1-\cos\beta)^2\ G_{20q}\ (e)\ \cos[2\tilde{\omega} - 2\alpha + (2+q)nt + 2\gamma] \Bigg\}.
\end{aligned}
\tag{5:1}
$$

Here $\tilde{\omega}$ represents the longitude of perihelion measured from the $\hat{I}$ axis, while the average distance $\bar{r}$ of Venus from the sun is identical to the semimajor axis of its orbit.

The G_{2pq} (e) appearing in eq. (5:1) above are the functions of eccentricity tabulated by Kaula (1964). In general, G_{2pq} (e) = $G_{2,2-p,-q}$ (e) is of order $e^{|q|}$ or higher in the orbital eccentricity e; in particular, Kaula (1964) gives

$$G_{210} \text{ (e) } = (1 - e^2)^{-3/2}, \quad G_{20-2} \text{ (e) } = G_{222} \text{ (e) } = 0 \quad . \qquad (5:2)$$

It is clear that expression (5:1) contains short-period terms. In order to find the secular contribution to the Hamiltonian, we must average $V_{\odot}$ with respect to time. As long as ω has no special value, the terms in (5:1) proportional to the equatorial asymmetry (B-A) vanish in the mean. The remaining terms are proportional to the dynamical oblateness $(2C-A-B = 2M_{\mathfemale} \, a^2 J_2)$; eq. (5:2) shows that the average of the second term also vanishes, while the first term becomes

$$V_s = \frac{GM_{\odot}}{2r^3} \text{ (2C-A-B) } (\frac{3}{4} \sin^2 \beta - \frac{1}{2}) (1 - e^2)^{-3/2} \qquad . \qquad (5:3)$$

The equatorial asymmetry can interact with the solar gravitation in the long run, provided that the planet turns the same hemisphere towards the sun on successive or alternating perihelia. These are known as spin-orbit resonances of the first kind, of which the $\omega = \frac{3}{2}$ n rotation of Mercury is the prime example. The terms in (5:1) containing 2 γ can thus contribute to the mean Hamiltonian in case 2ω/n is nearly an

integer (say m), so that their frequencies vanish, or become comparable to the secular rates. Averaging eq. (5:1) then leaves three additional terms with different dependences on the obliquity and eccentricity: a prograde-type contribution

$$V_p = - \frac{GM_\odot}{2r^{-3}} \frac{3}{8} (B-A) (1 + \cos \beta)^2 G_{20(m-2)} (e)$$

$$\cdot \cos (2\tilde{\omega} - 2\alpha + mnt - 2\gamma) \quad , \qquad (5:4)$$

a retrograde-type term

$$V_r = - \frac{GM_\odot}{2r^{-3}} \frac{3}{8} (B-A) (1 - \cos \beta)^2 G_{20}$$

$$\cdot \cos (2\tilde{\omega} - 2\alpha - mnt + 2\gamma) \quad , \qquad (5:5)$$

and an oblique-type term

$$V_o = - \frac{GM_\odot}{2r^{-3}} \frac{3}{4} (B-A) \sin^2 \beta \; G_{21m} (e) \cos (mnt - 2\gamma) . \qquad (5:6)$$

Because of their different resonant arguments, the three terms displayed above behave somewhat differently in the equations of motion.

As eq. (5:2) shows, V_p and V_r defined above vanish when $m = 0$, but V_o does not. Therefore the $\omega \approx 0$ resonance has purely oblique character, and would disappear altogether if the obliquity were 0 or 180°. This is worth noting because it is a common simplifying assumption in studies of this nature to let the planet's axis of greatest inertia be perpendicular to the orbit plane. Extra caution must be exercised in this particular case, though, because the planet would be practically nonrotating with respect to inertial space, and the basic

assumption of principal axis rotation may also be violated.

All of the other solar resonances contain terms of each type. Since the retrograde-type contribution is of higher order in e than the others, it only dominates for obliquities within about a degree of 180°. Except for the $\omega = n/2$ case, which contains mixed prograde and oblique terms of first order, and $\omega = 0$, all of the resonances have mainly prograde character for obliquities less than about 170°. The significance of this fact will be described shortly.

For certain rotation rates, the quadrupole moment of Venus can also interact with the orbits of the other planets; these are known as spin-orbit resonances of the second kind. The sidereal rotation period of Venus has been measured at $243.00 \pm .04$ days (Shapiro et al., 1978). If the period is actually 243.165 days, Venus would present the same face to the Earth at each inferior conjunction (Goldreich and Peale, 1966a, 1967, 1970). This situation is depicted in Fig. 11, where the position and orientation of Venus are viewed in a reference frame where the Earth and sun are fixed. Resonances with other planets such as Jupiter or Mercury are possible, but the nearest lie several days away from the observed period and are at least an order of magnitude weaker than the Earth resonance (Bellomo et al., 1967).

Figure 11

Resonant rotation of Venus as seen in a frame

of reference where the Earth and sun are fixed
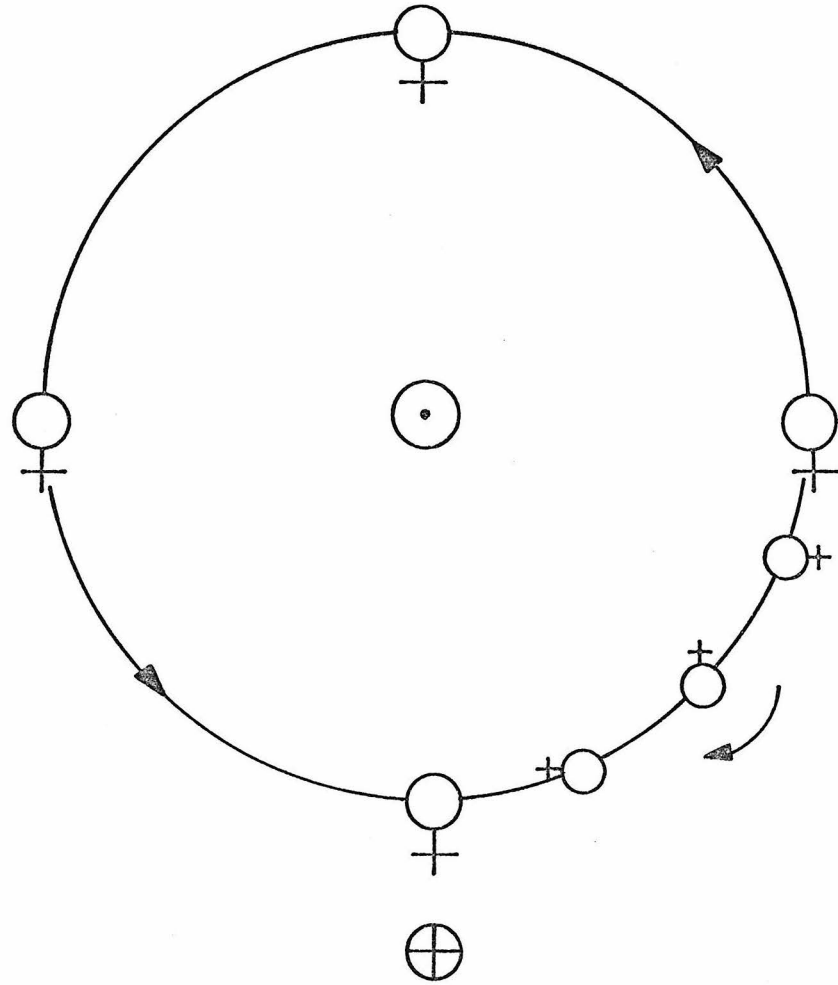
The Hamiltonian term $V_{\oplus}$ arising from the suspected Earth resonance can be developed in a parallel manner to the solar contribution described above. Goldreich and Peale (1970) have shown that the unperturbed eccentricities and mutual inclination between the orbits of the Earth and Venus can be ignored. The Earth resonance is then clearly of the retrograde type. If we choose the $\hat{1}$ inertial axis as well as the origin of time at some initial inferior conjunction, Goldreich and Peale's (1970) expression for the secular interaction becomes

$$V_{\oplus} \approx - \, 0.958 \, \frac{GM_{\oplus}}{r^3} \, \frac{3}{16} \, (B-A) \, (1 - \cos \beta)^2 \, \cos \, [-2\alpha + 5n_{\oplus} - 4nt + 2\gamma].$$

$$(5:7)$$

A square omitted from the factor $(1 - \cos \theta)$ in eq. (29) of Goldreich and Peale (1970) has been supplied in eq. (5:7) above, while the functions $F_{201}(\cos \theta)$ and $F_{220}(\cos \theta)$ in their equation (27) should be $F_{210}(\cos \theta)$ and $F_{222}(\cos \theta)$ respectively.

The strength T of a resonance may be defined as the greatest torque it can exert either for despinning or accelerating the rotation rate. For example, applying eq. (2:4) to (5:7) gives

$$\mathcal{T} = \max\ \frac{\partial V}{\partial \gamma} = 0.958\ \frac{GM_\oplus}{r^3}\ \frac{3}{8}\ (B-A)\ (1 - \cos\beta)^2 \approx 1.47 \times 10^{14}\ J$$

$$\cdot\ (1 - \cos\beta)^2 \cdot \qquad\qquad (5:8)$$

Here we have assumed $\dfrac{B-C}{C} = \dfrac{B-A}{.33\ M_\varphi a^2} = 2.21 \times 10^{-6}$, the same

value as for the Earth. Comparison of (5:8) above with eq.

(7:5) of Part I shows that the Earth resonance is probably

about an order of magnitude weaker than the torque due to

body tides.

Equations (5:4) through (5:6) yield similar expressions

for the strengths of the solar resonances, but the mass of

the Earth is replaced by the mass of sun and a factor depending

on the orbital eccentricity e of Venus. Since e is on the

order of 10^{-2} while $\dfrac{M_\odot}{M_\oplus} \approx 329000$ (including the mass of the moon),

the Earth resonance is stronger than all of the solar resonances

for $\omega \gtrsim 3n$. Furthermore, the orbital parameters of Venus vary on a

time scale of about 10^5 years, and the eccentricity occasionally

vanishes. Whenever this happens, only the $\omega = 0$ and $\omega = n$ resonances

exist, so that capture into any of the other solar resonances

is liable to be only temporary.

The generally accepted mechanism for capture into a spin-orbit resonance of the first kind cannot provide for capture of Venus into a spin-orbit resonance of the second kind (Goldreich and Peale, 1966b, 1967). However, an alternative capture mechanism (Goldreich and Peale, 1967, 1970) will be discussed in the next chapter. Once the rotation has been captured, the resonant argument librates about some mean with a period L given by

$$L = 2\pi \quad \sqrt{C/\Upsilon} \qquad \qquad \text{(5:9)}$$

Substituting Υ from eq. (5:8) into (5:9) above gives $L \approx 63000$ yr for the Earth resonance; the libration periods for the solar resonances scale accordingly. The frequency of libration may be regarded as defining the "linewidth" of a resonance; for example, $\frac{2\pi}{243d} \pm \frac{2\pi}{63000yr} \approx \frac{2\pi}{243 \pm .002d}$. The rotation period thus needs to be within about .002 d of the resonant value for the Earth substantially to affect the spin of Venus. The measured rotation period is almost a hundred times farther away (Shapiro et al., 1978), so that the resonant argument in eq. (5:7) would circulate through a full cycle about once every 500 years. On the other hand, the data do not altogether exclude the possibility of resonance (by about 4 standard deviations), especially considering that the measured

period is about a hundred times closer to this particular

resonance than to any others.

Suppose that the spin of Venus were trapped in a resonance

and the librations were damped out. Then the resonant argument would

adjust itself to some mean phase such that the solar tides just

balanced the resonant effect on the rotation rate. In the Hamiltonian

formalism employed heretofore, this may be expressed

$$0 = \frac{d\omega}{dt} = -\frac{1}{c}\frac{\partial}{\partial\gamma}(U+W+V) \rightarrow \frac{\partial}{\partial\gamma}V = -\frac{\partial}{\partial\gamma}(U+W) \quad . \qquad (5:10)$$

Equation (5:10) above may now be solved for V; that value can

then be inserted into (2:5) in order to find the behavior of

the obliquity within a resonance.

Instead of solving for the phase of the resonant argument

in each case, a clever substitution used by Goldreich and Peale

(1970) permits us greatly to simplify the problem. Equation

(2:5) for $\frac{d\beta}{dt}$ involves $\frac{\partial V}{\partial\alpha}$ and $\frac{\partial V}{\partial\gamma}$. Since $\frac{\partial V}{\partial\gamma}$ has already been

evaluated in eq. (5:8), we need only to relate it to $\frac{\partial V}{\partial\alpha}$.

When $\omega \approx 0$, only the oblique-type term (5:6) contributes

to V, so that $\frac{\partial V}{\partial\alpha} = 0$; however, the obliquity is then poorly defined

since eq. (2:5) involves dividing by ω. The $\omega \approx n/2$ resonance is of

mixed type, such that its behavior depends on the angle between

equinox and perihelion; we shall not go into it further.

All of the other solar resonances are of dominantly prograde

type, for which eq. (5:4) shows that $\frac{\partial V}{\partial \alpha} = \frac{\partial V}{\partial \gamma}$. Since the possible Earth resonance is mostly of retrograde type, (5:7) gives $\frac{\partial}{\partial \alpha} V_{\oplus} = - \frac{\partial}{\partial \gamma} V_{\oplus}$. Using the above along with (5:10) to replace V in eq. (2:5) then gives

$$
\begin{aligned}
\frac{d\beta}{dt} &= \frac{1}{\omega C} \frac{1}{\sin \beta} \frac{\partial}{\partial \alpha} (U+W+V) - \frac{1}{\omega C} \frac{\cos \beta}{\sin \beta} \frac{\partial}{\partial \gamma} (U+W+V) \\
&= \frac{1}{\omega C} \frac{1}{\sin \beta} \frac{\partial}{\partial \alpha} (U+W+V) = \frac{1}{\omega C} \frac{1}{\sin \beta} \left[\frac{\partial}{\partial \alpha} (U+W) \pm \frac{\partial}{\partial \gamma} V \right] \quad (5:11) \\
&= \frac{1}{\omega C} \frac{1}{\sin \beta} \left[\frac{\partial}{\partial \alpha} (U+W) \mp \frac{\partial}{\partial \gamma} (U+W) \right] \quad ,
\end{aligned}
$$

where the upper sign of the $\pm$ and $\mp$ refers to the solar resonances with $\omega \geqslant n$, and the lower sign refers to the Earth resonance. The net effect of resonance lock is as if the term V did not appear at all in eq. (5:11) above, but the factor $\cos \beta$ were replaced by +1 for prograde-type resonances and by -1 for retrograde-type resonances.

The above technique can now be applied to any suitable model of atmospheric and body tides. Figures 12 through 18 following show the rate of change of the obliquity versus the obliquity; in each case the scale factor is given in inverse years along the vertical axis. The solid curves, labeled with the symbols Δ, $+$, x, and $\lozenge$, correspond to rotation rates $\omega = n$, $\frac{3}{2}n$, $2n$, and $\frac{5}{2}n$, respectively. The dashed curves refer to the Earth commensurability with $\omega = \frac{2\pi}{243\ d} \approx .927n$. The graph on the left side of each figure shows the effects of the resonances from eq. (5:11); for comparison, the graph on the right corresponds to the same rotation rates, but without resonant trapping, according to eq. (3:12). The cases portrayed in Figs. 12 through 18 employ the same parameter values as Figs. 3-5 and 7-10; the right-hand curves in the former set therefore give $\frac{d\beta}{dt}$ along the appropriate semicircular cross-sections of the (X,Y)-plane in the latter. Note in particular that Figure 8 for the constant Q model of body tides can actually be extended to all rotation rates $\omega \geq n$, since $\omega \times \frac{d\beta}{dt}$ depends only on β in each of the five regions defined in eq. (3:24).

For every nonresonant case, inspection reveals that the rate of change of the obliquity vanishes at either end of

Figure 12

Spin evolution at resonance for the viscous model of body tides;

Δ: $\omega = n$; +: $\omega = \frac{3}{2} n$; x: $\omega = 2n$; $\Diamond$: $\omega = \frac{5}{2} n$. Dashed curves:

$\omega = \frac{2\pi}{243 \ d} \approx .927 \ n$.

Figure 13

Spin evolution at resonance for the constant Q model of body tides.

Figure 14

Spin evolution at resonance for the elasticoviscous model of body

tides.

Figure 15

Spin evolution at resonance for type 1 atmospheric tides plus

viscous body tides.

Figure 16

Spin evolution at resonance for type 2 atmospheric tides plus

viscous body tides.

Figure 17

Spin evolution at resonance for type 1 atmospheric tides plus

constant Q body tides.

Figure 18

Spin evolution at resonance for type 2 atmospheric tides plus

constant Q body tides.

SCALE FACTOR = 10⁻⁷

SCALE FACTOR = 10⁻⁷

199

SCALE FACTOR = 10⁻⁷

SCALE FACTOR = 10⁻⁷

202

SCALE FACTOR = 10^{-7}

SCALE FACTOR = 10^{-7}

OBLIQUITY

OBLIQUITY

$\frac{d\beta}{dt}$

$\frac{d\beta}{dt}$
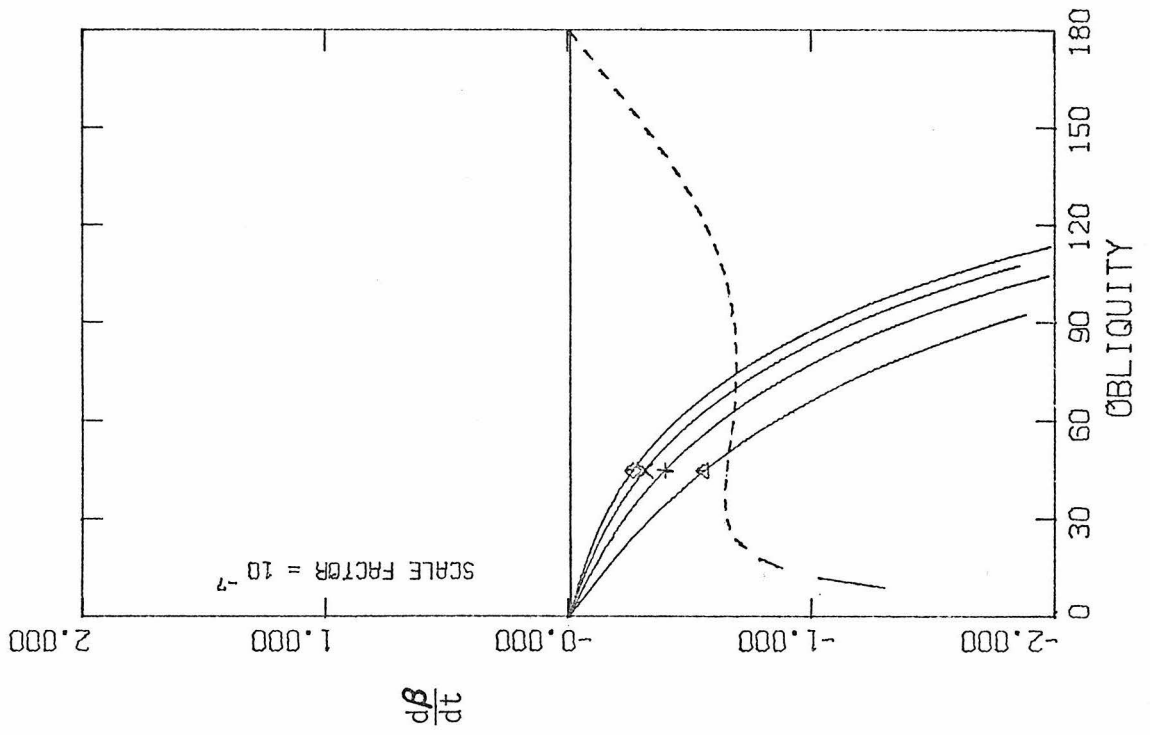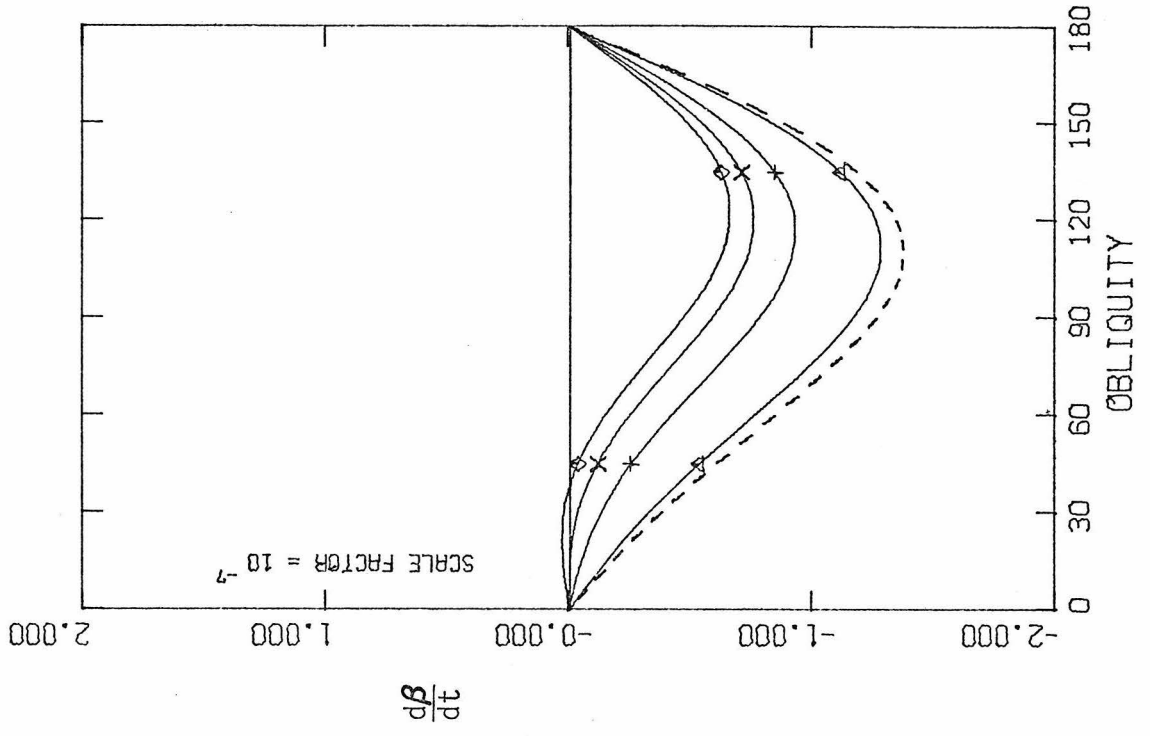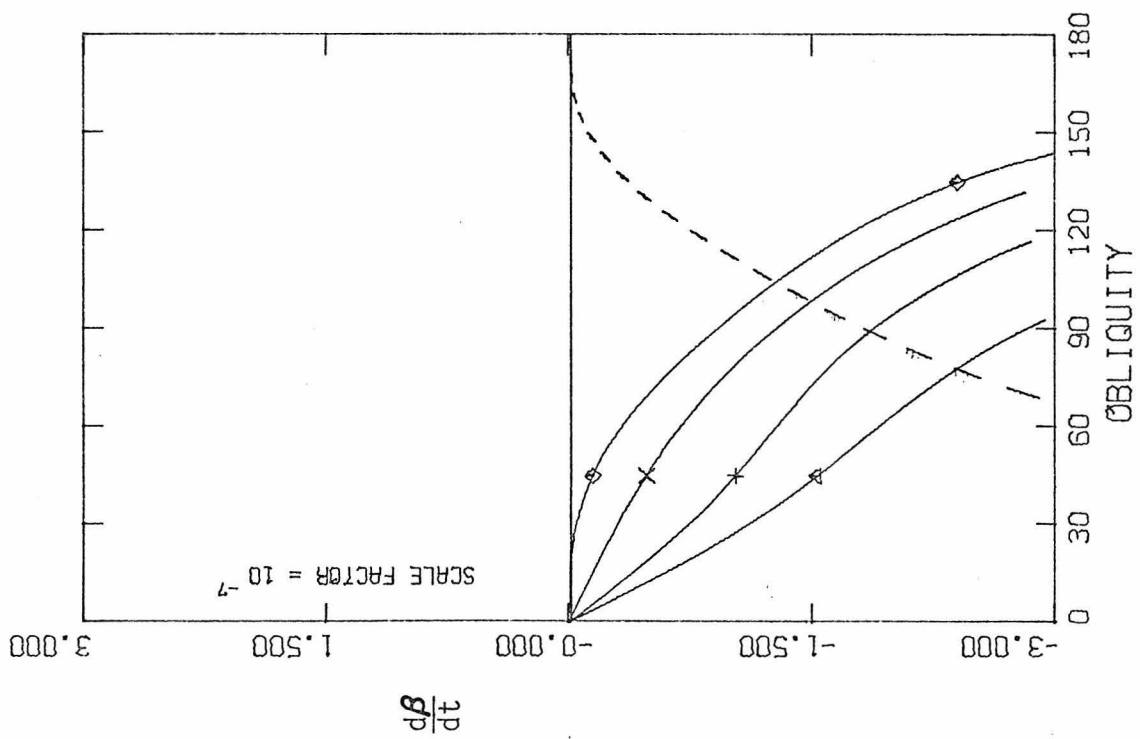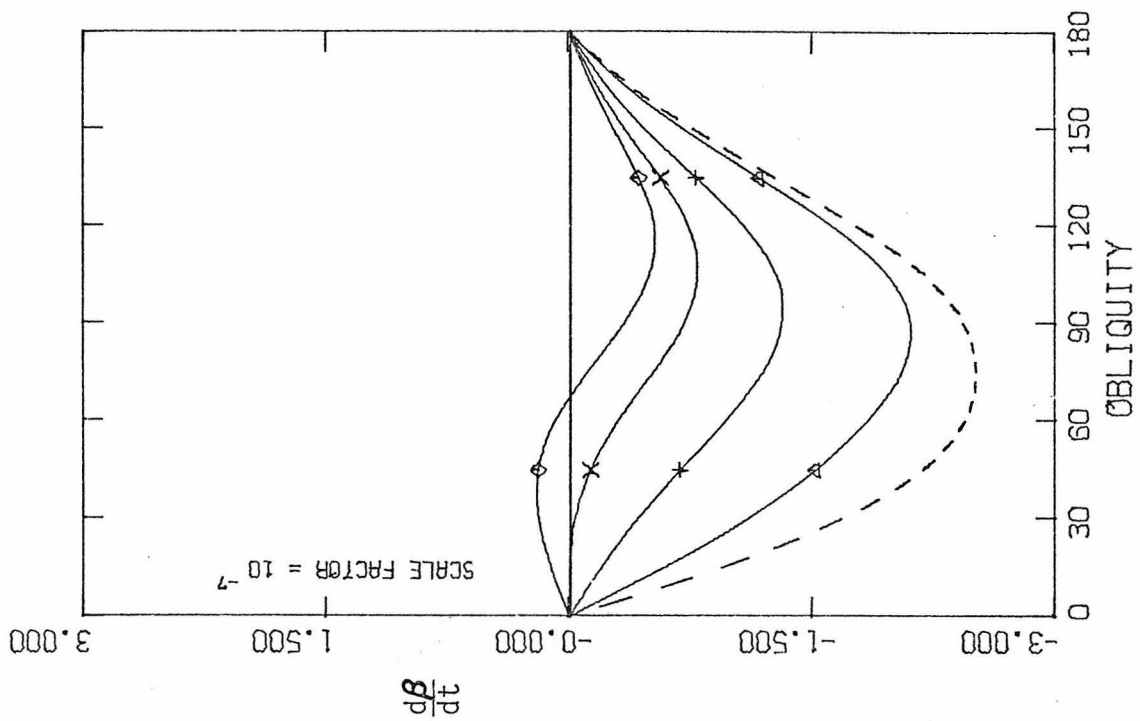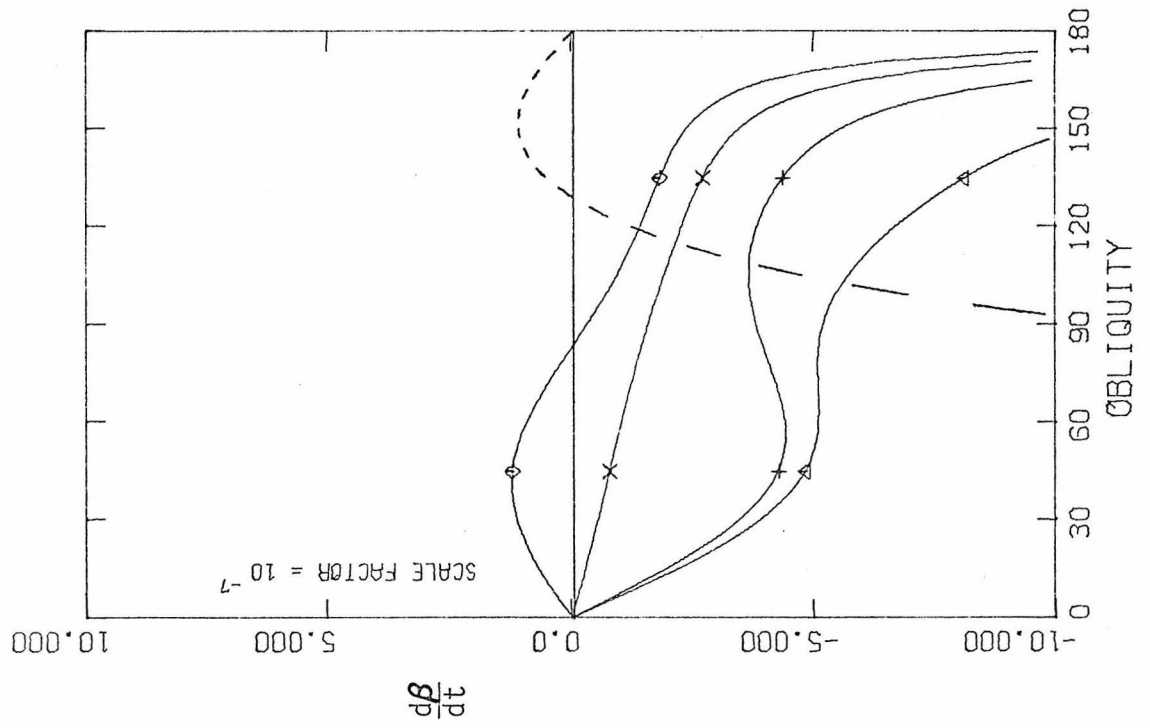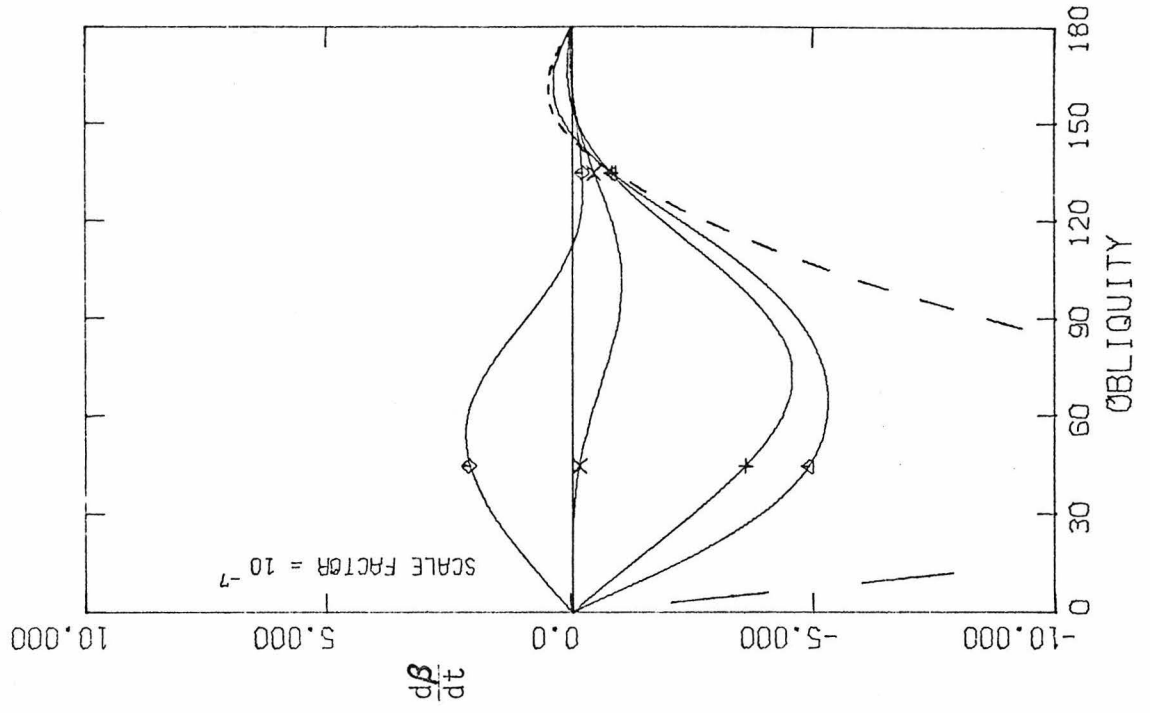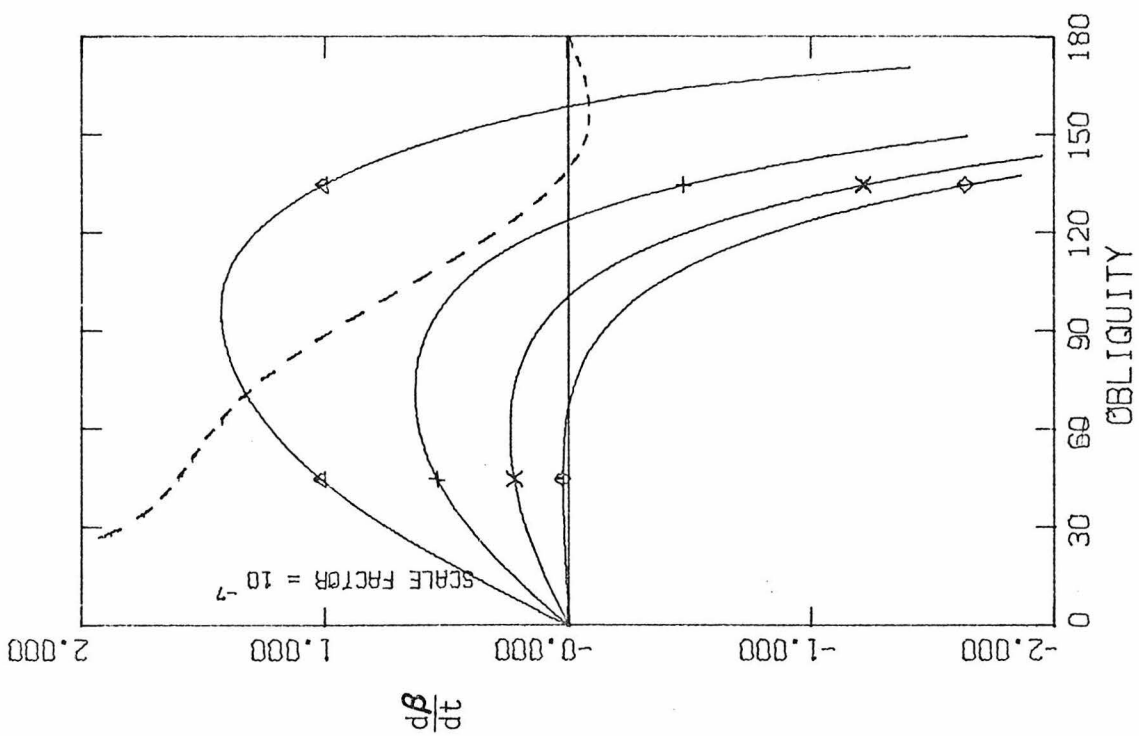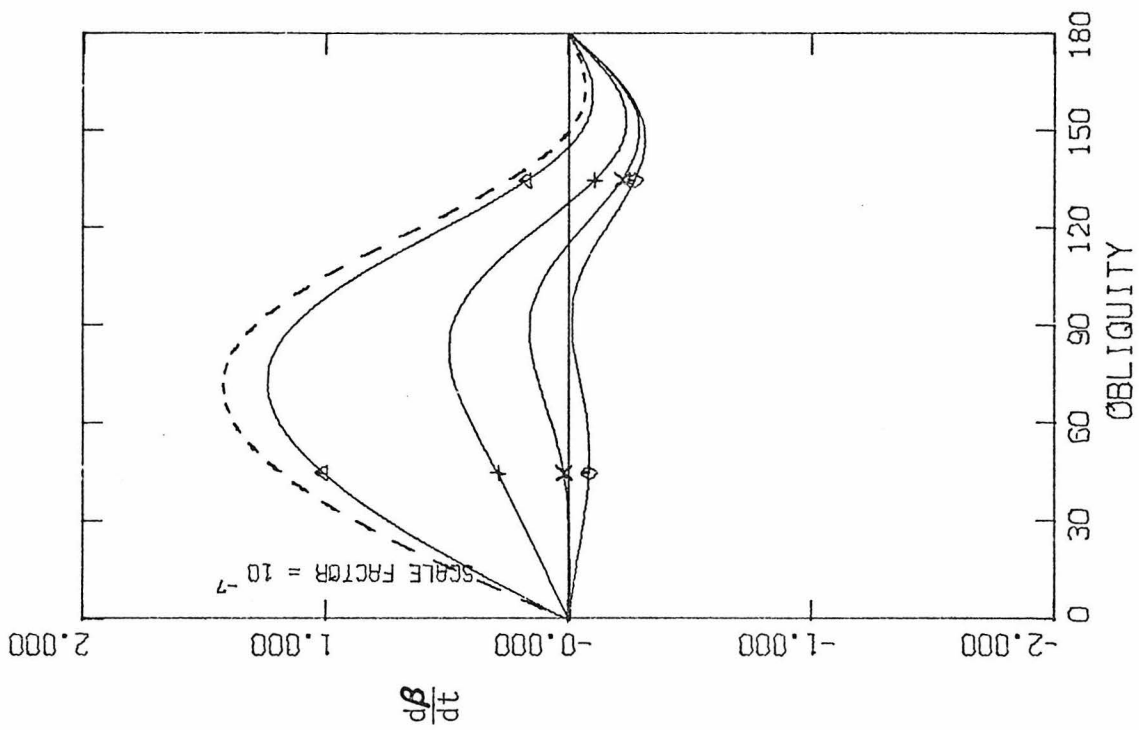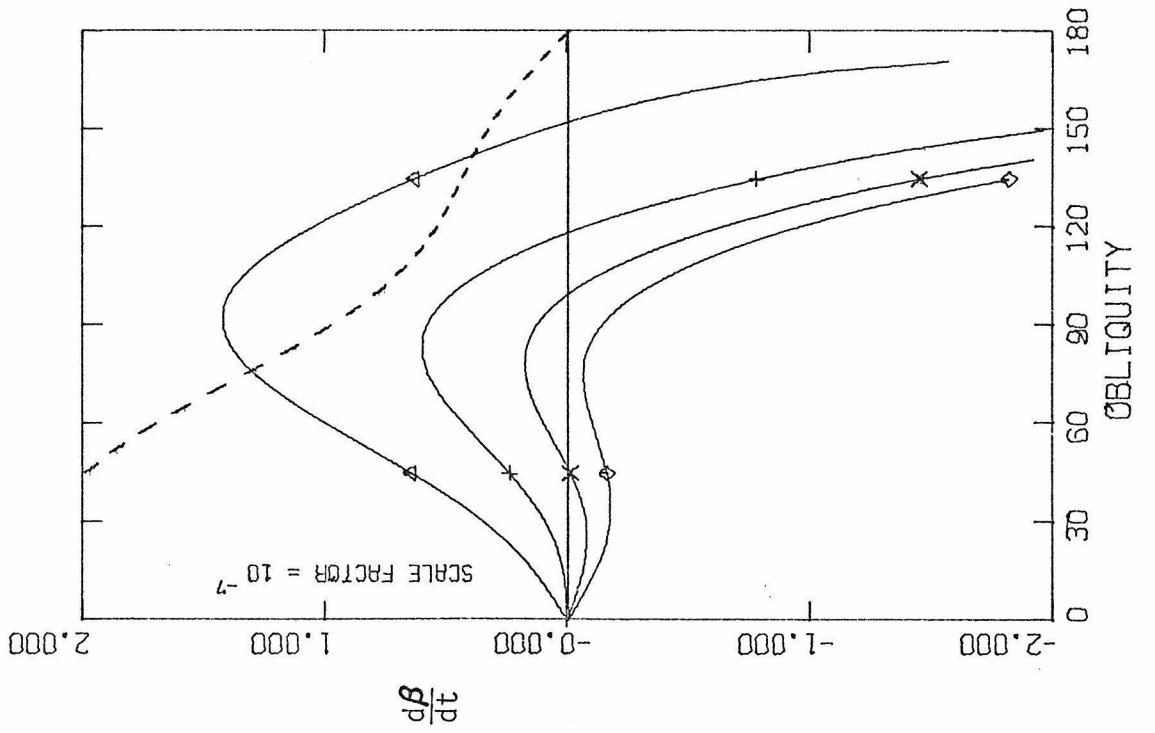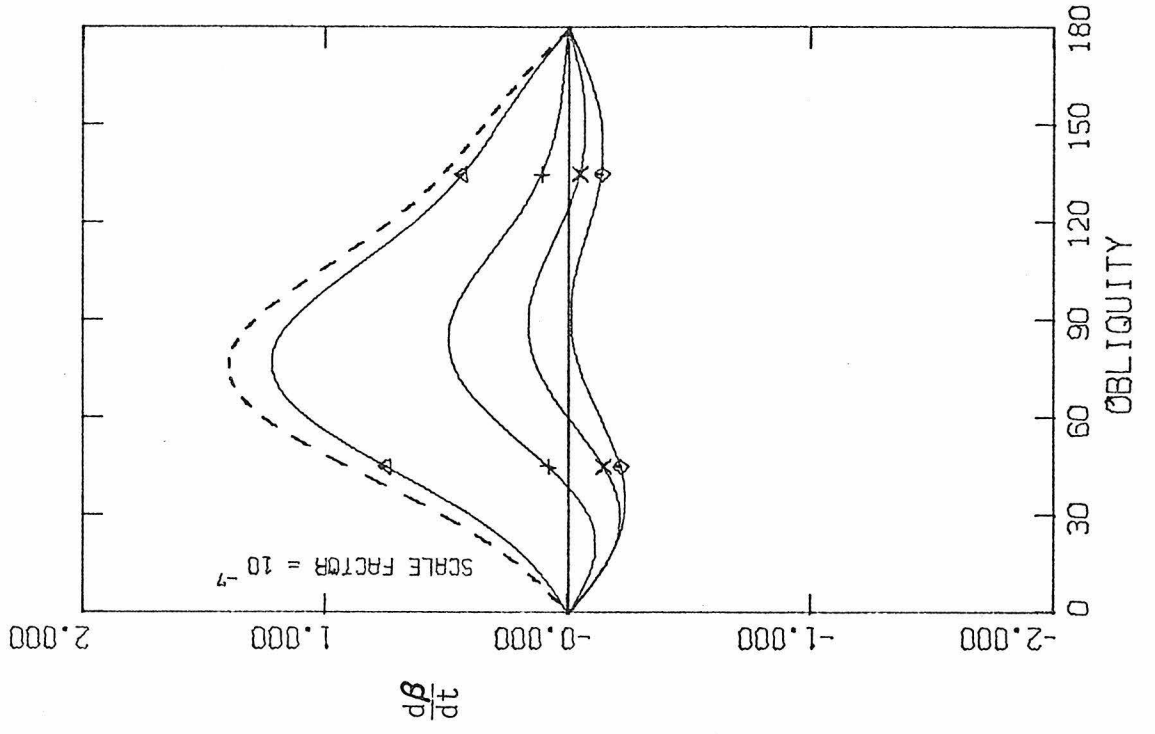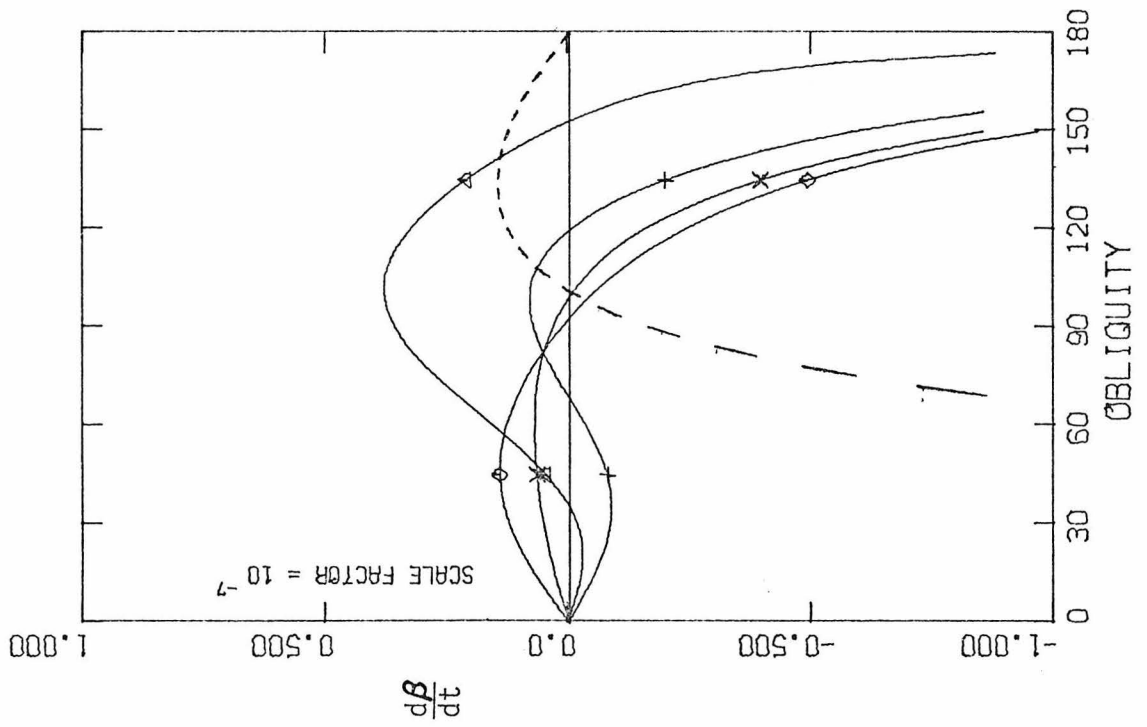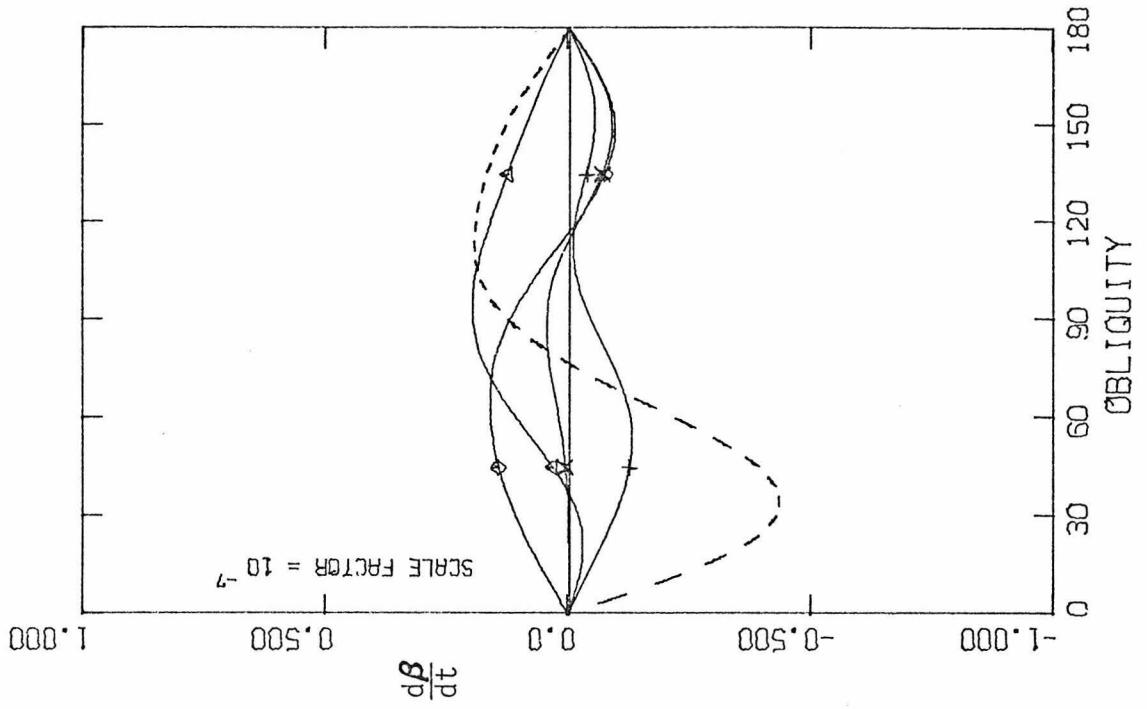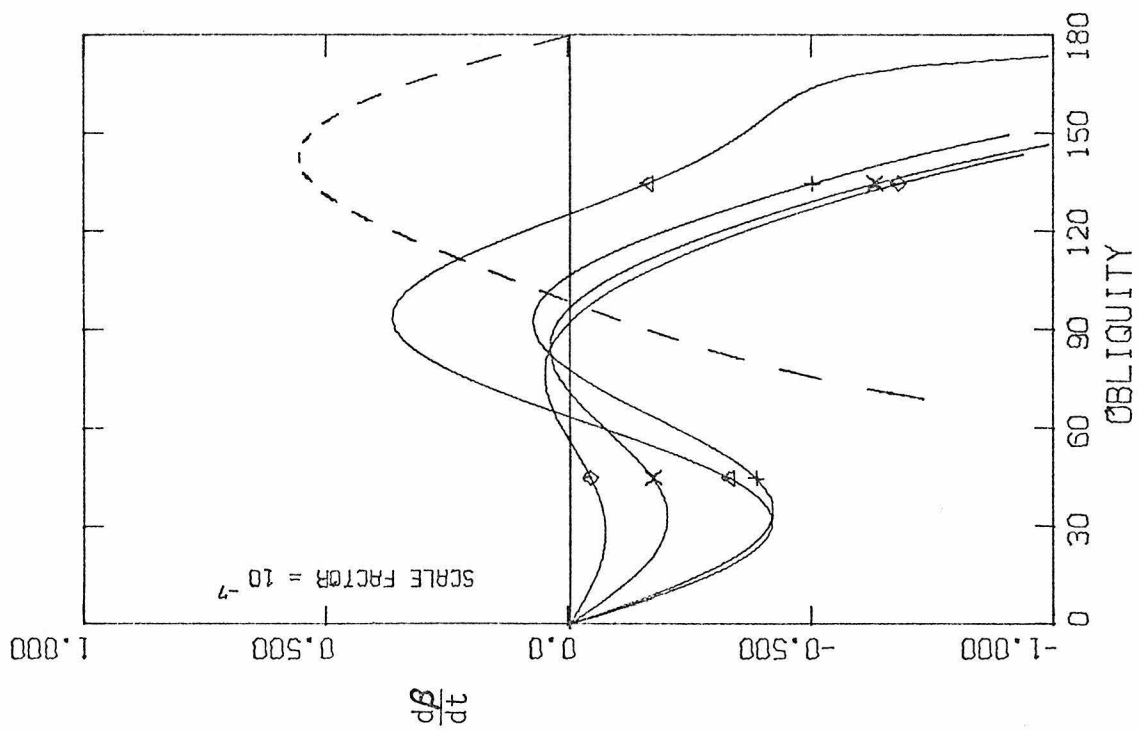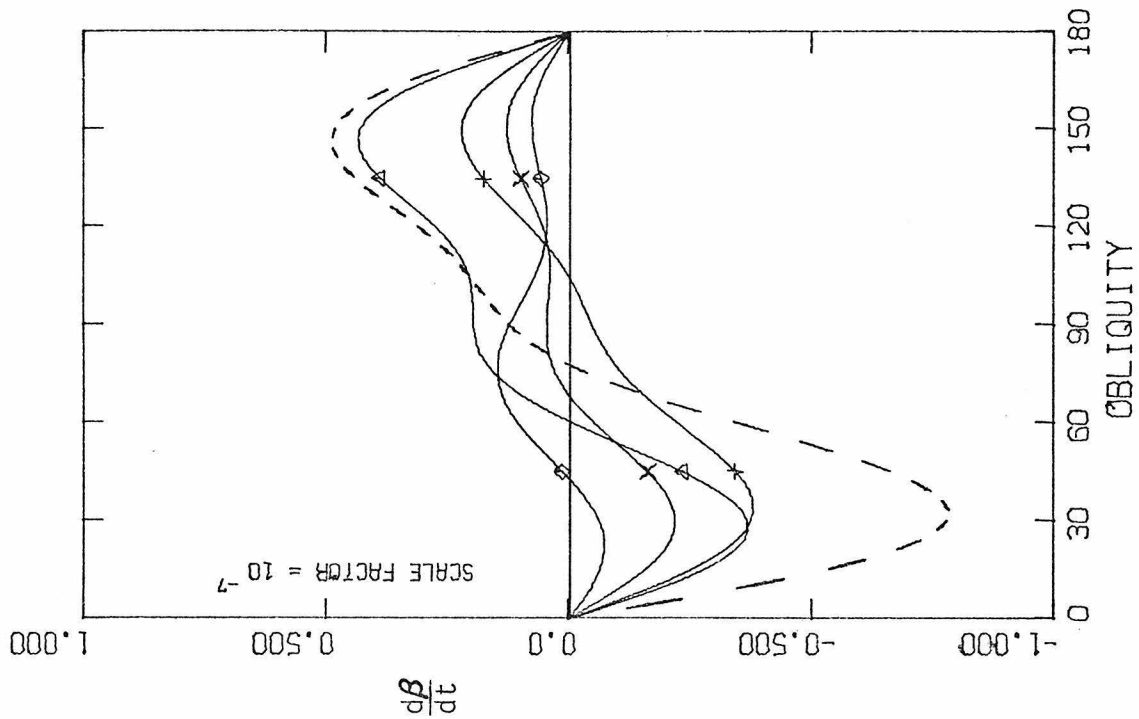
the scale, as it must. In contrast, within each of the solar resonances, $\frac{d\beta}{dt}$ becomes negatively infinite as β approaches 180°, and tends to destabilize a retrograde rotation. This cannot be taken literally, though, because the resonances change character and become much weaker at such high obliquities, so that the obliquity may be stabilized or the planet might escape from resonance altogether.

In contrast to the solar resonances, the Earth resonance is well behaved because of its retrograde character. This resonance only fades out or changes character for obliquities of less than a few degrees. Goldreich and Peale (1970) claim that expression (5:7) for the Earth-Venus interaction "... is only valid for θ (our β) somewhat greater then 90°, since the stability of the resonance decreases as θ approaches 90°." This remark appears to be inaccurate as it stands, but it would be apt if 90° were replaced by 0 in the above quotation.

When the net tidal torque on the planet is decelerating, eq. (5:11) shows that the Earth resonance has a stabilizing influence on an obliquity of 180°. Nevertheless, Figs. 12 and 13 confirm that this effect alone is not strong enough to maintain the present orientation of Venus against either the

viscous or constant Q models of body tides (compare Figs. 1, 2, and 4 of Goldreich and Peale, 1970). Yet if the rotation is already stable or nearly stable to begin with, resonance with the Earth distinctly augments its stability; witness Fig. 14 for the Darwin model of body tides.

The possibility of spin-orbit resonances revives the question of "roll-over". It is conceivable that Venus may once have evolved to a slow prograde rotation, and then been captured into a resonance of either the first or second kind. Subsequently it would travel along a circular arc in the (ω, β) plane at a fixed rotation rate. Because of the altered influence on its obliquity, Venus might then have turned from prograde to retrograde. If it were in the Earth resonance, it would remain there up to the present day; if in a solar resonance, it could be expected to escape as the resonance weakens at high obliquities, and finally to evolve a bit farther to the currently observed spin state. Unfortunately, the particular curves plotted in Figs. 12–18 show rather few instances where $\frac{d\beta}{dt}$ switches from negative to positive as a result of capture into a resonance. Furthermore, most of the solar resonances could not survive long enough for the obliquity to evolve substantially ($\sim 10^5$ years compared with $\sim 10^8$ years). We conclude that Venus is unlikely to have

turned retrograde because of resonant effects. The next
chapter deals with a much stronger constraint on the possibility
of "roll-over".

6. Precession, Nutation, and Related Phenomena

In order to specify completely the spin vector of Venus, yet a third coordinate is required. The simplest choice is α, the longitude of the equinox in the reference frame of the orbit. The greatest influence on α arises from the secular interaction of the dynamical oblateness with the sun; substituting V_s from eq. (5:3) into the equation of motion (2:6) yields

$$\frac{d\alpha}{dt} = - \frac{GM_\odot}{2r^{-3}} \frac{2C-A-B}{\omega C} \frac{3}{2} \cos \beta \, (1 - e)^{-3/2} = - I \frac{\cos \beta}{\omega} \qquad (6:1)$$

This represents uniform precession of the spin axis about the orbit normal. Measured values of $J_2 = \dfrac{2C-A-B}{2M_\male \, a^2}$ fall in the range of 10^{-6} (Howard et al., 1974),

corresponding to precession periods on the order of 10^4 or 10^5 yr. Additional contributions to $\frac{d\alpha}{dt}$ from $1/2 \, \omega^2 \, \Delta C$, U, and W are negligible by comparison, although V_o from (5:6) or V_p from (5:4) could be comparable to V_s in the $\omega = 0$ or $\omega = n$ solar resonances, respectively.

Suppose that Venus has a fluid core and a nearly rigid mantle. If these are strongly coupled, they will rotate about nearly the same axis with the same angular velocity ω. If they are only weakly coupled, the core can only respond to the long-term average direction of the mantle axis, and

ends up spinning almost normal to the orbit plane at the rate $\omega \left| \cos \beta \right|$. Between these two extremes, differential rotation will cause frictional dissipation of energy at the core-mantle boundary.

If the coupling is entirely viscous in nature, the core precesses at the same period as the mantle, but with a time lag given by

$$\tau_c = \frac{a_c}{\sqrt{\nu\omega}} \tag{6:2}$$

(Goldreich and Peale, 1967, 1970), where a_c represents the radius of the core, and ν its kinematic viscosity (viscosity divided by density). The precession rate for strong coupling $(\frac{d\alpha}{dt} \tau_c << 1)$ is given by eq. (6:1), while for weak coupling $(\frac{d\alpha}{dt} \tau_c >> 1)$ the precession rate is found by replacing the value of C in the denominator of (6:1) by C_m, the greatest moment of inertia of the mantle alone. Any deviation from this steady motion is exponentially damped with the same time constant τ_c from eq. (6:2) above (Goldreich and Peale, 1970).

Goldreich and Peale (1970) have also worked out the consequences of this process for the secular evolution of the obliquity and rotation period of Venus. In our notation, their results become

$$\left[\frac{d\omega}{dt}\right]_{CMF} = -\frac{C_c C}{C_o^2}\left(\frac{\omega}{\tau_c}\right)\frac{\sin^2\beta}{\left[1 + \left(\frac{d\alpha}{dt}\right)^{-2}\tau_c^{-2}\right]} = -\frac{C_c C}{C_o^2\, a_c}$$

$$\cdot\frac{\sqrt{\nu\omega^3}\sin^2\beta}{\left[1 + \dfrac{\nu\omega^3}{a_c^2 I^2\cos^2\beta}\right]} \tag{6:3}$$

$$\frac{d\beta}{dt} = \frac{\cos\beta}{\omega\sin\beta}\left[\frac{d\omega}{dt}\right]_{CMF} \qquad \cdot \tag{6:4}$$

The interpretation is even simpler in (X, Y)-coordinates:

$$\frac{dX}{dt} = 0 \quad , \quad \frac{dY}{dt} = \frac{1}{\sin\beta}\left[\frac{d\omega}{dt}\right]_{CMF} \qquad \cdot \tag{6:5}$$

In the above relations, C_c represents the maximum moment of inertia of the core, while the value of C_o lies somewhere between C_m for weak coupling and $C = C_m + C_c$ for strong coupling. The effects of core-mantle dissipation can simply be added to those of body and atmospheric tides; although strictly speaking they are not derivable from a potential, eqs. (6:3)-(6:5) above could be obtained by adding a term $-\frac{Y}{C}\left[\frac{d\omega}{dt}\right]_{CMF}$ to the Hamiltonian.

Fig. 19 depicts the evolution of a planet's rotation under the influence of core-mantle friction alone. This has the same format as Figs. 3-5 and 7-10, except that only half as many arrows are shown for the sake of clarity. As this figure clearly shows, the evolution is always straight down

Figure 19

Spin evolution under the influence of core mantle friction alone; time interval = 7.0×10^4y
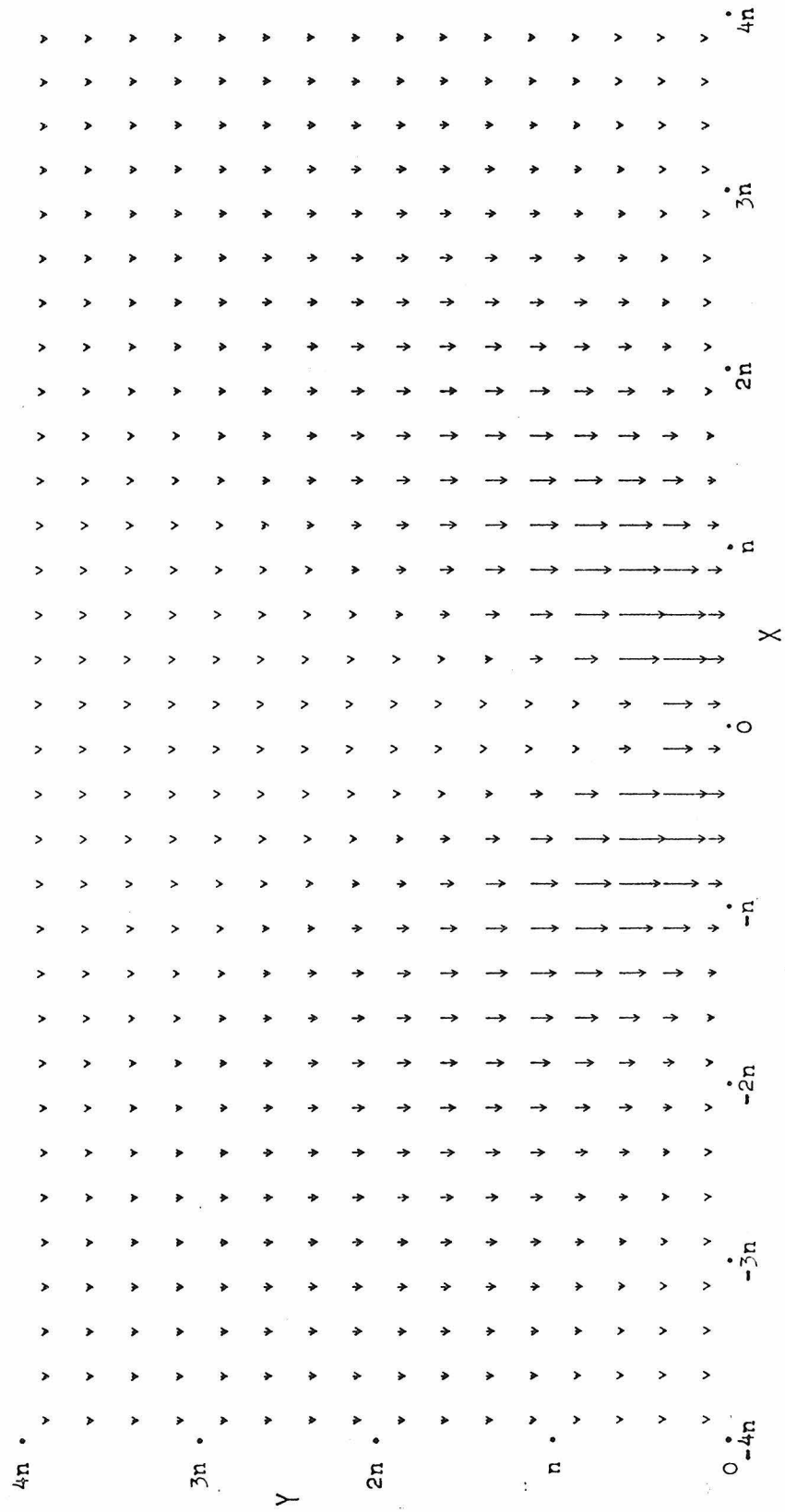
through the (ω, β)- plane. The Y-component of the mantle
rotation decays monotonically to zero, while the X-component
matches that of the core and is conserved. The rotation rate
ω is thus always reduced, while the obliquity β is driven away
from 90° toward either 180° or 0.

For the purposes of illustration, Fig. 19 is drawn using a
time interval of only 70,000 years, with a_c = 3.0 x 10^6 m, C_o = C
= .332 M_o a^2, C_c = .10 x C, and C_m = .90 x C. For rotation
periods longer than about 50 days, we have taken 2C-A-B
= 2.0 x 10^{-5} x C independent of ω, so that I $\approx$ 1.57 x 10^{-18} s^{-2}.
(For shorter rotation periods, hydrostatic flattening increases
the dynamical oblateness, but may also cause pressure forces
to replace viscosity as the dominant coupling mechanism
between the core and mantle (Goldreich and Peale, 1970). The
influence on the spin will increase again or continue to
decrease for more rapid rotations, depending on whether the
former or latter effect prevails.) For fixed values of these
parameters, core-mantle friction has the greatest influence
on the planet's spin when both terms inside the brackets in
eq. (6:3) are unity; accordingly we have also put

$$\tau_c = \left(\frac{d\alpha}{dt}\right)^{-1} \approx 6036 \quad yr \rightarrow \nu = \frac{a_c^2 E^2}{\omega_\male^3} \approx 3.38 \times 10^{-3} \quad m^2/s .$$

$$(6:6)$$

For this choice of the coupling constant, the core-mantle interaction has nearly 10^3 times greater influence on the current obliquity of Venus, and remains dominant for viscosities up to six orders of magnitude greater or less than the optimal value from (6:6). Core-mantle friction can thus be a very powerful mechanism for maintaining the obliquity of Venus near its present value. It also extends considerably the range of initial conditions which lead to an obliquity of 180°.

By the same token, since $\frac{d\gamma}{dt}$ is symmetric with respect to $\beta = 90°$, an initially prograde rotation is again prevented from "rolling over" and becoming retrograde.

In case the rotation rate ω is trapped in a resonance, a little algebraic analysis yields the generalization of eq. (5:9):

$$\frac{d\beta}{dt} = \frac{1}{\omega \, C \sin \beta} \left[\frac{\partial}{\partial \alpha} (U + W) \mp \frac{\partial}{\partial \gamma} (U \dotplus W) \right] \pm \frac{1}{\omega \sin \beta} \left[\frac{d\omega}{dt} \right]_{CMF} . \quad (6:7)$$

Using the same format as Figs. 12-18, Fig. 20 shows the effect of core-mantle dissipation on the obliquity, both in and out of resonance (compare Fig. 6 of Goldreich and Peale, 1970). The magnitude of $\frac{d\beta}{dt}$ is somewhat increased by spin-orbit resonances of the first kind; furthermore the obliquity is driven away from 180° to 90°, or even to 0. On the other hand, the Earth resonance again augments the stability of a retrograde

Figure 20

Spin evolution at resonance under

the influence of core-mantle friction
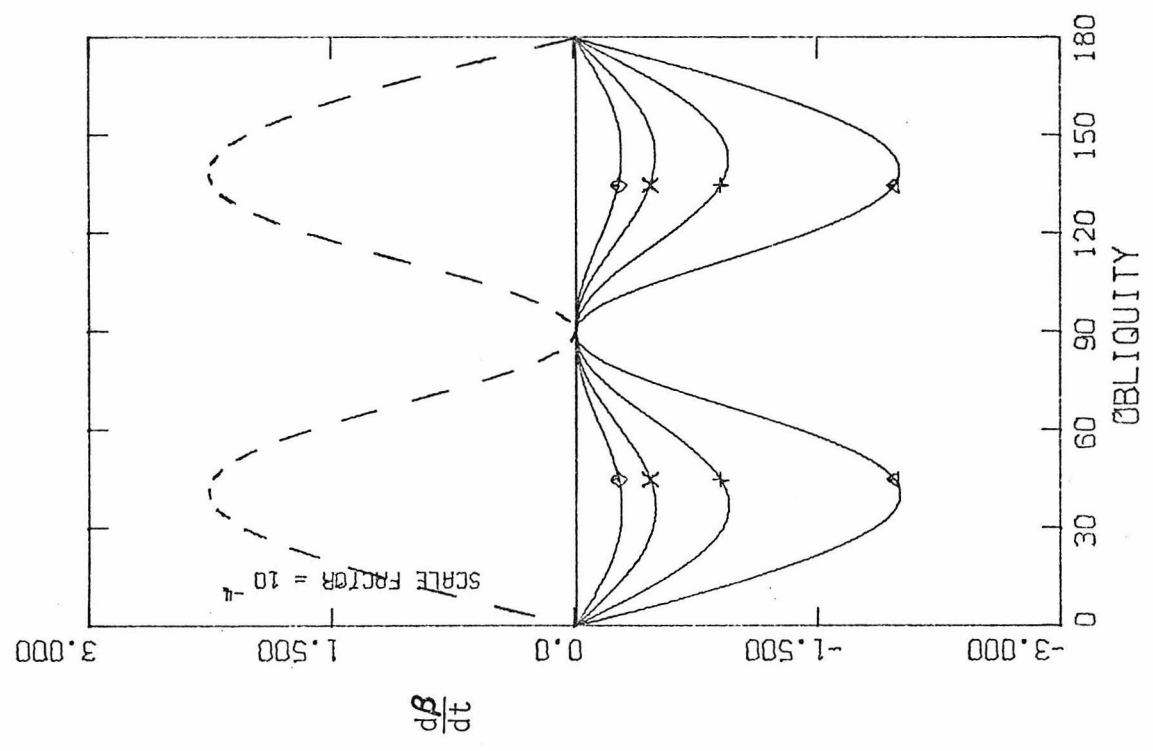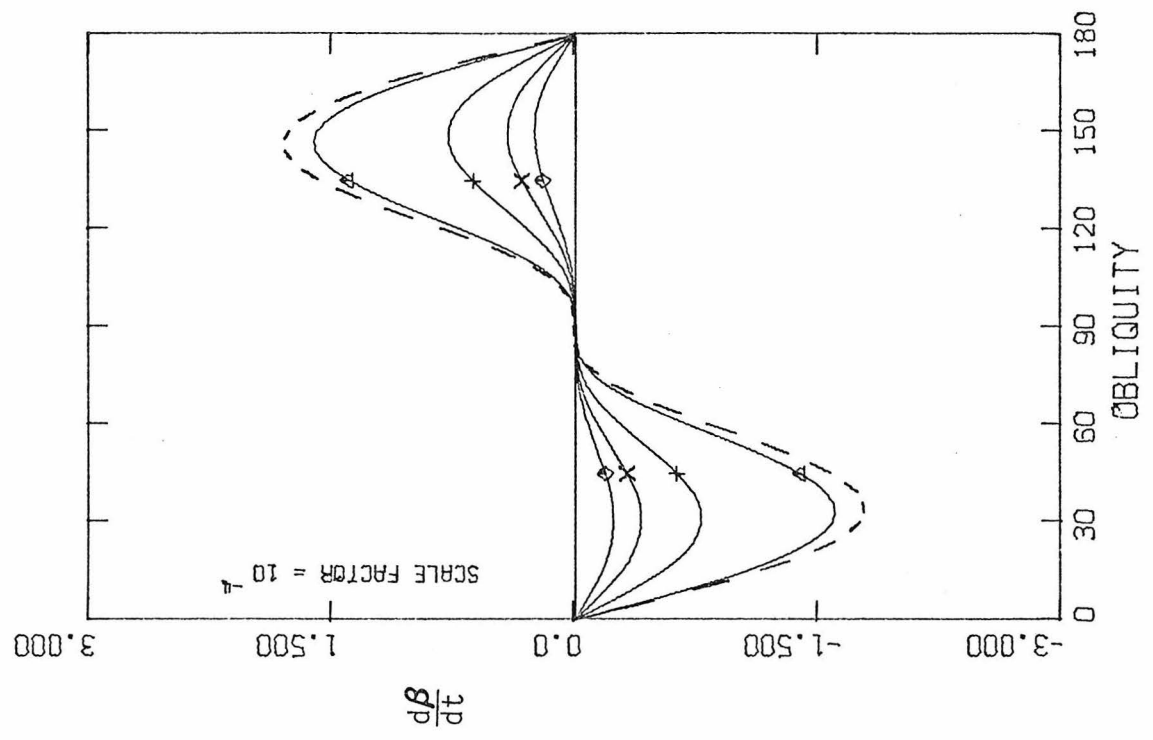
rotation, while a small obliquity tends to "roll over" toward 90° and possibly through to 180°! Unfortunately, this seems unlikely to have happened to Venus because its resonance with the Earth is so weak, particularly at low obliquities.

In addition to its strong stabilizing influence on the obliquity, core-mantle friction provides a mechanism for capture into the Earth resonance (Goldreich and Peale, 1967). It might also enhance the chances of capture into a spin-orbit resonance of the first kind, regardless of the frequency dependence of the tides. As the rotation rate ω of the mantle evolves across the resonant value, it is periodically increased and decreased slightly by the growing influence of the Earth or sun. Just as in the case of precession, the spin of the core lags the mantle. The resulting dissipation of energy may cause capture into the resonance, and subsequent damping of the librations. Provided that the resonance is stable, the greatest chance of capture occurs at $\tau_c \approx L/2\pi$, with significant capture probabilities for time constants on the same order of magnitude (Goldreich and Peale, 1967, 1968). Since the libration period L for the Earth resonance is on the same order as the precession period, the optimal coupling for stabilizing the obliquity also leads to a significant

likelihood of capture. Conversely, if the rotation period of
Venus is actually resonant with the orbit of the Earth, that
fact may be taken as evidence that core-mantle friction is
currently maintaining its obliquity near 180°.

The orbital plane of Venus also precesses with repect to
inertial space. The spin axis then cannot maintain a fixed
obliquity to the orbit normal unless both precession periods
are identical (or if the axial precession is much faster than
the orbital changes). Such commensurabilities are known as
generalized Cassini states, and have received much attention
in recent years; see, for example, Peale (1974) and Ward
and DeCampli (1978). It may thus be no coincidence that the
periods of precession and orbit variation are similar for Venus.
However, the motion of Venus' orbit relative to the invariable
plane is far from uniform, and complicates the problem considerably.
The ultimate orientation taken by the rotation axis then
depends not only on the details of the atmospheric and body
tides, core-mantle friction, and the precession rate, but
also on the history of Venus' orbit variations. At least the
resonant interaction with the Earth does not materially affect
the Cassini states for Venus. The pole position of Venus
determined by Shapiro et al. (1978) does not appear to match
the Cassini state predicted by Ward and DeCampli (1978); as
yet the interpretation is uncertain.

In the context of "roll-over", it is interesting to speculate that if the obliquity of Venus were ever near 90°, it might have been captured into an intermediate Cassini state (state 2). Subsequent despinning would have driven that Cassini state to a somewhat retrograde obliquity, and dragged the spin axis along. Ultimately Venus would have escaped from state 2 and evolved to its present configuration under the various other influences. Peale (1974) considered a similar scenario for Mercury, but found that it constrained the possible spin histories very little because of the small capture probability for Cassini state 2.

Since the differences among all three of its principal moments of inertia are probably comparable ($\frac{B-A}{C} \approx \frac{C-B}{A} \approx 10^{-5}$), Venus must be regarded as a triaxial body rather than simply oblate. Instead of precessing uniformly about the orbit normal, the spin axis of Venus might wander by about a degree in obliquity during each precession period (Lyttleton, 1973). While this effect is too small to affect the rotation of Venus substantially, it might be able to account for the difference between the measured pole position and the predicted Cassini state for Venus.

We are now in a position to examine the question of non-principal axis rotation. If a rigid body has principal moments of inertia C > B = A, and is freely rotating with

angular speed ω, in general the angle between its axis

of greatest inertia and the spin axis will vary at the Eulerian

period N for free nutation, where

$$N = \frac{C}{C-A} \; \frac{2\pi}{\omega} \; . \qquad\qquad (6:8)$$

Again taking $C-A = 1.0 \times 10^{-5} \times C$ in eq. (6:8) above gives

a very long nutation period of $N \approx 67000$ years. A simple

generalization of the above formula (Kaula, 1968) reveals

that for Venus, unlike the Earth, non-ridgidity has a negligible

effect on the period of nutation (Chandler wobble), although

the motion of the spin axis may be complicated by the triaxiality

of Venus.

Now Goldreich and Toomre (1969) have shown that the canonical

action integral associated with the free nutation of a rigid

rotator is an adiabatic invariant; in other words, the (properly

defined) "amount" of nutation is unaffected by changes in

the system which take much longer than a nutation period.

Unlike the Earth, however, the nutation period of Venus is

comparable to the estimated periods of axial precession,

orbit variation, and libration in resonance. The problem

then becomes very complicated, and each of these phenomena

might possibly pump up the amplitude of the nutation indefinitely,

unless it is damped somehow. If the only dissipation is

provided by the same mechanism "Q" that damps body tides,

the free nutation will decay on a timescale

$$\tau_Q \approx \frac{100 \, \mu \, Q}{\rho a^2 \, \omega^2} \qquad\qquad (6:9)$$

(Burns and Safronov, 1973; McAdoo and Burns, 1974). For the values
of these parameters estimated previously, this time constant
is on the order of 10^9 years, which seems too long to damp the
forced nutations effectively.

Table 2 following lists the estimates of the various
time scales most relevant to the rotational dynamics of Venus.
Inspection shows that they divide conveniently into one
group of about 10^5 years, and another of 10^8 years or longer.
The longer timescales pertain to the long-term evolution of
the spin, while the shorter ones are important to the problems
of Cassini states and core-mantle coupling. Because of this
coincidence of timescales, core-mantle friction is one of the
strongest possible stabilizing influences on the present spin
of Venus.

TABLE 2. TIME SCALES

FOR VENUS DYNAMICS

TIDAL TIMESCALE (TO DESPIN VENUS FROM FROM PRESENT ROTATION TO SYNCHRONISM)	$\sim 10^8$ YR
LYTTLETON'S TIME SCALE (FOR RANDOM WALK OF ROTATION VECTOR)	$\sim 10^{10}$ YR
PRECESSION PERIOD	$\sim 10^5$ YR
ORBITAL VARIATIONS	$\sim 10^5$ YR
LIBRATION PERIOD IN RESONANCE	$\sim 10^5$ YR
FREE NUTATION (CHANDLER WOBBLE) PERIOD	$\sim 10^5$ YR
TIME TO DAMP NUTATION BY Q ALONE	$\sim 10^9$ YR

7. Other Effects and Discussion

There is a variety of other phenomena that may affect the rotation of Venus, or which may have influenced its history. For example, the interaction of the solar wind with the planet's magnetosphere may produce an additional torque, although presently Venus does not appear to possess an intrinsic magnetic field. A more basic question concerns the fundamental behavior of atmospheric tides. John Lewis (1971) has suggested that the atmosphere of Venus is in thermochemical equilibrium with carbonate rocks on the surface. He proposes that energy absorbed by the ground raises its temperatures only slightly, but causes rapid outgassing of carbon dioxide (with a time constant on the order of a week; Lewis, 1971) via the reaction

$$Ca\ CO_3 + Si\ O_2 \rightarrow Ca\ Si\ O_3 + CO_2 \qquad . \qquad (7:1)$$
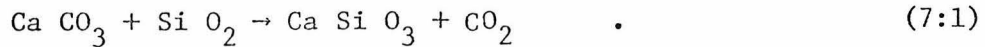
The resulting temperature change

$$\frac{dT_o}{dt} = \overline{T}_o\ F\ \frac{g}{\overline{\rho}_o}\ (2.09 \times 10^6\ J/kg)^{-2} \qquad (7:2)$$

is only on the order of a hundredth of a degree per Venus day, but the accompanying pressure variation

$$\frac{dp_o}{dt} = \frac{\overline{\rho}_o}{\overline{T}_o}\ \frac{dT_o}{dt}\ (2.09 \times 10^6\ J/kg) = Fg(2.09 \times 10^6\ J/kg)^{-1} \qquad (7:3)$$

amounts to several millibars, comparable to the largest effect of the atmospheric tides! Of course, the simple exchange of mass between the atmosphere and the soil cannot in itself alter the net torque on the planet. However, the resulting modification of the temperature and pressure fields could completely transform the pattern of atmospheric tides on Venus. For the time being, this remains merely an interesting speculation.

The most drastic explanation for the retrograde rotation of Venus invokes a collision with a sizeable interplanetary body capable of reversing an initially prograde spin (Singer, 1970, 1971; see also French, 1971). While such an event might indeed accomplish the desired effect, it must be considered improbable. Alternatively, body tides would by now have caused any sufficiently massive nearby retrograde satellites to crash onto the surface of Venus and make it rotate retrograde, regardless of its original orientation(McCord, 1968; Singer, 1970, 1971; Burns, 1973; Ward and Reid, 1973). The ad hoc nature of this hypothesis makes it unappealing but not unreasonable.

Another prime motivation for such proposals is a difficulty with the time scale for tidal evolution. Presuming that Venus began with a rotation period of about a day, like the other planets, and also that the tidal Q has remained constant, body tides alone could not have despun Venus to its present

slow rotation rate within the age of the solar system unless
$Q \leqslant 17$ (Goldreich and Soter, 1966). This range has been
regarded by some as implausibly low, compared to the other
planets; such a low Q would also preclude the possibility that
the current rotation period represents a balance between atmo-
spheric and body tidal torques. Of course, Q has not necessarily
been constant over such a length of time and so wide a range
of frequencies; these considerations can easily accomodate a
factor of two.

The retrograde obliquity of Venus presents a more
serious challenge. We have seen how difficult it is for a
prograde planet to "roll over" and become retrograde. Some
scenarios may permit a rapidly rotating prograde planet to
end up like Venus, but these all seem contrived. Barring
problematica like collisions, it appears necessary to conclude
that <u>Venus has always rotated retrograde.</u>

Especially considering the 98° obliquity of Uranus, we
prefer to postulate that Venus started out with an obliquity
in the neighborhood of 100° and a rotation period of a day or
two. Body tides and core-mantle friction would subsequently have
slowed its rotation rate to near the present value, and increased
the obliquity to nearly 180°. Finally the
evolution was halted by the growing influence of atmospheric
tides, or by capture into spin-orbit resonance with the Earth,

or both. The present rotation period of Venus thus represents
a balance between atmospheric and body tides, and perhaps also
the weaker influence of the Earth resonance. The obliquity is
maintained near 180° by a combination of these three torques
and the (probably dominant) effect of core-mantle friction.

What are the prospects for testing the above hypothesis?
More Earth-based radar observations are needed, since the measured
rotation period and pole position still contain substantial
uncertainties. As discussed in chapter 6, confirmation of the
suspected Earth resonance would also be positive evidence for
the importance of core-mantle friction.

The upcoming Pioneer Venus mission may not provide much
new information on the rotation vector, but gravitational
perturbations on the orbiter will reveal the planet's principal
axes and moment of inertia differences. In turn, this knowledge
will greatly improve our understanding of resonance, precession,
nutation, Cassini states, and related phenomena for Venus.
Much greater sensitivity would be required in order to detect
the induced tidal potential directly, though.

Remote sensing from a spacecraft like the proposed VOIR (Venus
Orbiting Imaging Radar) might be capable of measuring the
atmospheric and body tides independently. Tidal variations
of the surface pressure could be obtained from two-frequency
radar attenuation data, especially combined with altimetry,
since differential absorption of the signal depends on the

ntegrated column density of CO_2 (Shapiro et al., 1973). Unfortunetly, the absorptivity would also be affected by the temperature variations. Furthermore, sensitivities comparable to 10 cm of path length would be required, three or four orders of magnitude better than the state of the art for Earth-based radar.

One of the greatest shortcomings in our treatment of atmospheric tides is the equivalent gravity mode approach, described in chapter 5 of Part I, and the related ambiguity between type 1 and type 2 tides. These questions could be resolved by two-dimensional finite difference calculations like those of Lindzen and Hong (1974). However, such an undertaking is not warranted by the present uncertainties in the heating distribution and basic state of Venus atmosphere. In situ observations from the Pioneer Venus entry probes will substantially improve the state of our knowledge, and probably will make more elaborate calculations worth while.

Since the tidal temperature and pressure variations are so small at the surface of Venus, direct measurements of these would require a long-lived lander of delicate sensitivity and calibration, constituting a real engineering challenge. On the other hand, it was shown in chapter 6 of Part I that tidally driven winds of several m/s should occur in the thermal boundary layer. Unless these winds are considerably reduced by friction within a few meters of the ground, their speed and

direction could be measured by a network of short-lived landers or penetrators. (Note that the Venera 9 and 10 anemometer data are limited to wind speed only). The tidal wind field may then afford the best opportunity of examining the behavior of atmospheric tides on Venus.

APPENDIX I. Infinite Equivalent Depths

Consider the traditional tidal problem with ω = constant $\neq 0$. If the equivalent depth h becomes infinite under these circumstances, the solution of the Hough equation (2:33) of Part I must be a linear combination of the Legendre functions $P_{\ell s}$ (cos θ) and $P_{\ell-2,s}$ (cos θ), while the tidal frequency is

$$\sigma = \frac{2s\omega}{\ell(\ell-1)} \tag{I:1}$$

(Chapman and Lindzen, 1970). The only common case for which this occurs is the first antisymmetric sidereal diurnal tide, for which $\sigma = \omega$, s = 1, ℓ = 2, and $\Theta_{\ell,s}$ (θ) $\propto$ $\propto$ sin θ cos θ (Lindzen, 1965).

When h is infinite, the Hough operator (2:32) vanishes, and eq. (2:26) of Part I becomes simply

$$0 = \frac{\partial}{\partial x} \delta\eta - \delta\eta \rightarrow \delta\eta = \delta\eta_o \, e^x \quad . \tag{I:2}$$

However, (I:2) above can only satisfy the boundedness condition if $\delta\eta_o$ vanishes. Then eq. (2:27) of Part I may immediately be integrated to give the geopotential variations:

$$\delta\psi(x) = \delta\psi_o + \int_o^x \frac{\varkappa\delta J}{(i\sigma + 1/\tau)} \, dx' \quad . \tag{I:3}$$

Now if the gravitational forcing $\delta\eta$ is ignored, the lower boundary condition (2;37) of Part I yields identically $\delta\psi_o = 0$! This reproduces the classical result (Lindzen, 1965) that thermal tides can give rise to no surface pressure variation $\bar{\rho}_o\,\delta\psi_o$ nor its consequent torque on the atmosphere for modes whose equivalent depth is infinite. This may have significant consequences for the obliquity of Venus, as detailed in Part II of this dissertation.

The observed latitudinal differences in the ~ four-day rotation period of the Venus upper atmosphere (Suomi, 1974) will alter the equivalent depths h_ℓ, as well as the solutions Θ_ℓ to the Hough equation, for a given forcing frequency. This ensures that all of the equivalent depths in the stratosphere will remain bounded, and on the order of a hundred kilometers. However, the bottom of the atmosphere is likely to be corotating with the surface, so that the classical solution will apply locally and the equivalent depth for the antisymmetric diurnal mode may become infinite at the ground.

When h is taken as infinite throughout the troposphere, but finite in the stratosphere, the analysis in chapter 5 of Part I shows that the surface pressure variations vanish along with the quantity $(\xi_+ H_- - \xi_- H_+)^{-1}$. This is unrealistic, however, because mean winds probably occur at all levels except

within an infinitesimal distance of the surface. Since after
all this is the place not only where the lower boundary
condition is applied, but also where the pressure variations
are evaluated, the problem requires very careful treatment.
The following analysis is based on suggestions by A. P. Ingersoll.

We shall apply the Equivalent Gravity Mode method to the
case $\sigma = \omega$, $s = 1$, $\Pi = 1$. For simplicity, we shall again represent
the basic state by a vanishing stratification along with the
exponential wind model (3:2) of Part I. However, we will not
also adopt an exponential profile of the equivalent depth as
given by eq. (5:13) of Part I. Instead, it is convenient to
define

$$h = \mathcal{T}x^{-\nu} \quad \text{with } \nu \geq 0 \text{ for } x < x_c,$$
$$h = h_\infty = \text{constant for } x \geq x_c \qquad .$$

(I:4)

Then the tidal equation (5:8) of Part I may be written

$$\frac{\varkappa \delta J}{g \mathcal{T}} x^\nu = \frac{d^2}{dx^2} \delta \eta - \left(1 + 8f + \frac{\nu}{x}\right) \frac{d}{dx} \delta \eta + (1 + 5f)\left(3f + \frac{\nu}{x}\right) \delta \eta$$

(I:5)

for the troposphere, where the damping $1/\tau$ has been neglected
and $f \geq 0$. The classical vertical structure equation (2:30)
of Part I applies in the stratosphere.

We seek to solve eq. (I:5) above by the power series
method. Assume a homogeneous solution of the form

$$\delta\eta = \sum_{m=0}^{\infty} C_m x^{\mu+m} \quad , \quad \text{with } C_o = 1 \text{ and } \delta J = 0; \qquad (I:6)$$

(I:5) then becomes

$$0 = \sum_{m=0}^{\infty} (\mu+m)(\mu+m-1) C_m x^{\mu+m-2} - (1 + 8f + \frac{\nu}{x}) \sum_{m=0}^{\infty}$$

$$\cdot (\mu+m) C_m x^{\mu+m-1} \qquad (I:7)$$

$$+ (1 + 5f)(3f + \frac{\nu}{x}) \sum_{m=0}^{\infty} C_m x^{-\mu+m}$$

Gathering terms of each order in x and rearranging (I:7) gives

$$0 = \mu (\mu - 1 - \nu) \rightarrow \mu = 0 \text{ or } \mu = 1 + \nu;$$

$$0 = (\mu + 1)(\mu - 1 - 8f)c_1 + (1 + 5f)\nu, \text{ and}$$

$$0 = (\mu + m + 2)(\mu + m + 1 - \nu)C_{m+2} - [(\mu + m + 1)(1 + 8f)$$
$$+ (1 + 5f)\nu] C_{m+1} + 3g(1 + 5f) C_m \qquad . \qquad (I:8)$$

The above relations then provide two independent solutions

to the homogeneous part of eq. (I:5): one of order zero and

another of order $1 + \nu$ in x. We shall label these functions

$F(x)$ and $G(x)$, respectively. In the classical case where both ν and f

are zero, we recover the known solutions $F(x) = 1$ and $G(x) = e_x - 1$.

Since the coefficients in eq. (I:5) are all continuous for

x > 0, the easily verified general solution in the troposphere

is then

$$\delta\eta(x) = AF(x) + BG(x) - F(x) \int_0^x e^{-(1 + 8f)x'} G(x') \frac{\varkappa\delta J(x)}{g\mathcal{T}(1+\nu)} dx'$$

$$+ G(x) \int_0^x e^{-(1+8f)x'} F(x') \frac{\varkappa\delta J(x')}{g\mathcal{T}(1+\nu)} dx' \quad , \ x < x_c \ . \tag{I:9}$$

The general solution in the stratosphere is the same as eq. (5:17) of Part I.

The vertical velocity δw in the troposphere is given by eq. (5:12) of Part I, which for this case becomes

$$\delta w = \mathcal{T}x^{-\nu} \left(\frac{\omega_0}{\omega}\right)^2 \left[\frac{d}{dx} \delta\eta - (1 + 5f) \ \delta\eta\right] + H \ \delta\eta \quad . \tag{I:10}$$

When the gravitational forcing is left out, the lower boundary condition becomes $\delta w = 0$ at $x = 0$. In this limit, (I:10) above gives

$$0 = \frac{d}{dx} \delta\eta - (1 + 5f) \ \delta\eta = A \ \nu \left(\frac{1+5f}{1+8f}\right) - A \to A = 0 \quad , \tag{I:11}$$

as long as $\nu > 0$.

Ultimately we are interested in the pressure variations at the surface. Upon substitution by (I:9), expression (5:3) of Part I gives for the geopotential in the troposphere

$$\delta\psi(x) = \frac{gh}{i\sigma} x^{-\nu} \left[\frac{d}{dx} \delta\eta - (1 + 5f) \delta\eta\right]$$

$$= \frac{gT}{i\omega} B x^{-\nu} \left[\frac{d}{dx} G - (1 + 5f) G\right] \qquad (I:12)$$

$$- \frac{x^{-\nu}}{i\omega} \left[\frac{d}{dx} F - (1+5f) F\right] \int_0^x e^{-(1+8f)x'} G(x') \frac{\varkappa\delta J(x')}{1 + \nu} dx'$$

$$+ \frac{x^{-\nu}}{i\omega} \left[\frac{d}{dx} G - (1 + 5f) G\right] \int_0^x e^{-(1+8f)x'} F(x') \frac{\varkappa\delta J(x')}{1 + \nu} dx'$$

In order to evaluate $\delta\psi(0)$, we first take the following limits:

$$\lim_{x\to 0} \left\{ x^{-\nu} \left[\frac{d}{dx} F - (1+5f) F\right] \int_0^x e^{-(1+8f)x'} G(x') \frac{\varkappa\delta J(x')}{gY} dx'\right\}$$

$$= \left[\frac{d}{dx} F - (1+5f) F\right] \lim_{x\to 0} \left\{ \frac{\int_0^x e^{-(1+8f)x'} G(x') \varkappa\delta J(x') dx'}{x^\nu}\right\} \qquad (I:13)$$

$$= \left(\frac{1+5f}{1+8f}\right) \nu \lim_{x\to 0} \left\{ \frac{e^{-(1+8f)x} G(x) \varkappa\delta J(x)}{\nu x^{\nu-1}}\right\} = \left(\frac{1+5f}{1+8f}\right) \lim_{x\to 0}$$

$$\left\{ x^2 \varkappa\delta J(x)\right\} = 0$$

since δJ is integrable, and

$$\lim_{x\to 0} \left\{ x^{-\nu} \left[\frac{d}{dx} G - (1+5f) G\right]\right\} = 1 + \nu \qquad . \qquad (I:14)$$

Substituting the above results into eq. (I:12) then gives a simple expression for the surface pressure variation:

$$\delta p_o = \overline{\rho}_o \; \delta \psi_o = \overline{\rho}_o \; \frac{g \mathcal{T}}{i \omega_o} \; (1+\nu) \quad B \qquad \qquad . \qquad \text{(I:15)}$$

It only remains to evaluate the constant B. Consider for example the heating at the ground model, defined by eq (4:18) of Part I, since this case seems the most liable to be affected. Substituting this heating profile into eq. (I:9) gives

$$\delta \eta = G(x) \left[B + \frac{\varkappa \delta F}{P_o \; \mathcal{T} \; (1+\nu)} \right], \quad x < x_c \qquad . \qquad \text{(I:16)}$$

Meanwhile the solution in the stratosphere becomes

$$\delta \eta = C \; e^{\left(\frac{1}{2} + i \lambda_\infty\right)(x - x_c)} + D \; e^{\left(\frac{1}{2} - i \lambda_\infty\right)(x - x_c)}, \quad x \geq x_c \; ,$$
$$\text{(I:17)}$$

where λ_∞ is defined in eq. (5:18) of Part I.

The upper boundary condition yields $D = 0$. Matching (I:16) and (I:17) then gives

$$C = \left[B + \frac{\varkappa \delta F}{P_o \; \gamma \; (1+\nu)} \right] G(x_c) \qquad \qquad . \qquad \text{(I:18)}$$

We also require $\delta \psi$ to be continuous across the tropopause. Applying this condition to eq. (I:12) and using (I:18) above gives

$$\left[B + \frac{\varkappa \delta F}{P_o \, \gamma \, (1+\nu)} \right] \, \mathcal{T} x_c^{-\nu} \left[\frac{d}{dx} G \, (x_c) - (1+5f) \, G \, (x_c) \right]$$

$$= h_\infty \, (- \frac{1}{2} + i \, \lambda_\infty) \, C = h_\infty \, (- \frac{1}{2} + i \, \lambda_\infty) \left[B + \frac{\varkappa \delta F}{P_o \, \mathcal{T} \, (1+\nu)} \right] G(x_\infty) \; . \tag{I:19}$$

As long as the quantity $[B + \frac{\varkappa F}{P_o \mathcal{T}(1+\nu)}]$ is nonzero, dividing

by it through eq. (I:19) above leaves

$$\mathcal{T} x_c^{-\nu} \left[\frac{d}{dx} G \, (x_c) - (1+5f) \, G \, (x_c) \right] = h_\infty \, (- \frac{1}{2} + i \, \lambda_\infty) \, G(x_c) \tag{I:20}$$

This is just the condition for free oscillations, since B

may have any value when (I:20) is satisfied. As discussed

in chapter 5 of Part I, this is unlikely. Furthermore this

cannot occur for propagating modes, since then the right

hand side of (I:20) above is complex. In general, then, eq.

(I:19) along with eq. (I:15) implies

$$B = - \frac{\varkappa \delta F}{P_o \, \mathcal{T} \, (1+\nu)} \; \rightarrow \; \delta p_o = - \bar{\rho}_o \, \frac{g}{i \omega_o} \, \frac{\varkappa \delta F}{P_o} = i \, \frac{\varkappa \delta F}{\omega H_o} \; . \tag{I:21}$$

Now (I:21) above is essentially the same as the result (5:37)

of Part I for the heating at the ground model, where the

equivalent depth is everywhere bounded. Similar results are

expected for a distributed forcing. This justifies treating

the antisymmetric diurnal tide on the same footing as all of

the other tidal modes.

APPENDIX II. List of Symbols

A, B, C, principal moments of inertia, where $C \geq B \geq A$; also used as constants of integration

a strength of atmospheric tides, defined by eq. (4:5) of Part II

a radius of Venus; $a \approx 6050$ km

b strength of body tides; $b(\sigma) = k_\sigma \sin \epsilon_\sigma \approx \dfrac{k}{Q}$

c_p specific heat capacity at constant pressure; $c_p \approx$ 945 J/kg/K for CO_2

c_b specific heat capacity of soil; $c_b \approx 1000$ J/kg/K

D complex thermal skin depth

d distance from the center of Venus

e orbital eccentricity

F insolation of solar flux

f $= \sigma/2\omega$; also the exponential shear parameter defined in eq. (3:2) of Part I

G universal constant of gravitation; $G \approx 6.67 \times 10^{-11}$ $m^3/s^2/kg$

g acceleration of gravity; $g = GM_\varphi / a^2 \approx 8.6$ m/s^2

H scale height; $H = R\overline{T}/g$; also the Hamiltonian

$h_\ell^{\sigma,s}$ equivalent depths of tidal modes

I $= \dfrac{GM_o}{2r^{-3}} (2C-A-B) \dfrac{3}{2} (1-e^2)^{-3/2}$

i imaginary unit; $i = \sqrt{-1}$

J thermotidal heating per unit time per unit mass; $J = T\dfrac{dS}{dt}$

j	height Love number; $j \approx .42$ for Venus
K_a	eddy thermal conductivity of lower atmosphere
K_b	thermal conductivity of soil; $K_b \approx 10$ W/m/K
k	potential Love number; $k \approx .25$ for Venus
L	libration period in resonance
ℓ	degree of a Legendre function
$\bar{\ell}$	photon mean free path, or mean inverse of the gaseous absorption coefficient
$M_\odot$	mass of the sun; $M_\odot \approx 1.99 \times 10^{30}$ kg
$M_{\venus}$	mass of Venus; $M_{\venus} \approx M_\odot/408524 \approx 4.87 \times 10^{24}$ kg
$M_\oplus$	mass of Earth; $M_\oplus \approx M_\odot/332960 \approx 5.98 \times 10^{24}$ kg
m	surface mass distribution
N	Eulerian nutation period
n	orbital mean motion of Venus; $n \approx 2\pi/224.7$ d $\approx 3.236 \times 10^{-7}$ s^{-1}
$P_{\ell s}(\cos\theta)$	associated Legendre function of degree ℓ and order s (unnormalized)
p	pressure
Q	"quality factor" for body tides
R	specific gas constant; $R \approx 189$ J/kg/K for CO_2
r	distance between Venus and the sun; $\bar{r} \approx .72333$ AU $\approx 1.082 \times 10^{11}$ m
S	entropy per unit mass
s	integral wavenumber in longitude; also the order of an associated Legendre function

T	thermodynamic temperature; also tidal timescale
t	time
U	contribution to the Hamiltonian due to body tides
u	wind speed away from the right-hand rotational pole; $u = a \dfrac{d\theta}{dt}$
V	contribution to the Hamiltonian due to the permanent gravitational quadrupole moment
v	wind speed in the direction of rotation; $v = a \sin \theta \dfrac{d\varphi}{dt}$
$v_{\odot}$	speed of the subsolar point with respect to the surface; $v_{\odot} = a (\omega_{\varphi} + n) \approx 3.76$ m/s
W	contribution to the Hamiltonian due to atmospheric tides
w	vertical wind speed conjugate to altitude z; $w = \dfrac{dz}{dt}$
X	component of spin angular velocity in the orbit plane; $X = \omega \cos \beta$
x	dimensionless height coordinate; $x = -\ln(p/p_o)$
Y	component of spin angular velocity normal to the orbit plane; $Y = \omega \sin \beta$
y	$= \delta \eta \, e^{-x/2}$
Z	height of the crustal tide
z	altitude above mean radius
α, β, γ	Euler angles (see Fig. 1 of Part II)
Γ	stratification or static stability; $\Gamma = \dfrac{\partial}{\partial x} R\overline{T} + \varkappa R\overline{T}$ $= \varkappa \overline{T} \dfrac{\partial}{\partial x} \overline{S}$
Γ_{+}	$= \Gamma - \dfrac{1}{\Delta} (a \sin \theta \dfrac{\partial}{\partial x} \omega^2)^2$

Δ $\qquad = -\sigma^2 + \sin\theta\cos\theta\,\dfrac{\partial}{\partial\theta}\,\omega^2 + 4\omega^2\cos^2\theta$

δ $\qquad$ signifies a complex perturabtion quantity; also

$\qquad$ Dirac delta-function, where $\delta(x) = 0$ if $x \neq 0$, but

$\qquad \displaystyle\int_{0^-}^{0^+} \delta(x)\,dx = 1$

ϵ $\qquad$ tidal phase lag

ζ $\qquad$ local zenith angle of the sun

η $\qquad$ vertical wind speed conjugate to height x;

$\qquad \eta = \dfrac{dx}{dt} = -\dfrac{1}{p}\dfrac{dp}{dt}$

$\Theta_{\ell}^{\sigma,s}(\theta)$ $\qquad$ colatitudinal variation of tidal modes

θ $\qquad$ colatitude measured from the right-hand rotation

$\qquad$ pole

$\varkappa$ $\qquad = R/c_p \approx .20$ for CO_2

Λ $\qquad$ subscripted coefficients in differential equations;

$\qquad$ defined in text

λ $\qquad$ vertical wavenumber of atmospheric tides

μ $\qquad = \cos\theta$; also rigidity or shear modulus

ν $\qquad$ kinematic viscosity of the core

Ξ $\qquad$ forcing term in eq. (2:35), defined in eq. (2:36)

$\qquad$ of Part I

ξ $\qquad = \dfrac{1}{2} + \dfrac{f}{s^2} + \Pi\left(\dfrac{2f}{s^2}\right)$

Π $\qquad$ parity of tidal modes; $\Pi = 0$ for modes symmetrical

$\qquad$ with respect to the equator, but $\Pi = 1$ for

$\qquad$ antisymmetrical modes

ρ $\qquad$ gas density

ρ_b $\qquad$ soil density

σ amgular frequency of oscillations; $\sigma = \dfrac{s\bar{v}}{a\sin\theta} + \sigma_o$

σ_{SB} Stefan–Bolzmann constant; $\sigma_{SB} \approx 5.670 \times 10^{-8}$ $W/m^2/K^4$

τ thermal time constant of atmospheric damping; $1/\tau =$ Newtonian cooling coefficent

Γ strength of a resonance

ν tidal effective dynamic viscosity

Φ geopotential; $\Phi = \displaystyle\int_o^x g\, dz$

ϕ longitude in the direction of rotation

$\phi_\odot$ longitude relative to the subsolar point

ψ total potential; $\psi = \Phi + \Omega$

Ω tidal potential; $\Omega = \dfrac{3}{2}\, GM_\odot\, \dfrac{a^2}{r^3}\, (\cos^2\zeta - \dfrac{1}{3})$

ω rotation rate of the atmosphere; $\omega = \dfrac{\bar{v}}{a\sin\theta} + \omega_\female$

$\omega_\female$ rotation rate of the crust; $\omega_\female \approx \dfrac{2\pi}{243\ d} \approx 3.0 \times 10^{-7}$ $s^{-1} \approx \dfrac{1.809\ m/s}{a}$

$\tilde{\omega}$ longitude of perihelion

REFERENCES

Avduevskii, V. S., S. L. Vishnevetskii, I. A. Golov, Yu. Ta. Karpeiskii, A. D. Lavrov, V. Ya Likhushin, M. Ya. Marov, D. A. Mel'nikov, N. I. Pomogin, N. N. Pronina, K. A. Razin, and V. G. Fokin (1976b). Measurement of Wind Velocity on the Surface of Venus during the Operation of Stations Venera 9 and Venera 10. Cosmic Research, 14, 622-625.

Avduevskii, V. S., Yu. M. Golovin, F. S. Zavelevich, V. Ya. Likushin, M. Ya. Marov, D. A. Mel'nikov, Ya. I. Merson, B. E. Moshkin, K. A. Razin, L. I. Chernoshchekov, and A. P. Ekonomov (1976a). Preliminary Results of an Investigation of the Lighting Conditions in the Atmosphere and on the Surface of Venus. Cosmic Research, 14, 643-649.

Avduevsky, V. S., M. Ya. Marov, B. E. Moshkin, and A. P. Ekonomov (1973). Venera 8: Measurements of Solar Illumination through the Atmosphere of Venus. J. Atmos. Sci., 30, 1215-1218.

Avduevsky, V. S., M. Ya. Marov, A. I. Noykina, V. I. Polezhaev, and F. S. Zavelevich (1970). Heat Transfer in the Venus Atmosphere. J. Atmos. Sci., 27, 569-579.

Bellomo, I., G. Colombo, and I. I. Shapiro (1967). Theory of the axial rotations of Mercury and Venus. P. 193-211 in Mantles of the Earth and Terrestrial Planets, ed. S. K. Runcorn. Interscience Publishers, London. 584 pp.

Burns, J. A. (1973). Where are the Satellites of the Inner
Planets? Nature - Physical Science, 242, 23-25.

Burns, J. A., and V. S. Safronov (1973). Asteroid Nutation
Angles. Mon. Not. Roy. Astr. Soc., 165, 403-411.

Cazenave, A., and F. Fouchard (1977). Solid rotation of Venus:
role of the atmospheric tide. Presentation at the 1977
Spring Meeting of the AGU, in Washington, D. C. Abstract
in EOS, 58, 424.

Chapman, S., and R. S. Lindzen (1970). Atmospheric Tides.
Gordon and Beach, New York, 200 pp. Reprinted from Space
Science Reviews, 10, 3-188 (1969).

Darwin, Sir G. H. (1908). Scientific Papers, Volume II.
Tidal Friction and Cosmogony. Cambridge University Press, 516 pp.

Dickinson, R. E., and M. A. Geller (1968). A Generalization
of "Tidal Theory with Newtonian Cooling". J. Atmos. Sci.,
25, 932-933.

Flattery, T. W. (1967). Hough Functions. Technical Report
No. 21, Dept. of Geophysical Sciences, University of
Chicago. 168 pp.

French, B. M. (1971). How Did Venus Lose Its Angular Momentum?
Reply to Singer (1970). Science, 173, 169-170.

Gerstenkorn, H. (1967). The model of the so-called "weak"
tidal friction and the limits of its applicability. P. 229-234
in Mantles of the Earth and Terrestial Planets, ed. S. K.
Runcorn. Interscience Publishers, London. 584 pp.

Gierasch, P., and R. Goody (1968). A Study of the Thermal and Dynamical Structure of the Martian Lower Atmosphere. Planetary and Space Science, 16, 615-646.

Gold, T., and S. Soter (1969). Atmospheric Tides and the Resonant Rotation of Venus. Icarus, 11, 356-366.

Gold, T., and S. Soter (1971). Atmospheric Tides and the 4-Day Circulation on Venus. Icarus, 14, 16-20.

Goldreich, P., and S. Peale (1966a). Resonant Rotation for Venus? Nature, 209, 1117-1118.

Goldreich, P., and S. Peale (1966b). Spin-Orbit Coupling in the Solar System. Astron. J., 71, 425-438.

Goldreich, P., and S. Peale (1967). Spin-Orbit Coupling in the Solar System. II. The Resonant Rotation of Venus. Astron. J., 72, 662-666.

Goldreich, P., and S. Peale (1968). The Dynamics of Planetary Rotations. Ann. Rev. Astron. Astroph., 6, 287-320.

Goldreich, P., and S. Peale (1970). The Obliquity of Venus. Astron. J., 75, 273-284.

Goldreich, P., and S. Soter (1966). Q in the Solar System. Icarus, 5, 375-389.

Goldreich, P., and A. Toomre (1969). Some Remarks on Polar Wandering. JGR, 74, 2555-2567.

Goody, R. M. (1960). The Influence of Radiative Transfer on the Propagation of a Temperature Wave in a Stratified Diffusing Atmosphere. J. Fluid Mech., 9, 445-454.

Goody, R. M. (1964). Atmospheric Radiation. Oxford University
   Press, 436 pp.

Green, J. S. A. (1965). Atmospheric tidal oscillations: an
   analysis of the mechanics. Proceedings of the Royal Society,
   288A, 564-574.

Greenberg, R. (1974). Outcomes of Tidal Evolution for Orbits
   with Arbitrary Inclination. Icarus, 23, 51-58.

Hinch, E. J. (1970). The Rotation of Venus and Thermal Tides.
   (Unpublished.) P. 38-54 in Notes on the 1970 Summer Study
   Program in Geophysical Fluid Dynamics at the Woods Hole
   Oceanographic Institution; Volume II, Fellowship Lectures.

Holmberg, E. R. R. (1952). A Suggested Explanation of the Present Value
   of the Velocity of Rotation of the Earth, Mon. Not. Roy. Astr. Soc.
   Geophysical Supplement, 6, 325-330.

Howard, H., G. Tyler, G. Fjeldbo, A. Kliore, G. Levy, D. Brunn,
   R. Dickinson, R. Edelson, W. Martin, R. Postal, B. Seidel,
   T. Sesplaukis, D. Shirley, C. Stelzreid, D. Sweetnam,
   A. Zygielbaum, P. Esposito, J. Anderson, I. Shapiro, and
   R. Reasenberg (1974). Venus: Mass, Gravity Field, Atmosphere,
   and Ionosphere as Measured by the Mariner 10 Dual-Frequency
   Radio System. Science, 183, 1297-1300.

Ingersoll, A. P., and A. Dobrovolskis (1977). Calculations of
the Effects of Atmospheric Tides on the Rotation of Venus.
Presentation at the 8th annual meeting of the Division
for Planetary Sciences of the AAS, in Honolulu, Hawaii.
Abstract in BAAS, 9, 467.

Ingersoll, A. P., and A. R. Dobrovolskis (1978). Venus Rotation
and Atmospheric Tides. Accepted by Nature.

Irvine, W. M. (1968). Monochromatic Phase Curves and Albedos
for Venus. J. Atmos. Sci., 25, 610-616.

Kaula, W. M. (1964). Tidal Dissipation by Solid Friction and
the Resulting Orbital Evolution. Reviews of Geophysics,
2, 661-685.

Kaula, W. M. (1968). An Introduction to Planetary Physics.
John Wiley & Sons, New York. 490 pp.

Keldysh, M. V. (1977). Venus Exploration with the Venera 9 .
and Venera 10 Spacecraft. Icarus, 30, 605-625.

Kundt, W. (1977). Spin and Atmospheric Tides of Venus.
Astronomy and Astrophysics, 60, 85-91.

Kuo, H. L. (1968). The Thermal Interaction between the Atmosphere
and the Earth and Propagation of Diurnal Temperature Waves.
J. Atmos. Sci., 25, 682-706.

Kuzmin, A. D., and M. Ya. Marov (1975). Physics of the Planet
Venus. NASA Technical Translation TT-F-16226, from Fizika
Planety Venera (1974), Nauka Press, Moscow 328 pp.

Lacis, A. A. (1975). Cloud Structure and Heating Rates in the Atmosphere of Venus. J. Atmos. Sci., 32, 1107-1124.

Leovy, C. B. (1973). Rotation of the Upper Atmosphere of Venus. J. Atmos. Sci., 30, 1218-1220.

Lewis, J. S. (1971). Venus: Surface Temperature Variations. J. Atmos. Sci., 28, 1084-1086.

Lindzen, R. S. (1965). On the Asymmetric Diurnal Tide. Pure and Applied Geophysics, 62, 142-147.

Lindzen, R. (1967). Planetary Waves on Beta-Planes. Monthly Weather Review, 95. 441-451.

Lindzen, R. S. (1970a). Internal Gravity Waves in Atmospheres with Realistic Dissipation and Temperature. Part I. Mathematical Development and Propagation of Waves into the Thermosphere. Geophysical Fluid Dynamics, 1, 303-355.

Lindzen, R. S. (1970b). The Application and Applicability of Terrestrial Atmospheric Tidal Theory to Venus and Mars. J. Atmos. Sci., 27, 536-549.

Lindzen, R. S. (1971). Internal Gravity Waves in Atmospheres with Realistic Dissipation and Temperature. Part III. Daily Variations in the Thermosphere. Geophysical Fluid Dynamics, 2, 89-121.

Lindzen, R. S., and Donna Blake (1971). Internal Gravity Waves in Atmospheres with Realistic Dissipation and Temperature. Part II. Thermal Tides Excited Below the Mesopause. Geophysical Fluid Dynamics, 2, 31-61.

Lindzen, R. S., and S. Hong (1973). Equivalent Gravity Modes - An Interim Evaluation. Geophysical Fluid Dynamics, 4, 279-292.

Lindzen, R. S., and S. Hong (1974). Effects of Mean Winds and Horizontal Temperature Gradients on Solar and Lunar Semidiurnal Tides in the Atmosphere. J. Atmos. Sci., 31, 1421-1446.

Lindzen, R. S., and H.-L. Kuo (1969). A Reliable Method for the Numerical Integration of a Large Class of Ordinary and Partial Differential Equations. Monthly Weather Review, 97, 732-734.

Lindzen, R. S., and D. J. McKenzie (1967). Tidal Theory with Newtonian Cooling. Pure and Applied Geophysics, 66, 90-96.

Lyttleton, R. A. (1973). On the Status of the Rotation of Venus. Astrophysics and Space Science, 26, 497-511.

MacDonald, G. J. F. (1964). Tidal Friction. Rev. Geophys., 2, 467-541.

Marov, M. Ya., V. S. Avduevsky, N. F. Borodin, A. P. Ekonimov, V. V. Kerzhanovich, V. P. Lysov, B. Ye. Moshkin, M. K. Rozhdestvensky, and O. L. Ryabov (1973). Preliminary Results on the Venus Atmosphere from the Venera 8 Descent Module. Icarus, 20, 407-421.

McAdoo, D. C., and J. A. Burns (1974). Approximate Axial Alignment Times for Spinning Bodies. Icarus, 21, 86-93.

McCord, T. B. (1968). The Loss of Retrograde Satellites in the Solar System. JGR, 73, 1497-1500.

Moroz, V. I., N. A. Parfent'ev, N. F. San'ko, V. S. Zhegulev, L. F. Zasova, and E. A. Ustinov (1977). Preliminary Results of Narrow-Band Photometric Probing of the Cloud Layer of Venus in the 0.80-0.87-μ Spectral Region of the Venera 9 and Venera 10 Descent Vehicles. Cosmic Research, 14, 649-662.

Munk, W. H., and G. J. F. MacDonald (1975). The Rotation of the Earth. Reprinted with corrections from the 1960 edition. Cambridge University Press, Cambridge, England. 323 pp.

Peale, S. J. (1974). Possible histories of the obliquity of Mercury. A. J., 79, 722-744.

Pollack, J. B., and R. Young (1975). Calculations of the Radiative and Dynamical State of the Venus Atmosphere. J. Atmos. Sci., 32, 1025-1037.

Shapiro, I., P. Campbell, and W. DeCampli (1978). Submitted to Ap. J. Letters.

Shapiro, I. I., G. H. Pettengill, G. N. Sherman, A. E. Rogers, and R. P. Ingalls (1973). Venus: Radar Determination of Gravity Potential. Science, 179, 473-476.

Siebert, Manfred (1961). Atmospheric Tides. Advances in Geophysics, 7, 105-187.

Singer, S. F. (1970). How did Venus Lose Its Angular Momentum? Science, 170, 1196-1198.

Singer, S. F. (1971). How did Venus Lose Its Angular Momentum? Rebuttal of French (1971). Science, 173, 170.

Smith, J. C., and G. H. Born (1976). Secular Acceleration of Phobos and Q of Mars. Icarus, 27, 51-53.

Suomi, V. (1974). Cloud Motions on Venus. P. 42-59 in The Atmosphere of Venus: Proceedings of a conference held at Goddard Institute for Space Studies, New York, New York, October 15-17, 1974. J. E. Hansen, ed.

Ward, W. R., and W. M. DeCampli (1978). Comments on the Venus Rotation Pole (in preparation).

Ward, W. R., and M. J. Reid (1973). Solar Tidal Friction and Satellite Loss. Mon. Not. Roy. Astr. Soc., 164, 21-32.

Wilkes, M. V. (1949). Oscillations of the Earth's Atmosphere. Cambridge University Press, Cambridge, England. 75 pp.

Yoder, C. F., W. S. Sinclair, and J. G. Williams (1978). The Effects of Dissipation in the Moon on the Lunar Physical Librations. P. 1292-1293 in Abstracts of papers submitted to the Ninth Lunar and Planetary Science Conference, held March 13-17, 1978, in Houston, Texas.

Zurek, R. W. (1976). Diurnal Tide in the Martian Atmosphere. J. Atmos. Sci., 33, 321-337.